

AD613339

AD

USATRECOM TECHNICAL REPORT 64-67

ENGINE AND WHIRL TESTS,  
XV-9A HOT CYCLE RESEARCH AIRCRAFT

SUMMARY REPORT

BY

CARL W PIEPER

FEBRUARY 1965

DDC  
RECEIVED  
DDC IRA B

U S ARMY TRANSPORTATION RESEARCH COMMAND  
FORT EUSTIS VIRGINIA

CONTRACT DA 44 177-AMC-877(T)  
HUGHES TOOL COMPANY

1  
\$ 5.00  
\$ 1.25  
195 P



ARCHIVE COPY

### DDC Availability Notice

Qualified requesters may obtain copies of this report from DDC.

(This report has been furnished to the Department of Commerce for sale to the public.)

### Reproduction Limitations

Reproduction of this document in whole or in part is prohibited except with permission of the Commanding Officer, USAIRFECOM. However, DDC is authorized to reproduce the document for United States Government purposes.

### Disclaimer

The findings in this report are not to be construed as an official Department of the Army position, unless so designated by other authorized documents.

When Government drawings, specifications, or other data are used for any purpose other than in connection with a definitely related Government procurement operation, the United States Government thereby incurs no responsibility nor any obligation whatsoever, and the fact that the Government may have formulated, furnished, or in any way supplied the said drawings, specifications, or other data is not to be regarded by implication or otherwise as in any manner licensing the holder or any other person or corporation, or conveying any rights or permission, to manufacture, use, or sell any patented invention that may in any way be related thereto.

### Disposition Instructions

Destroy this report when it is no longer needed. Do not return it to the originator.

HEADQUARTERS  
U S ARMY TRANSPORTATION RESEARCH COMMAND  
FORT LUSTIS VIRGINIA 23604

Under the terms of Contract DA 44-177-AMC-877(T), Hughes Tool Company, Aircraft Division, has conducted engine and rotor whirl tests of the hot cycle propulsion system to be used on the XV-9A research aircraft. This testing was to accomplish a functional check-out of the propulsion system portion of the XV-9A to assure adequacy for flight and to obtain quantitative data on engine and rotor performance, rotor loads, and yaw valve operation.

During the tests performed from 28 October 1963 through 18 May 1964, satisfactory twin-engine operation with mixed gas flow through a common exhaust duct, isolation of individual engines through the use of J-85 diverter valves, and engine operation at different power levels were accomplished. Also, rotor whirl tests up to 23,000 pounds lift and tests through full ranges of cyclic and collective pitch control were accomplished. The test objectives were completed with satisfactory results, and no serious problems were encountered during the program.

Task 1D121401A14403  
Contract DA 44-177-AMC-877(T)  
USATRECOM Technical Report 64-67

February 1965

ENGINE AND WHIRL TESTS,  
XV-9A HOT CYCLE RESEARCH AIRCRAFT

SUMMARY REPORT

Report No. HTC-AD 64-23 (385-T-15)

Prepared by

Hughes Tool Company  
Aircraft Division  
Culver City, California

for

U. S. ARMY TRANSPORTATION RESEARCH COMMAND  
FORT EUSTIS, VIRGINIA

## ABSTRACT

A summary of engine and whirl testing of the rotor and power module portion of the XV-9A is presented. The results of engine testing include operation of two gas generators into a common exhaust duct with transient power conditions. Rotor whirl test results of the hot cycle rotor used on the XV-9A are reported and include functional check-out, performance evaluation and structural evaluation. Results of testing of a jet-reaction yaw control valve are included.

CONTENTS

	<u>Page</u>
ABSTRACT . . . . .	iii
LIST OF ILLUSTRATIONS . . . . .	vi
LIST OF TABLES . . . . .	x
1. INTRODUCTION . . . . .	1
2. SUMMARY . . . . .	3
3. DESCRIPTION OF TEST SETUP AND CONFIGURATION . . . . .	6
3.1 Engine Tests . . . . .	6
3.2 Whirl tests . . . . .	8
3.3 Changes to the Rotor System . . . . .	20
3.4 Changes to the Whirl Test Facility . . . . .	22
4. DESCRIPTION OF TESTS . . . . .	26
5. TEST RESULTS AND ANALYSIS . . . . .	31
5.1 Rotor Performance . . . . .	31
5.2 Rotor System Leakage . . . . .	39
5.3 Structural Temperatures - Blade and Hub . . . . .	42
5.4 Structural Loads . . . . .	47
5.5 Rotor Dynamics . . . . .	83
5.6 Rotor Control Deflections . . . . .	96
5.7 Yaw Control Valve Testing . . . . .	113
5.8 Rotor Downwash Velocity . . . . .	113
5.9 Rotor-Engine Sound Level . . . . .	113
5.10 Twin-Engine Test Results . . . . .	117
5.11 Simulated Emergencies . . . . .	140
6. POST-TEST INSPECTION . . . . .	145
6.1 Inspection Results . . . . .	145
7. TEST INSTRUMENTATION . . . . .	147
7.1 Description of Instrumentation . . . . .	147
7.2 Calibration Procedures . . . . .	153
7.3 Recording Instrumentation . . . . .	156
REFERENCES . . . . .	194
DISTRIBUTION . . . . .	195

## ILLUSTRATIONS

<u>Figure</u>		<u>Page</u>
1.	Engine Test Configuration . . . . .	11
2.	Engine Test Installation . . . . .	12
3.	Whirl Test Site and Equipment - Whirl Test in Progress . . . . .	13
4.	Test Operators' Control Console (Control Van) . . . . .	14
5.	XV-9A Power Module and Rotor . . . . .	15
6.	Hot Cycle Rotor During Whirl Test . . . . .	16
7.	Installation of Power Module and Rotor on Whirl Tower . . . . .	17
8.	Yaw Control Valve Installation . . . . .	18
9.	Blade-Tip Closure Valve Installation . . . . .	19
10.	Rotor Lift vs. Engine Discharge Pressure . . . . .	32
11.	Rotor Lift vs. Rotor Power Required . . . . .	36
12.	Engine Discharge Conditions During Rotor Operation . . . . .	37
13.	Leakage Measurement - Rotor System . . . . .	41
14.	Measurement of Diverter-Valve Leakage . . . . .	43
15.	Temperature Survey - Whirl Test . . . . .	45
16.	Typical Rotor Start-Up, RPM vs. Time . . . . .	50
17.	Front Spar Axial Load (Chordwise Moment) at Station 90.75" . . . . .	51
18.	Rear Spar Axial Load (Chordwise Moment) at Station 90.75" . . . . .	52
19.	Front Spar Axial Load (Chordwise Moment) at Station 149" . . . . .	53
20.	Rear Spar Axial Load (Chordwise Moment) at Station 149" . . . . .	54
21.	Hub Plate Stress - Aft . . . . .	55
22.	Hub Plate Stress - Forward . . . . .	56
23.	Blade Flapwise Bending at Station 63" Front Spar . . . . .	57
24.	Blade Flapwise Bending at Station 63" Rear Spar . . . . .	58
25.	Blade Flapwise Bending at Station 75.4" Rear Spar . . . . .	59
26.	Blade Flapwise Bending at Station 100" Front Spar . . . . .	60
27.	Blade Flapwise Bending at Station 100" Rear Spar . . . . .	61
28.	Blade Flapwise Bending at Station 140" Rear Spar . . . . .	62
29.	Blade Flapwise Bending at Station 220" Rear Spar . . . . .	63
30.	Blade Flapwise Bending at Station 270" Front Spar . . . . .	64
31.	Blade Flapwise Bending at Station 270" Rear Spar . . . . .	65
32.	Blade Skin Torsion at Station 38" . . . . .	66
33.	Blade Skin Torsion at Station 83" . . . . .	67

ILLUSTRATIONS (Continued)

<u>Figure</u>		<u>Page</u>
34.	Rotor Shaft Bending 90 Degrees to Blue Blade . . . . .	68
35.	Pitch Link Load, Blue Blade . . . . .	69
36.	Pitch Link Load, Yellow Blade . . . . .	70
37.	Pitch Link Load, Red Blade . . . . .	71
38.	Control Actuator Force, Starboard . . . . .	72
39.	Control Actuator Force, Port . . . . .	73
40.	Control Actuator Force, Longitudinal . . . . .	74
41.	Swash-Plate Drag Link Load . . . . .	75
42.	Blue-Blade Feathering Angle . . . . .	76
43.	Blue-Blade Flapping Angle . . . . .	77
44.	Gimbal Lug Bending Strain . . . . .	78
45.	Chordwise Shear at Station 23.0 . . . . .	79
46.	Rotor Blade Front Spar Axial Load vs. Rotor Shaft Bending . . . . .	81
47.	Engine No. 2 - Accessory Gearbox Pad Strain - Parallel to Eng. $\phi$ . . . . .	84
48.	Engine No. 2 - Accessory Gearbox Strain - 45 Degrees to Eng. $\phi$ . . . . .	85
49.	Engine No. 2 - Accessory Gearbox Strain - 90 Degrees to Eng. $\phi$ . . . . .	86
50.	Engine No. 2 Lower R. H. Pad Strain . . . . .	87
51.	Engine No. 2 Aft R. H. Pad Strain . . . . .	88
52.	Engine No. 2 Upper R. H. Pad Strain . . . . .	89
53.	Engine No. 2 Upper L. H. Pad Strain . . . . .	90
54.	Engine No. 2 Aft L. H. Pad Strain . . . . .	91
55.	Engine No. 2 Lower L. H. Pad Strain . . . . .	92
56.	First Chordwise Cantilever Mode Natural Frequency per Revolution vs. RPM . . . . .	93
57.	Coupled Pylon Blade Frequencies of Rotor on Whirl Stand vs. Rotor Speed . . . . .	95
58.	Lateral Cyclic Reversal, Run 31, 14 May 1964 $N_R = 99.6$ Percent . . . . .	97
59.	Lateral Cyclic Reversal, Run 31, 14 May 1964 $N_R = 99.6$ Percent . . . . .	99
60.	Longitudinal Cyclic Reversal, Run 31, 14 May 1964 $N_R = 97.1$ Percent . . . . .	101

ILLUSTRATIONS (Continued)

<u>Figure</u>		<u>Page</u>
61.	Longitudinal Cyclic Reversal, Run 31, 14 May 1964 NR = 97.4 Percent . . . . .	103
62.	Collective Pitch Transient, Run 30, 11 May 1964 NR = 98.4 Percent . . . . .	105
63.	Collective Pitch Transient, Run 30, 11 May 1964 NR = 98.4 Percent . . . . .	107
64.	Yaw Valve Thrust Measurement . . . . .	115
65.	Rotor Downwash Velocity vs. Blade Radial Station . . . . .	116
66.	Sound Pressure Level . . . . .	118
67.	Engine 010 in Twin-Engine Operation . . . . .	123
68.	Engine 026 in Twin-Engine Operation . . . . .	124
69.	Engine 026 Compressor Corrected Flow vs. Compressor Pressure Ratio . . . . .	126
70.	Engine 026 Compressor Corrected Flow vs. Corrected Engine Speed Twin-Engine Operation . . . . .	127
71.	Twin-Engine Operating Characteristics Rapid Accel- eration from Idle to Maximum Power . . . . .	128
72.	Twin-Engine Operating Characteristics Rapid Accel- eration to Maximum Power with Differential Starting Speeds . . . . .	129
73.	Twin-Engine Operating Characteristics Rapid Power Change from Maximum to 80 Percent NG and Return to Maximum . . . . .	130
74.	Twin-Engine Operating Characteristics Steady-State Engine Data at Differential Power Setting . . . . .	131
75.	T-64 Gas Generator Air Flow Characteristics . . . . .	135
76.	Pressure Loss Between Engine Exit (Station 5) and Hub (Station 6) . . . . .	137
77.	Strain-Gage Bridge Locations, Rotor Blades - Whirl Test . . . . .	173
78.	Thermocouple Locations, Rotor Blades and Hub Whirl Test . . . . .	175
79.	Engine Temperature and Pressure Probes . . . . .	177
80.	Thrust Load Cell Installation . . . . .	178
81.	Thrust Meter and Oscillograph Installation . . . . .	179
82.	Variable Area Exit Nozzle Probe Arrangement . . . . .	180
83.	Tip Pressure Transducer Installation . . . . .	181

ILLUSTRATIONS (Continued)

<u>Figure</u>		<u>Page</u>
84.	Hub Tilt Pickup Installation . . . . .	182
85.	Blade Geometry Pickup Installation . . . . .	183
86.	Engine Instrumentation Installation . . . . .	184
87.	Thrust Measuring System Calibration . . . . .	185
88.	Close-up of Hookup Used To Calibrate Thrust Measuring System . . . . .	186
89.	Slip Ring Installation . . . . .	187
90.	Engine T <sub>5</sub> Recorders . . . . .	188
91.	Temperature Recording Instrumentation . . . . .	189
92.	Rotor Thermocouple Switch Box Installation . . . . .	190
93.	Oscillograph and Balance Box Installation . . . . .	191
94.	Manometer and Camera Installation . . . . .	192
95.	Engine and Rotor Instrumentation Photographic Installation . . . . .	193

LIST OF TABLES

<u>Table No.</u>		<u>Page</u>
1.	Summary of Engine Tests . . . . .	27
2.	Summary of Whirl Tests . . . . .	29
3.	Leakage in the Rotor System and Rotor Components . .	40
4.	Component Temperatures . . . . .	44
5.	Oscillograph Setup Sheets . . . . .	109
6.	Yaw Control Valve Test Data . . . . .	114
7.	Sound Spectral Data . . . . .	119
8.	Rotor and Engine Performance, Rotor Geometry, and Control System Measurements . . . . .	158
9.	Strain Gage Installations . . . . .	160
10.	Rotor Thermocouple Summary . . . . .	165
11.	Structural Thermocouple Summary . . . . .	171

## 1. INTRODUCTION

The XV-9A Hot Cycle Research Aircraft engine and whirl tests were conducted in two parts from 28 October through 10 December, 1963, and from 27 March through 18 May, 1964. These tests were conducted by the Hughes Tool Company Aircraft Division at Culver City, California as called for by Contract No. DA 44-177-AMC-877(1). This report is submitted in compliance with the same contract.

The first phase of testing consisted of engine tests to verify the operation of two YT-64 gas generators installed in the power module portion of the XV-9A Hot Cycle Research Aircraft and to evaluate gas generator control and performance during twin-engine operation with mixed gas flow through a common-exhaust duct and exit nozzle. These tests provided a functional check-out and verification of the fixed-duct portion of the XV-9A including J-85 diverter valves, engine-diverter valve seals, transition ducts, and engine tailpipes.

Engine testing consisted of 17 hours 30 minutes of individual engine operation with gas flow through diverter valves in "over-board" position and 7 hours 48 minutes of twin-engine operation with mixed gas flow through the common-exhaust duct and exit nozzle. Quantitative data were recorded during these tests for evaluation and analysis of steady-state and transient twin-engine operating characteristics, individual and twin-engine performance as gas generators, and engine air flow measurement. Data are presented in this report for the most significant twin-engine test conditions.

The power module was removed from the whirl tower following completion of engine tests and was returned to the factory area for installation of the rotor, controls, and additional test instrumentation in preparation for the rotor whirl tests.

The second phase of testing consisted of rotor whirl tests to accomplish a functional check-out of the complete propulsion system portion of the XV-9A in order to assure adequacy for flight and to demonstrate compatibility of the rotor and the twin YT-64 power plant operation with associated controls, diverter valves, subsystems and ducting. Quantitative data were obtained from these tests to evaluate engine and rotor performance, rotor dynamic characteristics, structural loads and temperatures, rotor control characteristics, yaw valve operation, engine and rotor sound characteristics, and rotor downwash velocities.

The functional characteristics of the power plants, rotor, and systems were determined for rotor start-up, acceleration, cyclic and collective pitch reversals, steady-state operation at various rotor power and thrust levels, simulated emergencies and rotor shut-down. A functional check-out of the blade-tip closure valve was also accomplished during the whirl test phase. Whirl testing consisted of 15 hours 49 minutes of rotor operation. Test objectives were completed with satisfactory results, and no serious deficiencies or problems were encountered during the whirl test program.

The power module and rotor were removed following completion of whirl testing and returned to the factory area for teardown inspection, reassembly, installation of modified engines, and final mating with the XV-9A fuselage.

## 2. SUMMARY

The engine and whirl test phase of the XV-9A Hot Cycle Research Aircraft program was successfully completed in May 1964. The results and analysis of the significant portions of the test data are presented in this report.

The functional check-out of the complete XV-9A propulsion system including the rotor, YT-64 gas generators, J-85 diverter valves, engine and rotor controls, systems, and equipment was accomplished. In general the performance of systems and equipment was satisfactory. The need for the following component improvements was determined:

1. Replacement of diverter-valve hydraulic actuators.
2. Improvement of diverter-valve actuator hydraulic selector valves.
3. Reduction of diverter-valve leakage.
4. Revision of the rotor lubrication system to improve scavenging.
5. Scaling of the blade leading-edge segments to improve air flow.
6. Reinforcement of the yaw valve ducting.
7. Increased clearance for the movable vane of the blade-tip closure valve.
8. Increased clearance for the tri-duct within the hub area.
9. Improved heat blanket insulation for the Y-duct and tri-duct.
10. Improvement of the radial bearing oil seals.

A complete inspection of the rotor, power module, engines, and equipment was conducted after completion of whirl testing. The results of this inspection are presented later in this report.

The two YT-64 gas generators with mixed exhaust flow were successfully operated at a wide range of steady-state and transient conditions with a fixed common-exhaust nozzle and subsequently for rotor whirl tests. An individual gas generator was isolated by means of diverter-valve action and was then re-cycled to twin-engine operation.

The speed-power control characteristics of the hot cycle rotor and twin YT-64 gas generators were found to be satisfactory for the complete operating envelope utilizing the standard YT-64 fuel controls.

The predicted rotor lift and rotor power characteristics of the hot cycle rotor and YT-64 gas generators were substantiated by test measurements. The maximum measured rotor lift was 23,000 pounds for an engine pressure ratio of 2.62. The test data substantiated that the present hot cycle propulsion system has a lift capability of 25,500 pounds with the specification T-64 gas generators.

Operating temperatures of the various rotor components were either as predicted or lower at the maximum gas temperature attained during whirl test.

The leakage of the rotor ducts and seals was less than .2 percent of the total flow as measured before and after whirl test. Diverter-valve leakage was found to be higher than predicted by the manufacturer's data.

Structural load measurements taken during whirl tests substantiated the design of the various changes which were incorporated into the hot cycle rotor for the XV-9A program. With the exception of blade chordwise moments, all cyclic loads were of moderate magnitude and below endurance limits. Blade chordwise moments were near or slightly above endurance limits for the high rotor lift condition at 23,000 pounds.

The first mode blade chordwise bending frequency was determined to be 1.43/rev, an increase of 14 percent over the previous chordwise frequency prior to rotor modifications. There were no flapwise bending resonances within the normal rotor operating range.

Rotor control response and operating characteristics for large cyclic and collective transients and reversals were determined to be satisfactory for flight of the XV-9A aircraft. The XV-9A yaw control valve produced a measured thrust of 338 pounds, which was in excess of the design objective.

Measured sound levels were approximately the same as had been predicted from previous whirl test data. In general, the noise

level was not considered as objectionable as that for previous whirl test with a J-57 engine.

### 3. DESCRIPTION OF TEST SETUP AND CONFIGURATION

#### 3.1 ENGINE TESTS

The basic engine test configuration consisted of two YT-64 gas generators installed in the XV-9A power module, with the fixed-duct portion of the propulsion system including two J-85 diverter valves, engine-diverter valve seals, transition ducts, and tailpipes. The power module assembly was installed on top of the whirl tower utilizing the mounting structure and test support systems provided for these tests and for subsequent rotor whirl testing. This placed the engines approximately 30 feet above ground level. The engine test configuration is shown in Figures 1 and 2.

Three YT-64 generators were used during the engine test program. Engines S/N 250010-4 and 250013-5, which are ground test engines, were installed initially with Engine 010-4 in the left (No. 1) nacelle and Engine 013-5 in the right (No. 2) nacelle. Following the failure of Engine 013-5 during Run 6, Engine 250026-1A, the first flight-quality YT-64 gas generator received by Hughes Tool Company, was installed in No. 2 nacelle.

A standard bellmouth containing air flow instrumentation was installed on Engine No. 1 for Runs 1 - 16 for air flow calibration tests. A Hughes Tool Company inlet, P/N 385-7503, containing the same instrumentation was installed on Engine No. 2 for Runs 1 - 16. The bellmouth was removed from Engine No. 1 and installed on Engine No. 2 for Run 17 and the Hughes Tool Company inlet installed on Engine No. 1 to obtain bellmouth air flow data from both engines.

The original hot cycle heavyweight Y-duct was used for the engine tests to provide support for the large, common-exhaust duct used to simulate gas flow through the rotor. The common-exhaust duct, having an adjustable plug-type nozzle at the upper end to permit varying exit area, was installed on top of the Y-duct.

Power module attachment to the upper tower structure was by the four spar attachment fittings on the front and rear spars which are used for mating to the XV-9A fuselage. The four load cells for measurement of rotor lift force were installed in the whirl tower support structure but were not used for this phase of the testing.

The engine control system consisted of two separate power levers, cable, pulley, and bell-crank systems running from the control van to the individual power control shafts on the fuel controls. The  $N_f$  governing system was not used, and the engine fuel control load signal shafts were mechanically fixed.

Engine controls, instruments, switches, circuit breakers, and test instrumentation were contained in the control van approximately 75 feet from the base of the tower (see Figures 3 and 4).

JP-4 fuel was supplied to the engines from a trailer-tanker at ground level by means of a common 1-1/2-inch-diameter supply line and boost pump which delivered fuel through a flow divider to the individual fuel control inlets at 20 psig.

The 28-volt DC generators and the 3,000-psi hydraulic pumps were not installed on the engines for these tests. Electrical power and hydraulic pressure for diverter valve operation were supplied from ground carts.

Engine starting was accomplished by means of MA-1 gas turbine compressor starting unit located at ground level. The air-start valve on the MA-1 cart was wired to the "start" switch on the operator's control panel to control the air flow from the compressor.

Engine starting by the YT-64 air impingement starting (AIS) system was very satisfactory, and no "hot starts" were experienced during this program. Air delivery pressure to the engine AIS manifold connection of 43 psig was maintained while accelerating the engine to 30 percent  $N_G$ .

An external engine lubrication system consisting of a 5-gallon reservoir, water-oil cooler, supply, return, and vent lines was installed for each engine. Oil temperatures were maintained below 175 degrees F for all engine conditions by regulating the flow of water through the coolers.

The engine control quadrant installed in the control van was a flight-type control quadrant which was to be used in the XV-9A. Stops were provided for off, idle, and maximum power-lever angle settings by the engine control system. This was adequate for individual and twin-engine operation.

### 3.2 WHIRL TESTS

The basic whirl test configuration consisted of the XV-9A power module and rotor assembly with test instrumentation installed on the whirl tower. (See Figures 3, 5, and 6.) The rotor contained the following modifications, which were incorporated as part of the XV-9A program:

1. Laminated steel spars
2. Revised blade retention straps
3. Reinforced articulate duct clamps
4. Reduced weight stationary swashplate
5. Reduced weight Y-duct and tri-duct
6. Revised rotor shaft and spoke assembly
7. Reinforced hub gimbal lugs and added hub gimbal lug thrust bearings

The power module included the YT-64 gas generators, diverter valves, transition ducts, tailpipes, rotor support structure and rotor shaft bearings and the following systems and equipment:

1. Flight controls
2. Hydraulic systems
3. Electrical system
4. Engine lubrication system
5. Engine fire extinguishing system
6. Fuel system components
7. Rotor accessory gearbox
8. Rotor lubrication system

The power module and rotor assembly were mounted on the whirl tower by means of the four attachment fittings which are also used to mate this portion of the aircraft to the XV-9A fuselage. (See Figure 7.) The support structure for the power module contained the four strain-gage load cells which were used for rotor thrust measurements. The power module contained YT-64 gas generators S/N 250010-4 and S/N 250026-1A, which were the same engines used during the earlier engine tests. Engine 250010-4, which was qualified for ground test only, was installed in the left nacelle. Engine 250026-1A, which was a flight-quality engine, was installed in the right nacelle. At this time the engine did not have the first-stage compressor modification which was later incorporated on this and subsequent flight engines utilized on the XV-9A.

The XV-9A flight control system was installed including the flight-type hydraulic servo actuators. The rotor cyclic and collective pitch controls were located in the control van at the test operator's station. A section of a Hughes 269A helicopter cockpit, including the controls and mixer, was installed in the control van for this purpose. The collective and cyclic pitch controls were connected to the input spools of the hydraulic servo actuators by a cable and push-rod system extending from the control van to the power module on top of the tower.

The engine control system used was the same as for the engine tests. A collective pitch-power coordination system consisting of a cam and push-rod mechanism for interconnecting the power lever quadrant with the collective pitch control was installed but was removed because of high operating forces which were encountered from the long cable runs and resultant friction between the control van and the tower.

A control van was located approximately 75 feet from the base of the tower and contained test instrumentation and recorders, a two-man test operators' console, engine and rotor controls, and various test equipment (see Figure 3). The test operators' console contained typical helicopter cyclic and collective control sticks, instruments, switches, and circuit breakers for operation of the YT-64 gas generators and rotor (see Figure 4).

The dual engine-driven hydraulic systems were installed in the power module and provided the hydraulic power for operation of the flight controls and diverter valves. A 28-volt DC 150-ampere generator was installed on each engine for test evaluation of the generator control and regulation system.

The flight-type engine lubrication system, consisting of the oil reservoir, air-oil cooler, and plumbing, was installed in each engine nacelle. The air-oil coolers were evaluated during initial whirl tests and found to be satisfactory. However, the water-oil coolers were reconnected during the latter whirl test runs to evaluate the effect of the  $P_3$  bleed on engine and rotor performance.

The engine fire extinguishing system, consisting of the extinguishing agent bottle, solenoid valve, lines, and discharge ring, was installed, and the electrical portion of the system was functionally checked out. The system was not discharged during whirl tests, as no serious engine fires were encountered.

The portions of the fuel system which are contained in the power module, including the lines, shutoff valves, and filters, were installed.

The rotor accessory drive gearbox, including the rotor tachometer generator and rotor lubrication pump, was installed for functional check-out during whirl tests.

The revised rotor lubrication system was installed and functionally tested during whirl tests. An electrical scavenge pump was added to the system to provide adequate oil scavenging from the upper and lower bearings during rotor start-up and shut-down when the speed of the rotor-driven pump was low.

The yaw control valve was installed on the whirl tower for functional check-out and evaluation during Runs 24 and 25 (see Figure 8). The valve was mounted on an auxiliary supporting structure built up on the whirl tower upper work platform. The installation included two strain-gaged links for measurement of yaw control valve thrust and an electrical actuator for positioning the valve at various openings. The actuator was controlled from a switch on the cyclic control stick in the control van. A short portion of the aircraft yaw control system ducting was used to connect the valve to the gas supply ports on the Y-duct. The yaw control valve rotor was positioned at various openings for the test by means of the electric actuator controlled by the switch located on the cyclic control stick. An indicator showing the amount of yaw control valve opening was mounted on the test operators' console.

The two-position XV-9A blade-tip closure valve was functionally tested during Runs 28 through 30 by mounting the valve assembly on the yaw control valve support structure and using the yaw control valve supply duct as the high-energy gas source (see Figure 9). The solenoid valve and the high-pressure air supply bottle for the blade-tip closure valve actuator were located at the base of the whirl tower to simulate the relative location of components as they will be installed in the aircraft. The solenoid valve for operation of the blade-tip closure valve from normal to single-engine position was controlled by a switch on the test operators' console. The results of this test are reported in Reference 6.

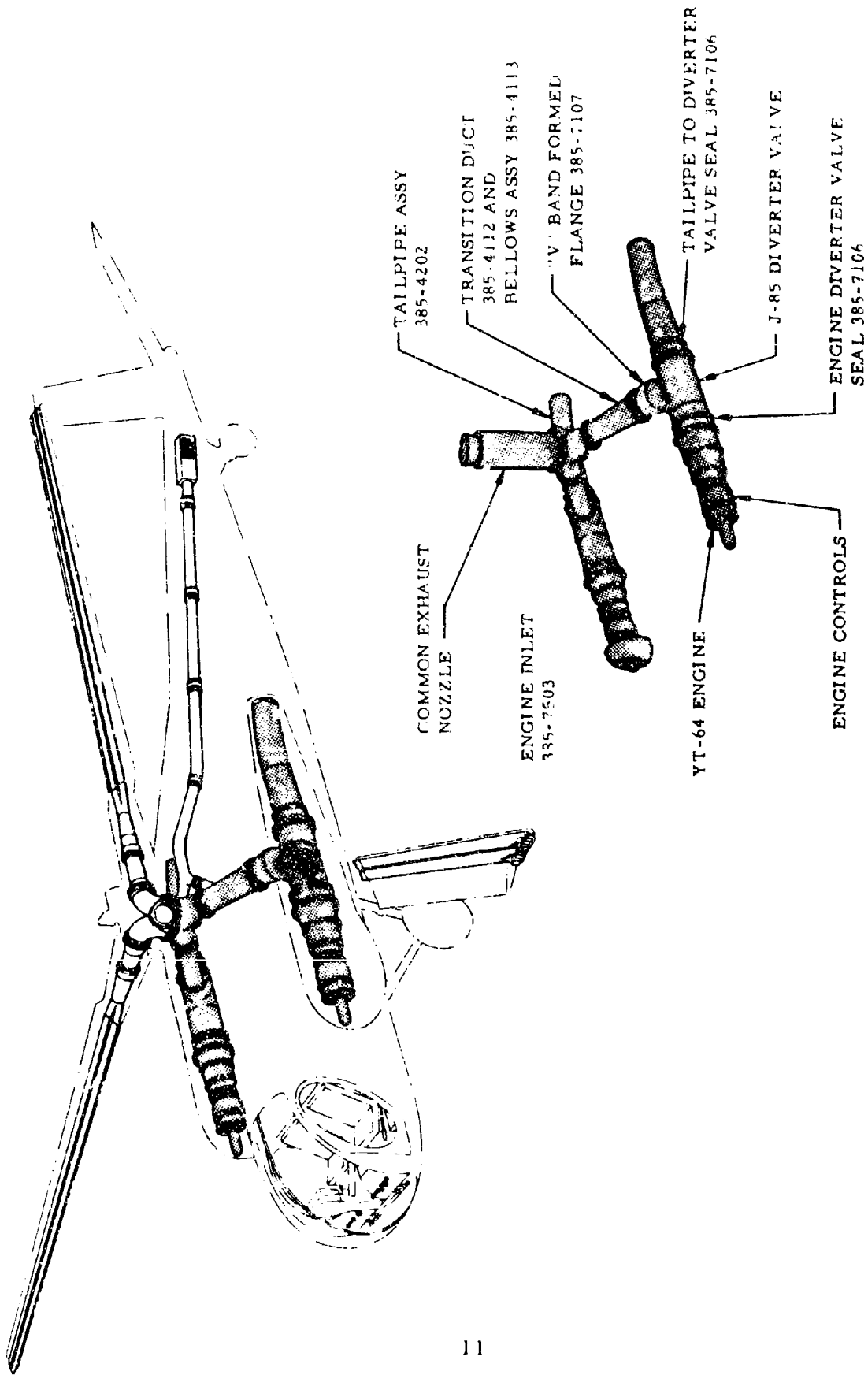


Figure 1. Engine Test Configuration

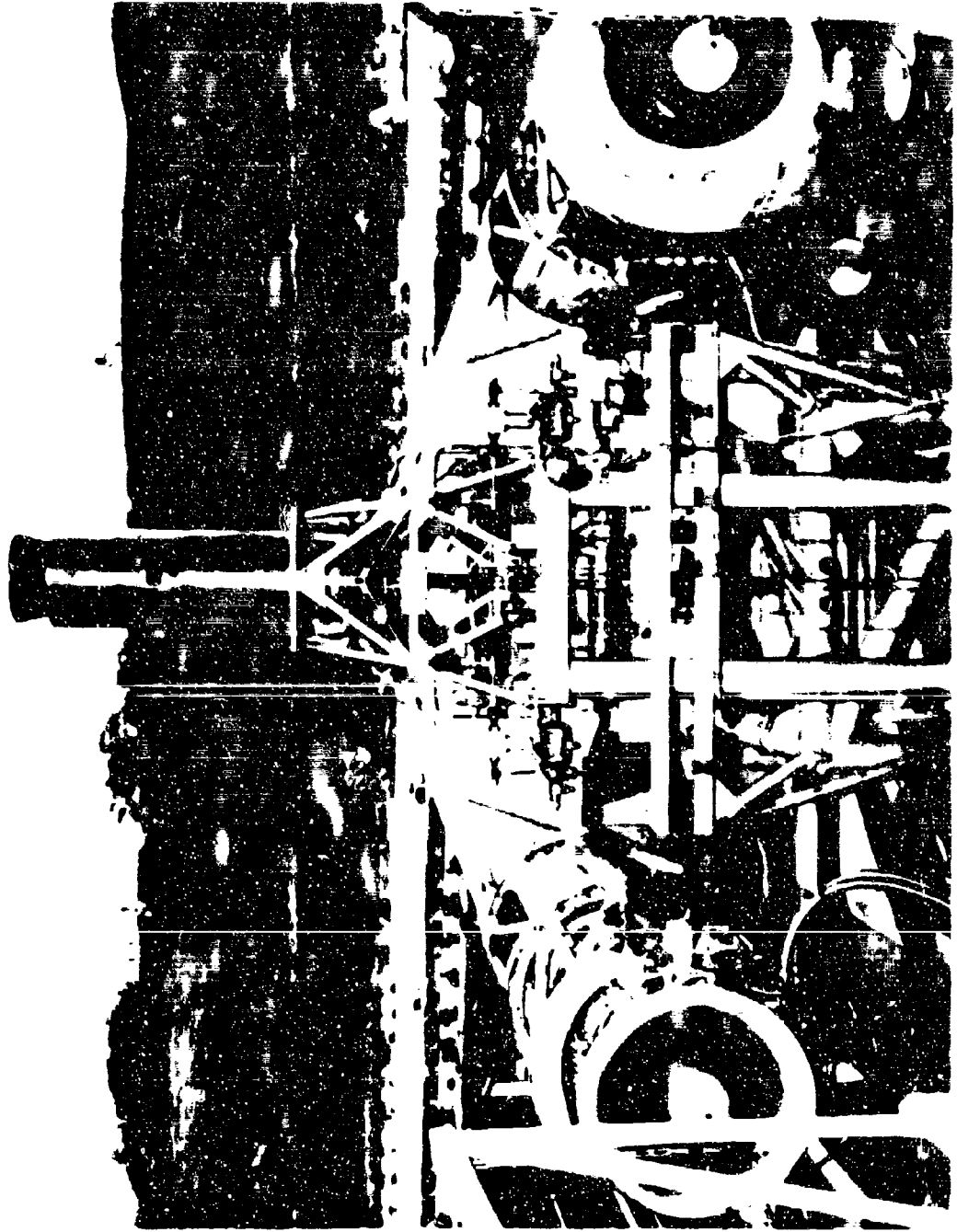


Figure 2. Engine Test Installation



Figure 3. Whirl Test Site and Equipment. Whirl Test in Progress.

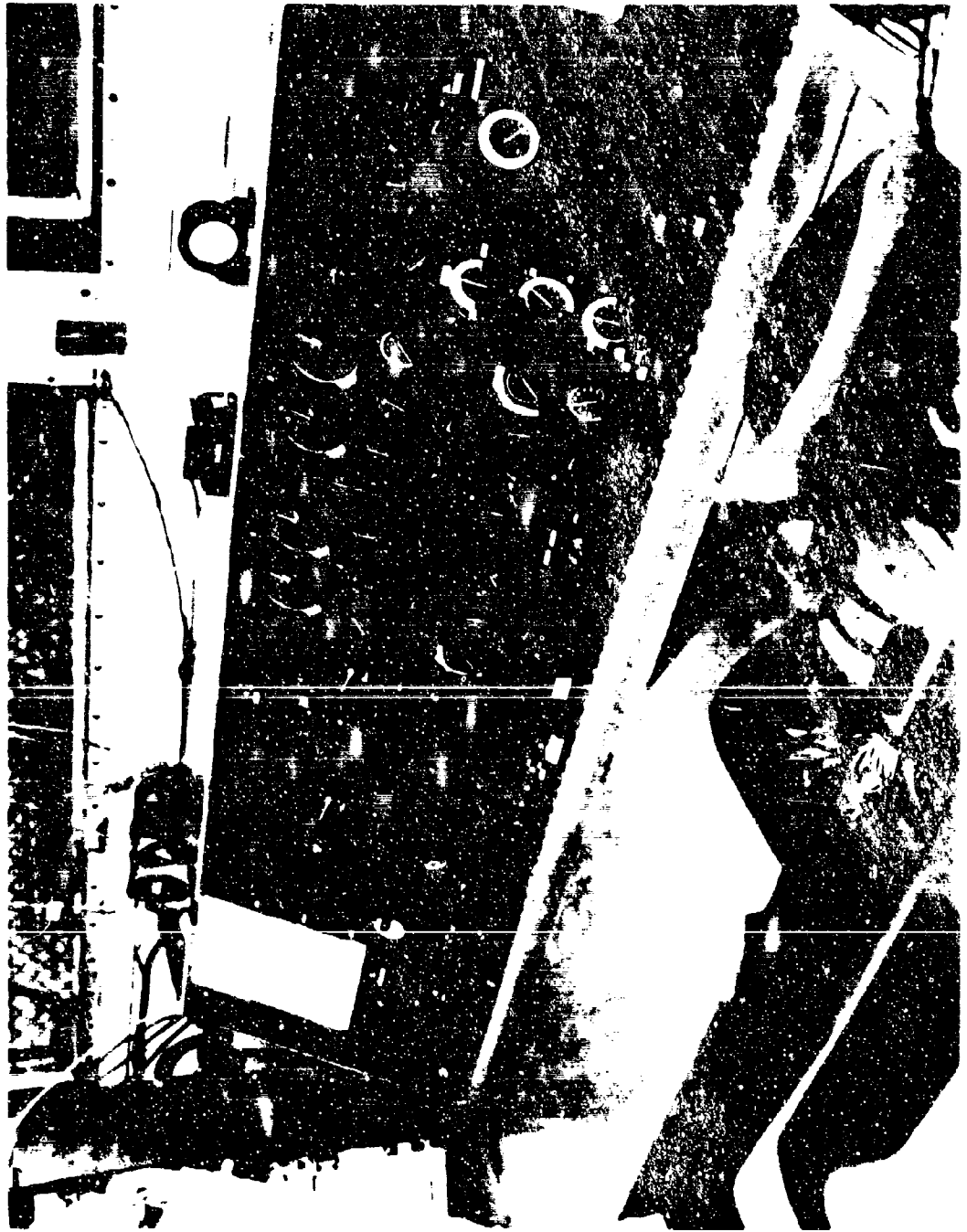


Figure 4. Test Operators' Control Console (Control Van)



Figure 5. XV-9A Power Module and Rotor



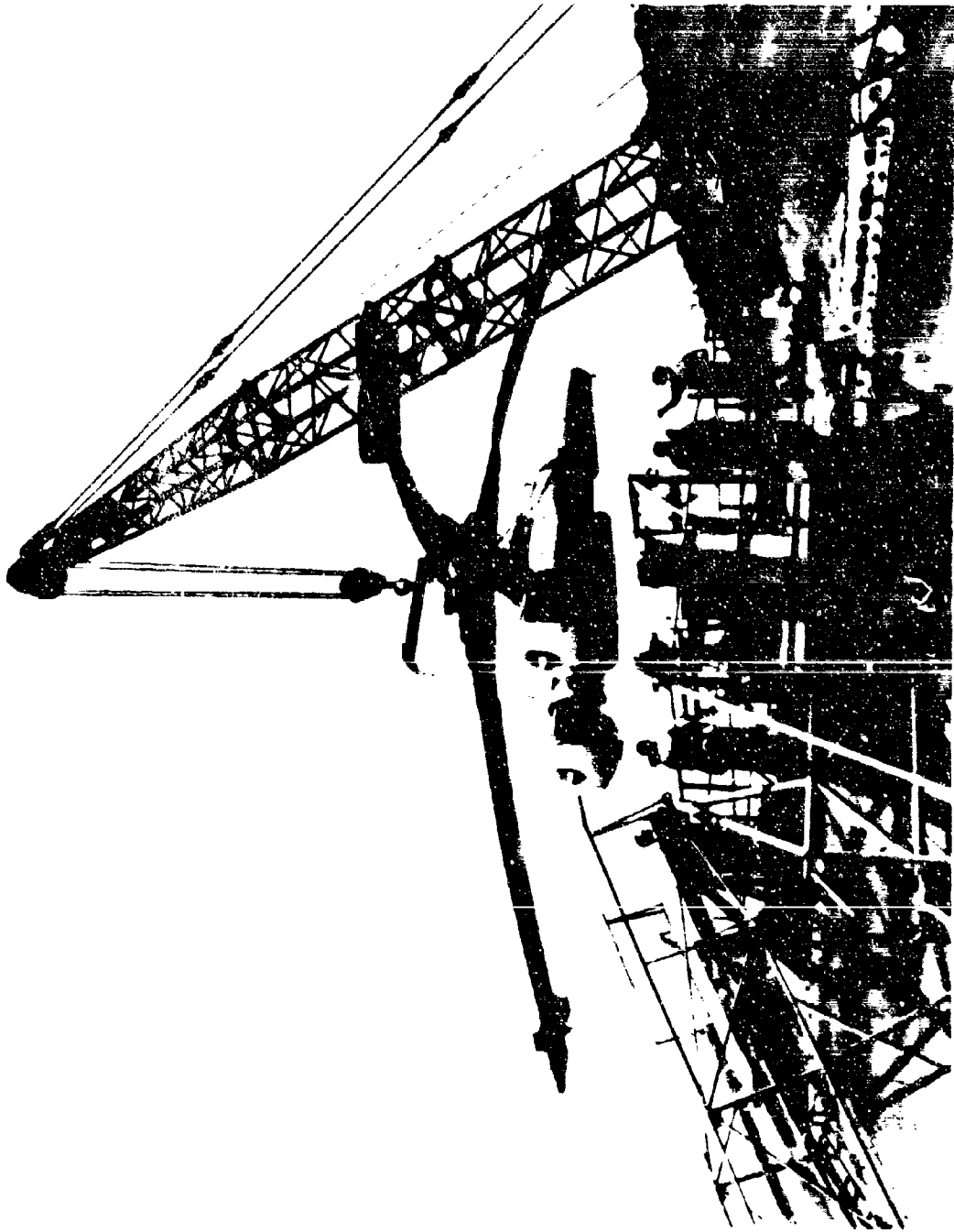


Figure 7. Installation of Power Module and Rotor on Whirl Tower

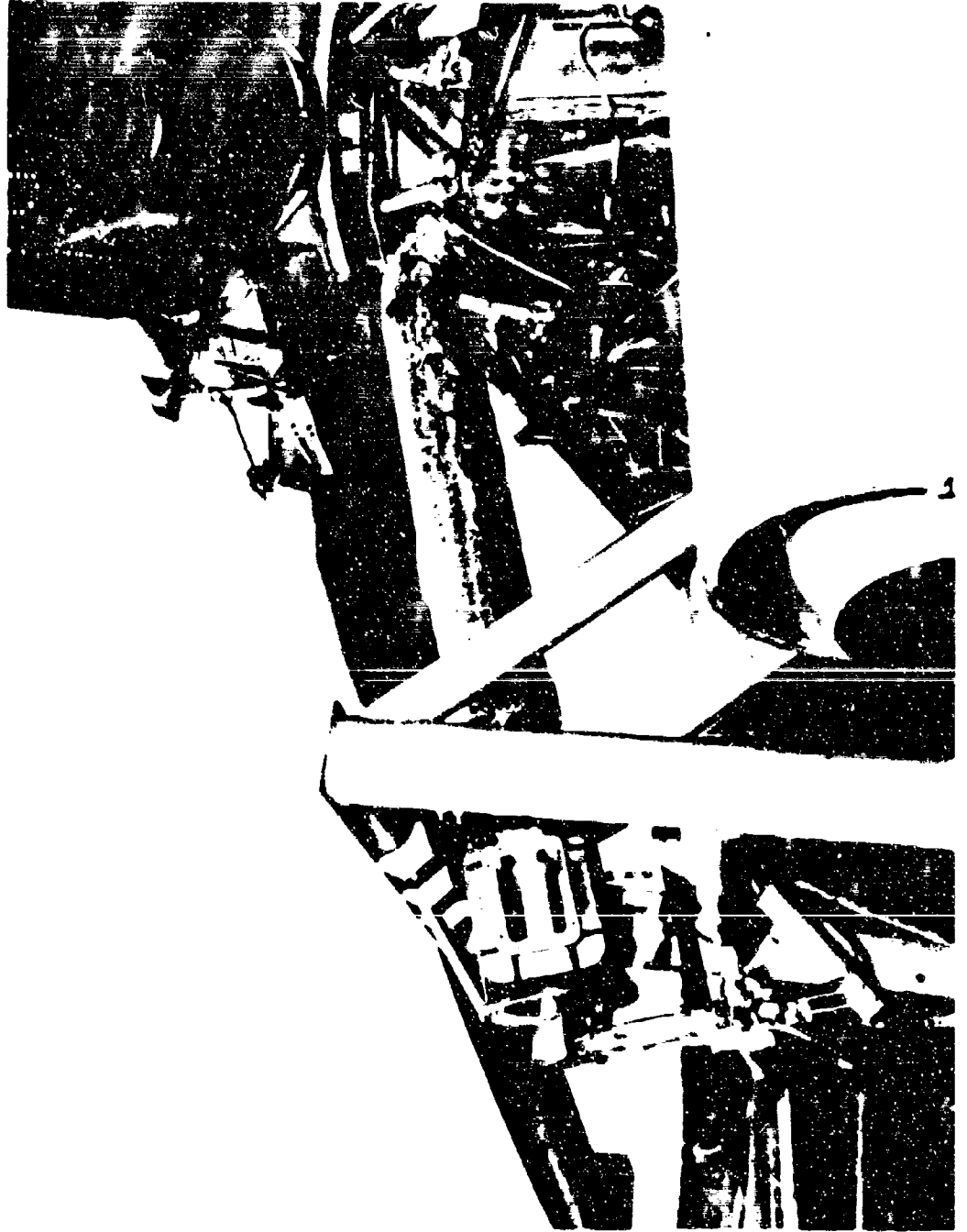


Figure 8. Yaw Control Valve Installation.

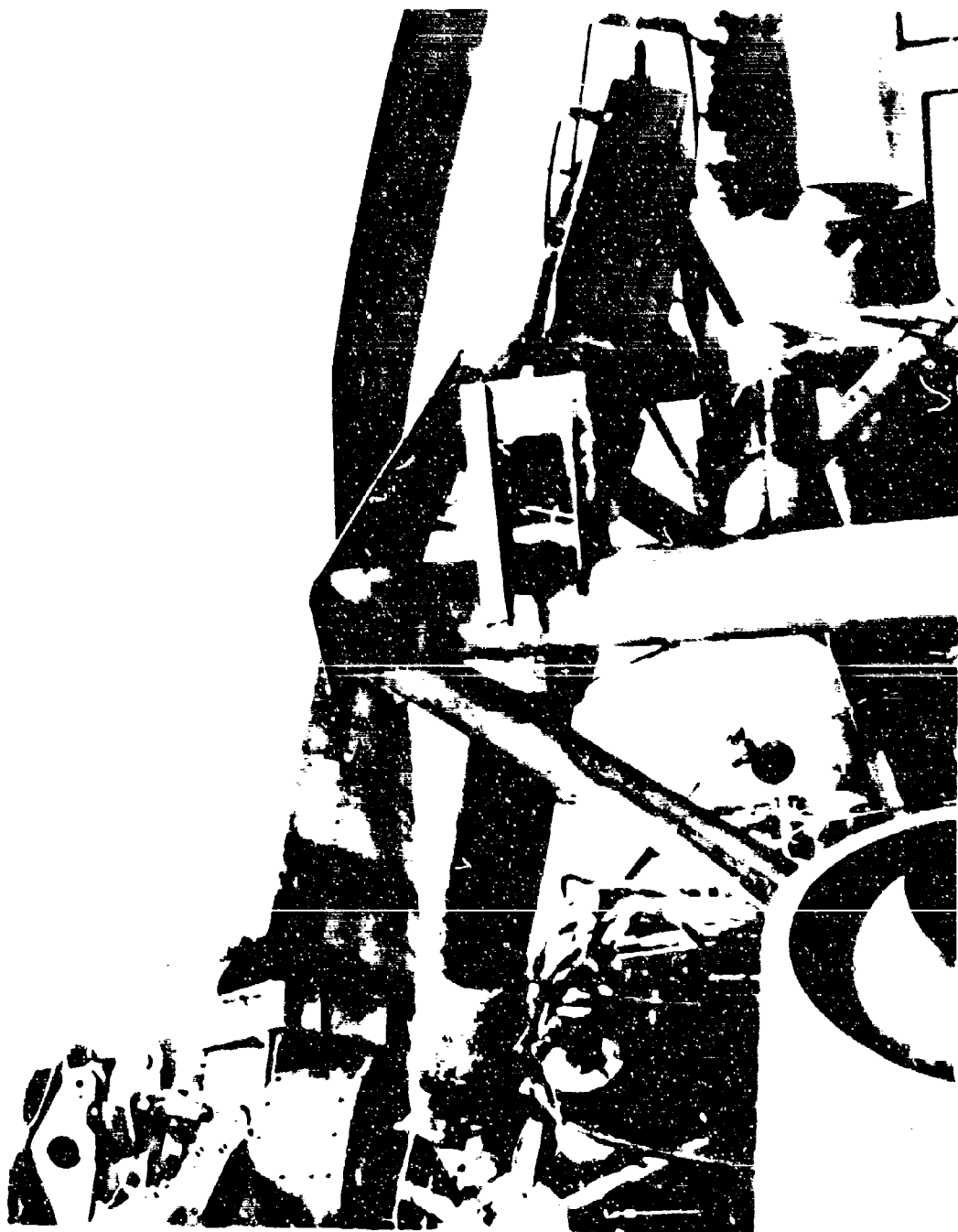


Figure 9. Blade-Tip Closure Valve Installation

### 3 3

### CHANGES TO THE ROTOR SYSTEM

The following changes to the rotor system were accomplished prior to start of whirl testing in order to improve structural integrity, to reduce weight, and to improve performance of the hot cycle system.

1. Replacement of solid machined titanium spars with laminated steel spars
2. Installation of new blade retention strap packs.
3. Installation of reinforced articulate duct clamps.
4. Installation of a new, lighter weight, stationary swashplate.
5. Installation of a new, lighter weight Y-duct and tri-duct.
6. Installation of a new rotor shaft and radial bearing support spoke.
7. Installation of a new hub gimbal assembly having strengthened hub gimbal lugs and added thrust bearings.
8. Installation of a rotor accessory drive gearbox.
9. Installation of a new rotor lubrication system.

#### 3. 3. 1

#### Laminated Steel Spars

The new laminated steel spars were fabricated from AM 355 CRT stainless-steel material. The spar assembly consists of the laminated section and a machined spar root fitting also of AM 355 CRT

The laminations were bonded together and to the spar root fitting with a high-temperature adhesive. The spar cross-sectional area was tapered by dropping off laminations at intervals along the length of the spar.

The spar assemblies were bolted to the blade segments and blade root sections using the same attachments as were used for the previous spars. A shim of low-friction material (Armalon) was installed between the spars and the blade segments to prevent fretting

#### 3. 3. 2

#### Blade Retention Straps

The chordwise natural bending frequency of the blades in cantilever mode was increased by the design and fabrication of new

blade retention strap packs having increased stiffness. The new strap packs consist of two strap packs per blade, each having 22 laminations of AM 355 CRT stainless steel of increased width over previous straps.

### 3.3.3 Reinforced Articulate Duct Clamps

The articulate duct clamps were reinforced to eliminate duct leakage during severe maneuvers.

### 3.3.4 Stationary Swashplate

The stationary swashplate was redesigned to reduce weight and to provide for the flight-type hydraulic servo actuators. A weight reduction of approximately 30 pounds was achieved.

### 3.3.5 Y-duct and Tri-duct

The stationary Y-duct and rotating tri-duct were redesigned and fabricated from drop-f mmer-formed Inconel 718 sheet material. A weight saving of approximately 105 pounds was achieved.

### 3.3.6 Rotor Shaft and Support Spoke

The rotor shaft was redesigned to increase strength and to incorporate a gear for use in driving the accessory drive gearbox. The three-armed spoke utilized in transmitting shaft radial loads to the upper bearing was also redesigned to increase strength.

### 3.3.7 Hub Gimbal Bearing Reinforcement

The existing hub gimbal assembly was revised to provide for reinforcement of the hub gimbal lugs in order to increase the strength of the hub gimbal system for in-plane loads and by the addition of thrust bearings to provide a direct load path for in-plane loads.

### 3.3.8 Rotor Accessory Drive Gearbox

A rotor-driven accessory drive gearbox was designed and fabricated to provide drive pads for the rotor lubrication system pump, rotor tachometer generator, emergency hydraulic pump, and rotor speed governing units. The gearbox is driven through a cogged-

tooth timing belt from a drive gear added to the rotor shaft. The gearbox is a basic off-the-shelf unit modified by the addition of a 90-degree drive unit.

### 3.3.9 Rotor Lubrication System

A flight-type rotor lubrication system was designed to supply circulating oil for the rotor upper radial bearing and the lower rotor thrust bearing. The system employs a combination pressure and scavenge pump driven by the accessory drive gearbox. An electrically driven scavenge pump was used to provide adequate oil scavenging at low rotor speeds.

## 3.4 CHANGES TO THE WHIRL TEST FACILITY

The following changes and additions were accomplished to the whirl test facility prior to the start of engine and whirl tests in order to accommodate the XV-9A power module and rotor installation.

1. Removal of ducting, rotor supports, J-57 engine mount, and various systems and equipment used for the previous whirl test.
2. Design and fabrication of a new upper work platform.
3. Revision of the movable blade work platform.
4. Revision of the rotor mounting structure.
5. Design and installation of a rotor thrust measuring system.
6. Design and installation of an engine lubrication system.
7. Design and installation of an engine and rotor control system.
8. Design and installation of a 28-volt DC electrical system.
9. Revision of whirl site electrical power facilities.

### 3.4.1 Removal of Ducting, Rotor Support Structure, J-57 Engine Mount, and Various Equipment

The large, vertical, hot-gas supply ducts, rotor support structure, J-57 engine mount, and the equipment and systems used for operation of the J-57 engine and hot cycle rotor during previous whirl

tests were no longer needed and were removed to permit installation of the new equipment.

#### 3.4.2 Design and Fabrication of a New Upper Work Platform

A work platform of steel construction was fabricated and installed on the whirl tower to provide access to the power module, the YT-64 gas generators, and the rotor hub area.

#### 3.4.3 Revision of the Movable Blade Work Platform

The movable blade work platform, which provides access to the entire blade length and blade tip when in the "up" position, was shortened and relocated to be compatible with the new upper work platform. A hydraulic actuating system was used to raise or lower the movable work platform as required.

#### 3.4.4 Revision of Rotor Mounting Structure

The mounting structure used to support the rotor pylon truss during the previous whirl test was modified to accommodate the rotor thrust measuring load cells and the power module support adapter. The power module and rotor were mounted on the revised structure.

#### 3.4.5 Design and Installation of a Rotor Thrust Measuring System

A rotor thrust measuring system utilizing four strain-gage load cells was designed and installed. The load cells and their attachment fittings formed the power module support system. The thrust measuring system provided a summing meter read-out of the four load cells in addition to individual recording of each load cell on oscillograph recorders.

#### 3.4.6 Design and Installation of a New Fuel System

A fuel system was designed and installed to provide JP-4 fuel to the YT-64 gas generators installed in the power module at the top of the tower. A boost pump, pressure regulator, filter, and shut-off valve were located at the base of the tower. A single 1-1/2-inch-diameter supply line carried fuel to a flow divider at the top of the tower which provided fuel supply to each engine fuel control inlet.

3. 4. 7 Design and Installation of an Engine Starting System

An engine starting system was designed and installed to provide "air starting" of the YT-64 gas generators by means of the engine AIS manifold. An MA-1 ground turbine compressor was used to provide the "air start" air flow and pressure. The engine starting system consisted of an individual air supply line with couplings and connections for the MA-1 nozzle and the engine AIS manifold.

3. 4. 8 Design and Installation of an Engine Lubrication System

A separate engine oil reservoir and oil cooler were required during engine tests to permit using the standard bellmouth for air flow measurements. The system consisted of a reservoir, oil cooler, check valves, and suction and return lines for each engine.

3. 4. 9 Design and Installation of an Engine and Rotor Control System

The engine and rotor control systems consisted of cables, pulleys, bellcranks, and push-pull rods to provide remote control of the rotor servo actuators and the engine power control shafts from the control van at ground level approximately 75 feet from the base of the whirl test tower.

The rotor controls in the control van consisted of a portion of a typical helicopter cockpit containing cyclic pitch and collective control sticks.

The engine control quadrant used in the control van was the XV-9A flight unit.

3. 4. 10 Design and Installation of a 28-Volt DC Electrical System

A 28-volt DC electrical system was designed and installed to interconnect with the power module electrical system and to provide electrical power distribution for the various test instrumentations and equipment.

Electrical power was supplied either from a 28-volt DC external power rectifier cart or from the engine-driven 28-volt DC generators.

3. 4. 11 Revision of Whirl Site Electrical Power Facilities

Additional 60-cycle, 440-volt electrical power was provided to the whirl test facility by means of a diesel generating unit and power distribution system. The additional power was required to operate test equipment and for operation of component tests (Reference 6) concurrently with rotor whirl tests.

#### 4. DESCRIPTION OF TESTS

A summary of test runs for engine and whirl tests is shown in Tables 1 and 2. Tests were conducted in accordance with the objectives and procedures outlined by Reference 1. Test Runs 1 - 17 were engine tests without the rotor installed. Test Runs 18 - 32 were whirl tests of the complete XV-9A propulsion system. The results and analysis of testing are presented in Section 5 of this report.

TABLE I  
ENGINE TEST SUMMARY

Run No.	Date	Purpose/Objective	Engine Operating Time			
			Engine #1 S/N 250010-4		Engine #2 S/N 250013-5	
			Run Total	Cumulative	Run Total	Cumulative
1	10-28-63	Engine & Systems Shakedown, Engine #1	00:22	00:22	---	---
2	10-29-63	Engine & Systems Shakedown, Engine #2	---	00:22	00:38	00:38
3	10-31-63	Steady-State Operating Data, Engine #2	---	00:22	1:02	1:40
4	11-1-63	Steady-State Operating Data, Engine #1	00:49	1:11	---	1:40
5	11-4-63	Engine #1 Topping Check & Single-Engine Transients Twin-Engine Operation at Idle Diverter Valve Functional Check-out	1:24	2:35	00:21	2:01
6	11-5-63	Engine #2 Topping Check & Single-Engine Transients Twin-Engine Steady-State Operating Data (Engine 013-5 Failure Occurred)	00:40	3:15	1:24	3:25 Engine Removed
7	11-21-63	Air Flow Calibration, Engine #1 Single-Engine Transients	1:40	4:55	Installed Y/T-64 Engine S/N 250026-1A	
8	11-23-63	Engine Shakedown, Engine #2 (250026-1A)	---	4:55	00:39	00:39
9	11-26-63	Steady-State Operating Data, Engine #2	---	4:55	00:52	1:31
10	11-27-63	Steady-State Operating Data, Engine #2	---	4:55	1:07	2:38
11	11-29-63	Engine #1 Topping Check Variable Geometry Schedule Check, Engine #2 Effect of Tailpipe "Tabbing," Engine #2, 5 in <sup>2</sup> Tabs added	00:39	5:34	00:58	3:36
12	12-2-63	Air Flow Calibration, Engine #1	1:40	7:14	---	3:36
13	12-3-63	Engine #2 Topping Check, Variable Geometry Schedule Check, Air Flow Calibration Data	---	7:14	1:49	5:25

TABLE 1 (Continued)  
ENGINE TEST SUMMARY

Run No.	Date	Purpose/Objective	Engine Operating Time	
			Engine #1 S/N 250010-4 Run Total Cumula- tive	Engine #2 S/N 250026-1A Run Total Cumula- tive
14	12-5-63	*Twin-Engine, Steady-State Operating Data Exhaust Nozzle Area = 109.6 in <sup>2</sup>	1:23 8:37	1:08 6:33
15	12-6-63	*Twin-Engine Steady-State Operating Data Twin-Engine Transients & Mismatch Exit Area = 109.6 in <sup>2</sup>	3:20 11:57	3:07 9:40
16	12-7-63	*Rapid Twin-Engine Transients & Mismatched Accelerations Exit Area = 109.6 in <sup>2</sup>	2:11 14:08	2:05 11:15
17	12-10-63	*Twin-Engine Steady-State Data with Reduced Exit Area Rapid Twin-Engine Transients with Reduced Exit Area HTC Inlet Air Flow Data for Calibration Exit Area = 98.6 in <sup>2</sup>	1:57 16:05	1:51 13:36

\*Gas flow through diverter valves & common exhaust nozzle.

Run No.	Date	Purpose/Objective	Engine Operating Time				Rotor Operating Time	
			Engine #1 S/N 250010-4		Engine #2 S/N 250026-1A			
			Run	Total	Run	Total		
18	3-24-64	Engine & Systems Shakedown	00:32	16:37	00:31	14:07	---	---
19	3-27-64	Rotor Shakedown - (Run aborted because of rotor oil leak)	00:38	17:15	00:33	14:40	00:01	00:01
20	4-2-64	Rotor & Systems Shakedown	1:01	18:16	00:52	15:32	00:23	00:24
21	4-3-64	Rotor Speed Build-up & Rotor Tracking Checks Rotor Thrust Build-up & Performance; $\Theta = 40^\circ, 60^\circ, \& 80^\circ$	2:04	20:20	2:00	17:32	1:52	2:16
22	4-7-64	Rotor Thrust Build-up & Performance; $\Theta = 100^\circ \& 110^\circ$	00:55	21:15	00:53	18:25	00:38	2:54
23	4-9-64	Simulated Emergency - Rapid Rotor Shut-Down Rotor Performance $\Theta = 110^\circ \& 120^\circ$	2:19	23:34	1:42	20:07	1:00	3:54
24	4-22-64	Yaw Valve Functional Check-out & Thrust Meas. Cyclic Control Response & Blade Dynamic Characteristics Diverter Valve Leakage Measurement	1:55	25:29	1:51	21:58	1:21	5:15
25	4-27-64	Yaw Valve Thrust & Power Measurements Engine & Rotor Sound Spectral Data	2:32	28:01	2:25	24:23	1:39	6:54
26	5-1-64	Rotor Performance; $\Theta = 70^\circ$ Diverter Valve Leakage Measurements Engine Nacelle Dynamic Characteristics	1:34	29:35	1:29	25:52	1:29	7:24
27	5-7-64	Tri-Duct Displacement - Run Aborted Because of Ground Equipment Failure	00:23	29:58	00:18	26:10	00:04	7:28

TABLE 2  
WHIRL TEST SUMMARY

TABLE 2 (Continued)  
WHIRL TEST SUMMARY

Run No.	Date	Purpose/Objective	Engine Operating Time		Rotor Operating Time			
			Engine #1 S/N 250010-4	Engine #2 S/N 250026-1A	Run	Total	Run	Total
28	5-8-64	Blade Tip Closure Valve Functional Check-out Blade Dynamic Characteristics with Simulated Mass of New Tip Cascades Diverter-Valve Leakage Measurements Cyclic Control Reversals	2:00	31:58	1:58	28:08	1:38	9:06
29	5-9-64	Engine Topping Adjustments Pilot Familiarization (Run aborted because of loose tape on blade leading edge)	00:55	32:53	00:50	28:58	00:02	09:08
30	5-11-64	Blade Tip Closure Valve - Functional Check-out Cyclic Control Reversals Collective Control Reversals Rotor Down-wash Data Y-Duct Cross Flow Vane Data	3:16	36:09	3:04	32:02	2:30	11:38
31	5-14-64	Rotor Performance; Maximum Topping, Sealed L. E. Segments & Cleaned Compressors $\Theta = 30^\circ, 50^\circ, 70^\circ, 90^\circ, 100^\circ, 110^\circ, 120^\circ$ Collective Control Reversals Cyclic Control Reversals Rotor Acceleration Characteristics Y-Duct Cross Flow Vane Data Simulated Emergencies	4:38	40:47	4:16	36:18	3:39	15:17
32	5-18-64	Structural Frequency Investigation D C Generator Regulation & Adjustment Revised Rotor Lube System Check-out	00:51	41:38	00:48	37:06	00:32	15:49

## 5. TEST RESULTS AND ANALYSIS

This section presents the significant data and analysis for the test objectives which were accomplished by the engine and whirl tests. The following subjects are included:

1. Rotor performance
2. Rotor system leakage
3. Structural temperatures
4. Structural loads
5. Rotor dynamics
6. Control system characteristics
7. Yaw control valve characteristics
8. Rotor downwash
9. Rotor-engine sound characteristics
10. Twin-engine test results
11. Simulated emergencies
12. Component maintenance and repair

### 5.1 ROTOR PERFORMANCE

#### 5.1.1 Summary

In the hot cycle system, rotor lift is directly related to input pressure. A plot of rotor lift vs. engine discharge pressure thus provides a comprehensive and over-all check of system performance. In this manner, Figure 10 presents the results from rotor whirl test.

As the ambient conditions prevailing during the test program closely corresponded to a standard day at sea level, for practical purposes the plot represents rotor performance on a standard day at sea level. The effect of parameters other than pressure is negligible. An effort was made to identify the effect of measured wind and rotor rpm. No visible trend due to wind or rotor rpm could be established within the scatter of test points. It was also found that increasing the exit area by opening the yaw control valve did not influence the relation between rotor lift and pressure. However, opening of the yaw control valve did cause a pressure drop and therefore a loss of rotor lift at a constant engine power setting.

The predicted curve of rotor lift vs. engine discharge pressure has been included on the plot for comparison and as a means for estimation of system behavior with specification T-64 engines.

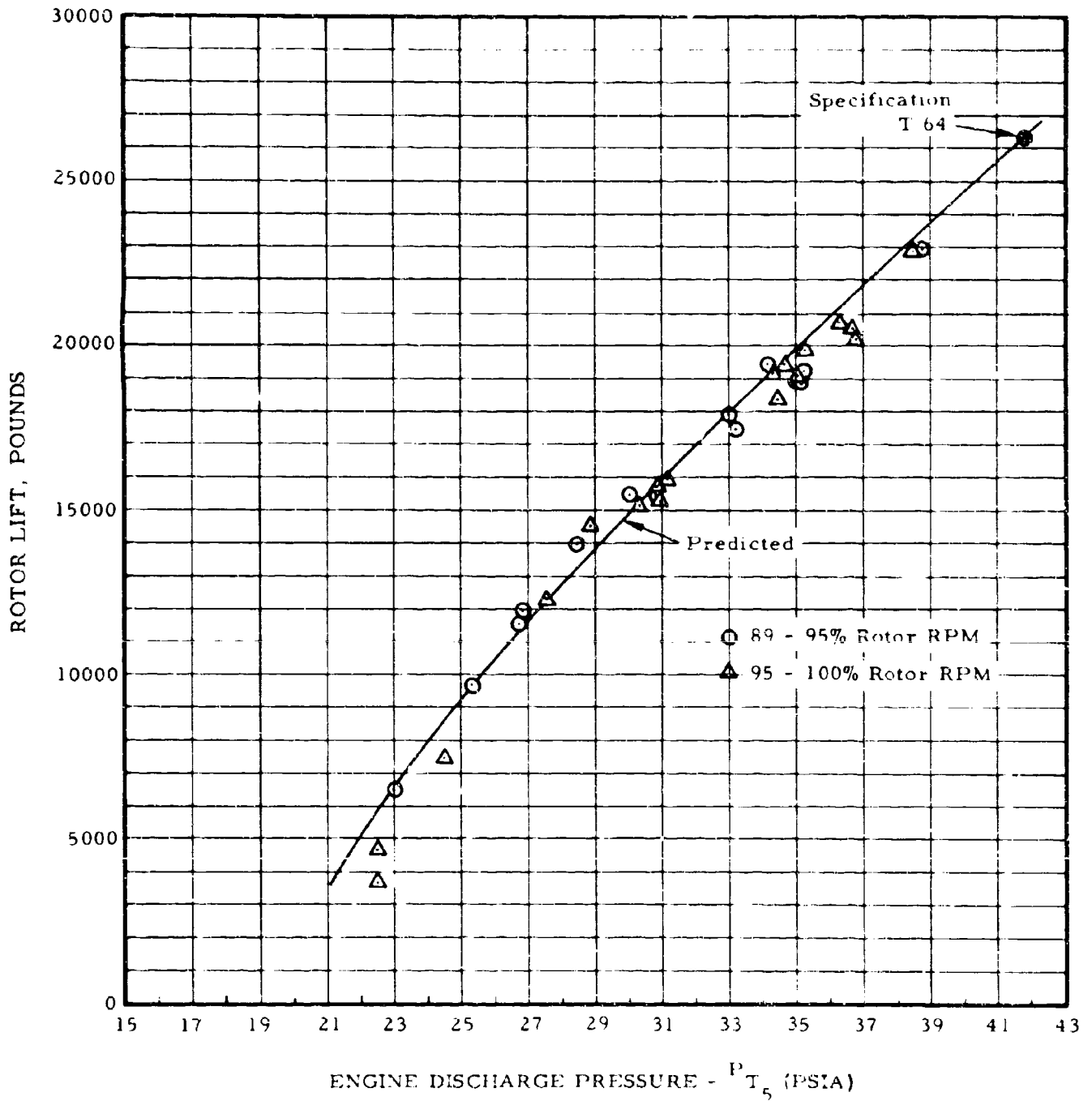


Figure 10. Rotor Lift vs. Engine Discharge Pressure

Evaluating the whirl test results shown in Figure 10, the following conclusions can be made:

1. The rotor lift shown as a function of the input pressure very closely follows previous predictions. The maximum value of measured lift is shown to be 23,000 pounds at a discharge pressure of 38.6 psia.
2. On the basis of test results, the present propulsion system when powered with specification T-64 engines and without introducing any improvements can lift 25,500 pounds out of ground effect at a discharge pressure of 41.8 psia. In this regard, performance of the rotor was considered as very satisfactory.
3. The results of the whirl test currently reported confirm the results from previous whirl testing reported in Reference 2. The improved instrumentation and better test methods are evidenced by the greatly reduced scatter of test points. Higher lift resulted from the higher pressure produced by the YT-64 gas generators when compared to the J-57 gas generator used in previous tests.

#### 5.1.2 Discussion

The performance tests of the hot cycle rotor system covered in this report were fulfilled in two different phases of the test program.

The power plant tests, twin-engine operation, mass flow calibration, and measurement of pressure loss in the stationary ducting were accomplished prior to installation of the rotor system. Results from the above tests are described later in this report.

The whirl test performance data of the complete hot cycle propulsion system are reported in this section. About one-third of the accumulated whirl test time was devoted to performance measurements. All measurements, with the exception of the last two test points, were made at power settings restricted by the temperature limitation of the ground test engine. Just before the completion of whirl testing, this limitation was lifted to allow a measurement of lift at a power level approximating that of the YT-64 flight engines.

Three basic groups of performance data were recorded as follows:

1. Power supplied to the rotor system was measured in terms of blade tip exhaust pressure ( $P_{T7}$ ), tip temperature ( $T_{T7}$ ), and mass flow ( $W_7$ ).
2. Rotor aerodynamic performance was determined by measurement of the rotor lift and a comparison with theory.
3. The measurement of engine discharge conditions ( $P_{T5}$ ,  $T_{T5}$ , and  $W_5$ ) and rotor tip pressure ( $P_{T7}$ ) produced data which were used in determination of subsystem and component performance.

The over-all system performance has been summarized in Figure 10, which shows rotor lift vs. engine discharge pressure. The maximum value of measured lift was seen to be 23,000 pounds at the discharge pressure of 38.6 psia.

#### 5.1.2.1 Power Supplied to the Rotor

In order to define the power supplied to the rotor, rotor tip instrumentation was installed, consisting of pressure and temperature probes which were located at the inlets to the blade-tip cascade nozzles. It is important to note that the tip pressure instrumentation operated at variable temperature levels and in a centrifugal field exceeding 500 g's. These conditions and lack of space restricted the number of pressure probes that could be installed at that station. The pressure test data recorded on the oscillograph were consequently subjected to various corrections. In addition, using the classical theory of flow in straight ducts, all tip pressure readings (taken near the duct centerlines) were adjusted to represent the average total pressure at the measuring station ( $P_{T7}$ ). The tip temperatures were recorded on a servo-balanced strip recorder and did not present any problem.

Values of power required by the rotor based on the rotor tip measurements vs. rotor lift are shown in Figure 11, which is discussed

in the next section. Values of engine discharge temperature and mass flow rate are shown as a function of engine discharge pressure in Figure 12. These values, plus Figure 10, completely define the quantity and quality of gas flow to the rotor as a function of rotor lift during tests on the whirl tower.

The equation used in calculating the power required by the rotor was the same as that described in Reference 2,

$$\text{RHP} = \frac{W_7}{g \times 550} (C_{V_e} V_{j_i} - V_T) V_T$$

In this equation,  $V_{j_i}$ , the ideal jet velocity, is obtained by classical methods, using  $P_{T_7}$  and  $T_{T_7}$ .  $V_T$  is blade tip speed. The determination of flow at station 7 ( $W_7$ ) was based on measurements at the engine station ( $W_5$ ) combined with measurements of the major source of leakage -- that through the diverter valves. The diverter-valve leakage was found to be 2.5 percent, as reported later in this report. Post-whirl test measurements of hub and blade leakage indicated a value of less than 0.2 percent.

The velocity coefficient  $C_{V_e}$  used in the above calculations was .955, which was presented in Reference 2.

In order to allow for the power required to pump spar cooling air, to drive accessories, and to overcome bearing friction, an arbitrary allowance of 100 horsepower was subtracted from the power calculated by using the above equations.

#### 5.1.2.2 Rotor Aerodynamic Performance

The computed hovering thrust of the rotor vs. power required (as influenced by ground effect on the whirl tower) is shown in Figure 11 for 100 percent and 90 percent rpm. The calculations of induced power, profile power, and ground effect are based on standard NACA methods presented in Reference 3. The profile power coefficient used in the present calculations was increased 17 percent to allow for the 18 percent thickness in the hot cycle blades compared to the blades of 12 percent thickness upon which the profile power coefficient given in Reference 3 was based. The calculations include correction for the design blade twist of -8 degrees as given on page 85 of Reference 3.

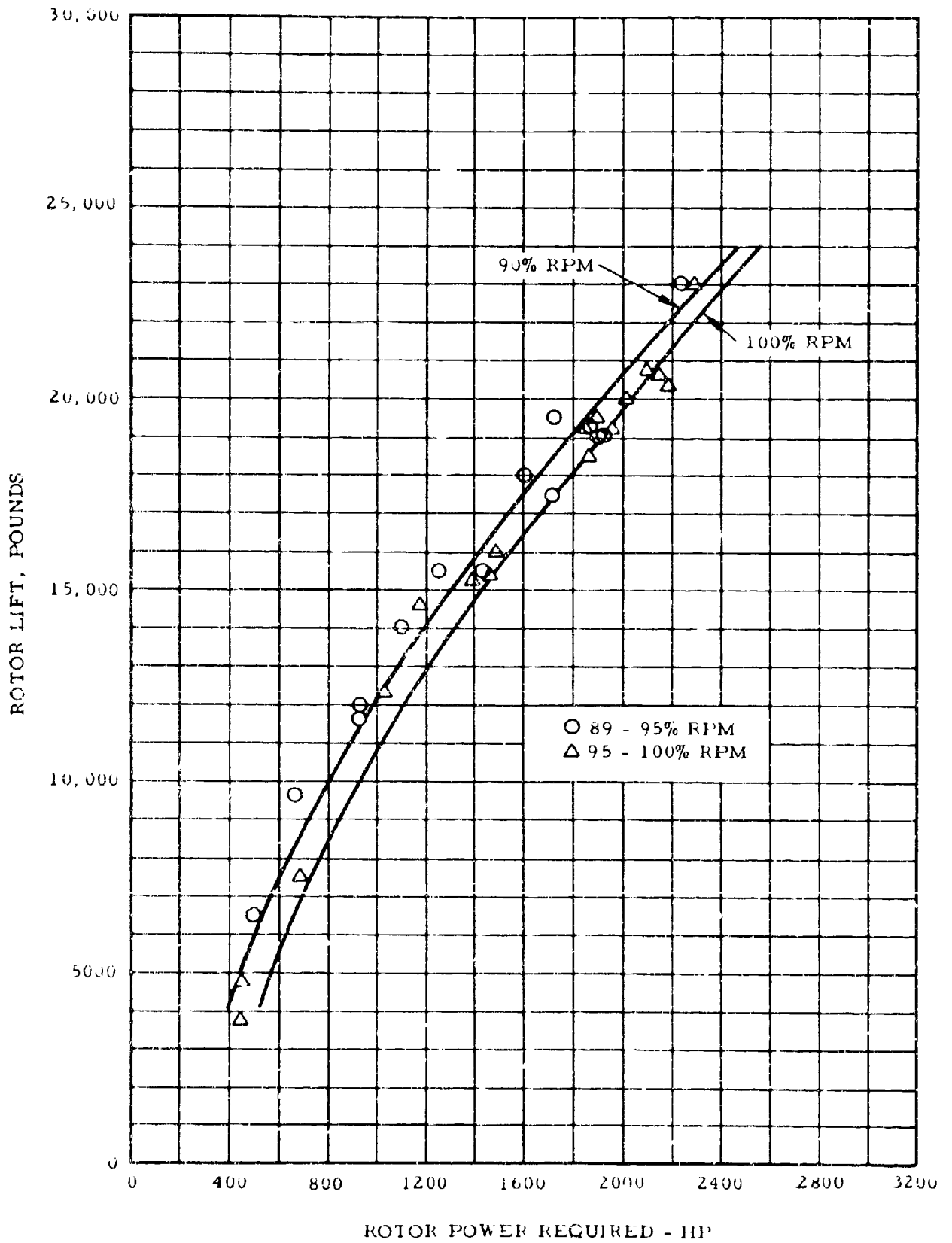
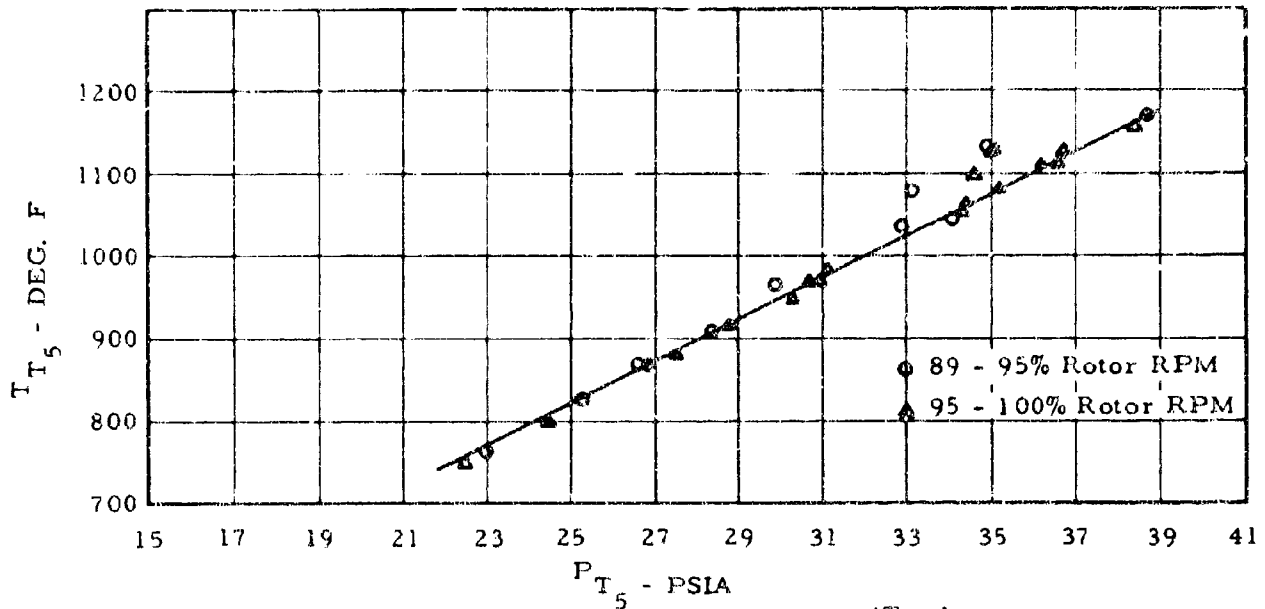
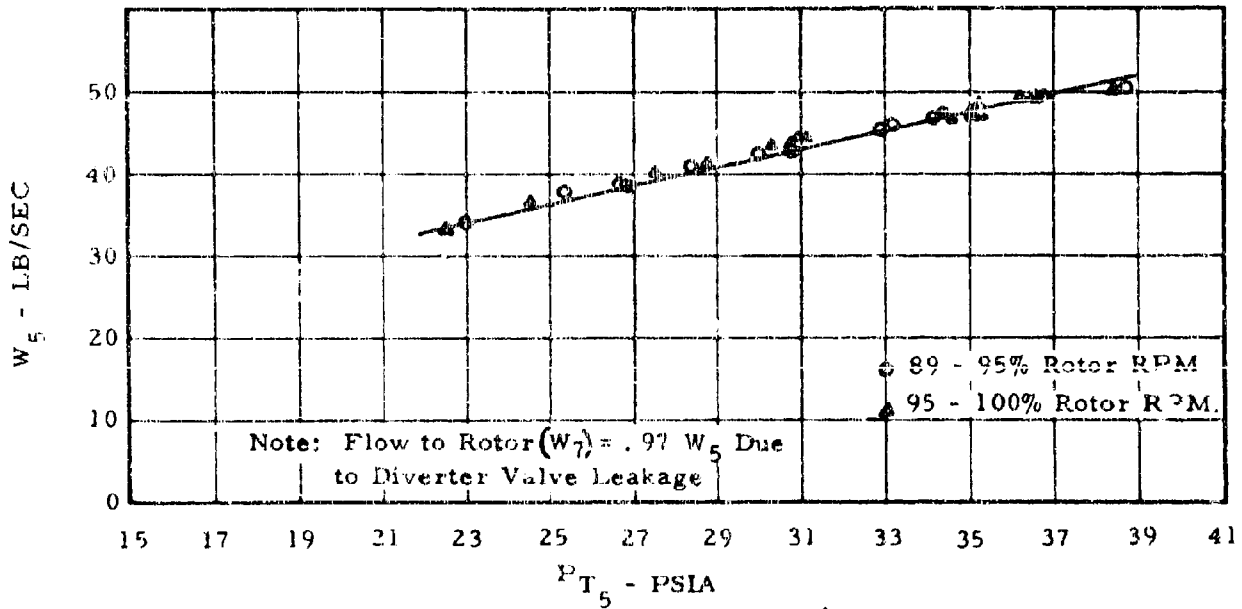


Figure 11. Rotor Lift vs. Rotor Power Required



a) Engine Discharge Temperature ( $T_{T_5}$ ) vs.  
Engine Discharge Pressure ( $P_{T_5}$ )



b) Engine Discharge Flow Rate ( $W_5$ ) vs.  
Engine Discharge Pressure ( $P_{T_5}$ )

Figure 12. Engine Discharge Conditions During Rotor Operation

Applying the above factors, the equation for power coefficient vs. thrust coefficient becomes (using procedures from pages 85 and 112 of Reference 3 and symbols as defined in that reference):

$$C_p = C_i \left[ \frac{C_T^{3/2}}{\sqrt{2} B} \left( \frac{T_\infty}{T} \right)^{3/2} + 1.17 \frac{\sigma \delta_o}{8} + \frac{2}{3} \frac{\delta_1}{a} \frac{C_T}{B^2} + \frac{4 \delta_2}{\sigma a^2} \left( \frac{C_T}{B^2} \right)^2 \right]$$

Inspection of Figure 11 indicates that the calculated aerodynamic performance agrees quite well with the measured performance.

#### 5.1.2.3 Over-all System Performance

The measured values of tip pressure, temperature, and mass flow previously discussed were used to reduce component system performance (friction coefficient, flow coefficient, etc.), and a calculation of rotor power available versus engine pressure ratio was made. Using the curve of rotor thrust versus power required (Figure 11, discussed above), a calculated curve of rotor lift versus engine discharge pressure was obtained and was plotted in Figure 10. This curve is essentially the same as Figure 5.1.1 of Reference 2, when a 4 percent allowance is made for extra pressure drop between the rotor hub station (used in Reference 2) and engine discharge (used here).

The specification T-64 engines have a discharge pressure of approximately 41.8 psia at maximum power. Referring to Figure 10, a calculated rotor thrust of 26,400 pounds inside ground effect is predicted, consistent with the height of the whirl tower, which introduces about a 4 percent thrust increase with constant power available. On this basis, the XV-9A helicopter, powered with specification T-64 engines, should lift 25,500 pounds outside ground effect.

It should be noted that the lift performance shown in Figure 10 is obtained in the presence of 2.5-percent diverter-valve leakage. It is anticipated that this leakage can be reduced in future work, with consequent increase in system performance.

#### 5. 1. 2. 4 Effect of Wind on Power Required

Due to the tight schedule of the whirl test program, a number of tests were unavoidably conducted under wind conditions which developed after the test was in progress. Since the Figure 11 curve of thrust vs. power required was prepared for a zero-wind condition, it was necessary to examine the possible effect of wind on Figure 11. As discussed below, it was concluded that, for the range of rotor parameters tested, and for the highest wind velocities encountered (20 mph), the wind does not change the power-required curve for a rotor in ground effect, which is the case for the whirl tower.

An explanation of this result, which apparently contradicts the conventional reduction of power required (out of ground effect) vs. forward speed, is given in Reference 4. That report points out that, for a lifting rotor in ground effect (i. e., for rotor height/rotor radius value of the whirl tower), power required is essentially constant from hovering out to the speeds measured during the whirl test.

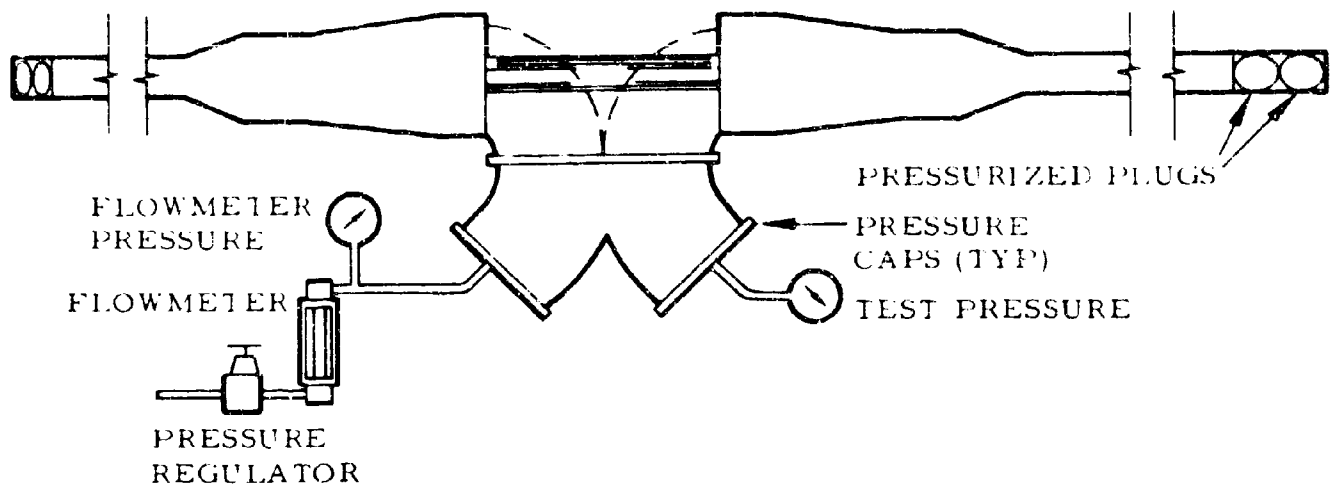
#### 5. 2 ROTOR SYSTEM LEAKAGE

The component and system leakage was determined in a series of leakage checks conducted before and after the whirl test program. The results from these tests are presented in Table 3. It is shown that leakage in the rotor ducts and seals amount to less than 0.2 percent of the total flow. This quantity is negligible and the rotor, after passing through two whirl tests, may be considered as practically leakproof. A rate of less than 1/2 percent leakage was measured during the laboratory tests of the engine-diverter valve seals. This test is described in Reference 6. The highest leakage was observed in the diverter valves through the valve door when seated in the "rotor" position. The resulting "overboard" flow was measured at the tail-pipe during rotor operation. The portion of gas flow escaping through both diverter valves amounted to about 2-1/2 percent of the total flow.

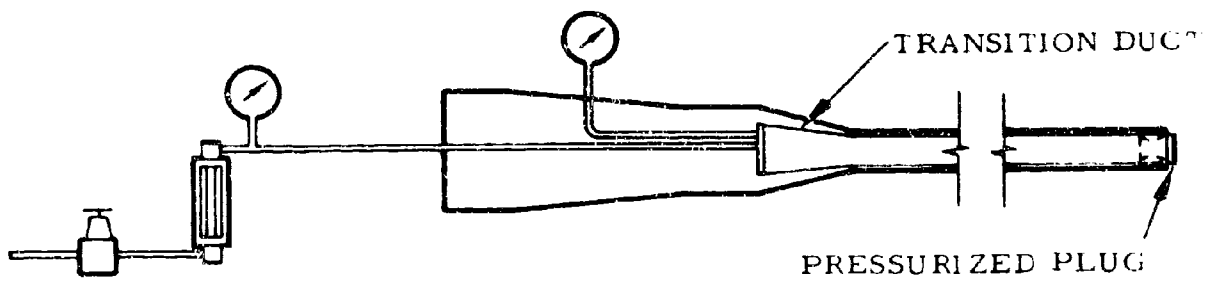
With the exception of diverter valves, all other components and assemblies of the duct system were tested with air at ambient temperature. The typical test arrangements are shown in Figure 13. The shop air supply was used with pressure regulated at 27.5 psig to represent the typical operating pressure. A rotameter in conjunction with two pressure gages was used to measure air flow caused by the leakage. Pressure was measured at the exit end of the rotameter and

TABLE 3  
LEAKAGE IN THE ROTOR SYSTEM AND  
ROTOR COMPONENTS

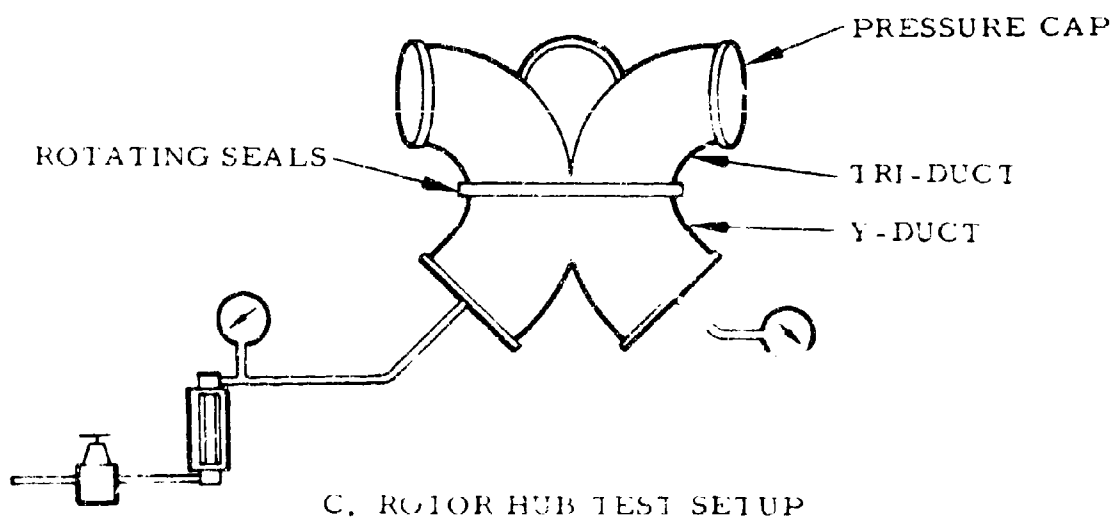
% of Total Flow			
Component:	After 1961/62 Whirl Test	Before 1964 Whirl Test	After 1964 Whirl Test
Blue Blade	0.052	0	0
Red Blade	0.103	0.006	0.03
Yellow Blade	0.085	0.0015	0.032
Rotor Hub	<u>0.114</u>	<u>0</u>	<u>0</u>
Total Rotor System	0.168	0.125	0.183
Inboard Articulated Duct Seals (total in 3 blades)	-	-	-
Outboard Articulated Duct Seals (total in 3 blades)	-	-	0.075



A. ROTOR SYSTEM TEST SETUP



B. ROTOR BLADE TEST SETUP



C. ROTOR HUB TEST SETUP

Figure 13. Leakage Measurement - Rotor System

in the component undergoing the test. The recorded readings from the rotameter were subsequently converted to standard cubic feet per minute. Leakage area is referred to the total exit area of the blade-tip cascade nozzles. This definition of leakage makes the results from the cold tests directly applicable to any operating conditions.

Leakage through the diverter valves was measured during operation of the rotor system. The test arrangement is shown in Figure 14. A cone-type orifice was designed to reduce the tailpipe exit area and to raise back pressure enough for the application of standard flow measuring techniques. A calibration curve was prepared relating leakage (pound/second) with the differential head across the orifice (inches  $H_2O$ ). Using this method, leakage through both diverter valves was found to be about 2-1/2 percent of the total gas flow.

### 5.3 STRUCTURAL TEMPERATURES, BLADE AND HUB

A continuous record of temperature distribution in the rotor and power plant system was kept throughout the test program. The temperatures of typical components measured during the hottest run of the whirl test program are shown in Table 4. The corresponding predicted temperatures and the measurements taken during the 1961/62 whirl test are included in the same table for comparison. It is shown that the hot-gas ducts and flexures operated at predicted or slightly lower temperatures. The spar and the outer blade skin were consistently cooler than predicted (Reference 5). No component temperatures over design limits were encountered during the conduct of the test program. Figure 15 shows the location of all thermocouples, which are marked with maximum temperatures recorded during the same test run.

The pattern of temperature distribution in the rotor system is similar to one discussed in more detail in Reference 2. The highest temperature recorded in steel parts close to the engine (not shown on the Figure) did not exceed 300 degrees F. The temperature of aluminum parts was below 250 degrees F.

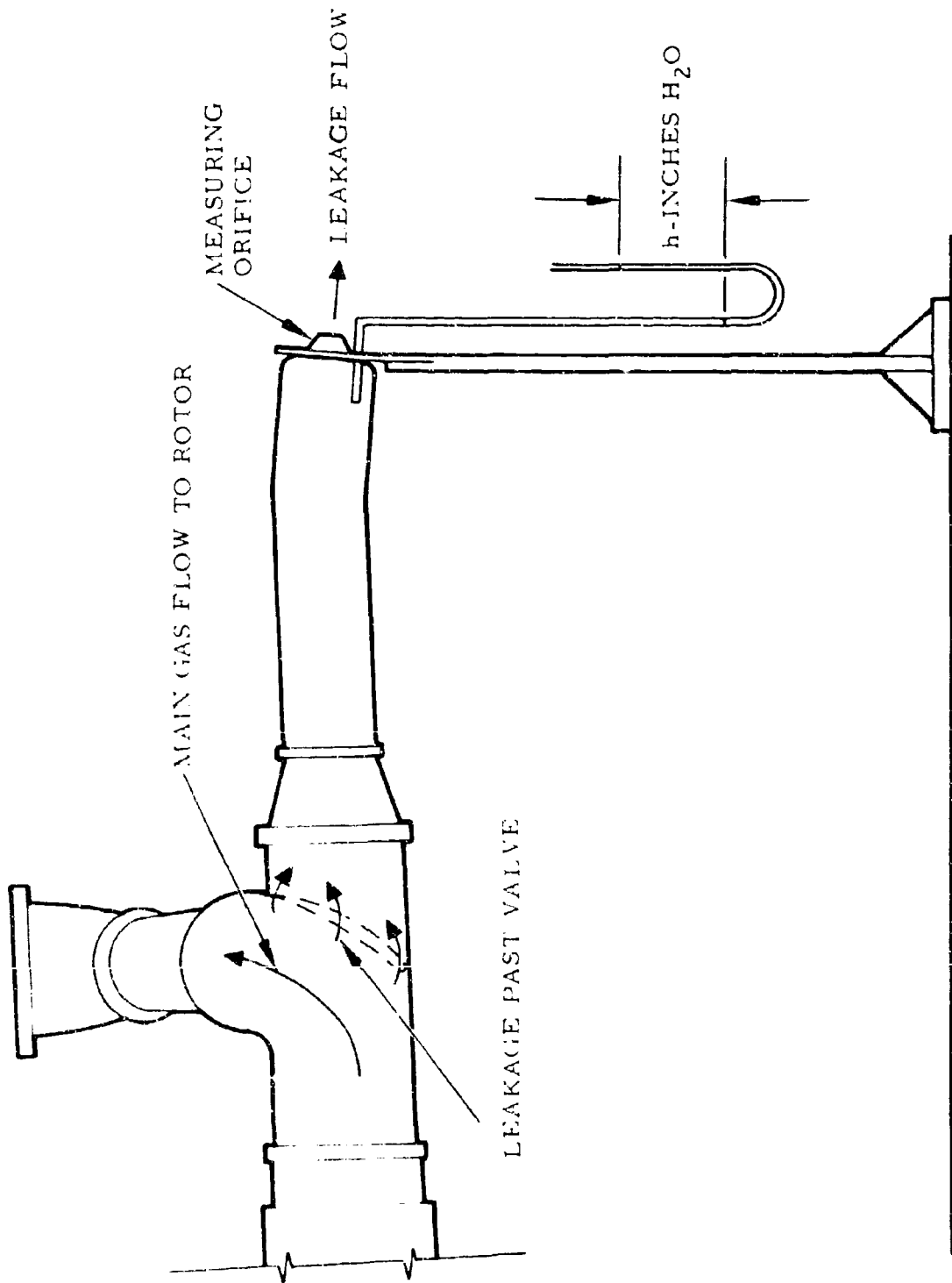


Figure 14. Measurement of Diverter Valve Leakage

TABLE 4  
COMPONENT TEMPERATURES

Component	Measured During 1961/62 Whirl Test @ Gas Temp. 1176°F °F	Measured During 1964 Whirl Test (Run 31) @ Gas Temp. 1151°F °F	Predicted At Gas Temp. 1151°F °F	Component Temp (1964) With Refer- ence to Prediction
Duct Wall 3/8" from Chord Line Station BS-1	1105	1102	1120	27° (2.4%) Cooler
Duct Wall-Top Station BS-18	1070	1060	1060	As Predicted
Outer Skin on the Rib Station BS-18	272	251	449	198° (40.1%) Cooler
Rear Spar Segment 11 and 18	240	218	415	107° (47.5%) Cooler
Flexure Average Temperature At Station BC <sub>2</sub>	640	547	621	74° (12%) Cooler

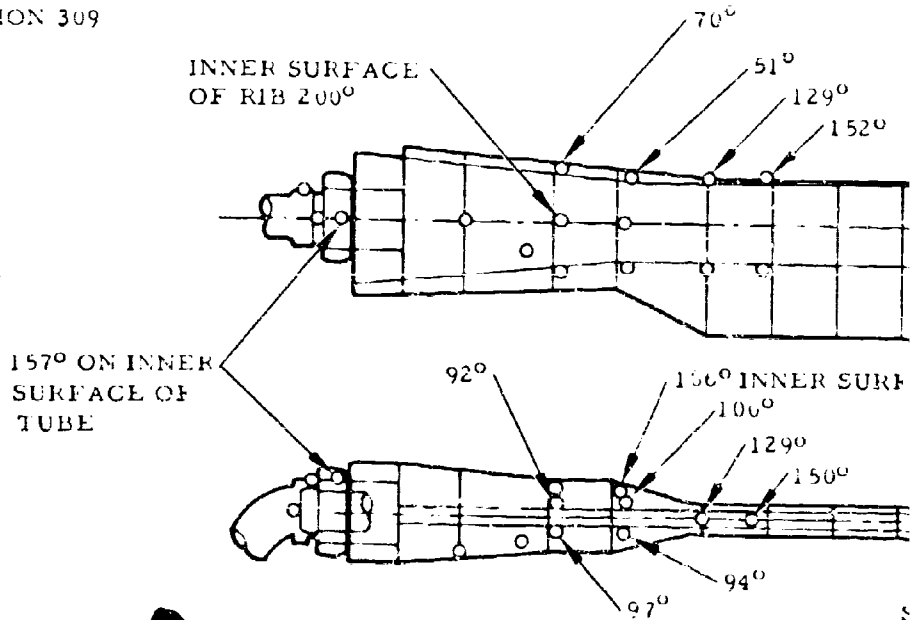
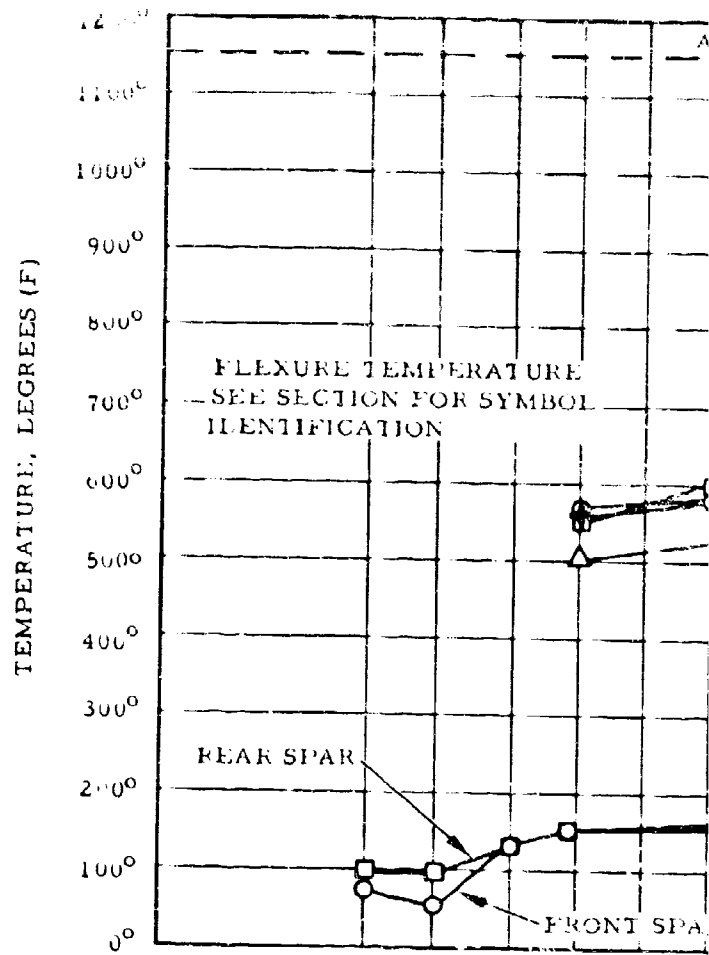
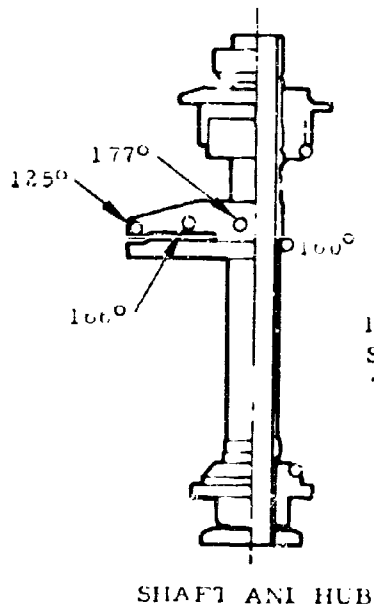
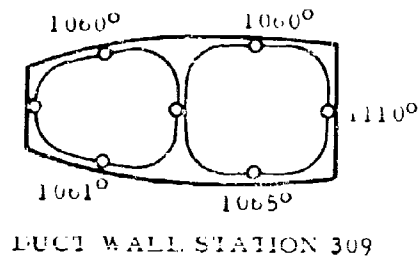
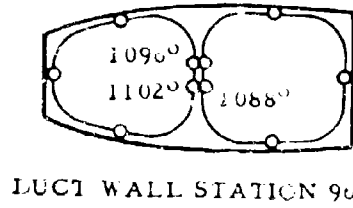
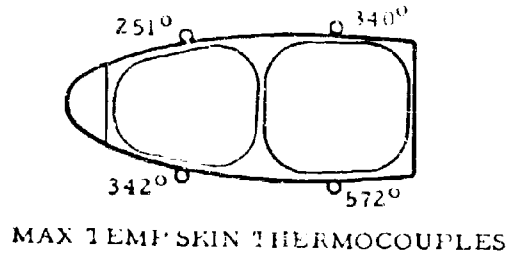
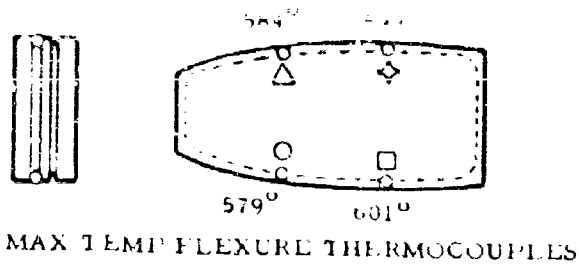
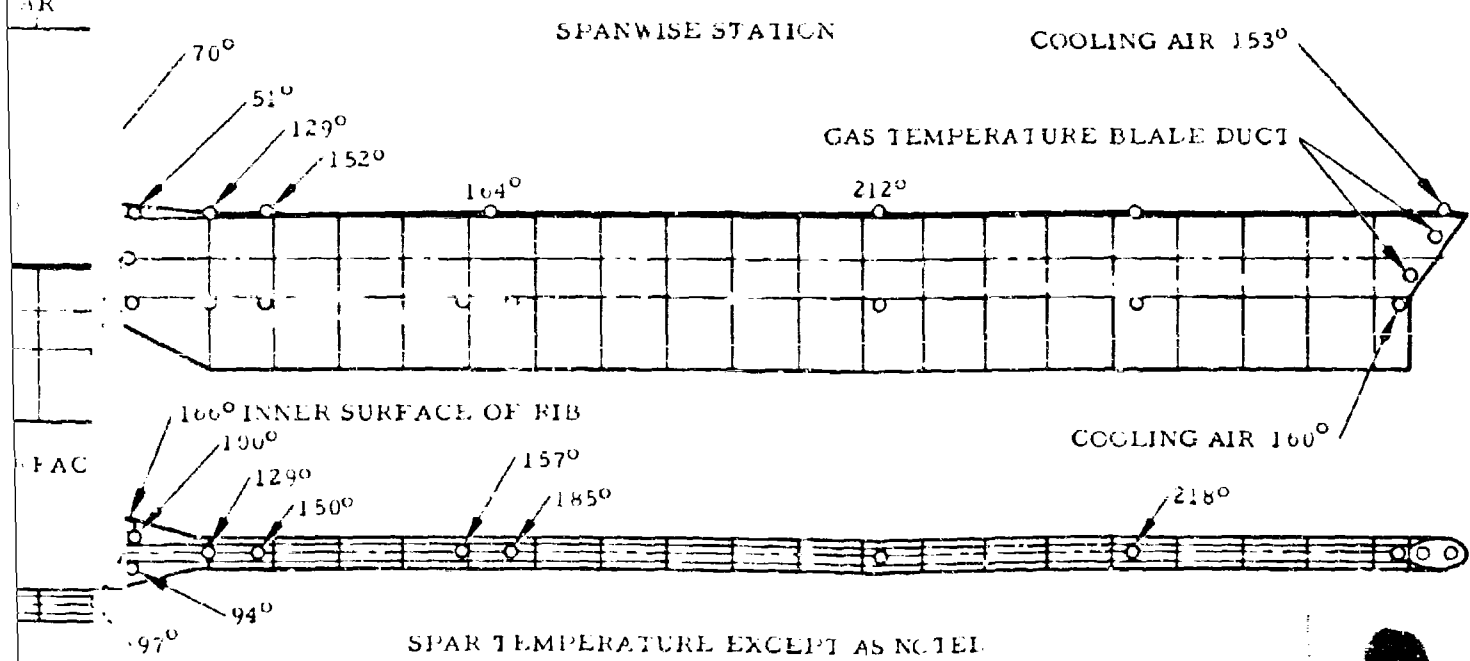
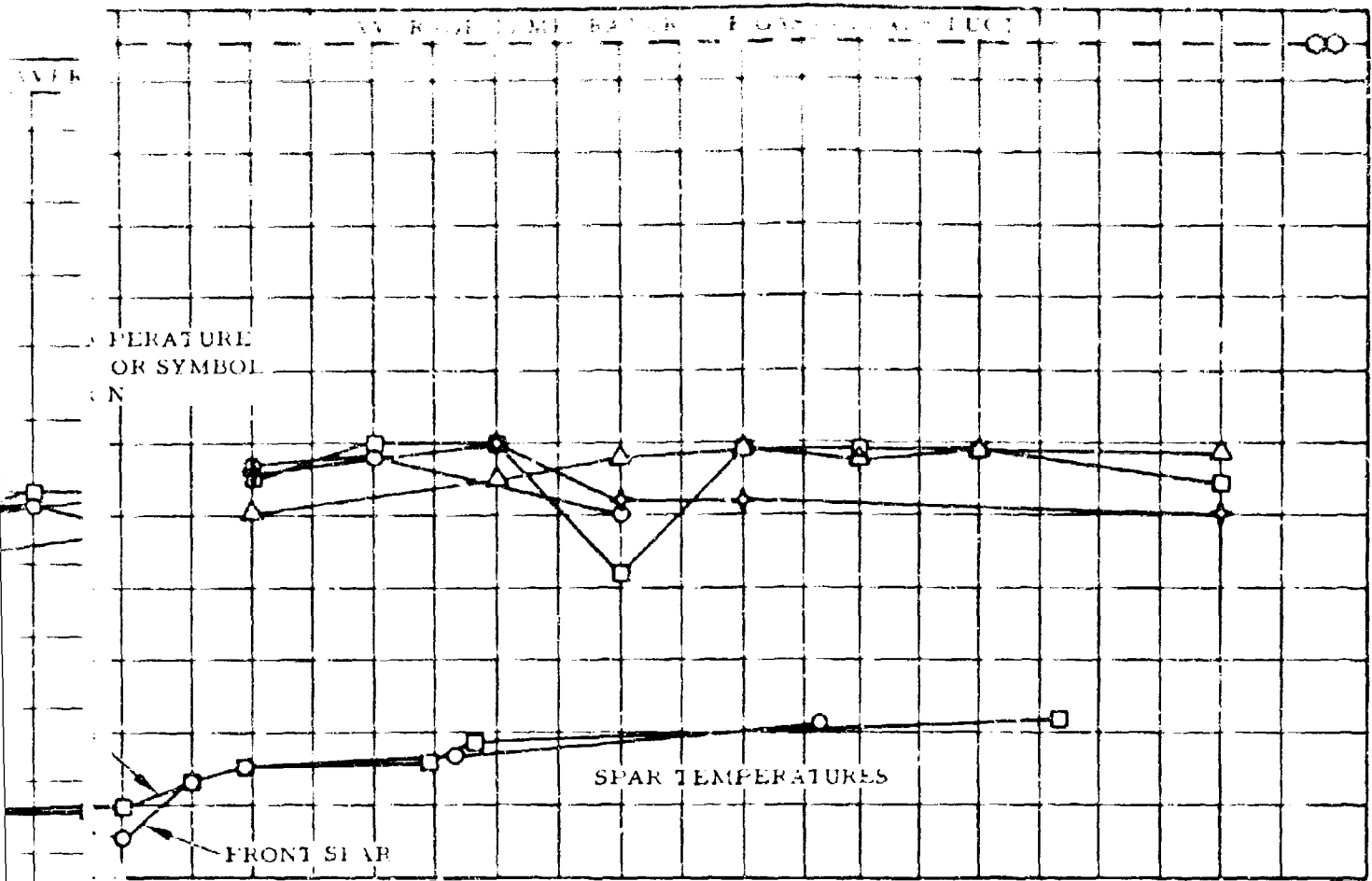


Figure 15. Temperature S



5. Temperature Survey - Whirl Test



Load measurements were taken during the whirl test program and were scrutinized for critical loading of the various components. With the exception of blade chordwise moments, all cyclic structural loads were of moderate magnitude and below their endurance limits (see Reference 7). High 1/rev and 2/rev chordwise bending moments, some of which slightly exceeded endurance limits, occurred during operation at high thrust in high winds (15 - 20 mph). As shown in the section on rotor dynamics, the 2/rev chordwise moments were a characteristic of the rotor mounted on the whirl tower due to the coupling between blade chordwise bending and whirl tower pylon bending.

All structural loads measured during normal start-ups and shut-downs were at acceptable levels. Loads during an emergency shut-down were also at acceptable levels. Fairly high flapwise bending loads are generated when collective pitch is used to slow the rotor during shut-down; therefore, collective pitch should not be used for this purpose. Figure 16 is a plot of rotor rpm vs. time during a normal start-up

Included as Figures 17 through 45 are plots of significant structural loads vs. rpm (as well as blade flapping and feathering angles vs. rpm). The limiting endurance stress or load shown is the value selected for use in the design of the component for cyclic loading. The limiting mean stress or load shown is the permissible value of steady load corresponding to the limiting endurance value. Strain gages utilized for measuring blade flapwise bending at Station 75.4 front spar, Station 140 front spar and Station 220 front spar and for vertical shear at Station 23 were inoperative during this testing. These figures give the following mean and cyclic measurements:

<u>Figure Number</u>	<u>Item</u>
17.	Front spar axial load (chordwise moment) at Sta. 90.75
18.	Rear spar axial load (chordwise moment) at Sta. 90.75
19.	Front spar axial load (chordwise moment) at Sta. 149
20.	Rear spar axial load (chordwise moment) at Sta. 149

Figure  
Number

Item

21. Hub plate stress-aft
22. Hub plate stress-forward
23. Blade flapwise bending at Sta. 63 front spar
24. Blade flapwise bending at Sta. 63 rear spar
25. Blade flapwise bending at Sta. 75.4 rear spar
26. Blade flapwise bending at Sta. 100 front spar
27. Blade flapwise bending at Sta. 100 rear spar
28. Blade flapwise bending at Sta. 140 rear spar
29. Blade flapwise bending at Sta. 220 rear spar
30. Blade flapwise bending at Sta. 270 front spar
31. Blade flapwise bending at Sta. 270 rear spar
32. Blade skin torsion at Sta. 38
33. Blade skin torsion at Sta. 83
34. Main rotor shaft bending  $90^{\circ}$  to blue blade
35. Pitch link load, blue blade
36. Pitch link load, yellow blade
37. Pitch link load, red blade
38. Control actuator force, starboard
39. Control actuator force, port
40. Control actuator force, longitudinal

<u>Figure Number</u>	<u>Item</u>
41.	Swashplate drag link
42.	Blue blade feathering angle
43.	Blue blade flapping angle
44.	Gimbal lug bending strain
45.	Chordwise shear at Sta. 23.0

#### 5. 4. 1 Chordwise Blade Loading

A correlation was found to exist between 1/rev chordwise moment and 1/rev shaft moment, as shown in Figure 46. During trimmed flight, shaft 1/rev moment is a function of thrust vector tilt with respect to the shaft. Thrust vector tilt is a function of aircraft weight and C. G. position, fuselage drag, and fuselage moment from the down load on the tail surfaces. The bending moments shown in Figure 46 are associated with the rotor mounted on a whirl stand, where untrimmed forces can exist. During hover when all forces on the helicopter are in trim, the only moments that are imposed on the rotor shaft are those due to C. G. offset, and a shaft 1/rev moment of 28,200 inch-pounds will be developed at maximum C. G. offset and design gross weight. From Figure 46 it is seen that this will result in an axial 1/rev load of 4100 pounds, which is only about 75 percent of the chordwise design endurance limit. Calculations at high-speed trimmed flight (125 knots) with the C. G. near the rotor shaft indicate that a shaft 1/rev moment of the same order of magnitude as the 1/rev shaft moment during hover with full C. G. offset will be applied. As a result, this high-speed forward flight condition will have no higher chordwise moments than the maximum value while hovering with full forward C. G. when, as pointed out above, stresses are below the endurance limit. It should be noted that these moments anticipated in forward flight could be reduced by locating the C. G. more forward. Therefore, it appears that chordwise 1/rev moments can be optimized during the flight program by control of aircraft C. G. position and that the high chordwise loads experienced during whirl test (Figures 17 and 18) will not occur during flight test.

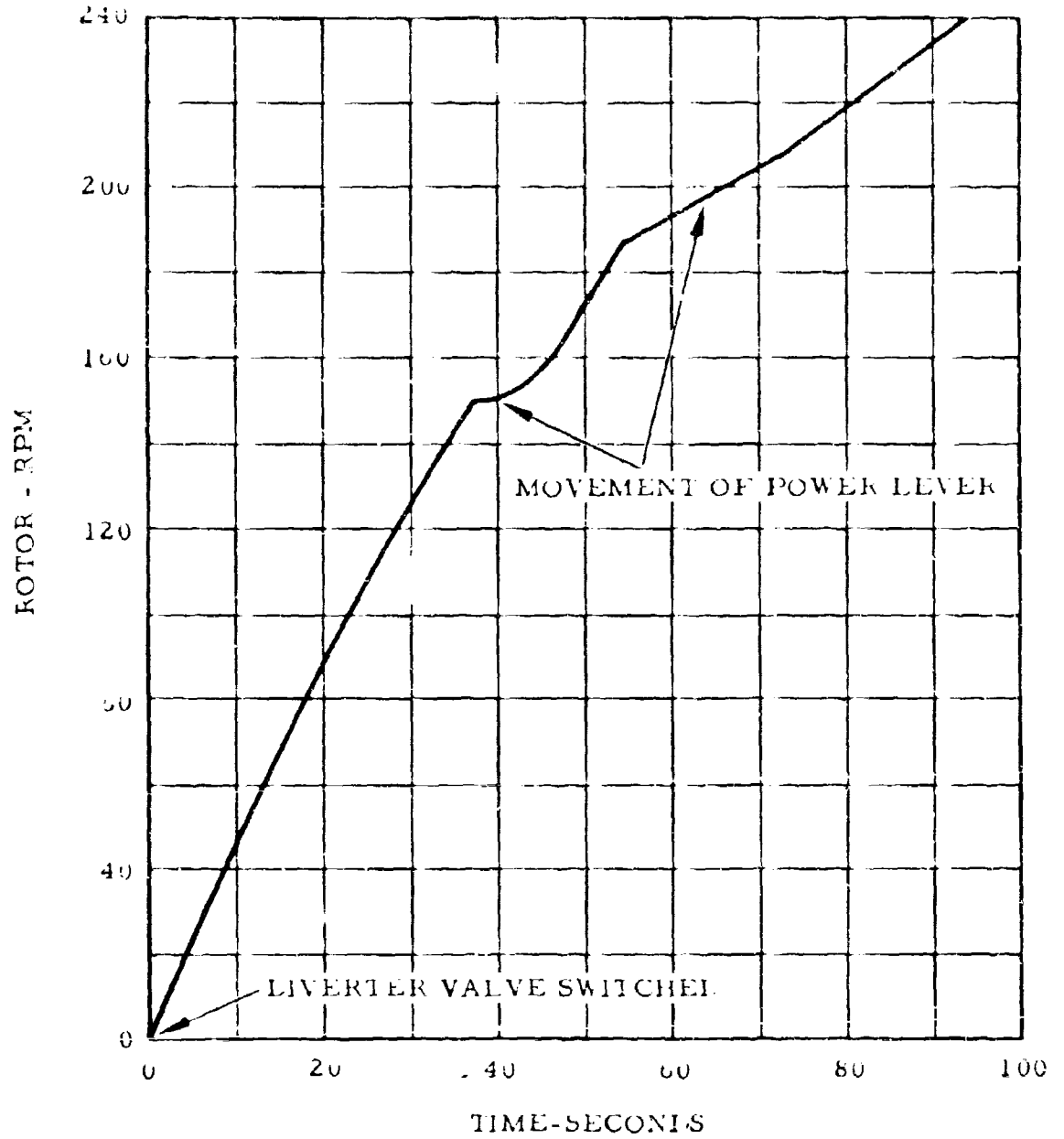


Figure 16. Typical Rotor Start-Up, RPM vs. Time

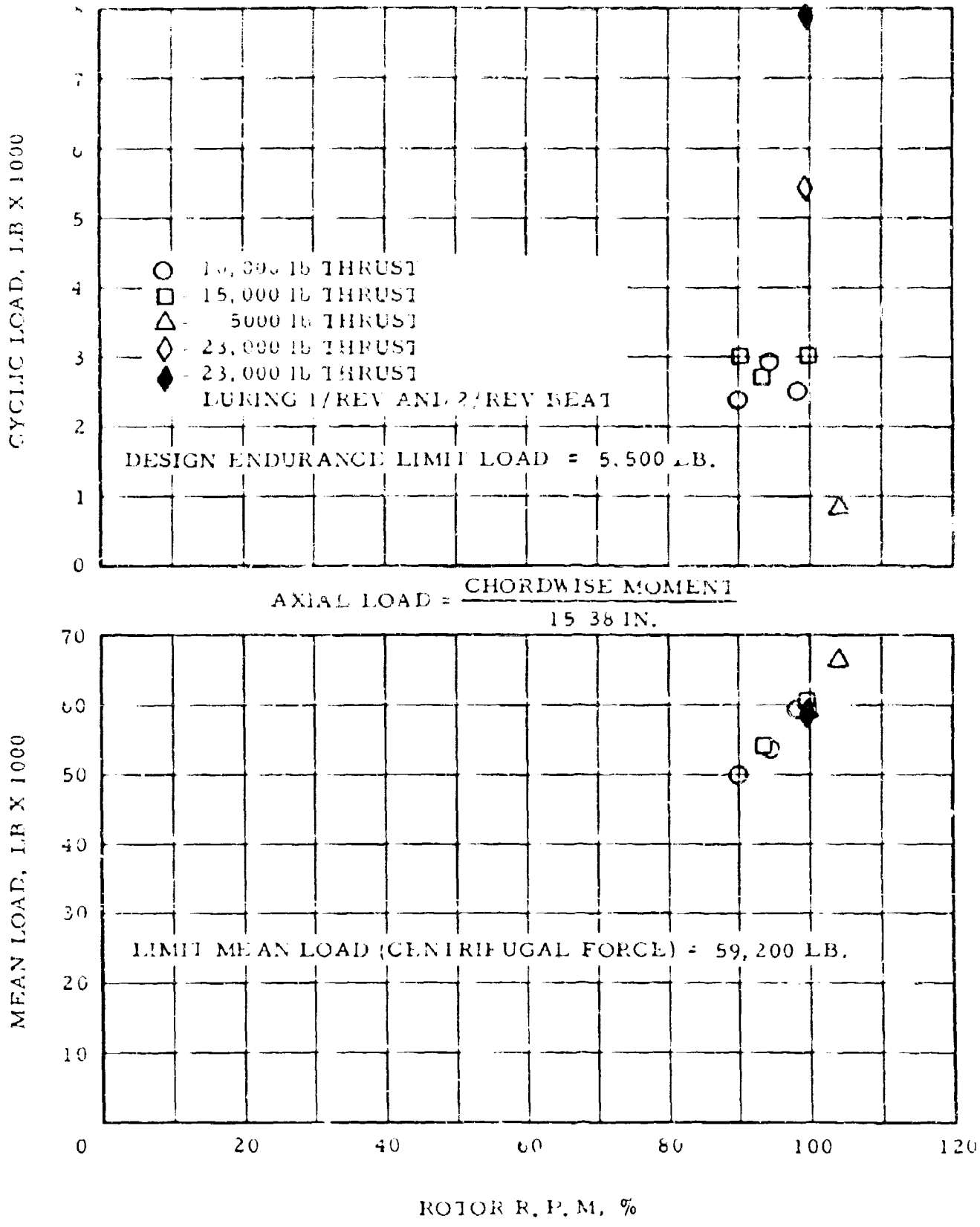


Figure 17. Front Spar Axial Load (Chordwise Moment) at Station 90.75

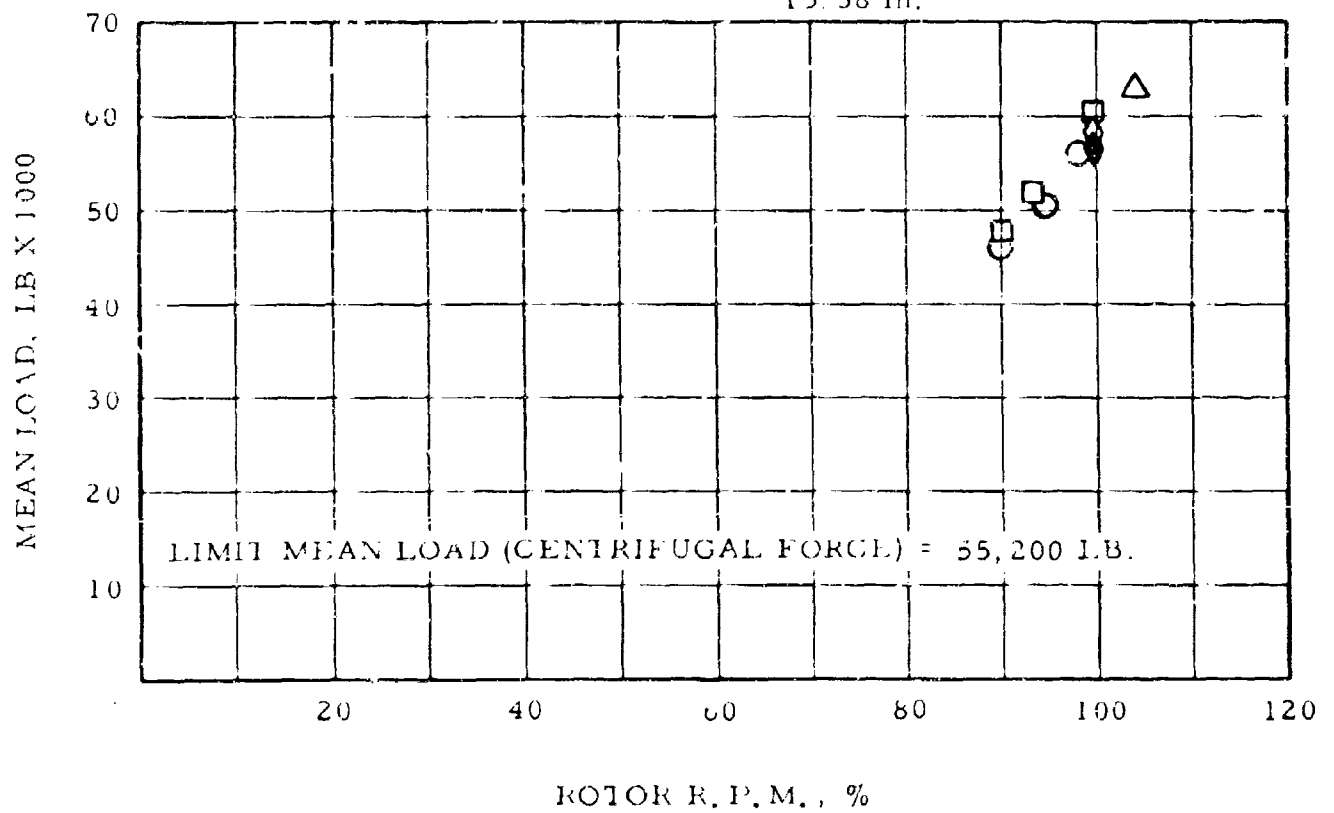
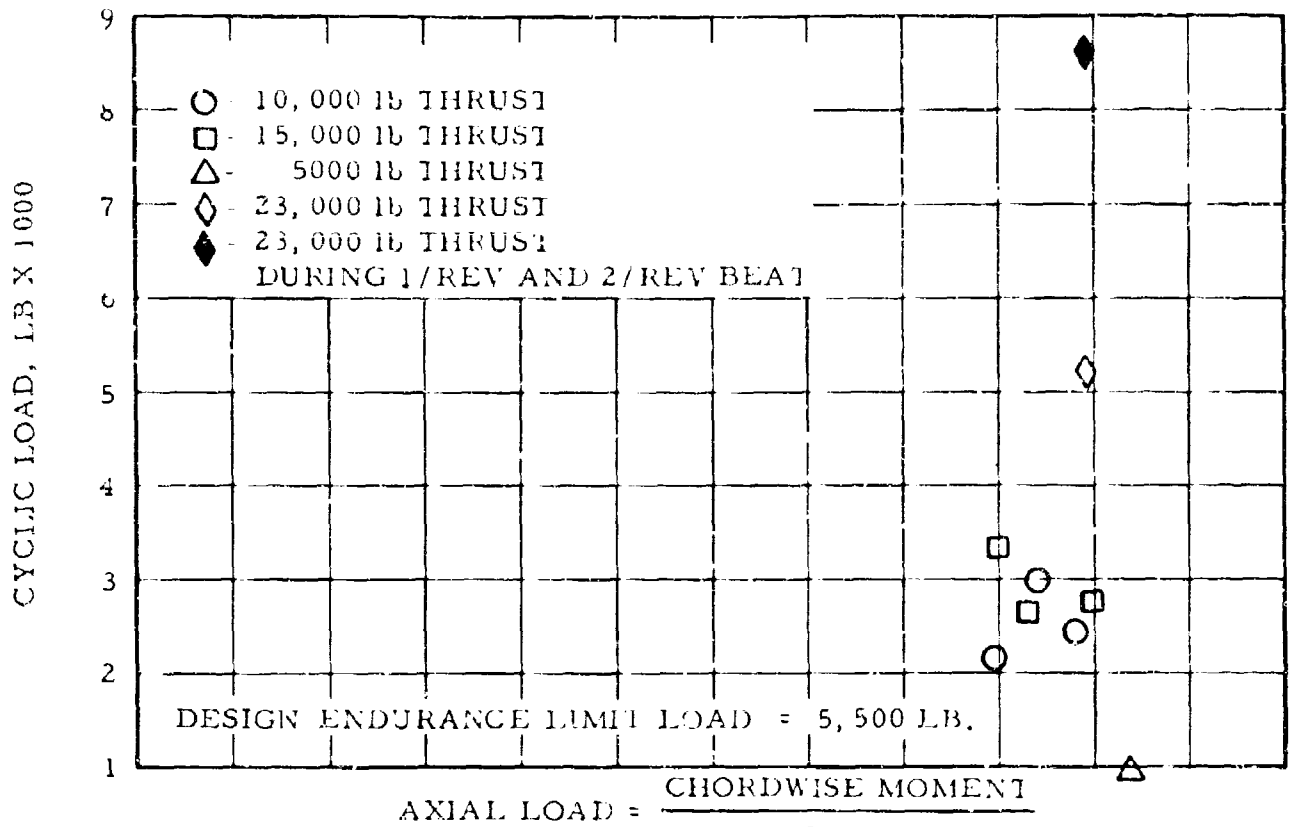
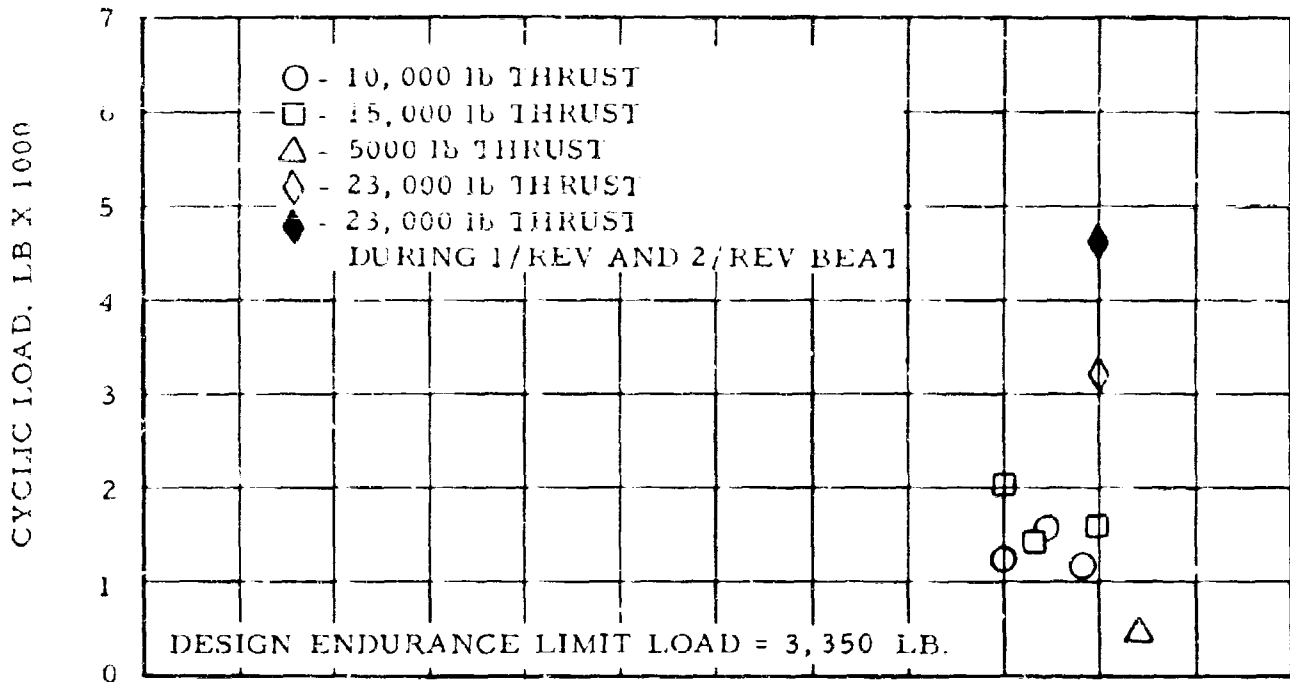


Figure 18. Rear Spar Axial Load (Chordwise Moment) at Station 90.75"



AXIAL LOAD = CHORDWISE MOMENT / 15.38 in.

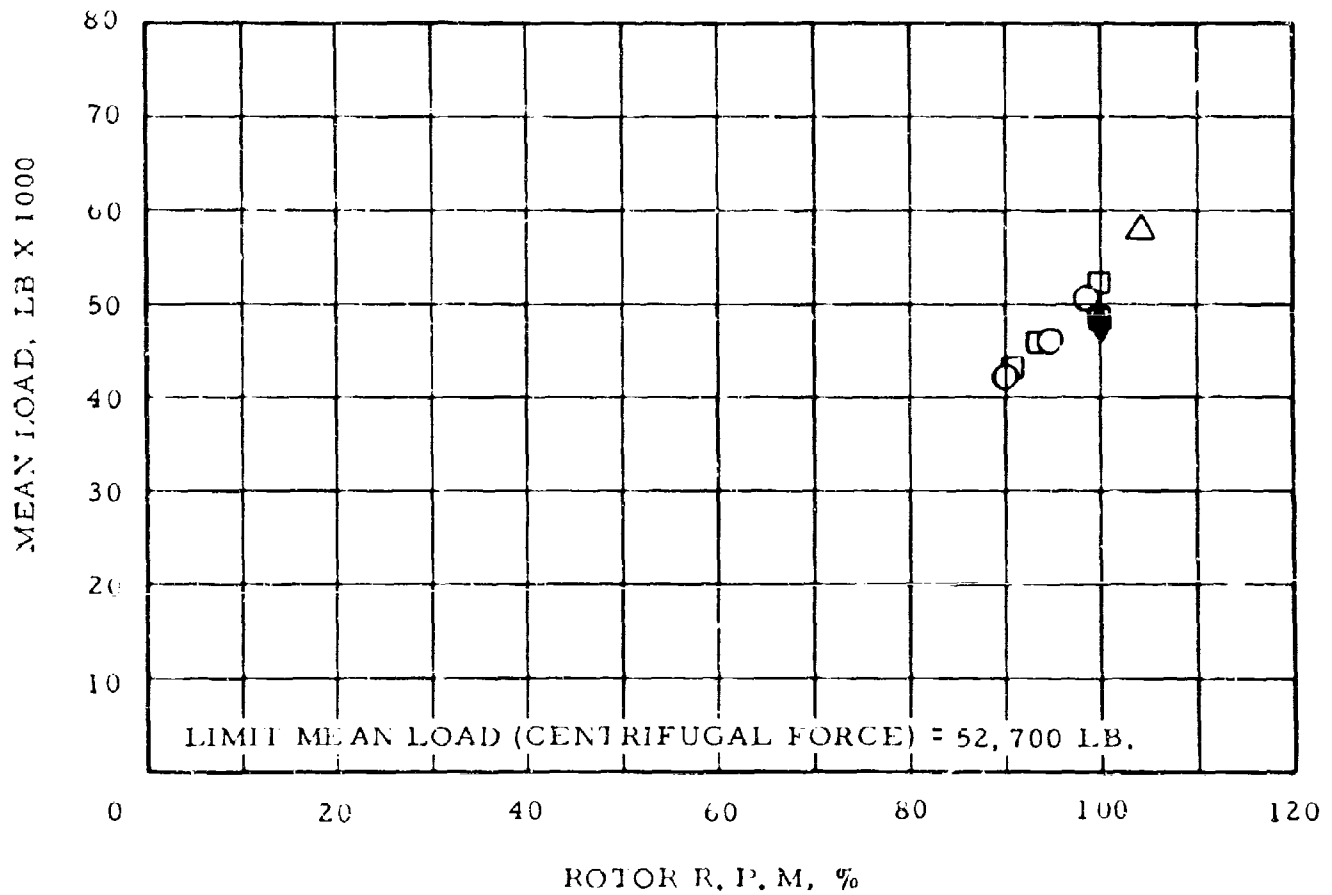


Figure 19. Front Spar Axial Load (Chordwise Moment) at Station 149"

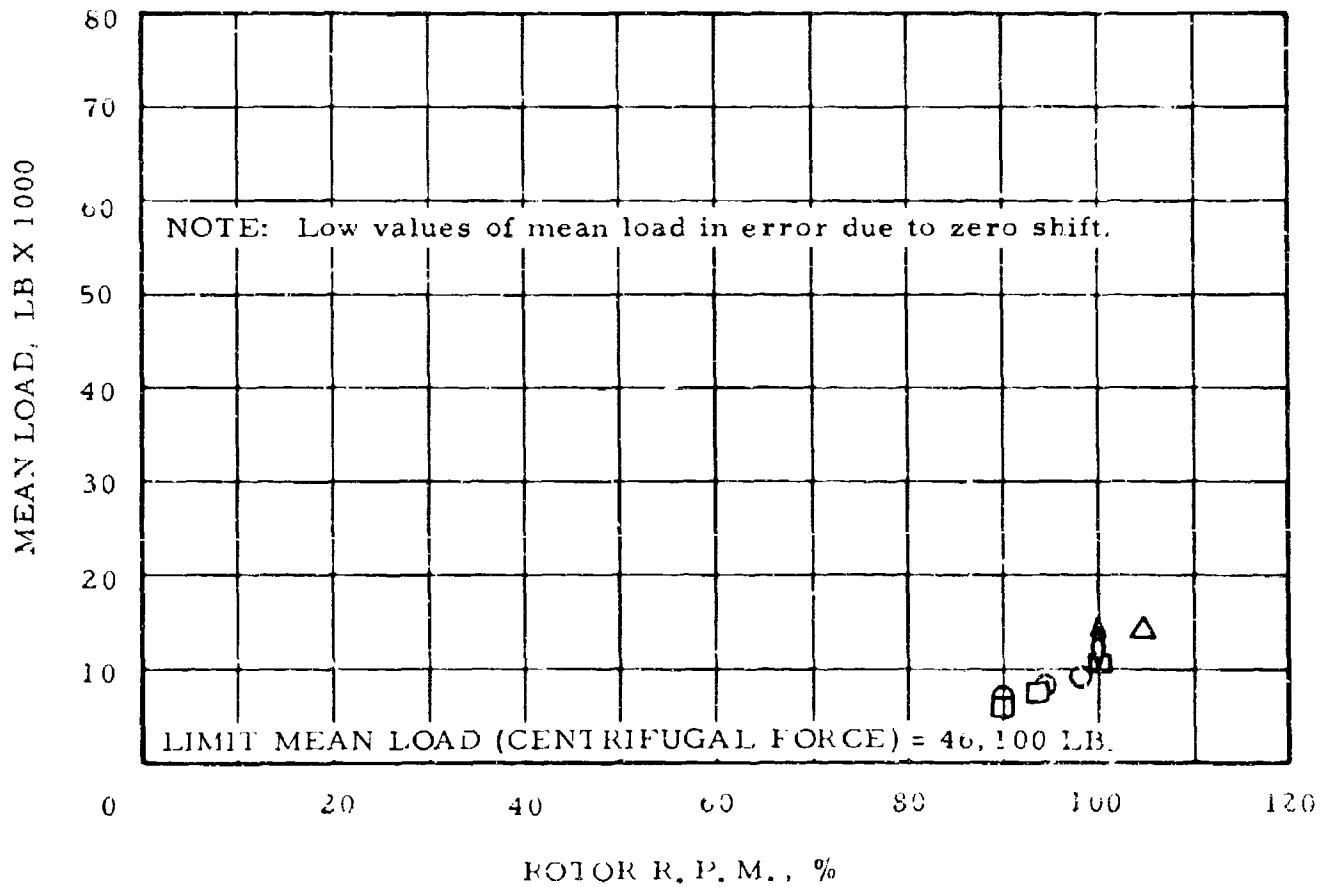
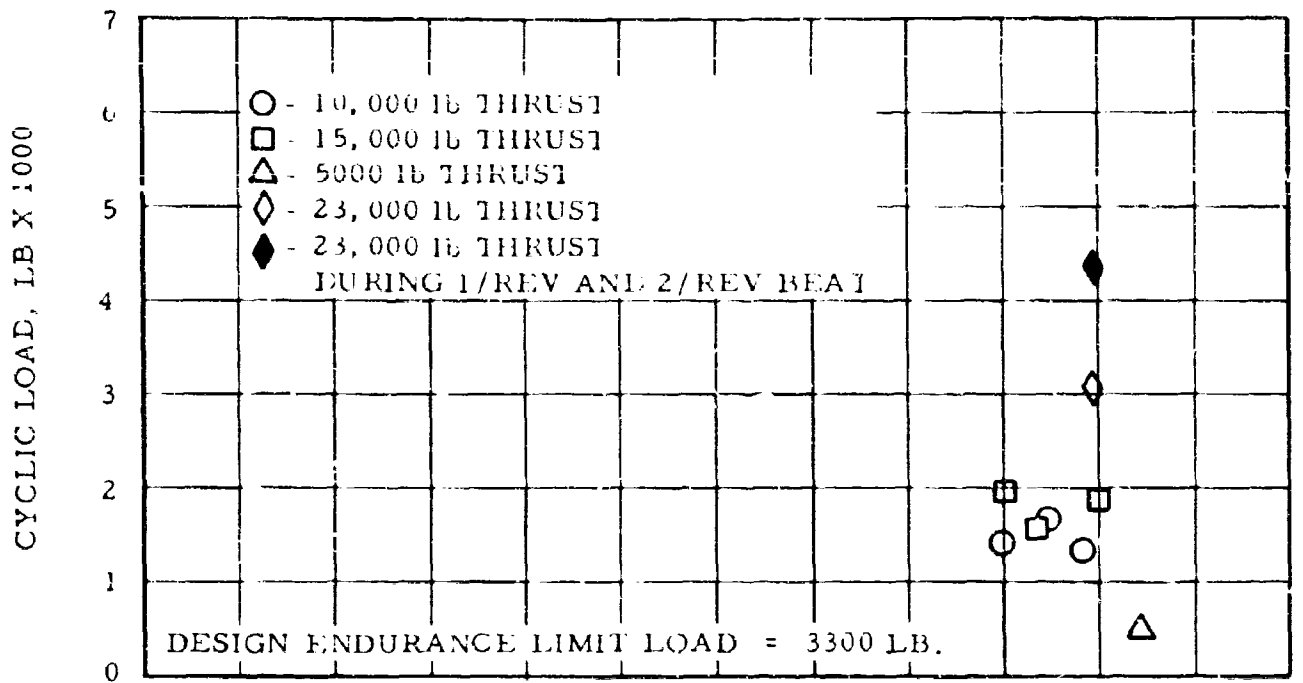
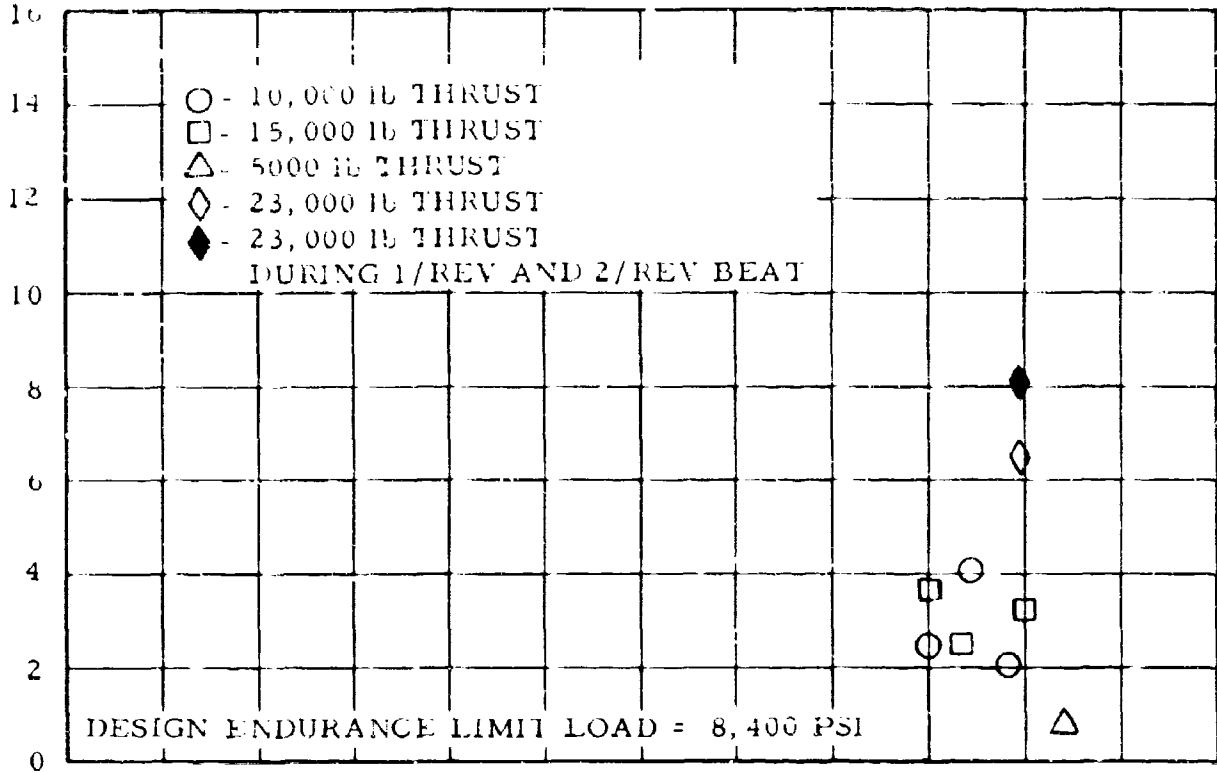


Figure 20. Rear Spar Axial Load (Chordwise Moment) at Station 149"

CYCLIC LOAD, P.S.I. X 1000



MEAN LOAD, P.S.I. X 1000

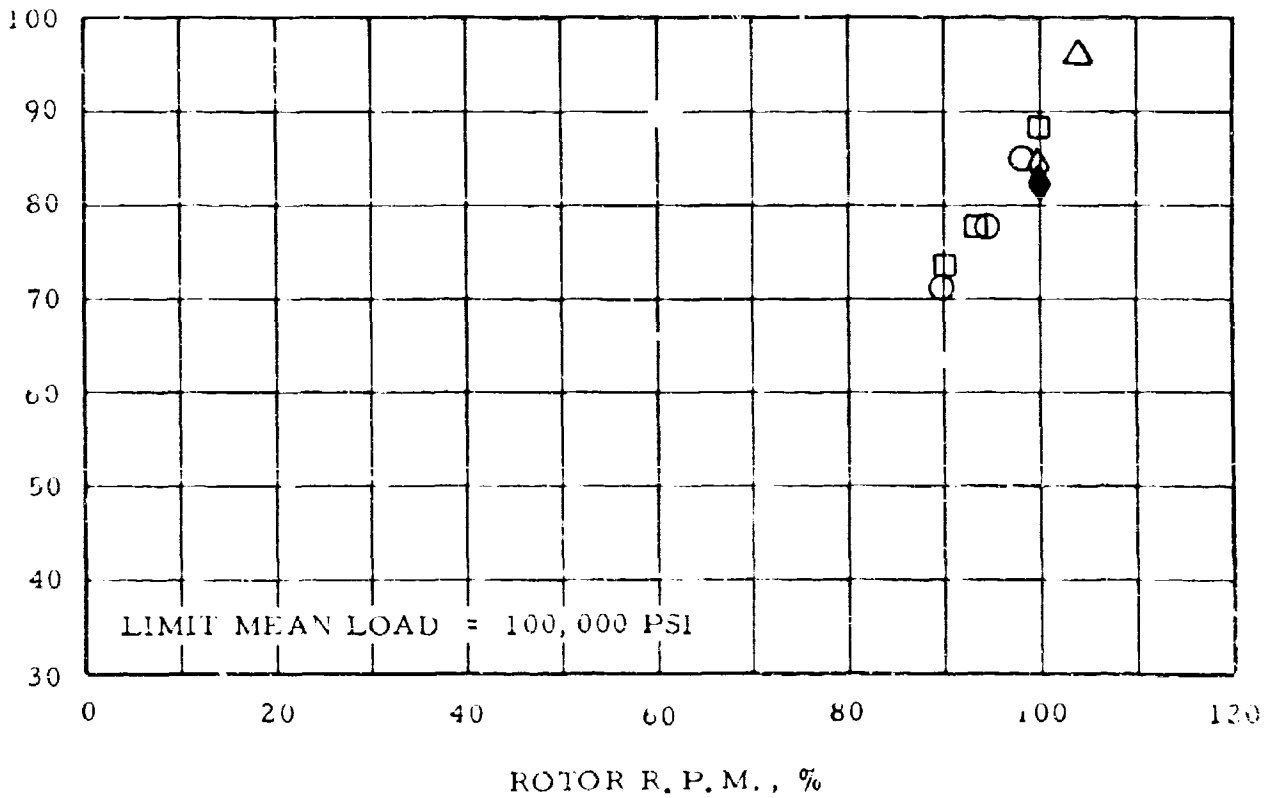


Figure 21. Hub Plate Stress - Aft

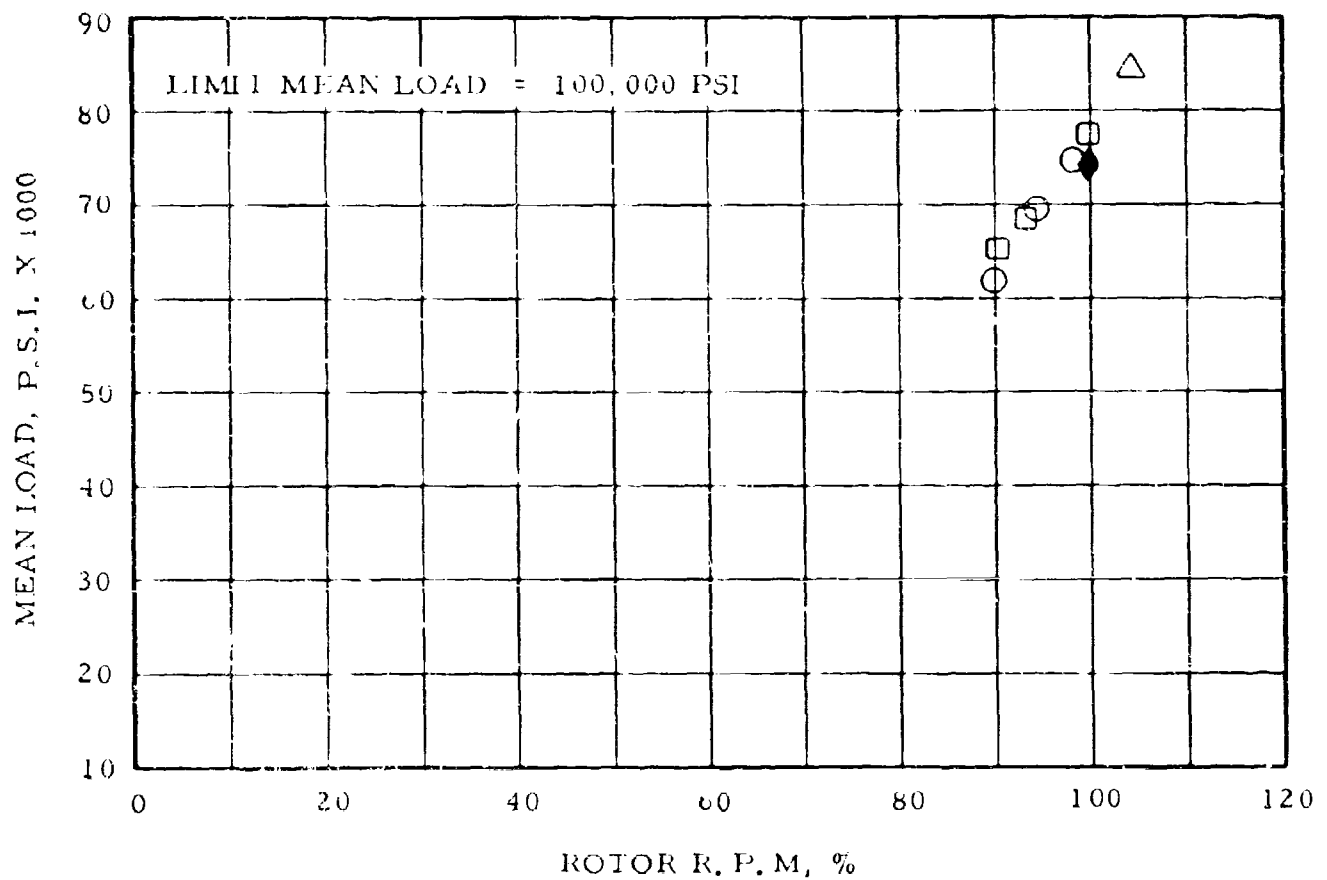
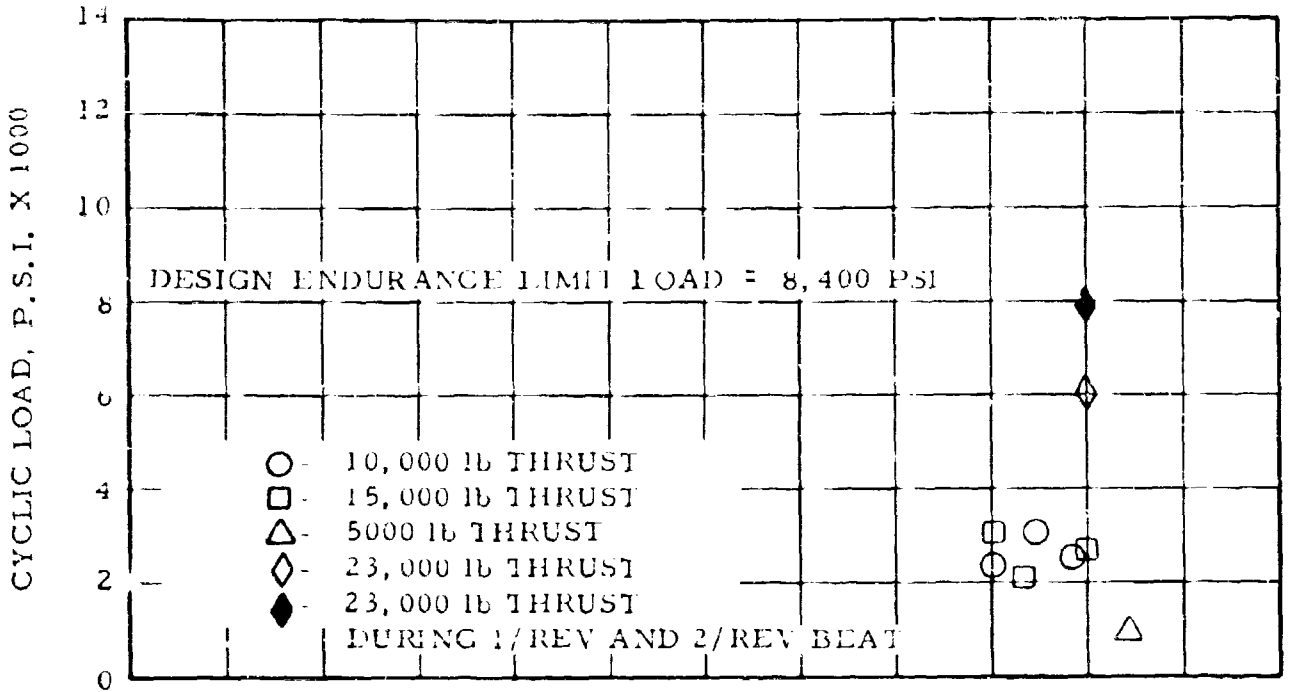


Figure 22. Hub Plate Stress - Forward

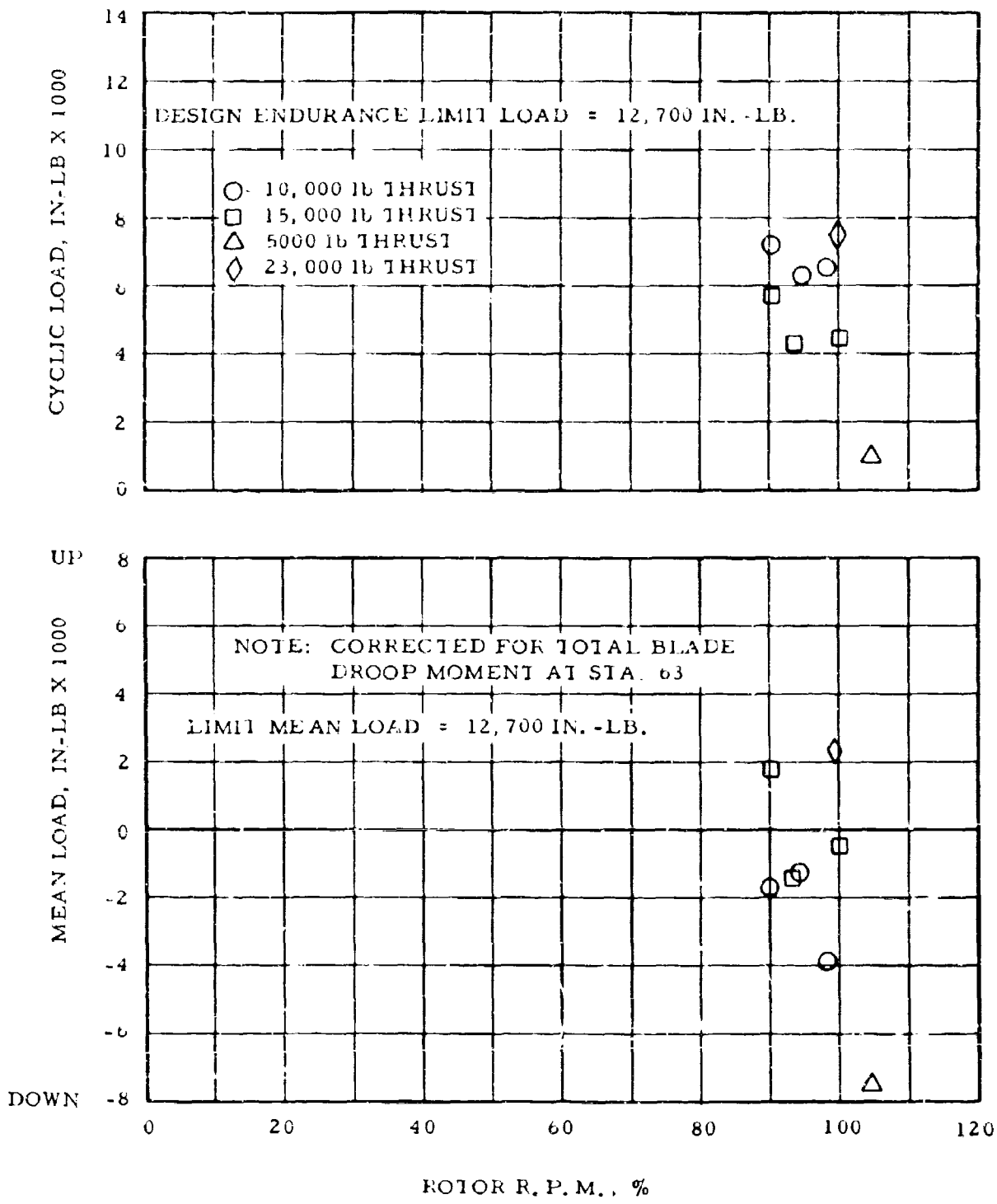


Figure 23. Blade Flapwise Bending at Station 63" Front Spar

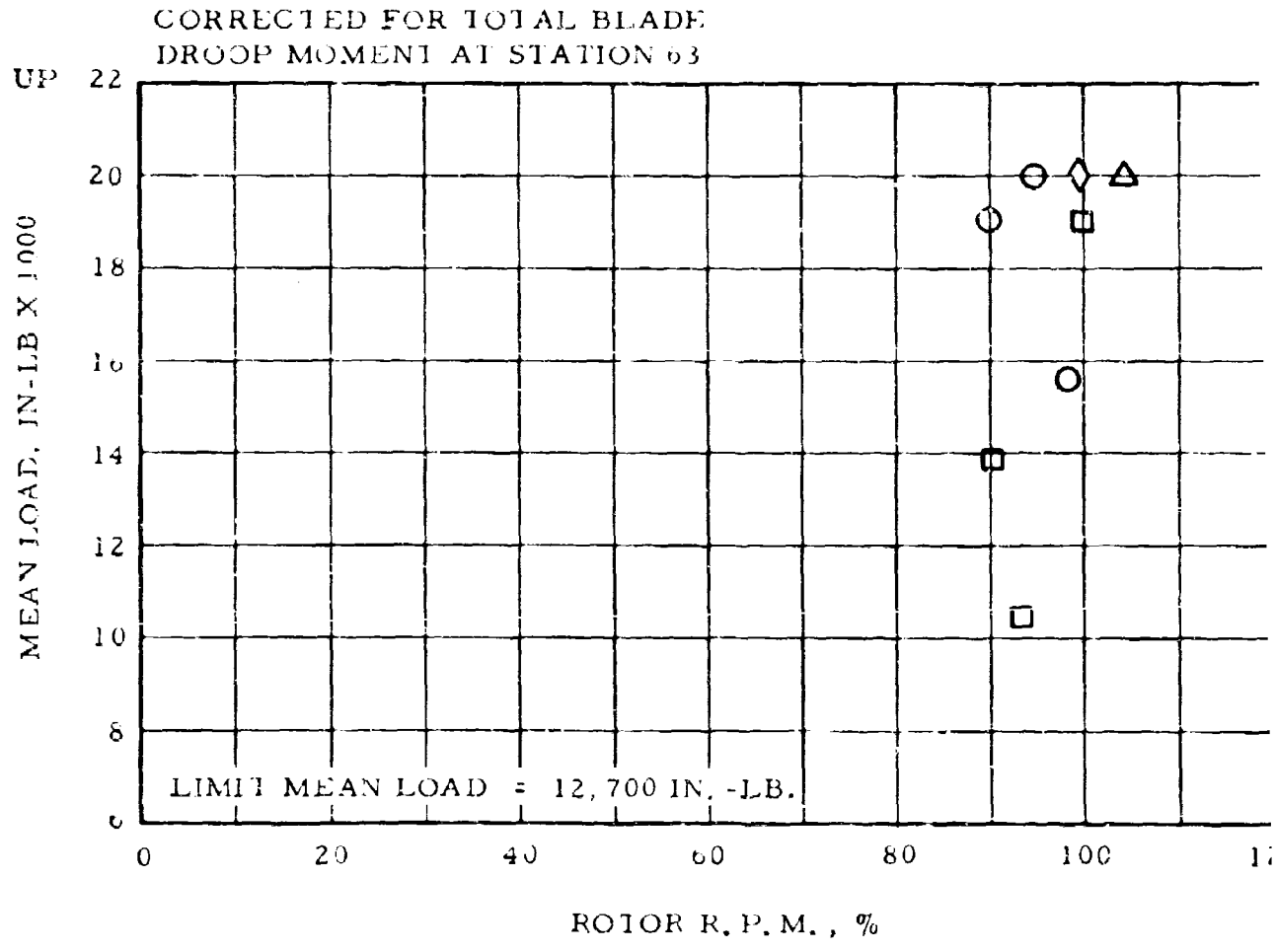
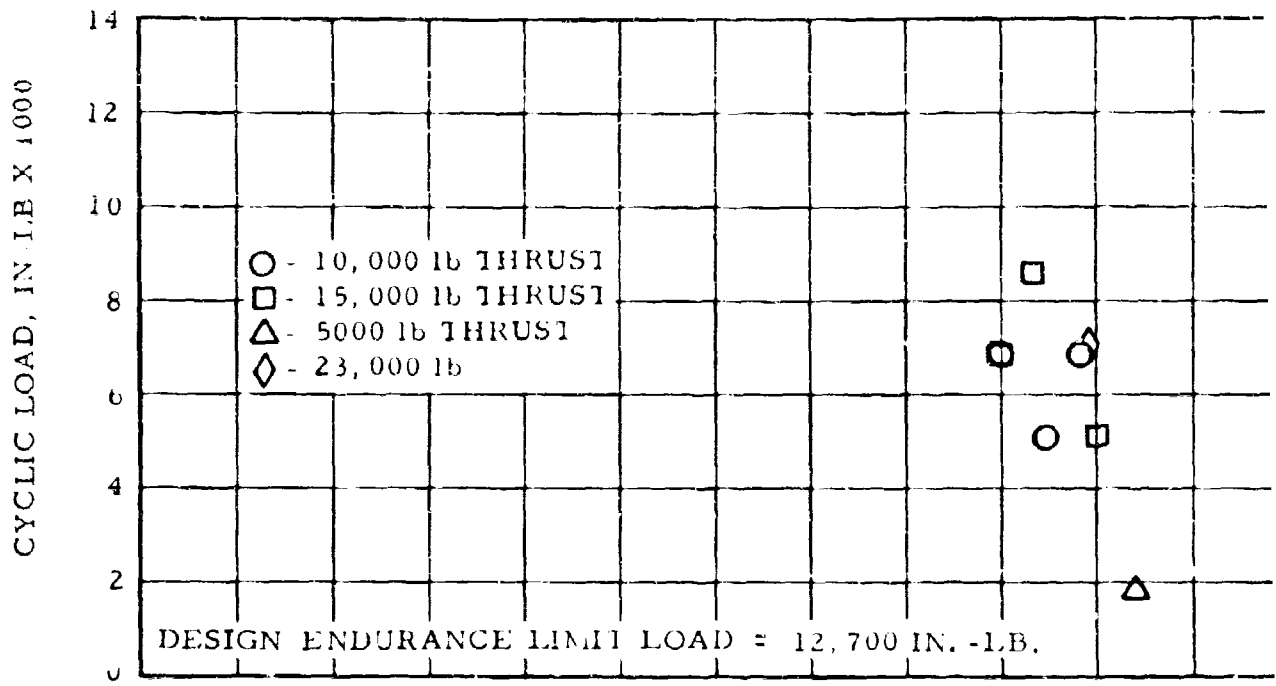


Figure 24. Blade Flapwise Bending at Station 63" Rear Spar

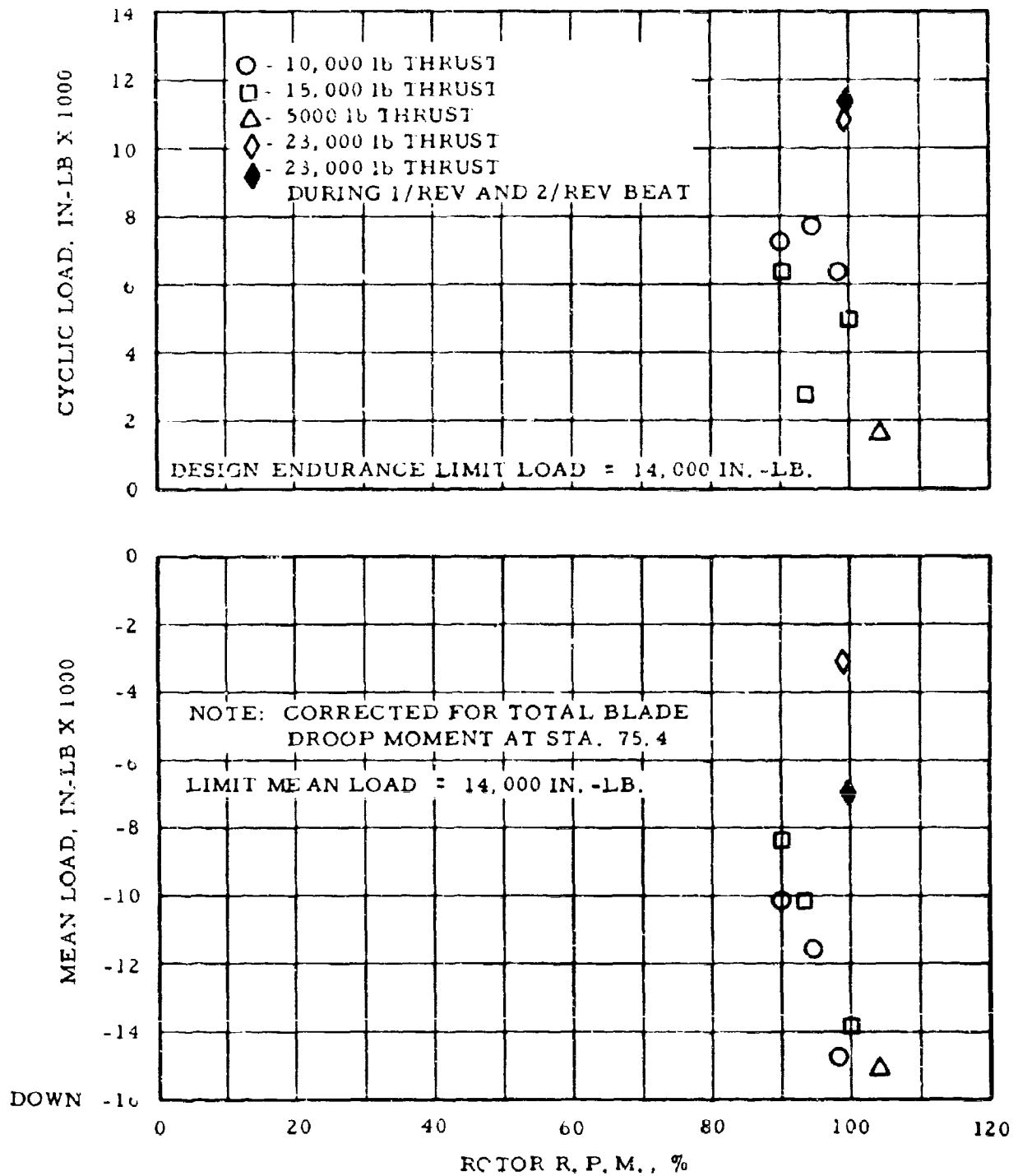


Figure 25. Blade Flapwise Bending at Station 75.4' Rear Spar

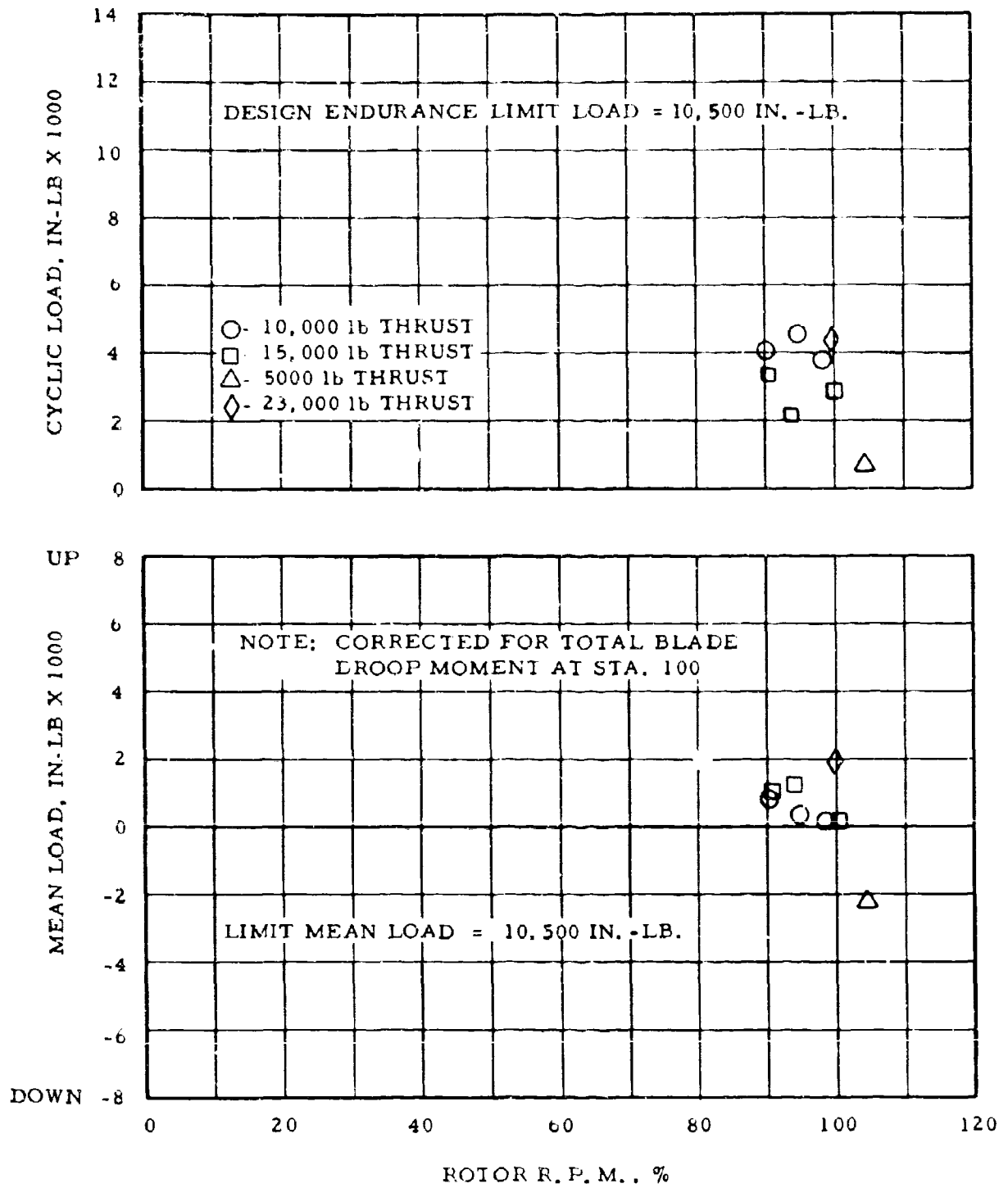


Figure 26. Blade Flapwise Bending at Station 100" Front Spar

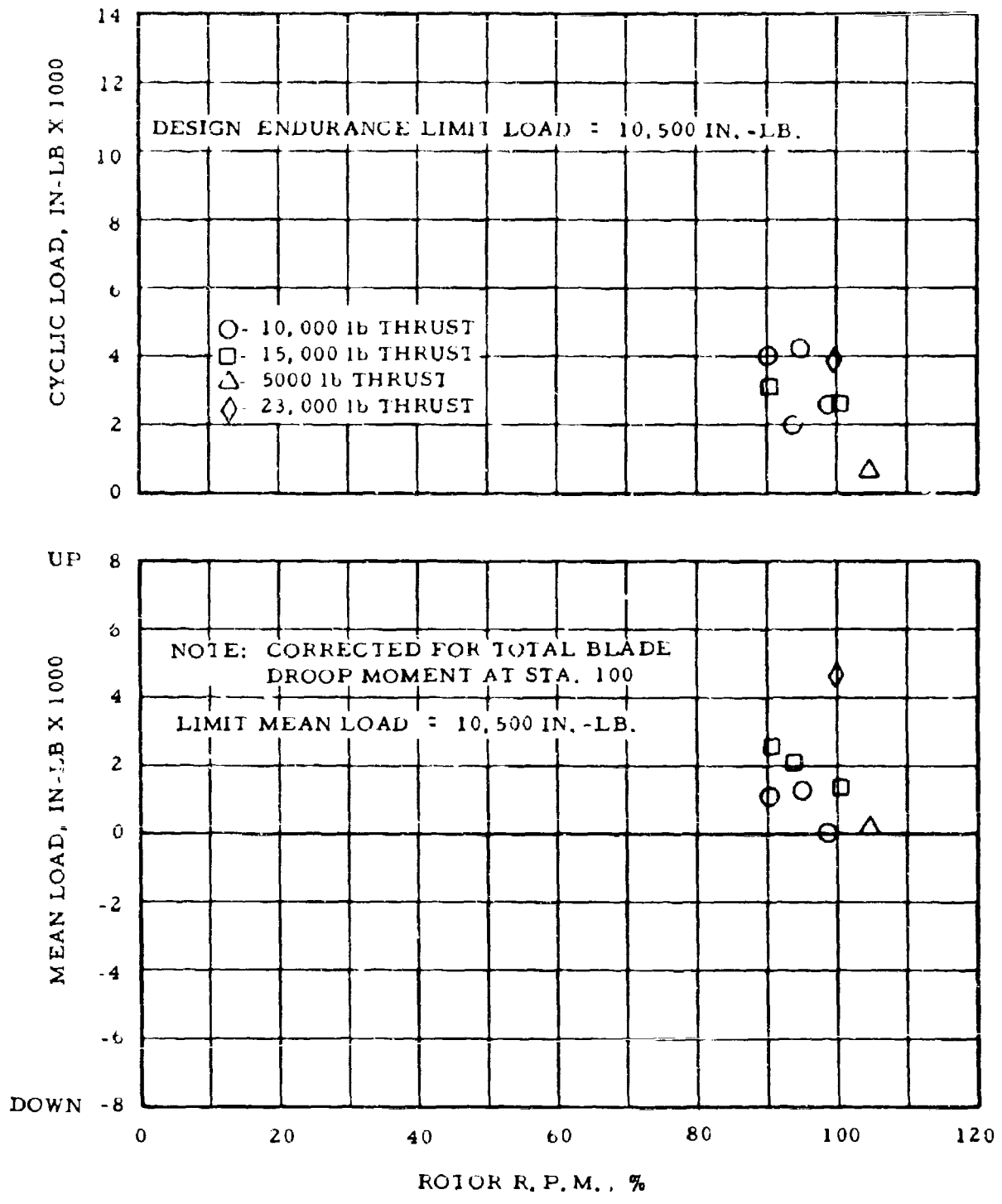


Figure 27. Blade Flapwise Bending at Station 100' Rear Spar

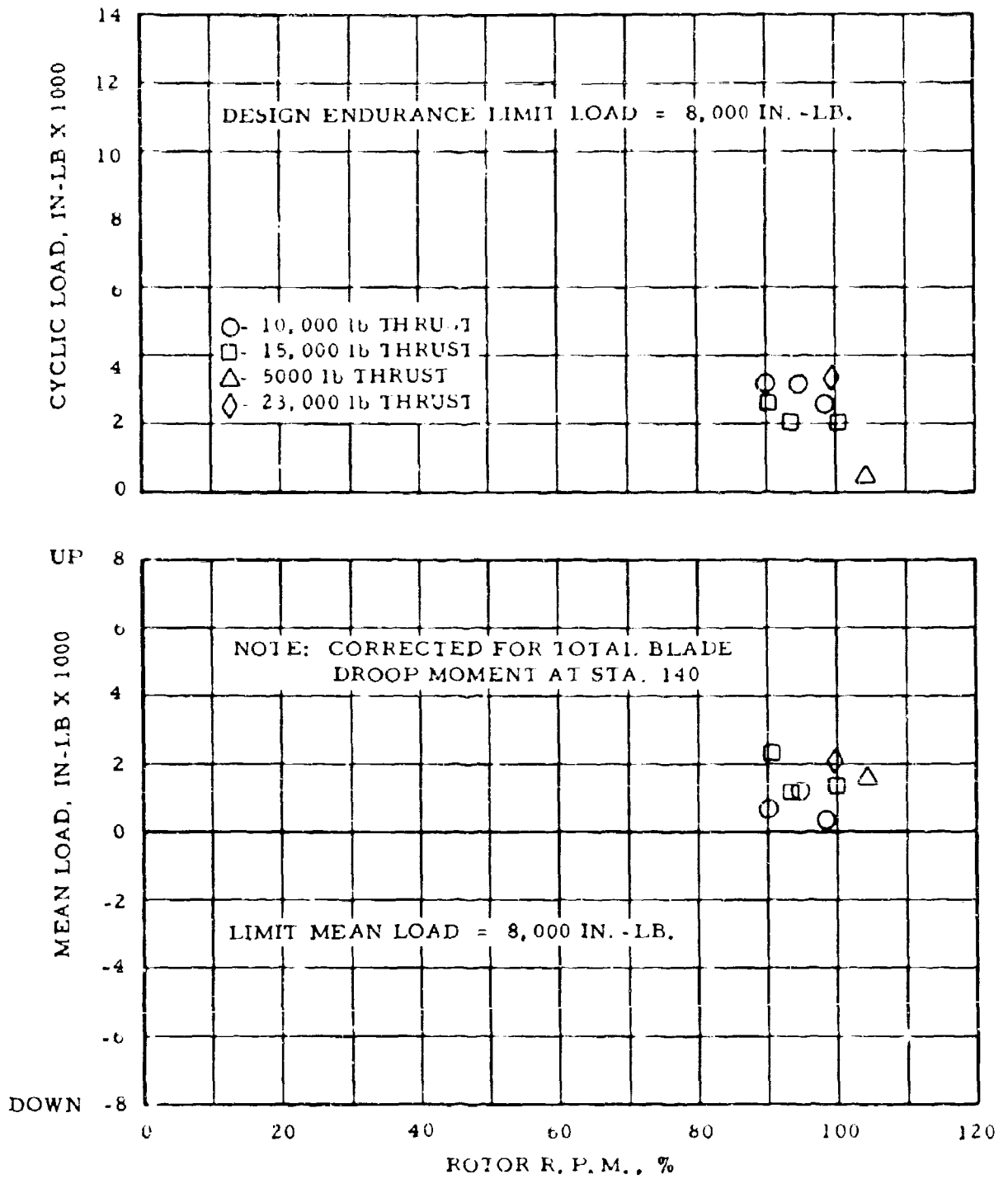


Figure 28. Blade Flapwise Bending at Station 140'' Rear Spar

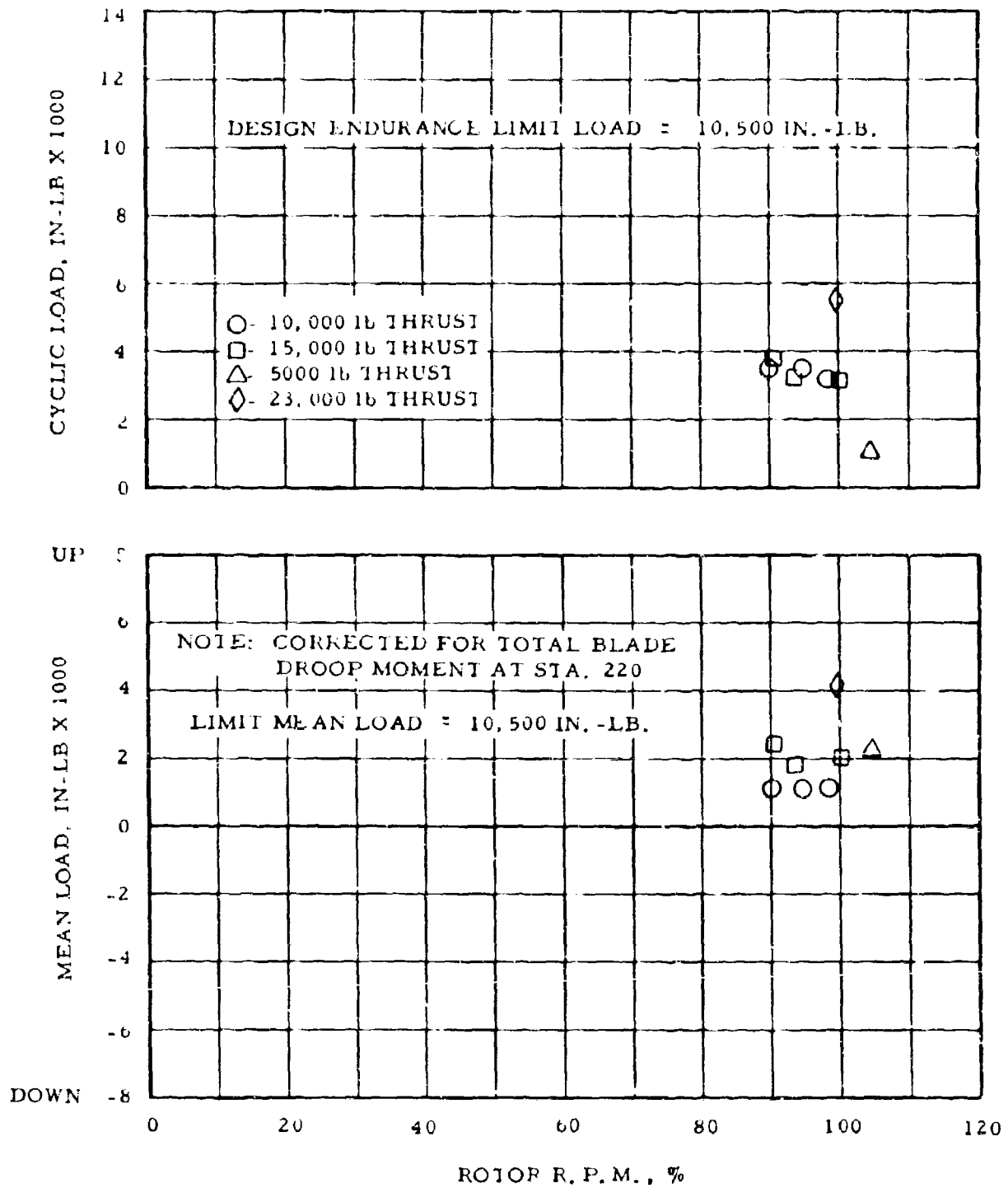


Figure 29. Blade Flapwise Bending at Station 220" Rear Spar

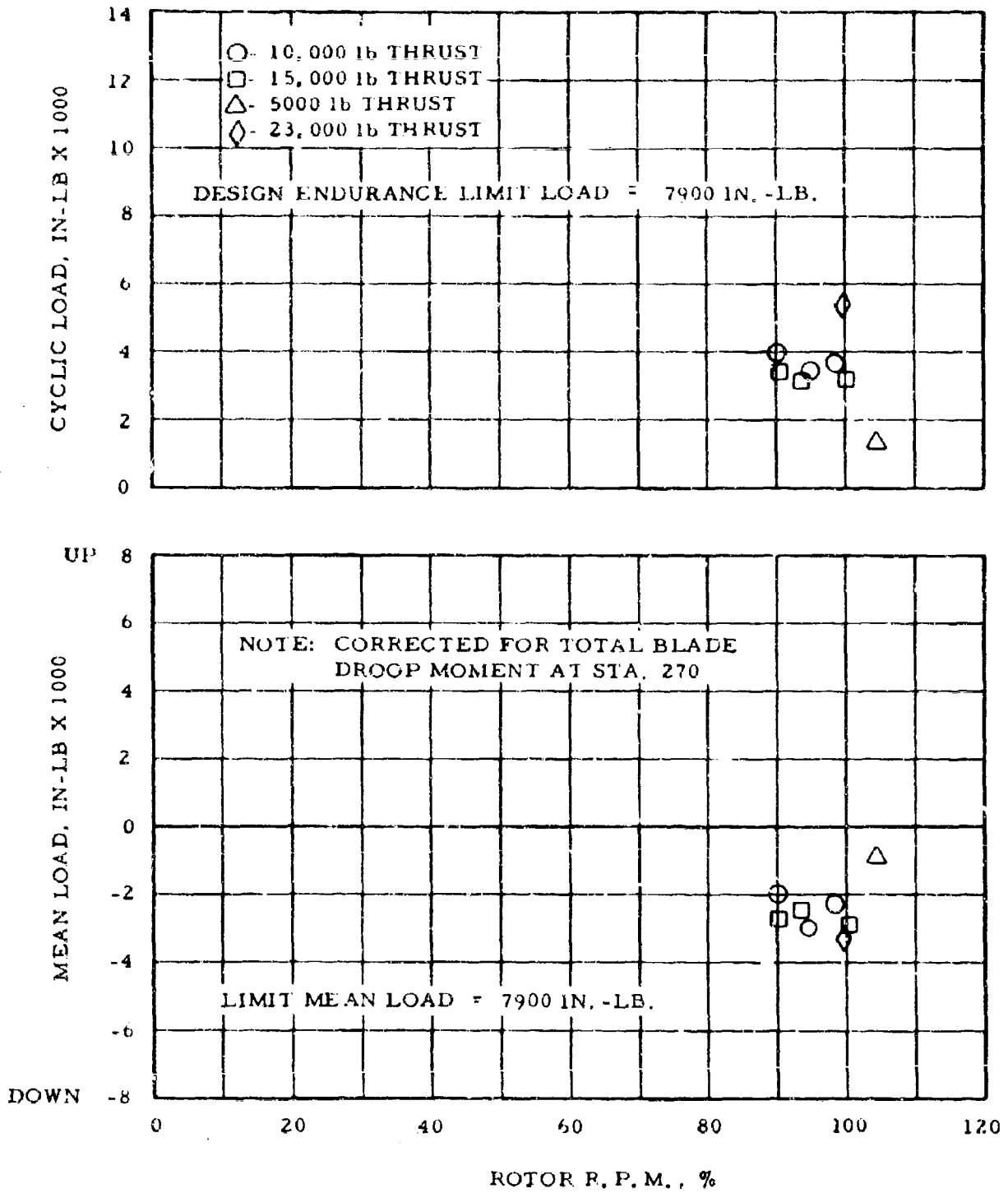


Figure 30. Blade Flapwise Bending at Station 270" Front Spar

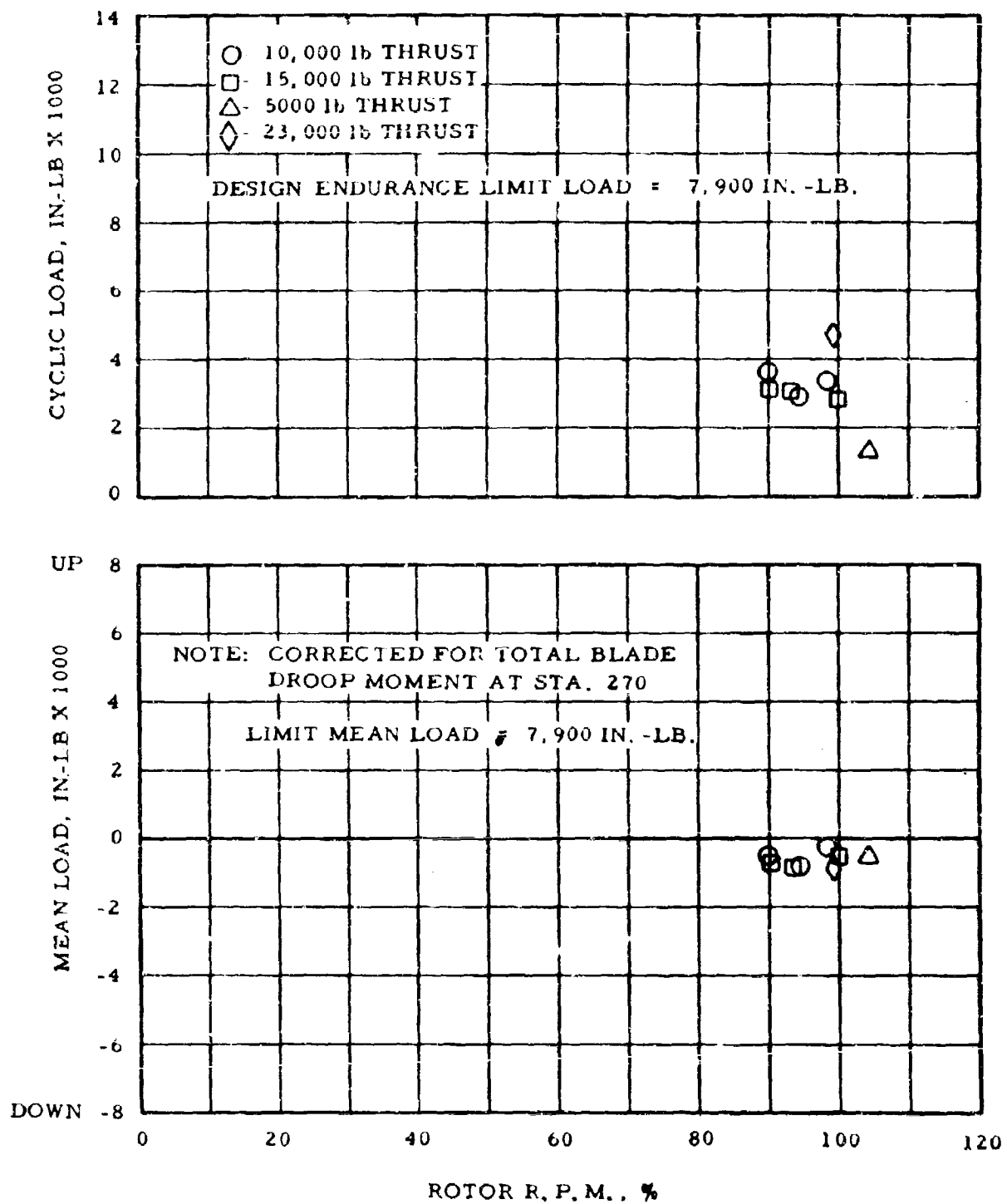


Figure 31. Blade Flapwise Bending at Station 270" Rear Spar

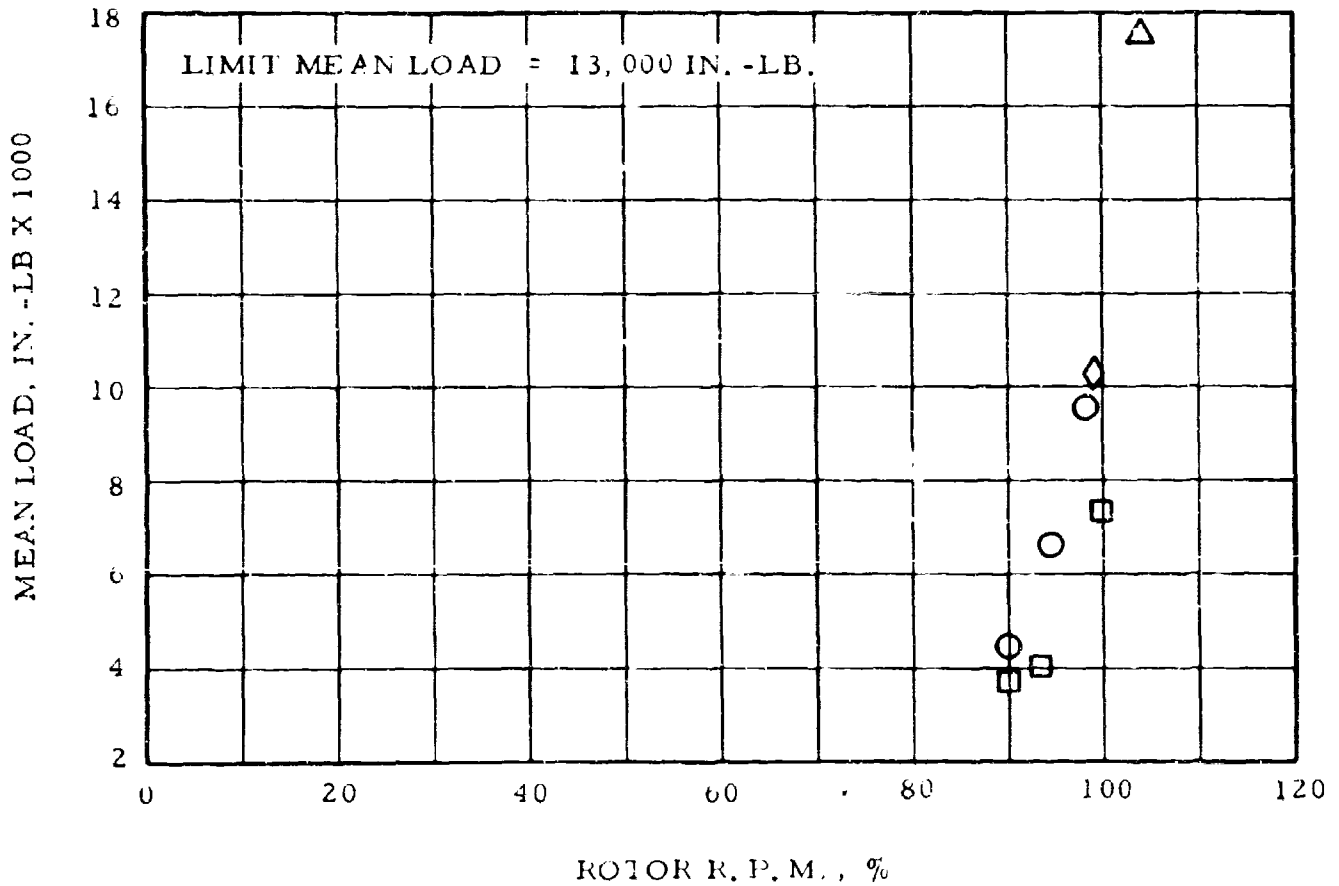
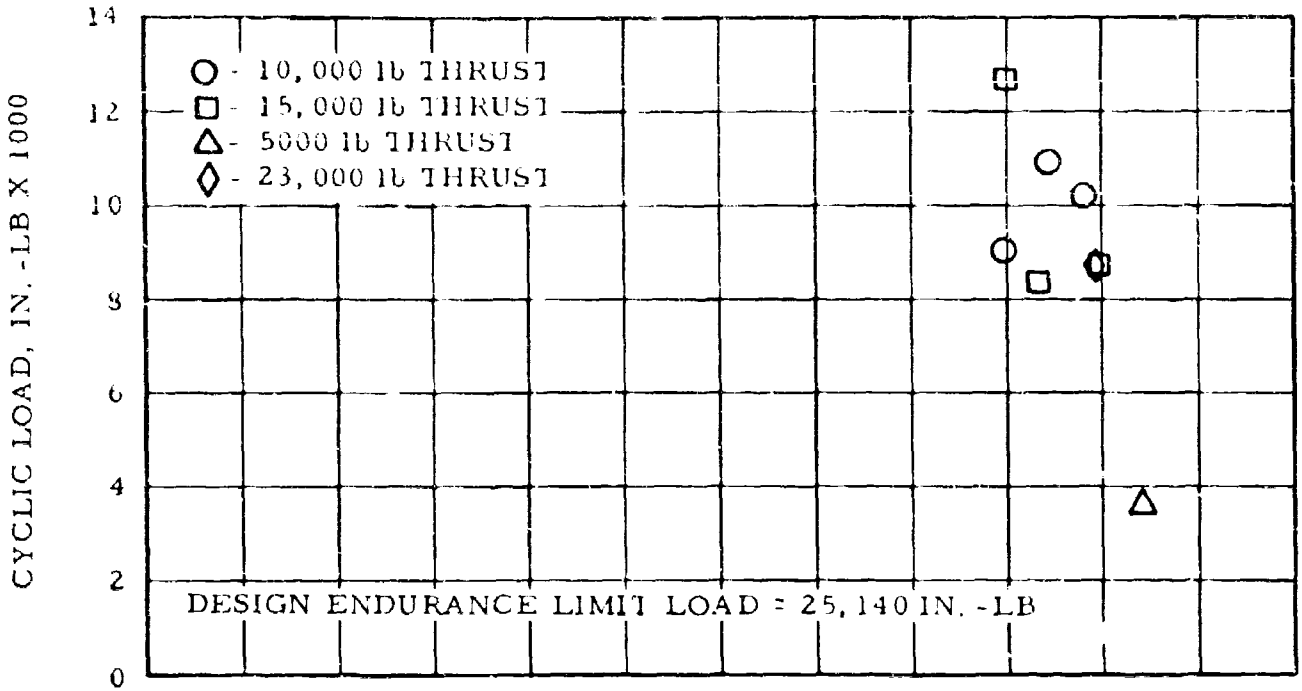


Figure 32. Blade Skin Torsion at Station 38"

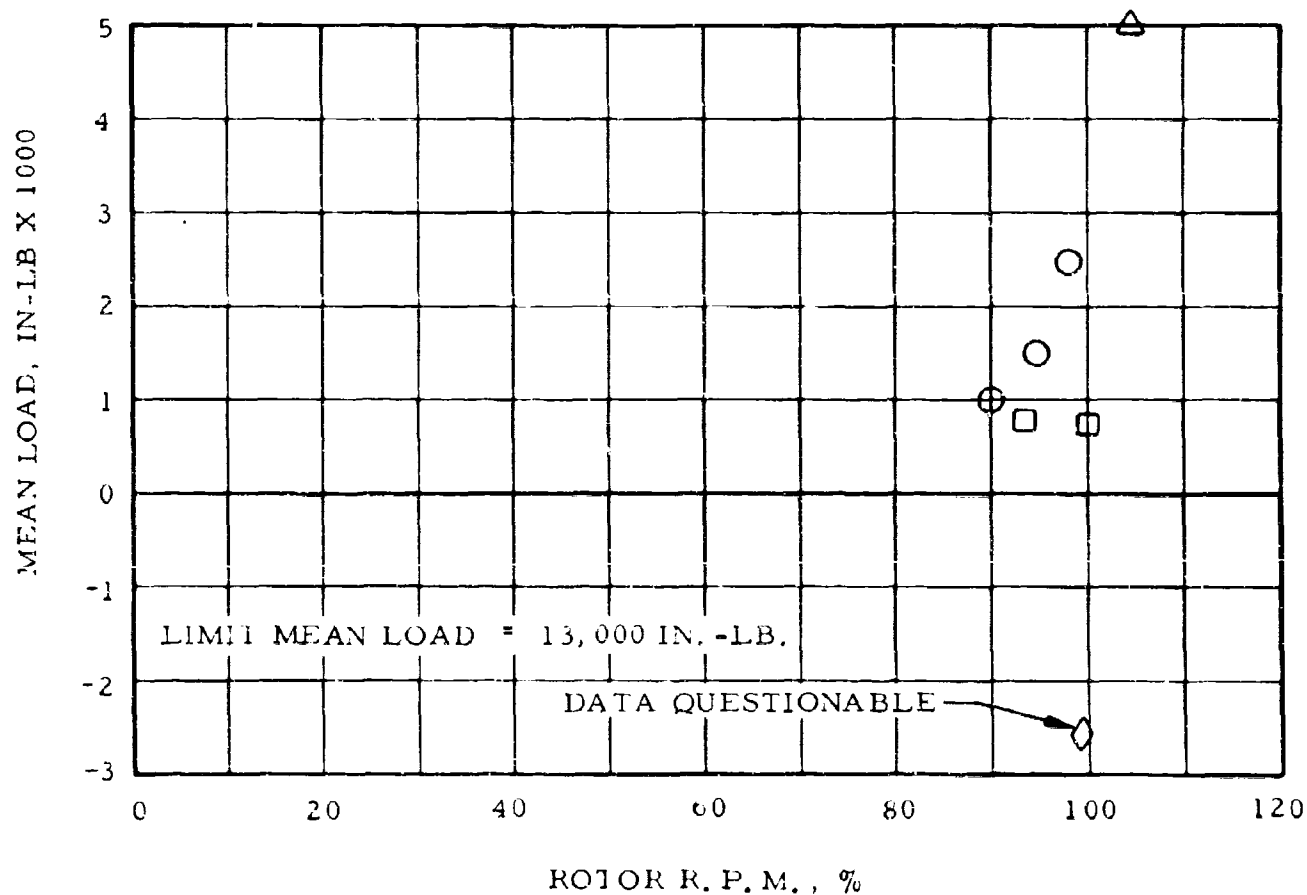
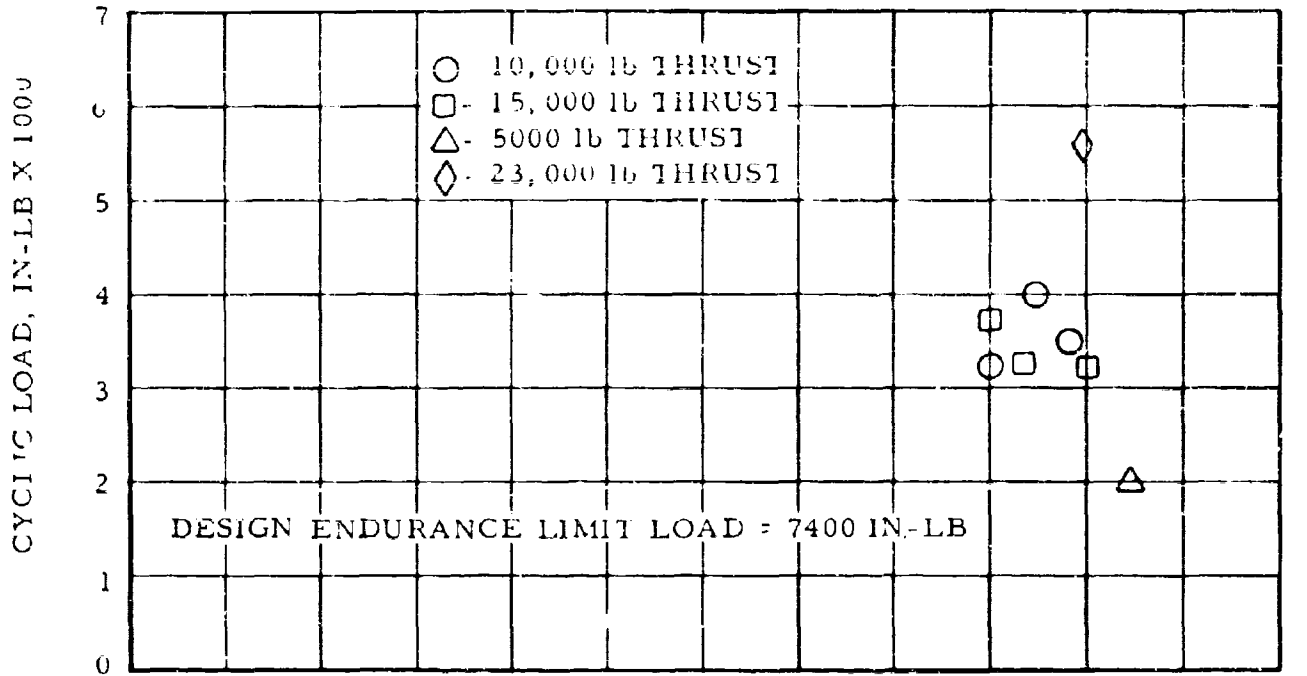


Figure 33. Blade Skin Torsion at Station 83"

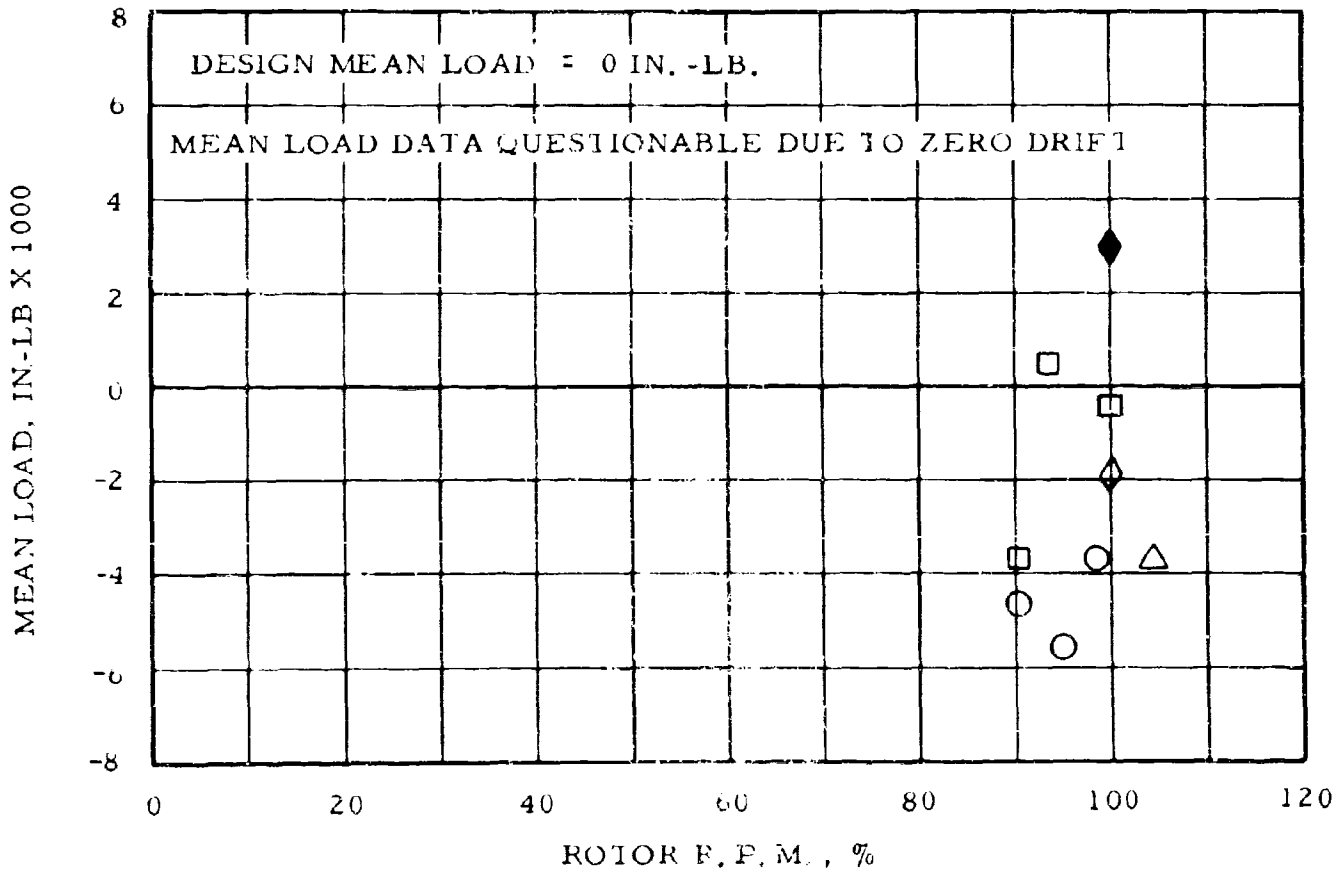
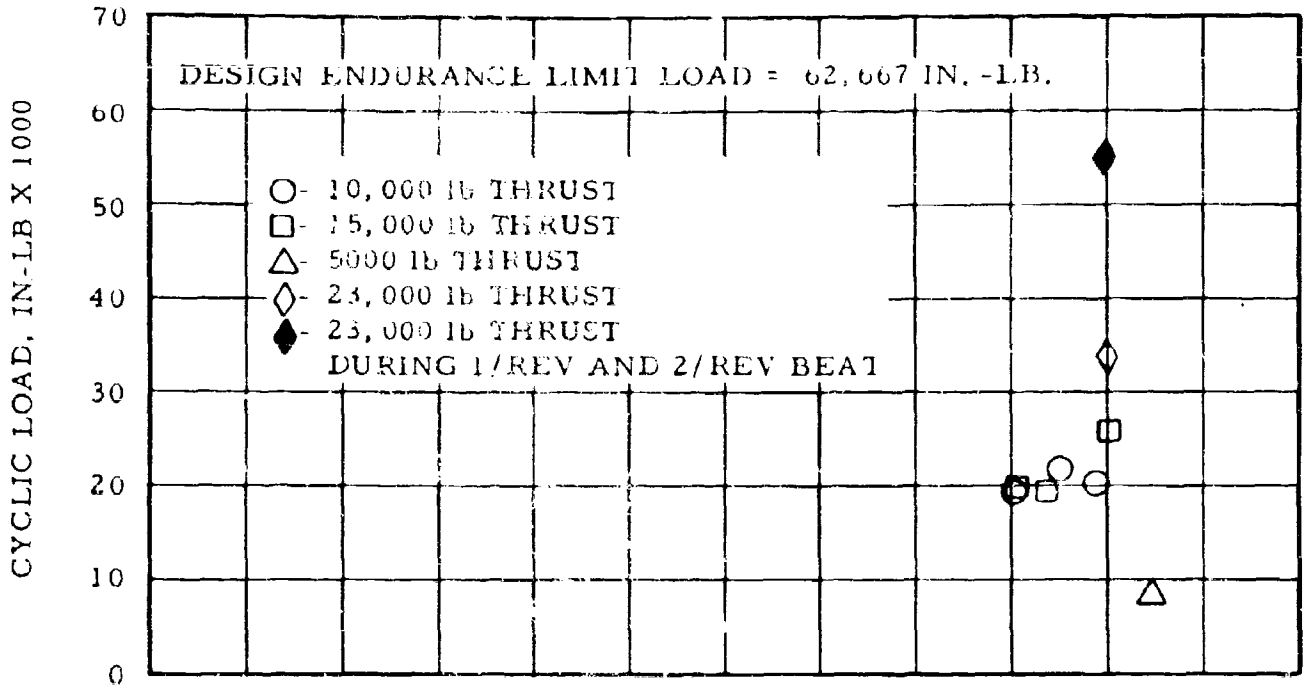


Figure 34. Rotor Shaft Bending 90 Degrees to Blue Blade

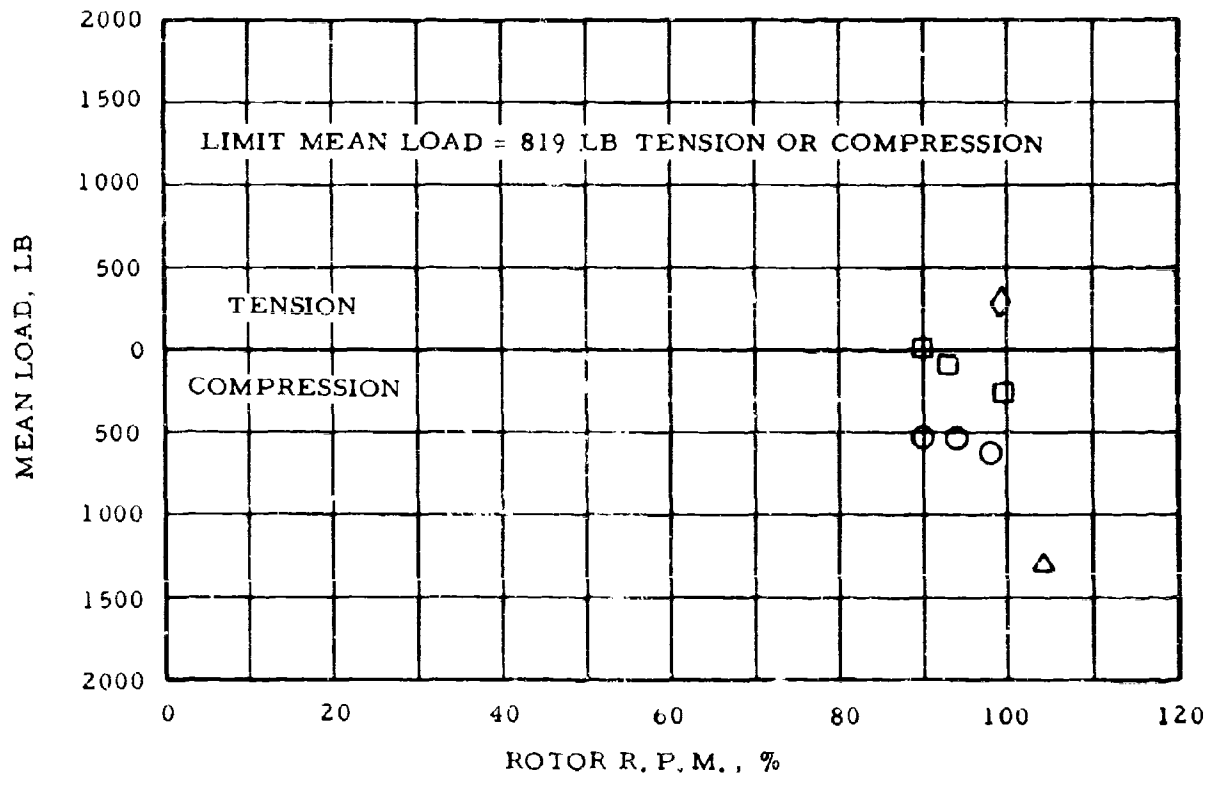
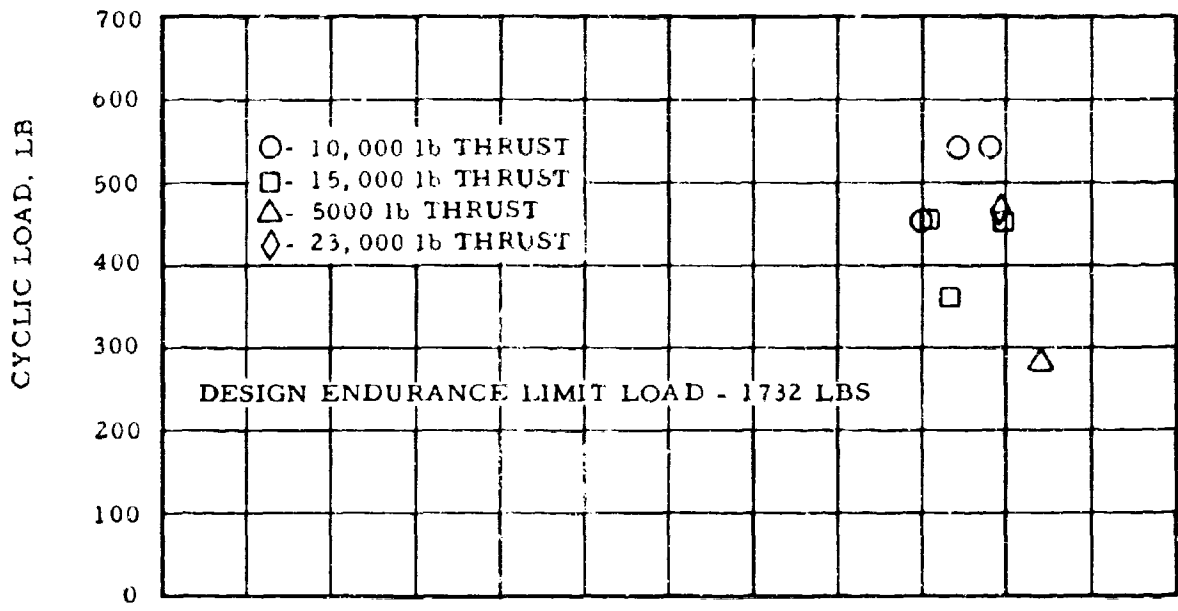


Figure 35. Pitch Link Load, Blue Blade

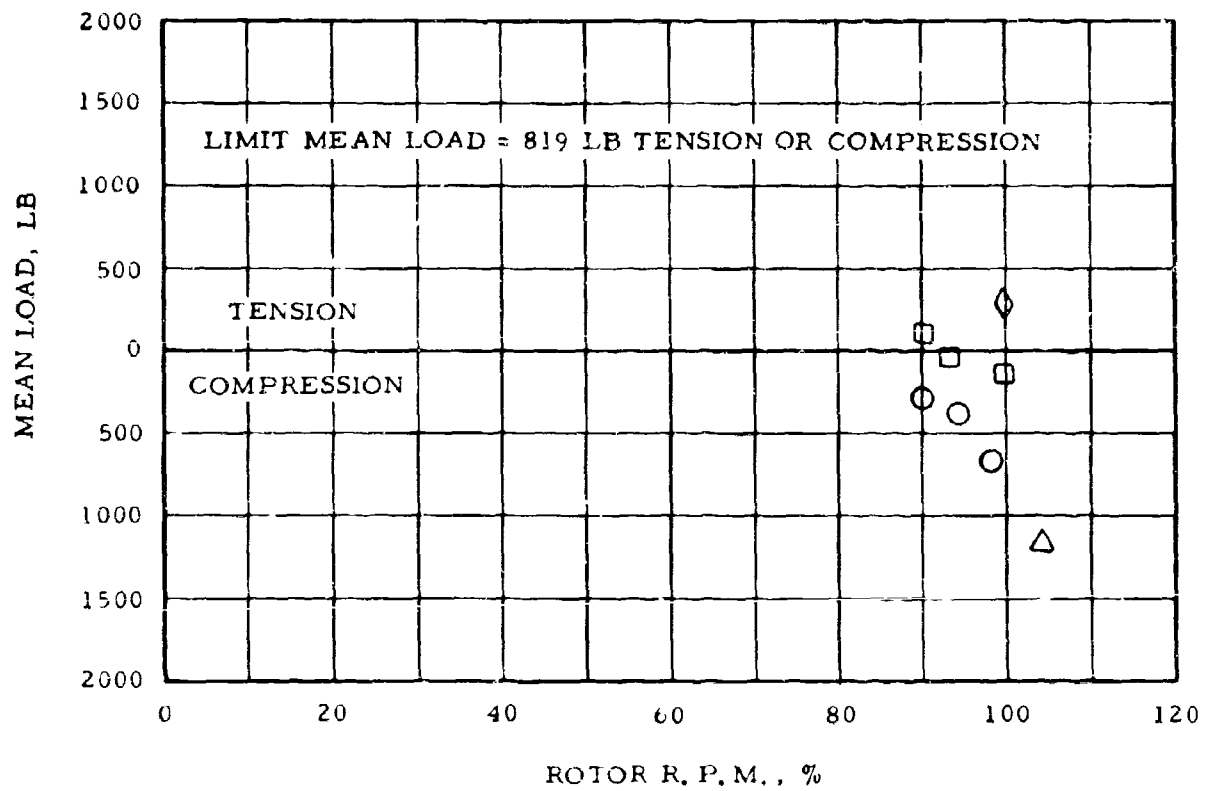
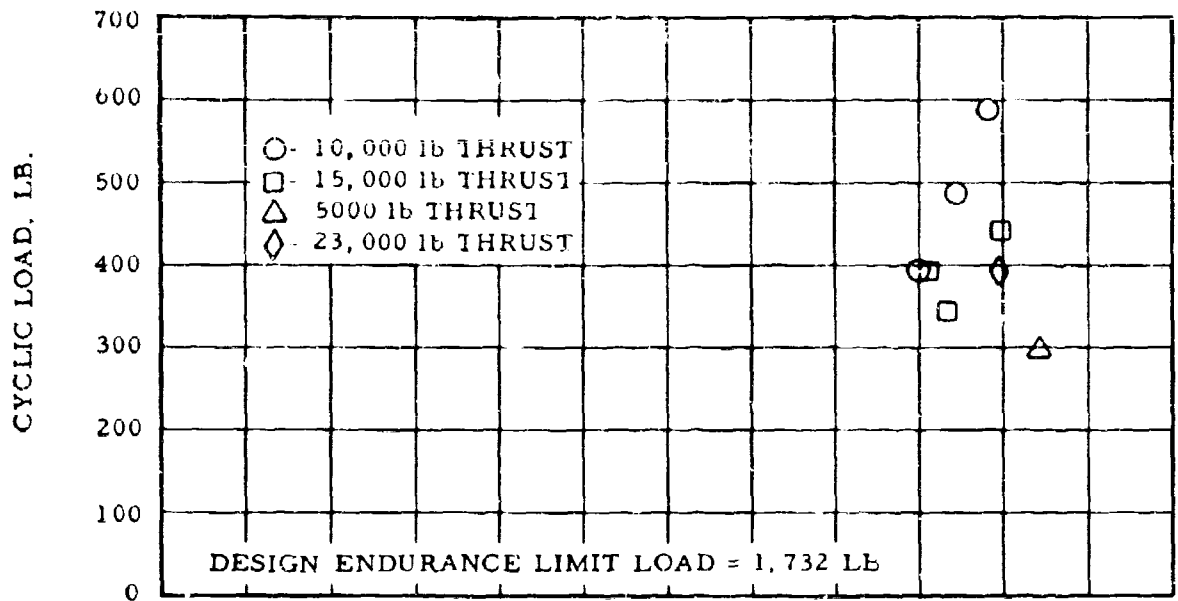


Figure 36. Pitch Link Load, Yellow Blade

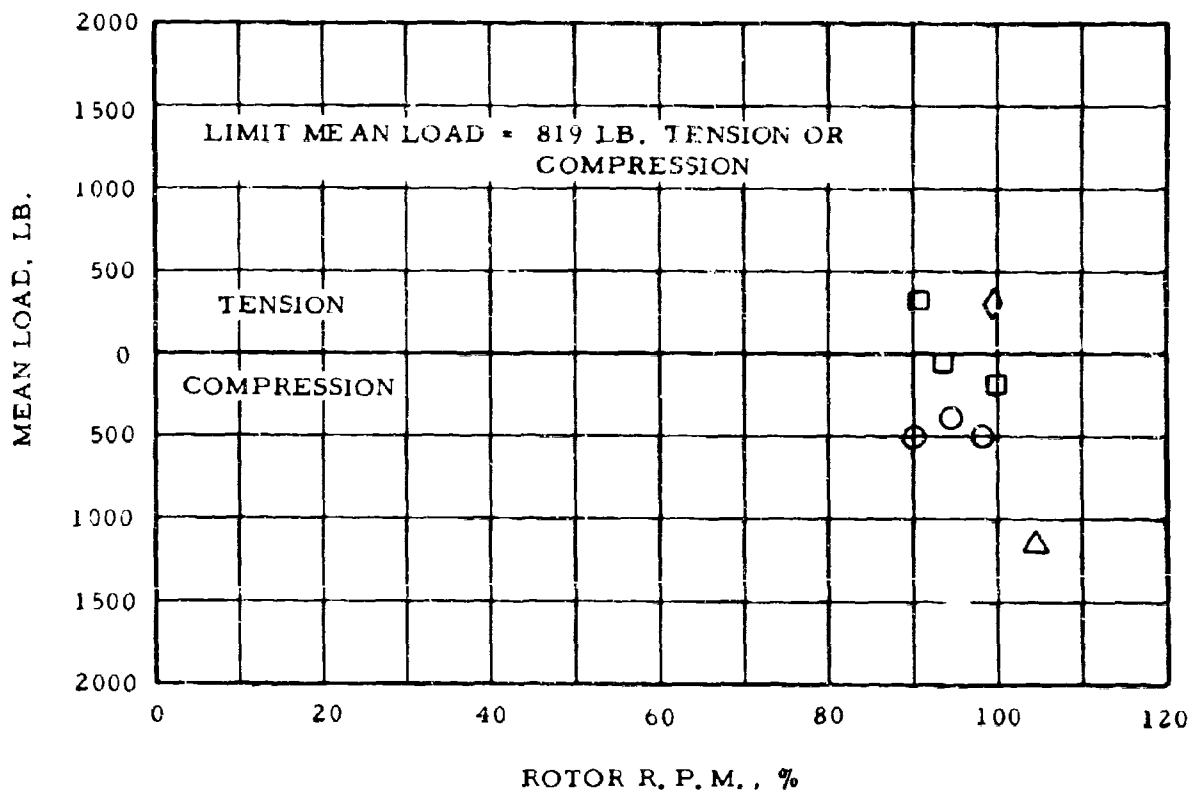
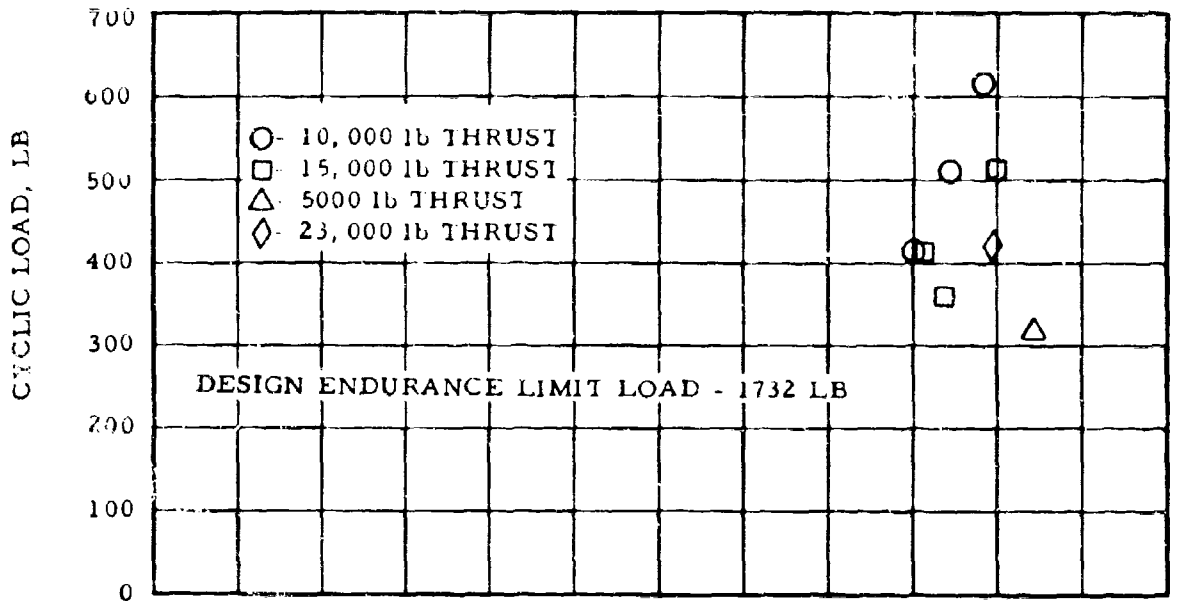


Figure 37. Pitch Link Load, Red Blade

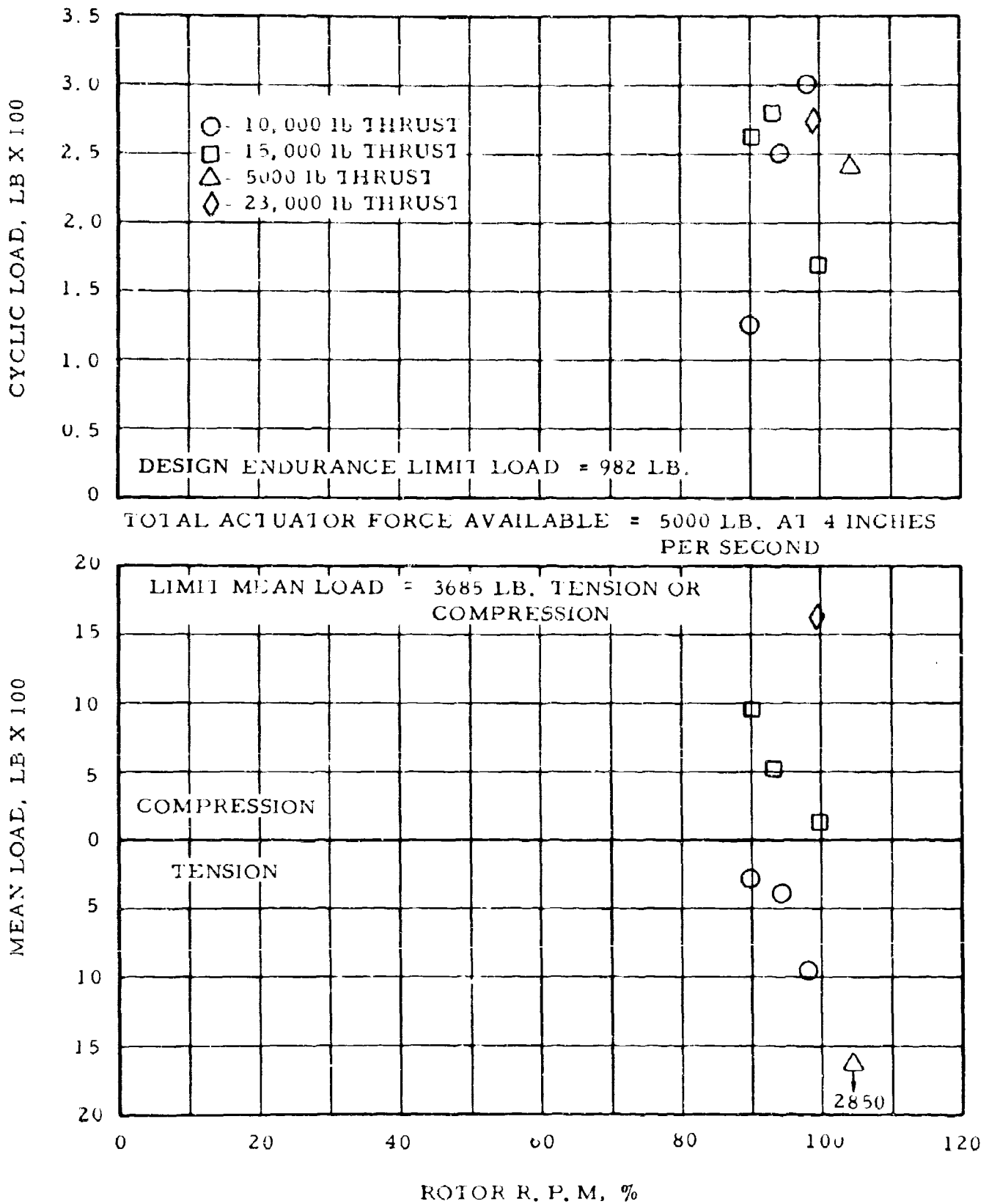
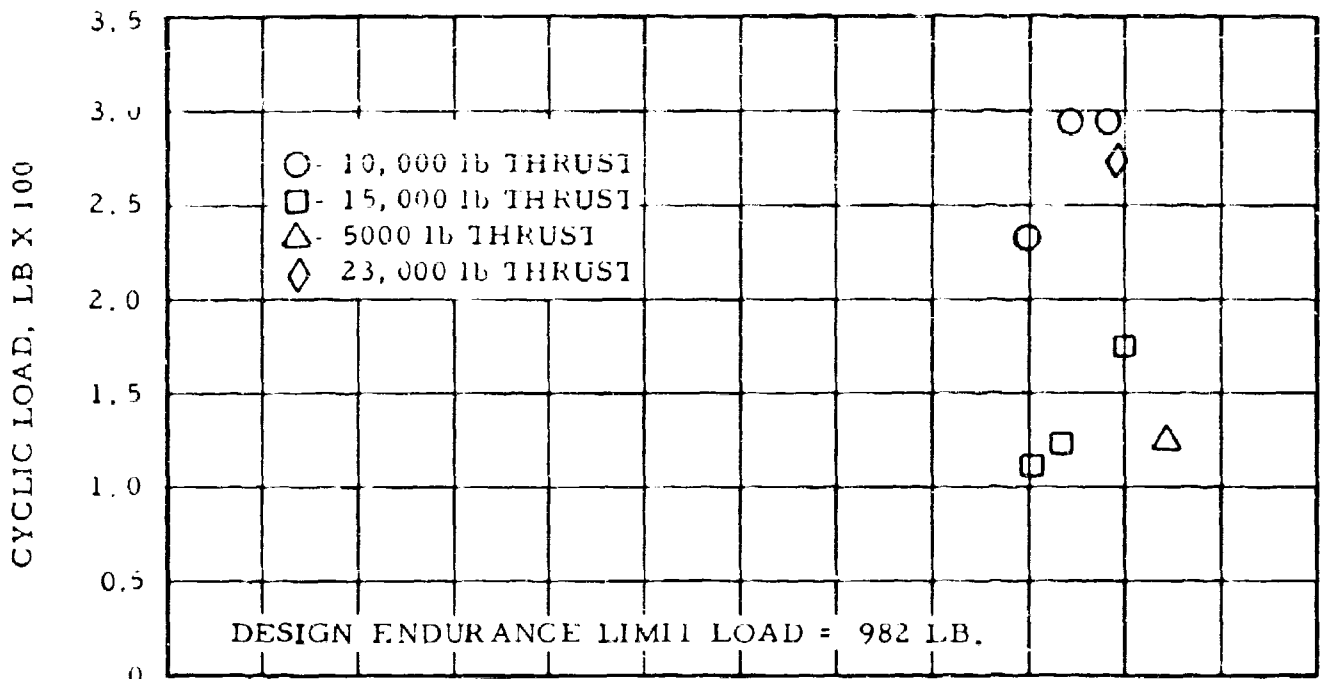


Figure 38. Control Actuator Force, Starboard



TOTAL ACTUATOR FORCE AVAILABLE = 5000 LB AT 4 IN/SEC

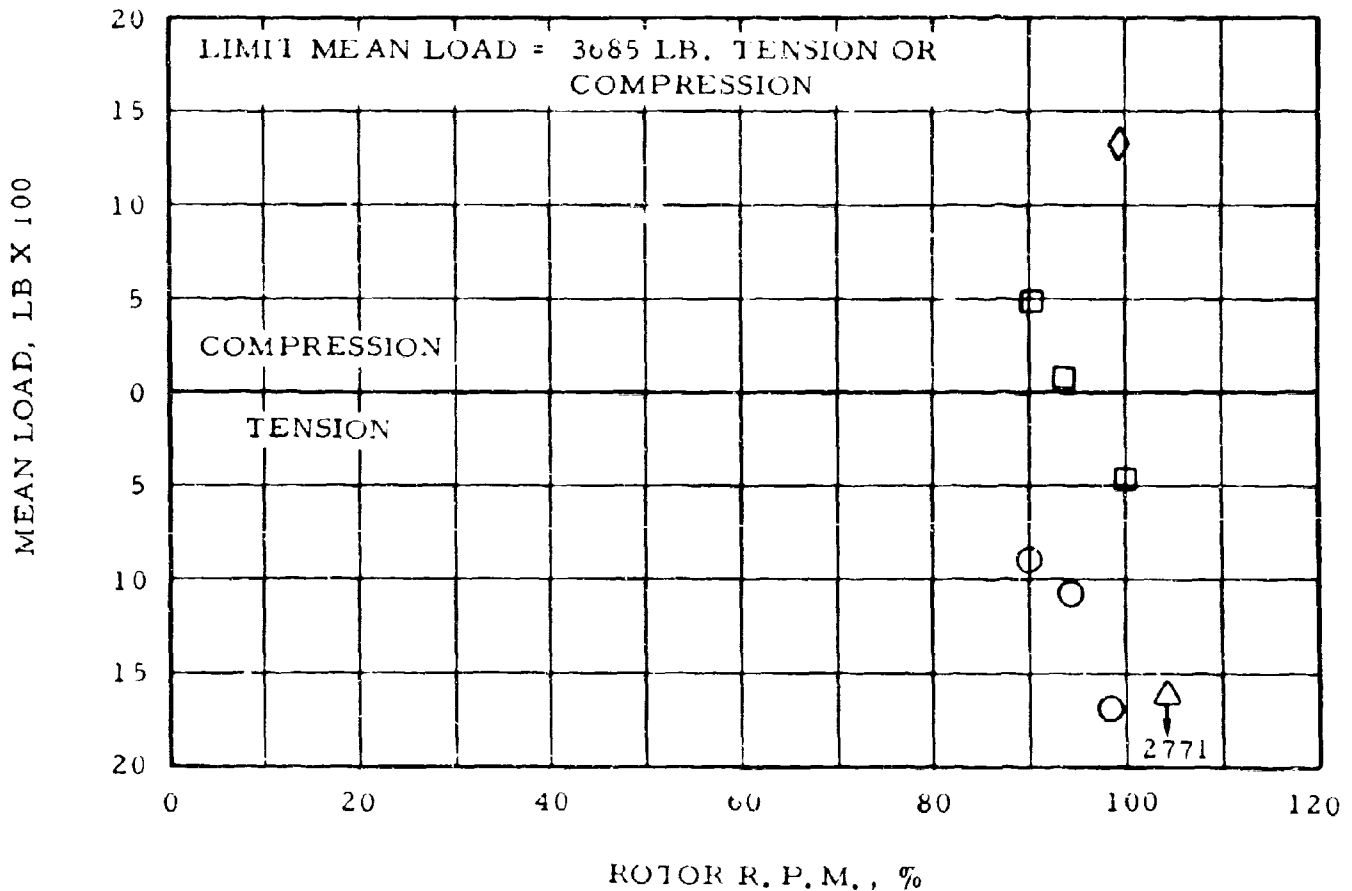
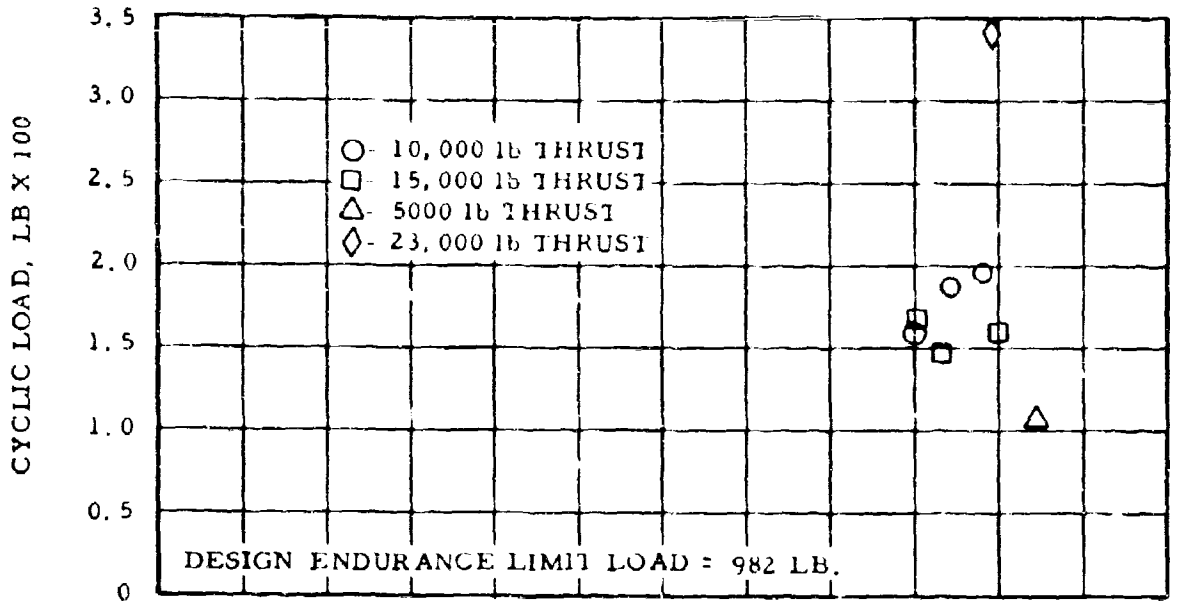


Figure 39. Control Actuator Force, Port



TOTAL ACTUATOR FORCE AVAILABLE = 5000 LB AT 4 INCHES PER SECOND

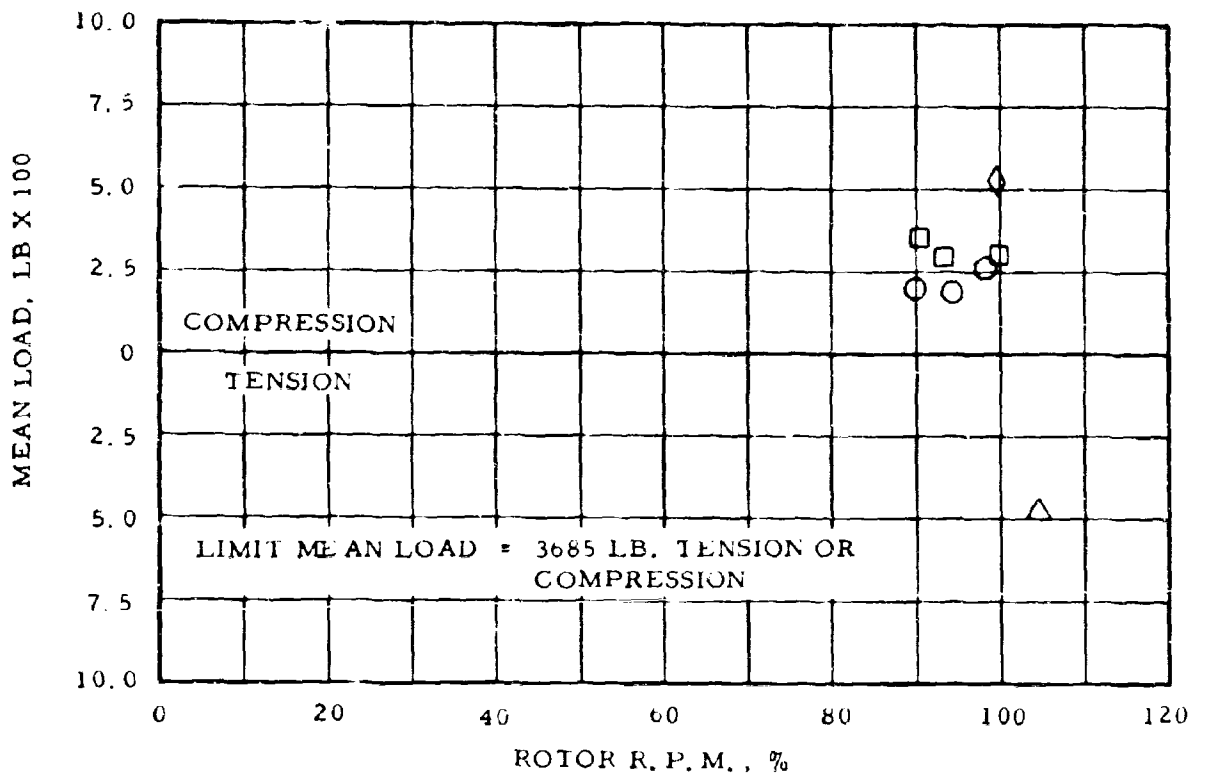


Figure 40. Control Actuator Force, Longitudinal

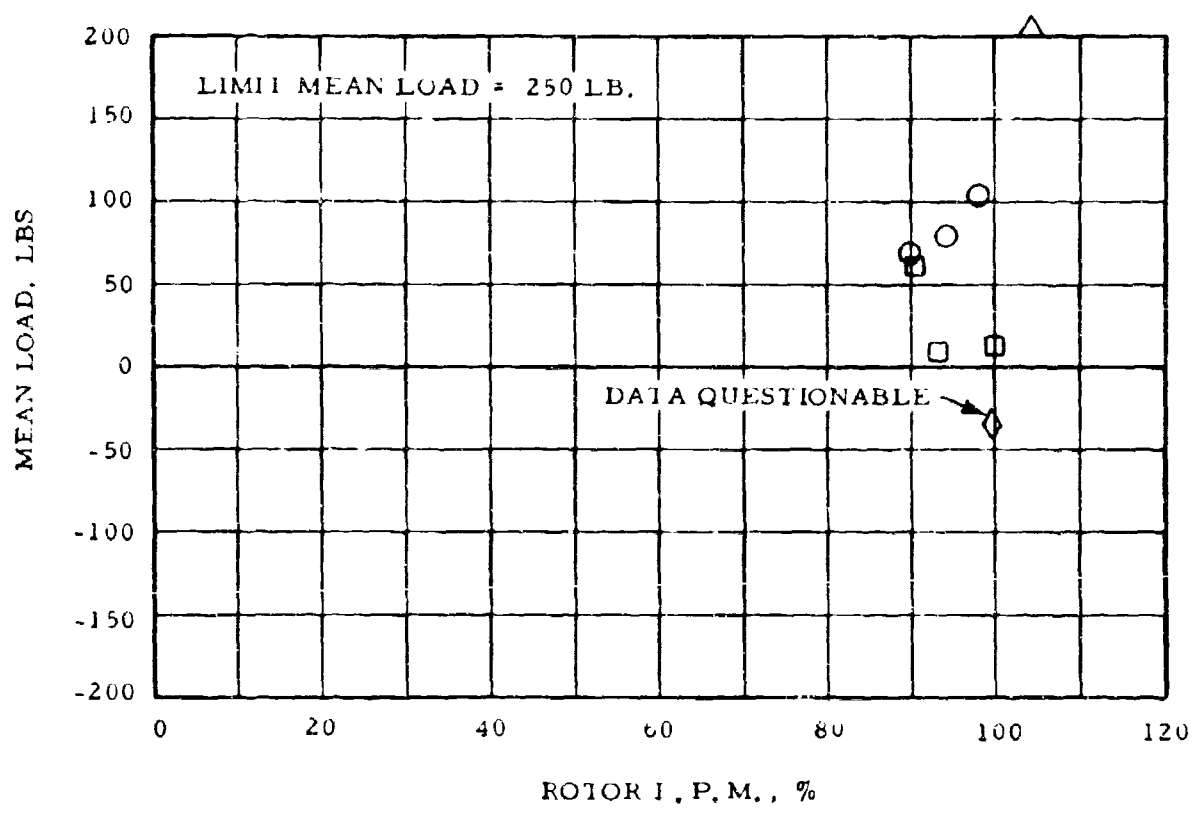
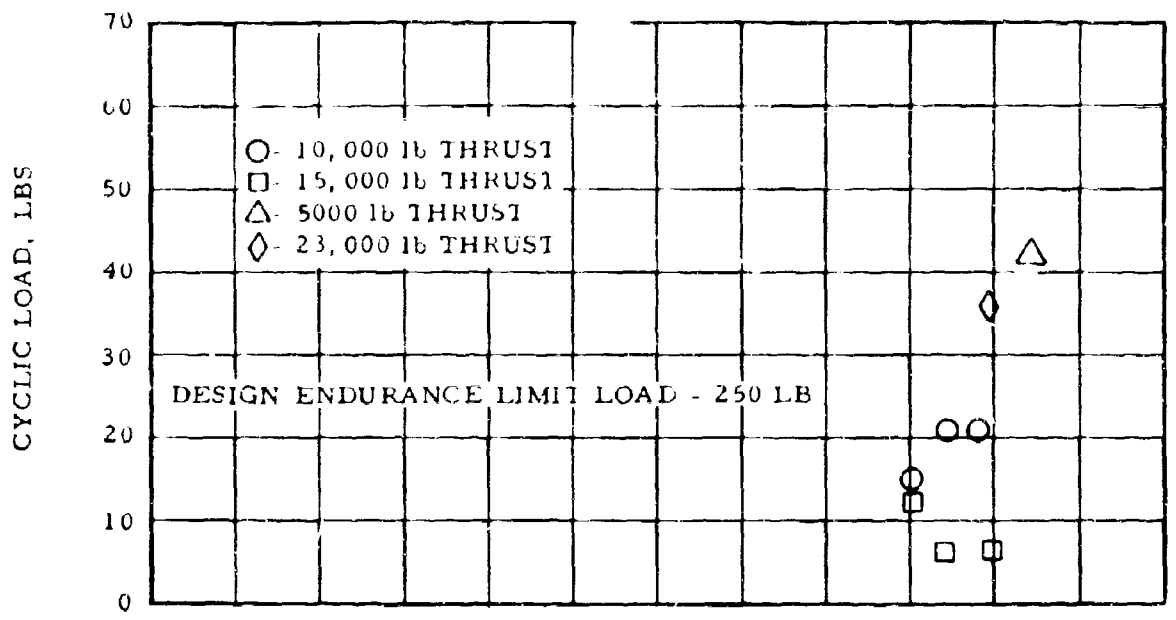


Figure 41. Swash-Plate Drag Link Load

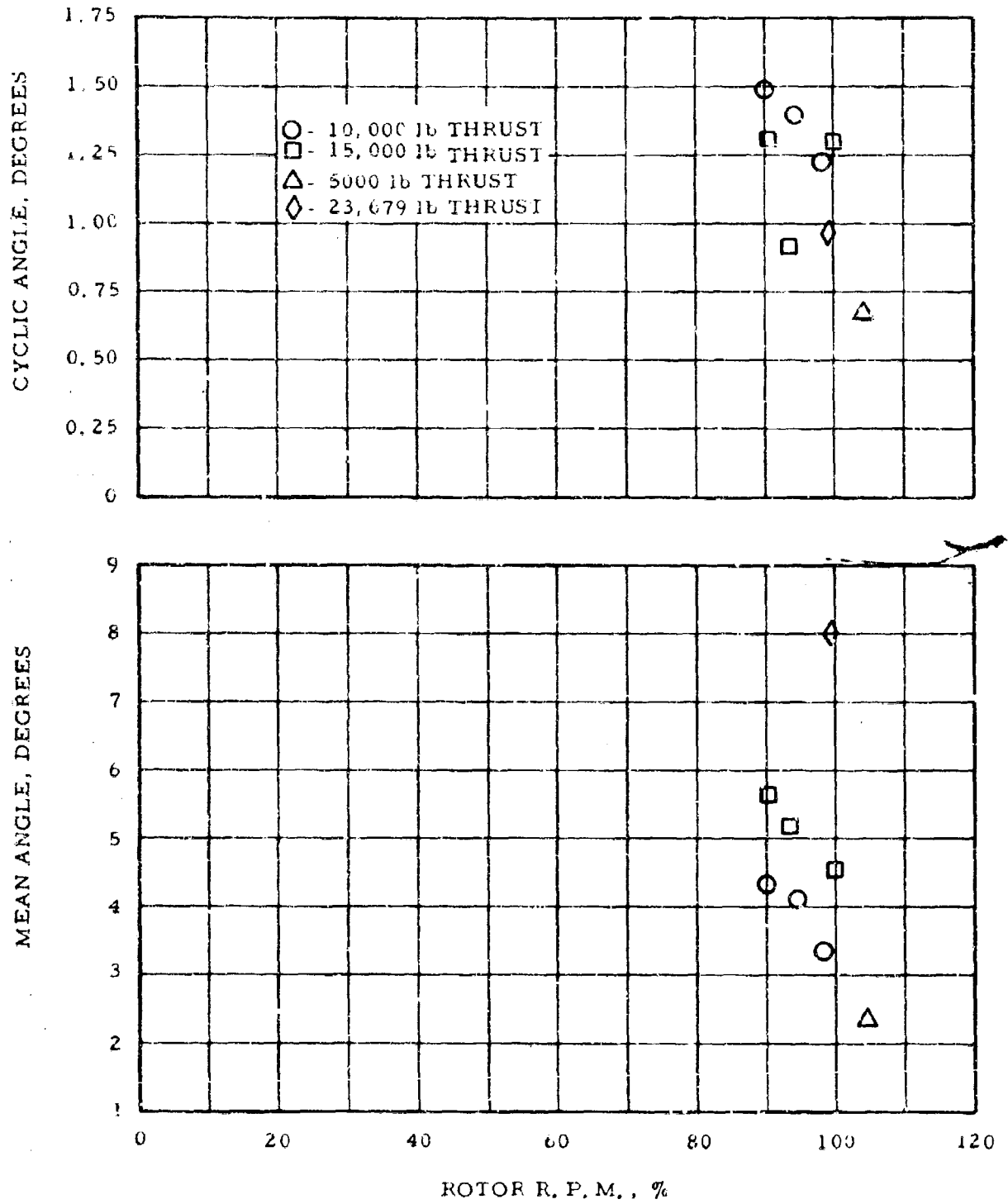


Figure 42. Blue-Blade Feathering Angle

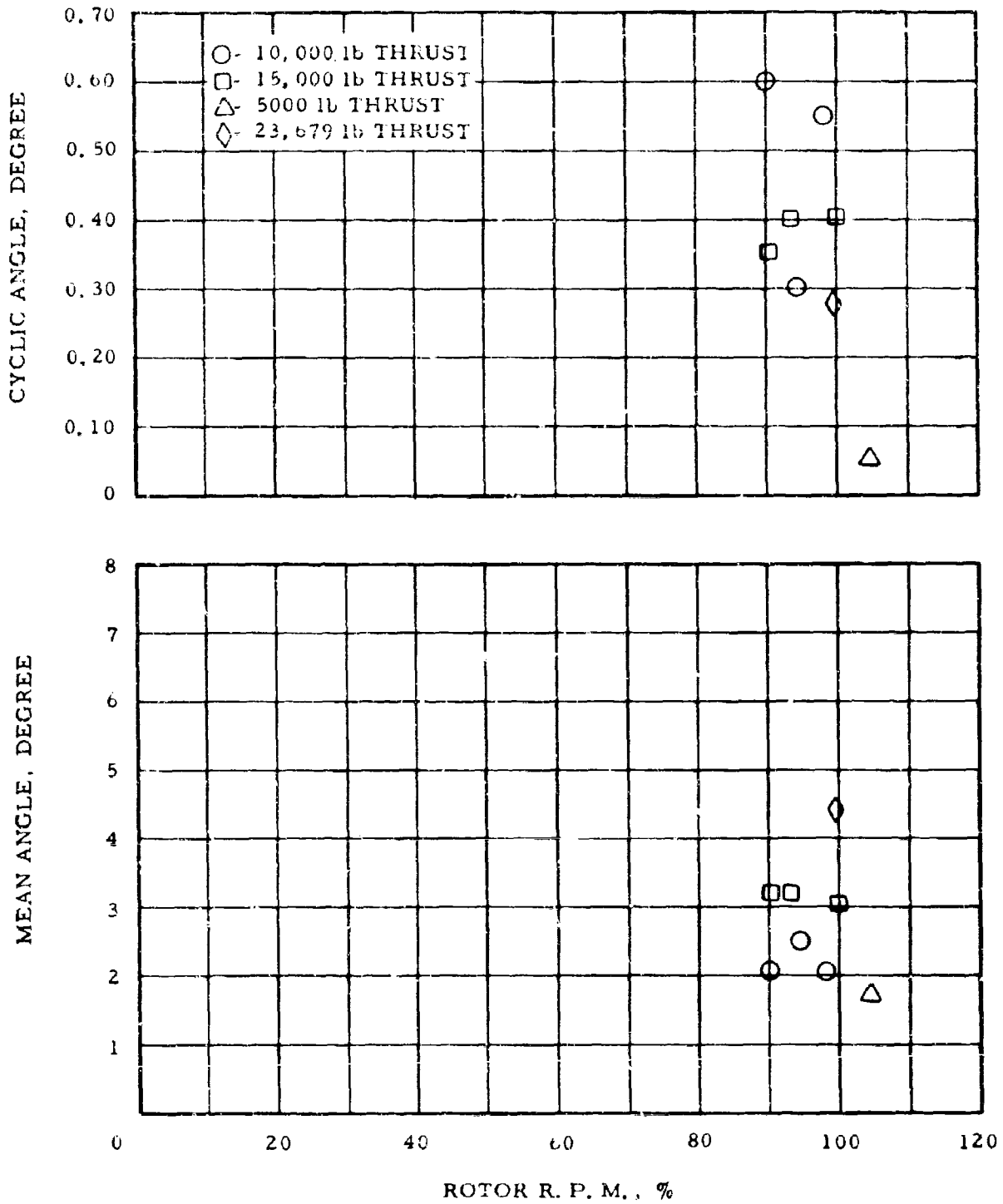


Figure 43. Blue-Blade Flapping Angle

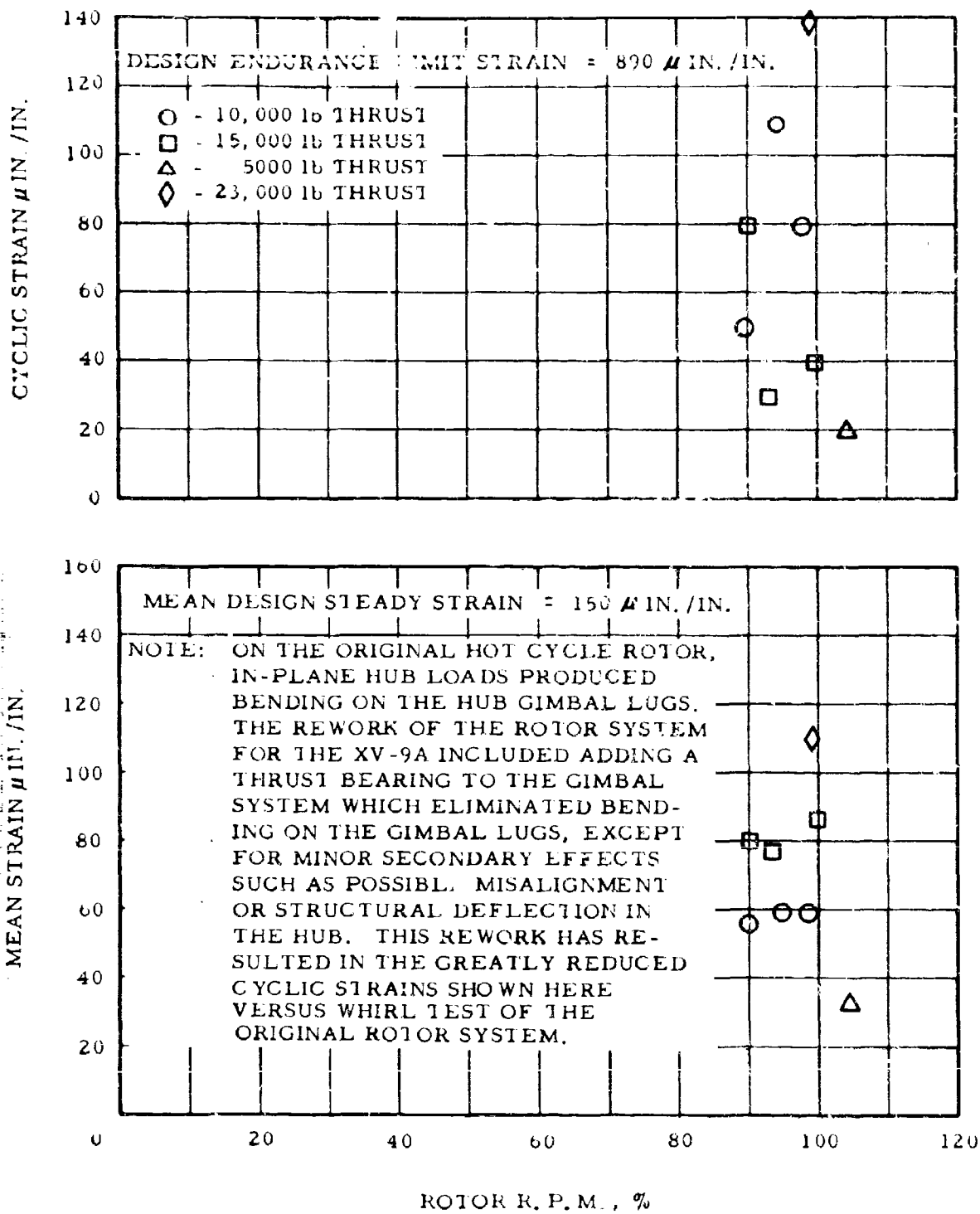


Figure 44. Gimbal Lug Bending Strain

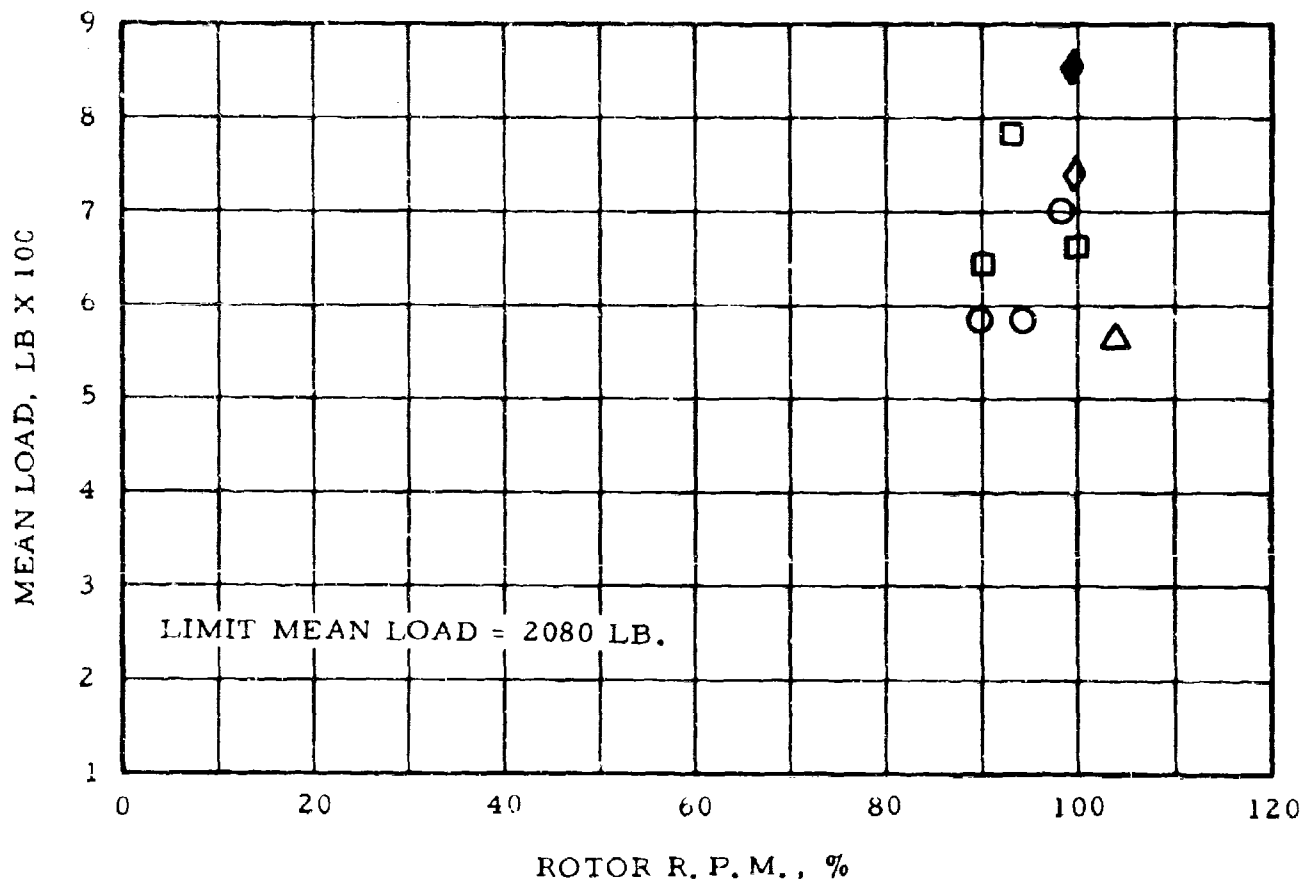
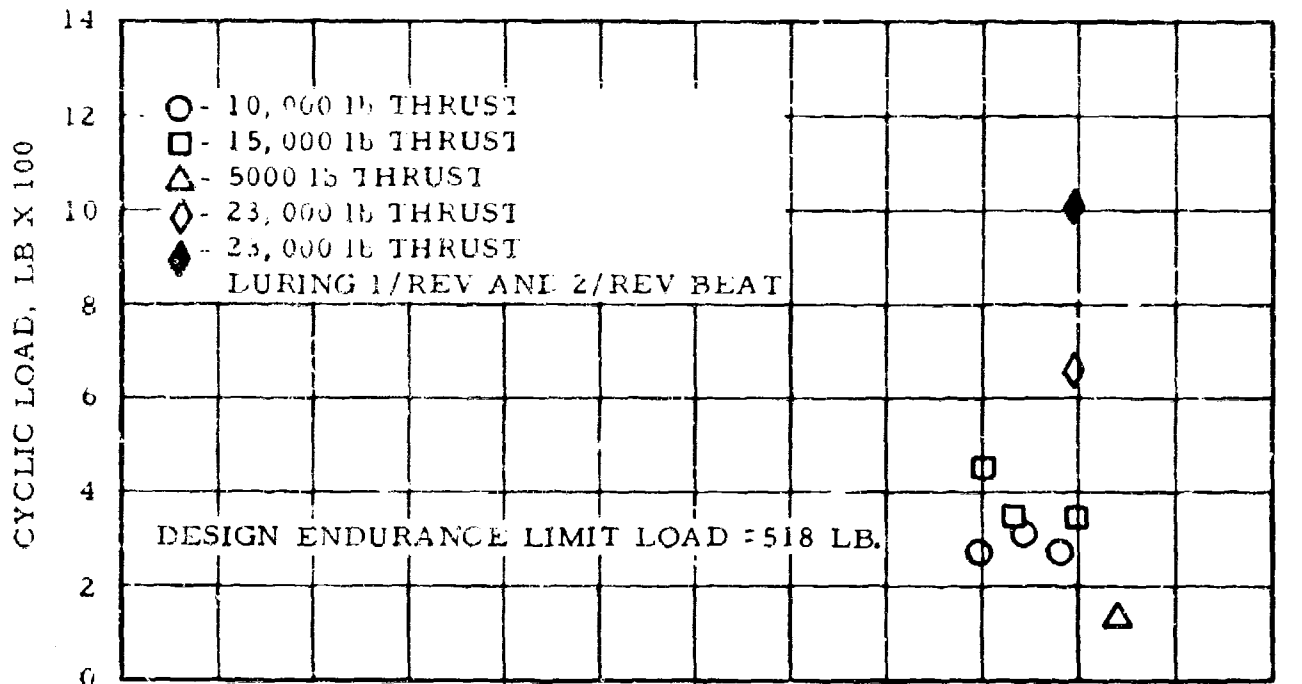


Figure 45. Chordwise Shear at Station 23.0

ROTOR BLADE FRONT SPAR AXIAL LOAD (CYCLIC 1/REV)  
(CHORDWISE MOMENT/15.38IN.), LBS X 1000 AT STA. 90.75

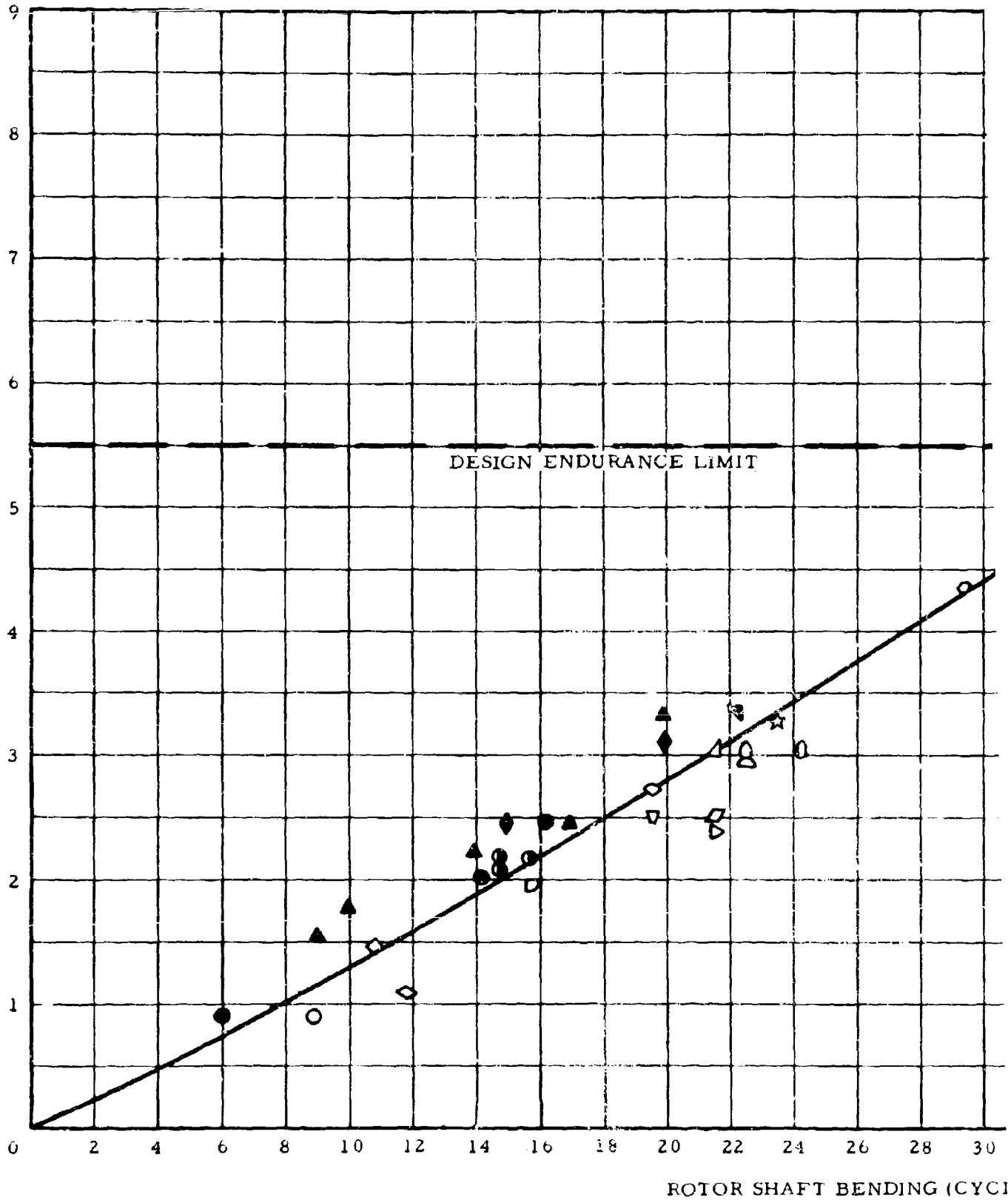
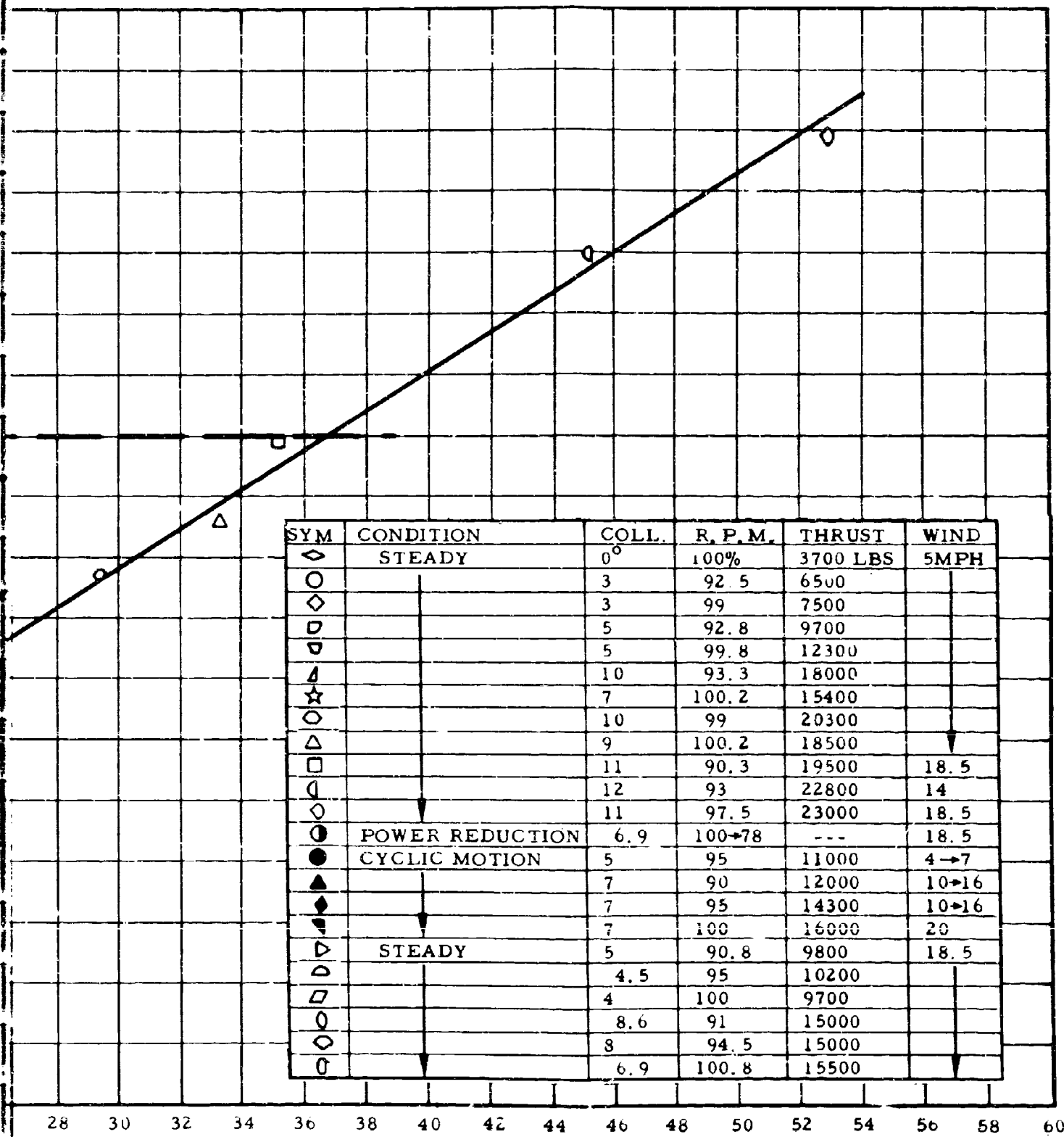


Figure 46. Rotor Blade Front Spar Axial



0 BENDING (CYCLIC 1/REV), IN. -LB X 1000

CLF Spar Axial Load vs. Rotor Shaft Bending

#### 5.4.2 Engine Vibration

During the whirl test program, engine vibration in the low-frequency range (0 - 12 cps) was measured by means of accelerometers, and the level exceeded the engine operating limits during some transient conditions. The installation of strain gages on the engine front frame was subsequently accomplished in accordance with instructions supplied by the engine manufacturer. The resulting stress measurements taken during the whirl test program were well within the allowable fatigue area for the critical front frame areas as established by the engine manufacturer (see Figures 47 through 55). Additional engine vibration measurements were to be obtained during tie-down and flight tests.

#### 5.5 ROTOR DYNAMICS

##### 5.5.1 First Mode Blade Chordwise Bending Frequency

A significant aspect of the present tests was determination of the first mode blade chordwise bending frequency. During the original whirl testing (reported in Reference 2), it was found that this frequency was 1.25/rev, which was close enough to 1/rev excitation that high chordwise stresses were obtained. Prior to the present tests, the spar stiffness was increased. During whirl tests, cyclic control pulses of varying severity were applied at different rotor rpm. In addition, a slow rpm sweep was made to locate resonance points at reduced rotor speed. Results of these (summarized in Figure 56) indicate that the first mode chordwise natural frequency is 1.43/rev. This increased frequency causes the blade to have a lower response to 1/rev excitation and results in lower blade stresses than measured on the original blade under similar conditions.

##### 5.5.2 Blade Flapwise Bending Frequencies

Computations were made of the flapwise (and chordwise) blade bending frequencies for the collective mode (3, 6, 9/rev) and cyclic mode (1, 2, 4, 5, 7, and 8/rev) when the rotor is mounted on a rigid pylon. The results of these calculations are shown in Figures 44 and 45 of Reference 7. These figures indicated that no flapwise resonances should be found in the normal rotor operating range of 225 to 255 rpm. Examination of the flapwise bending gages taken during the whirl tests showed that, as predicted, no flapwise bending resonances are located in the normal rotor operating rpm range.

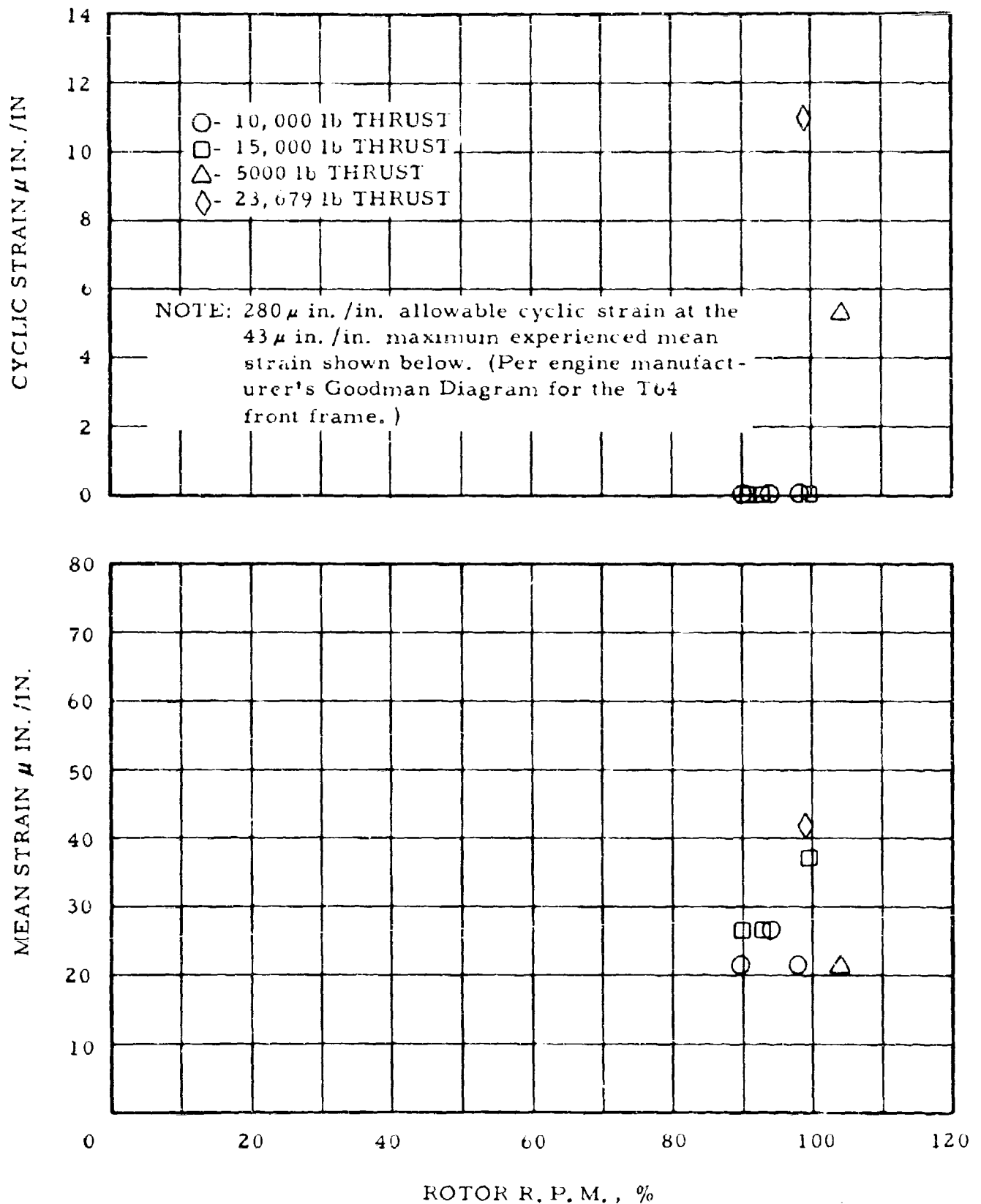


Figure 47. Engine No. 2 - Accessory Gearbox Pad Strain - Parallel to Eng.  $\phi$

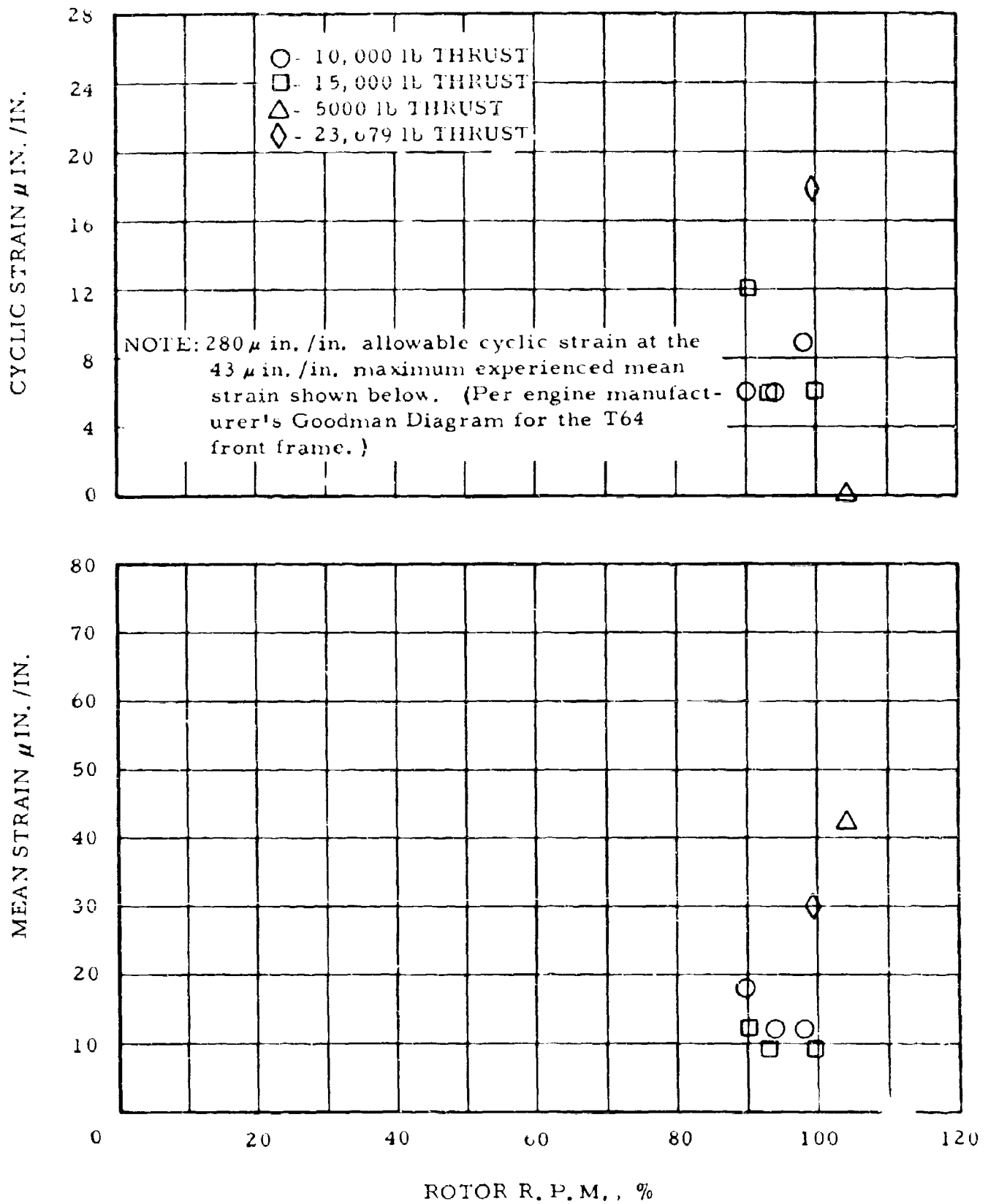


Figure 48. Engine No. 2 - Accessory Gearbox Strain - 45 Degrees to Eng.  $\phi$

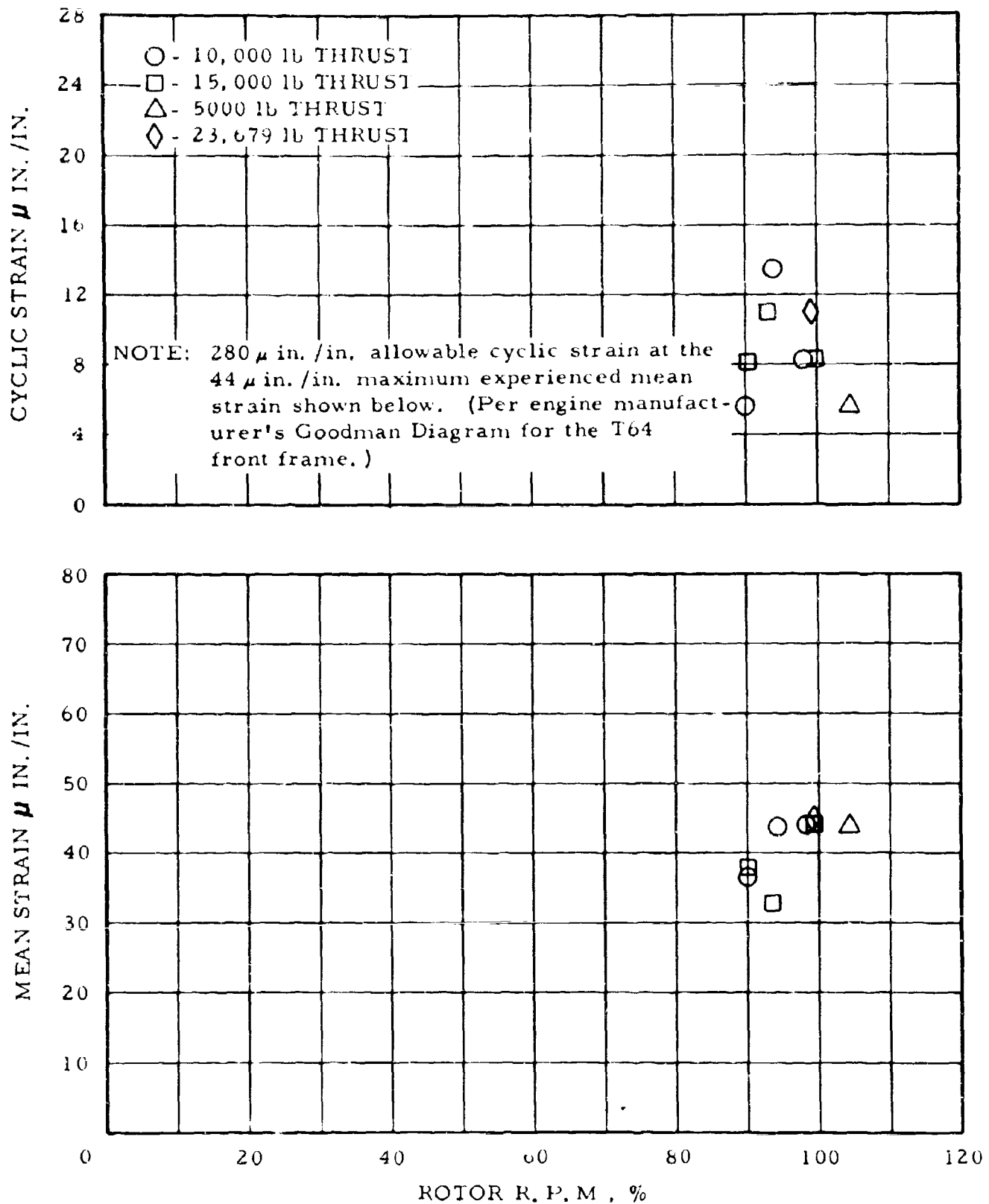


Figure 49. Engine No. 2 - Accessory Gearbox Strain - 90 Degrees to Eng.  $\phi$

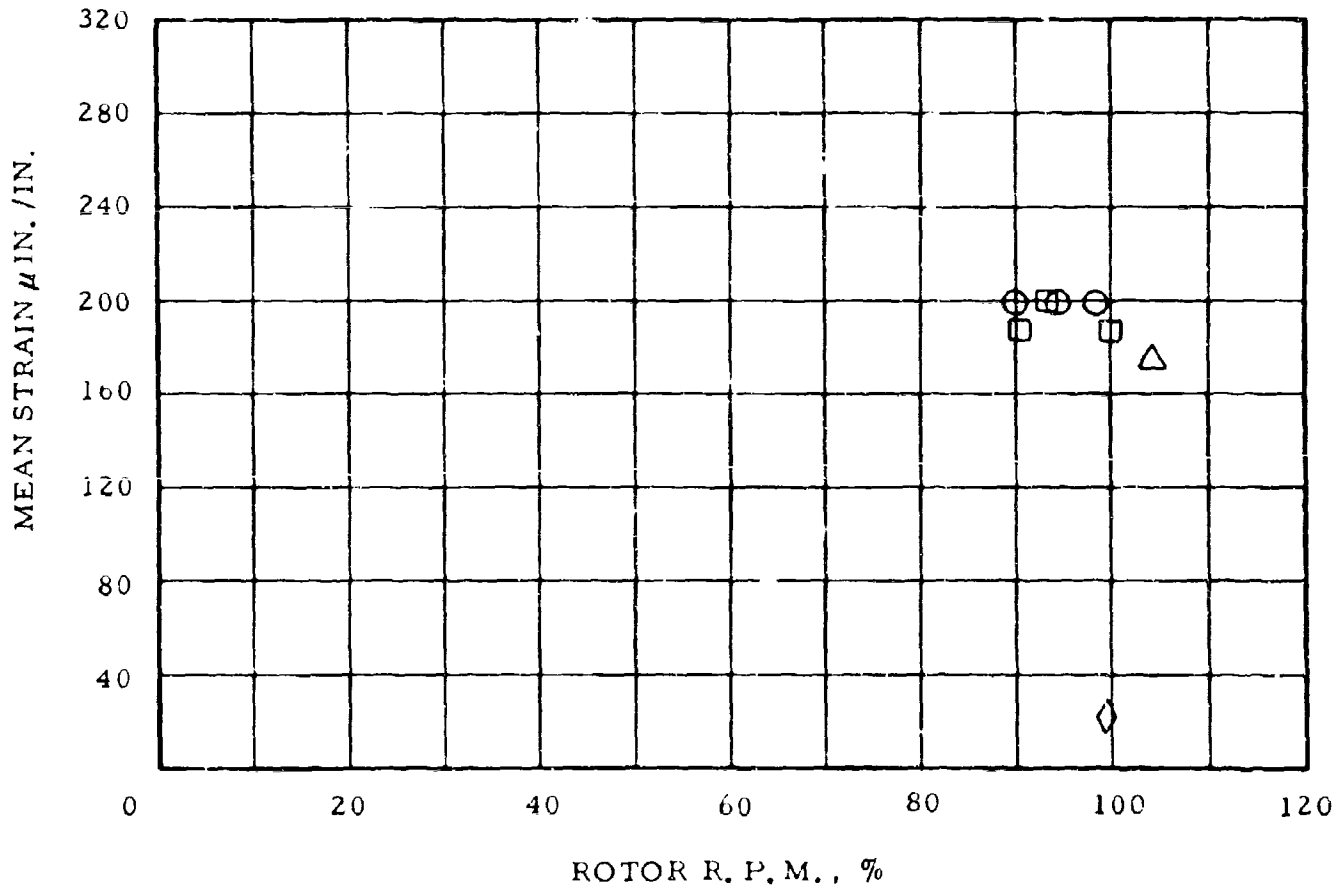
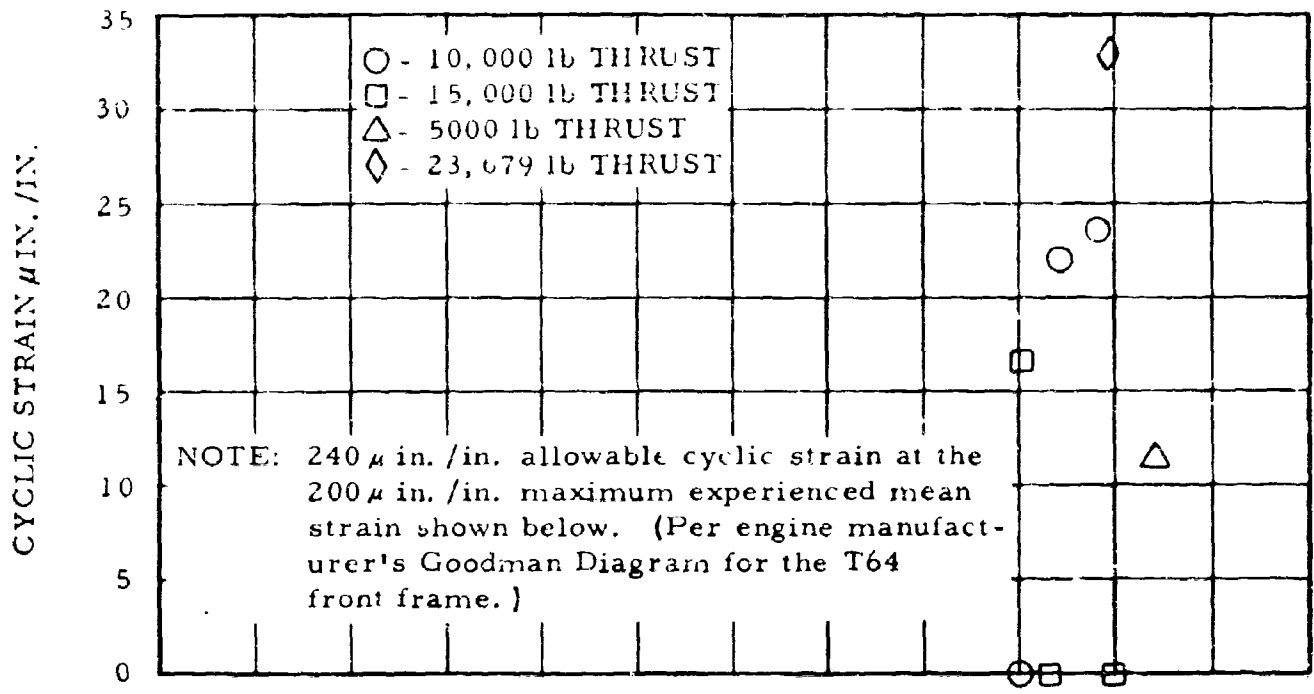


Figure 50. Engine No. 2 Lower R. H. Pad Strain

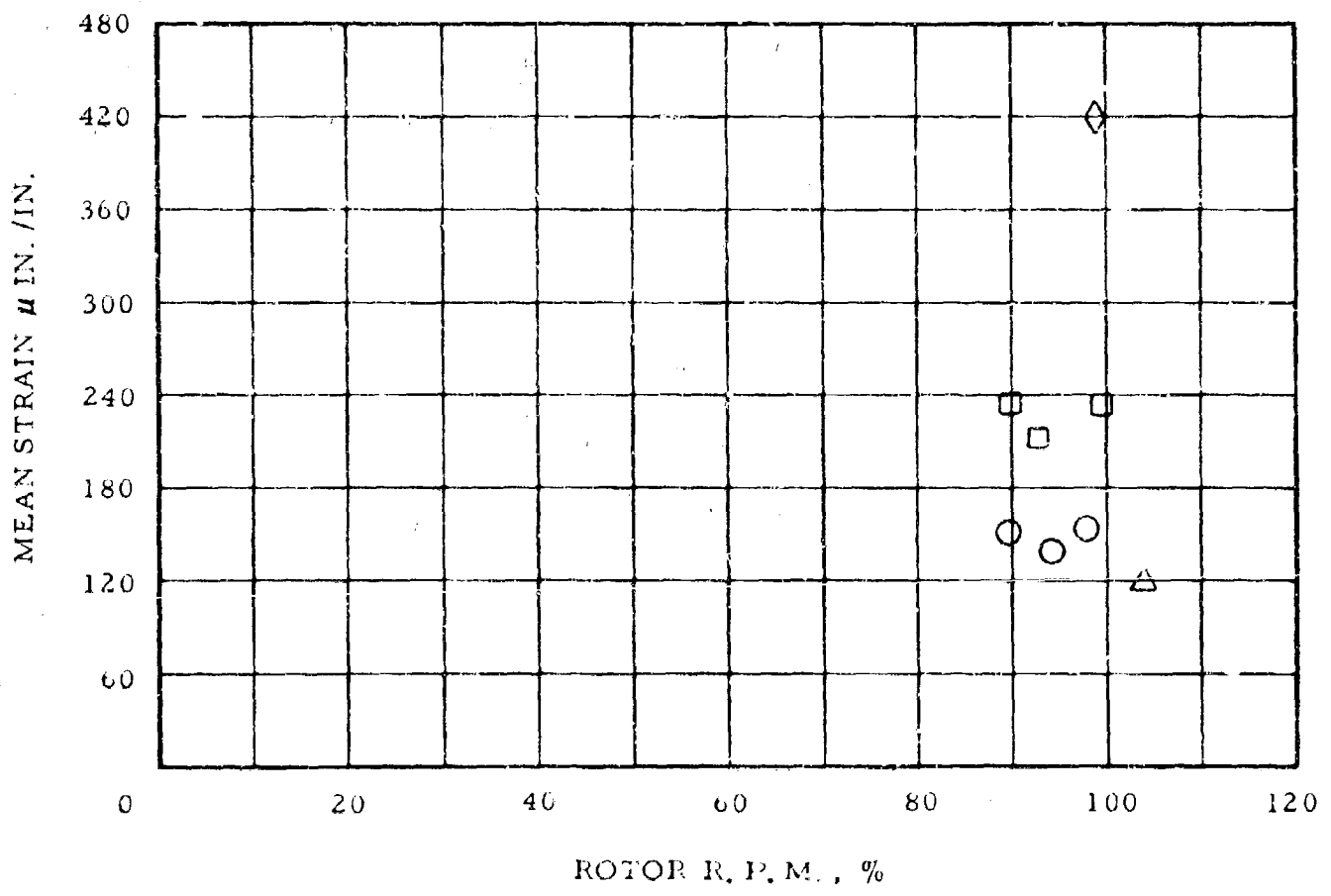
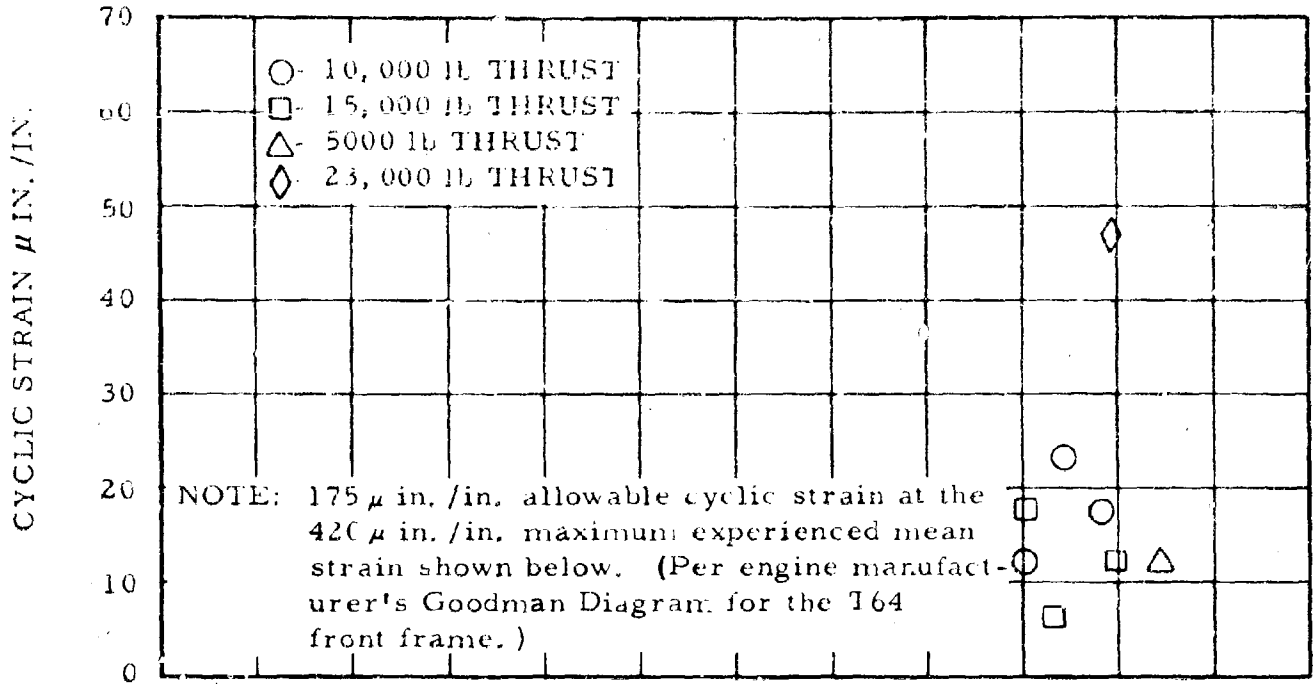


Figure 51. Engine No. 2 Aft R. H. Pad Strain

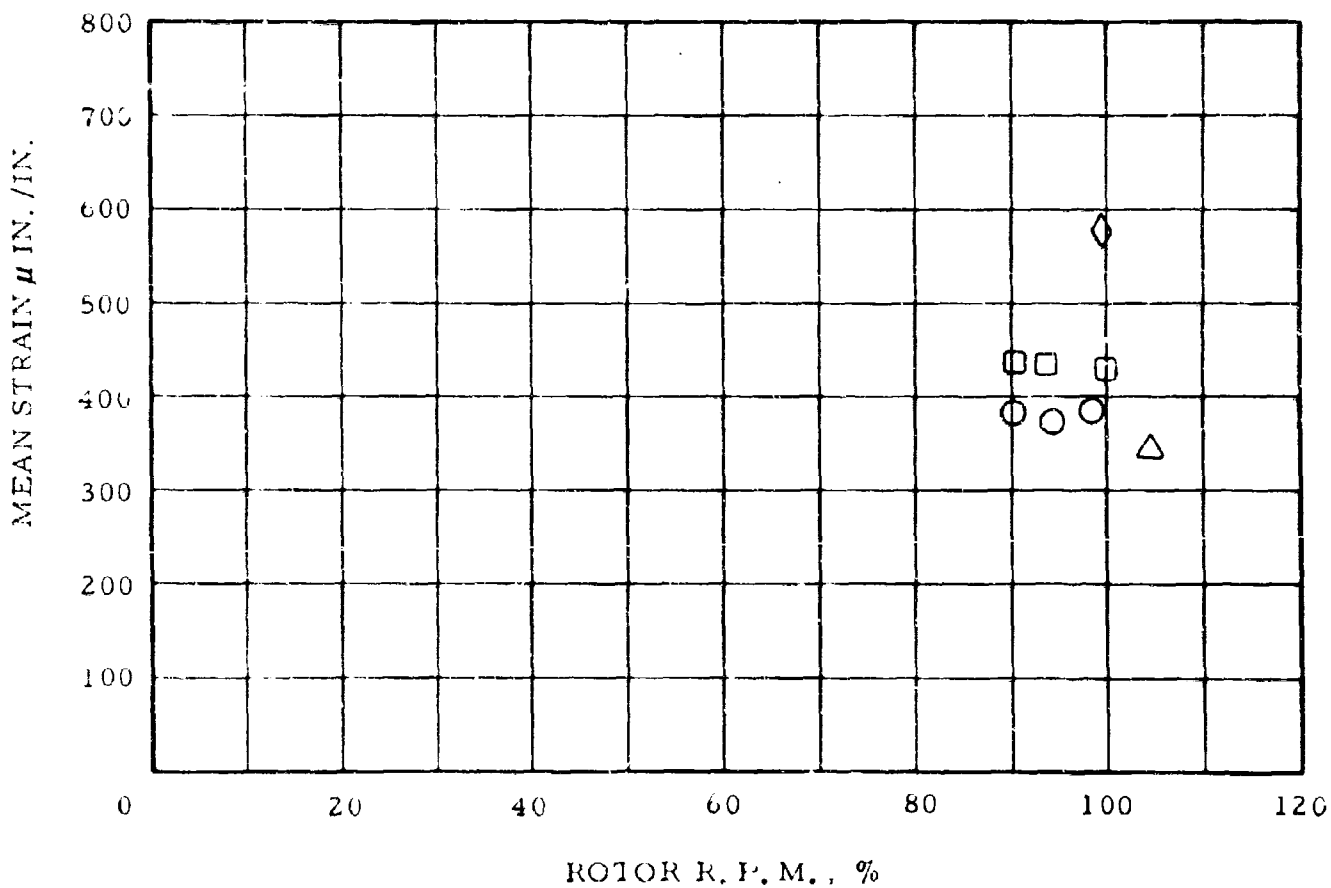
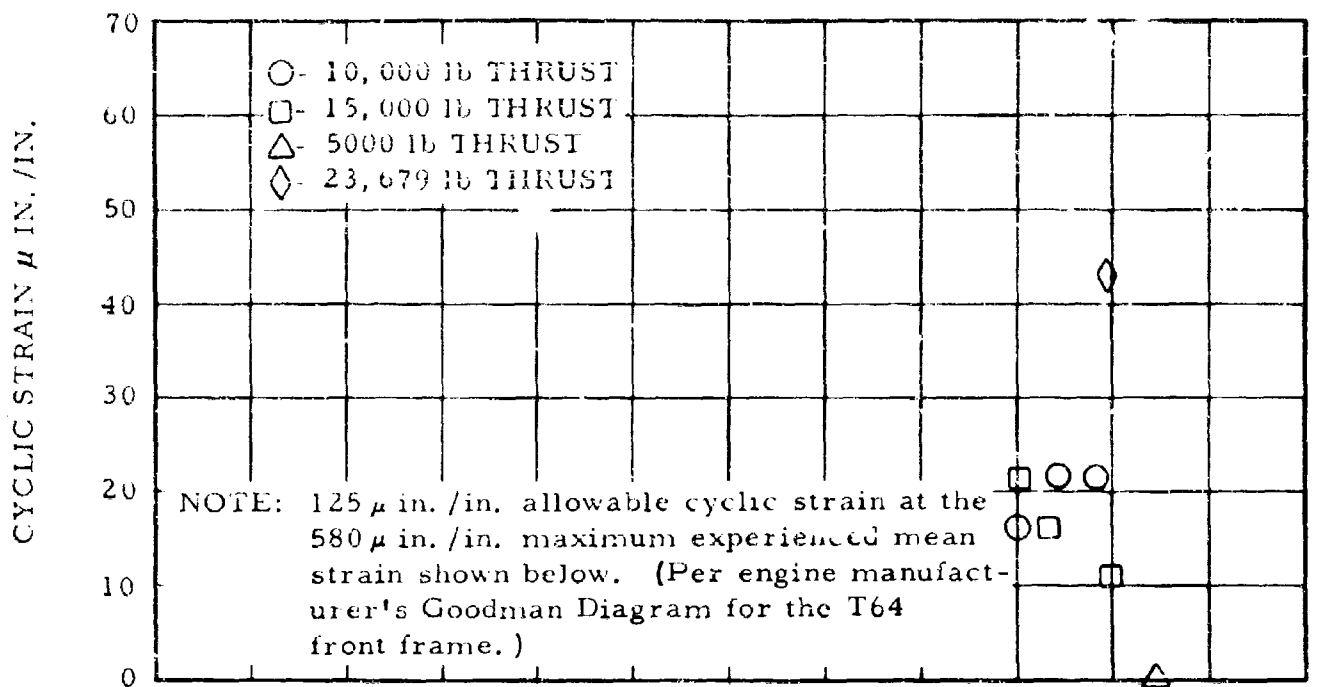


Figure 52. Engine No. 2 Upper R. H. Pad Strain

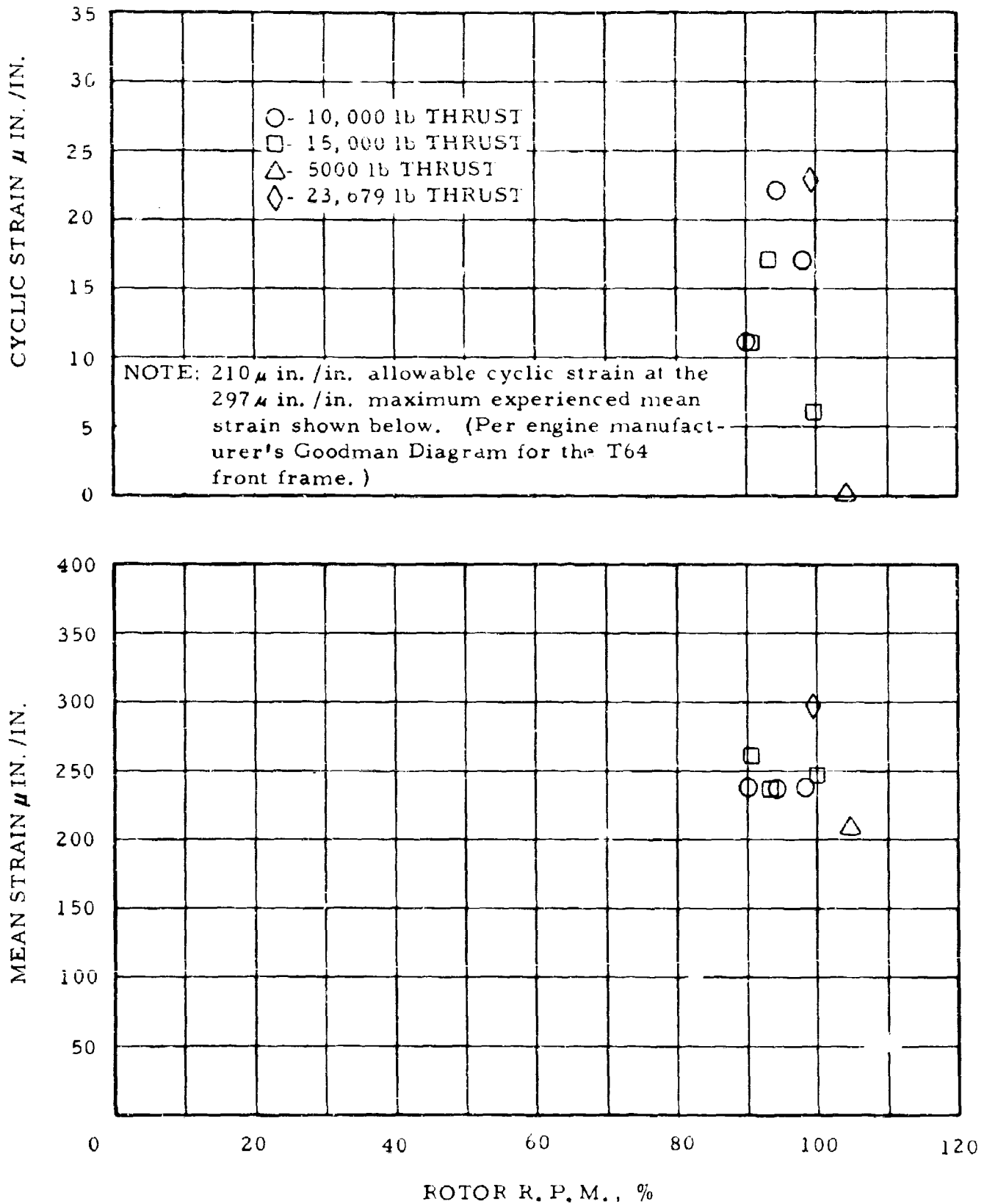


Figure 53. Engine No. 2 Upper L. H. Pad Strain

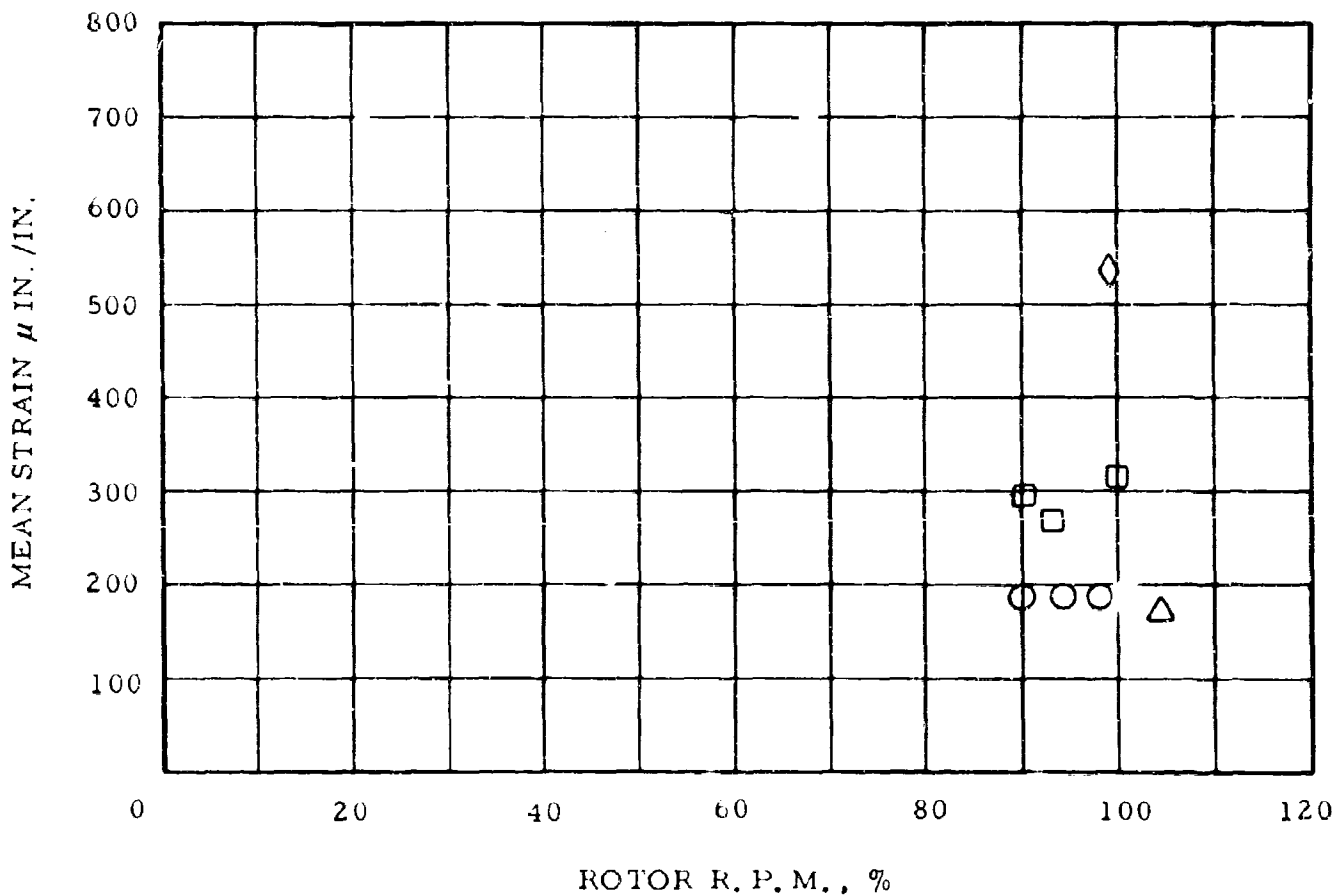
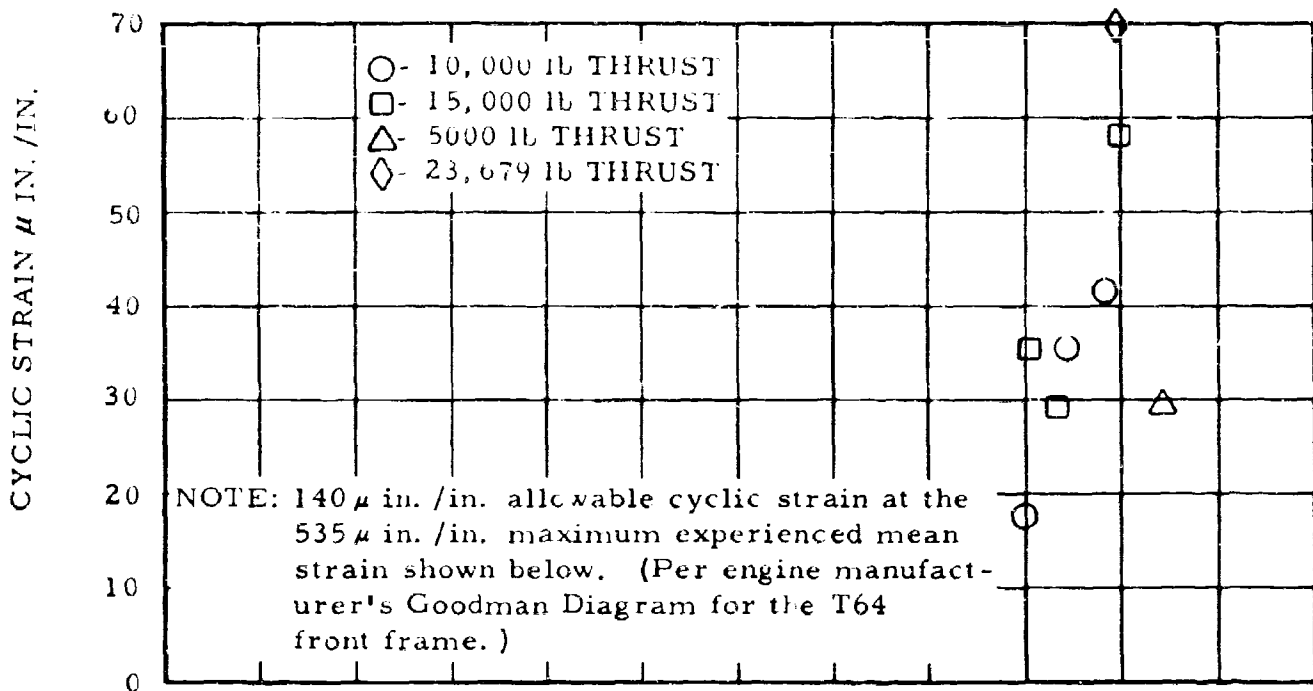


Figure 54. Engine No. 2 Aft L. H. Pad Strain

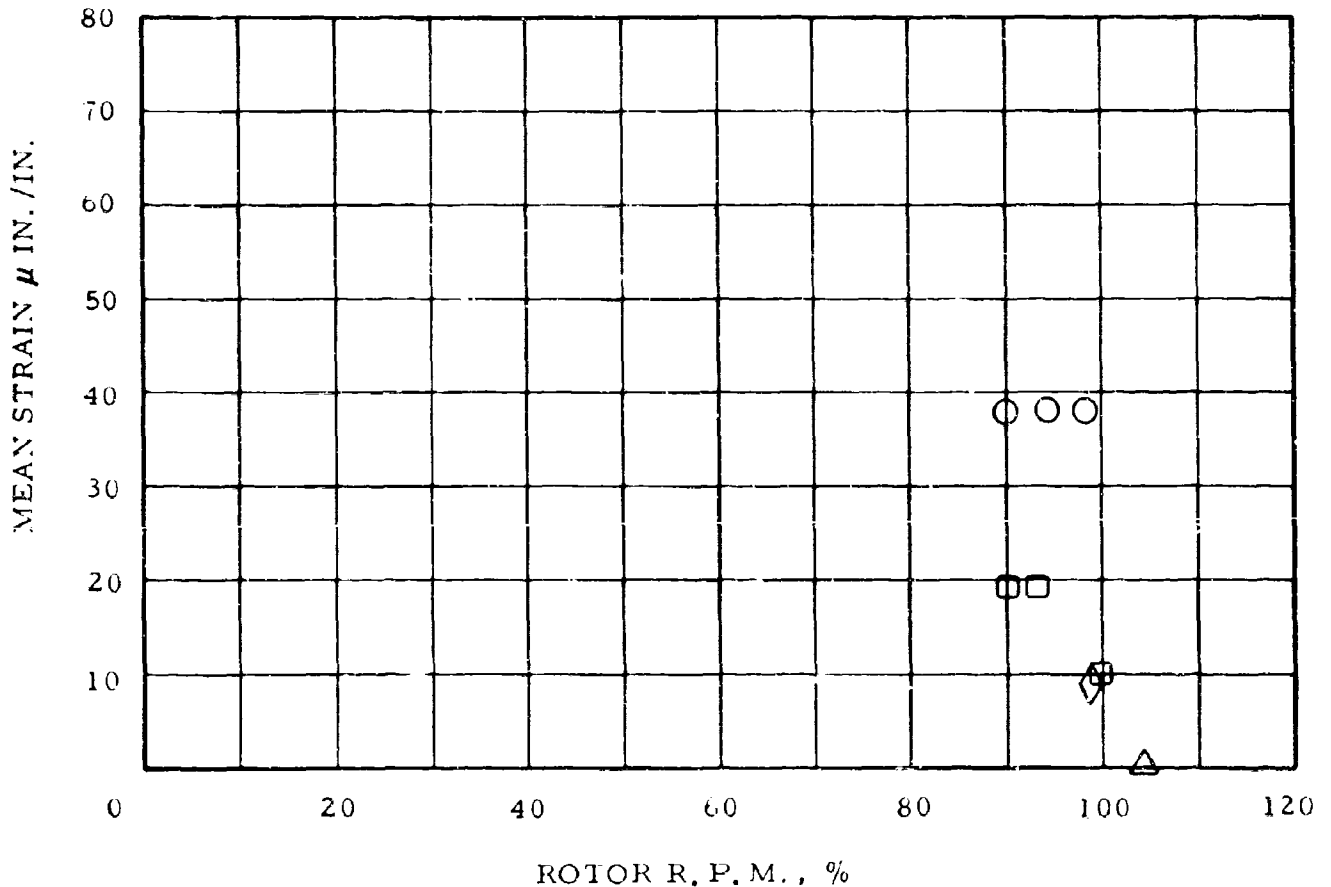
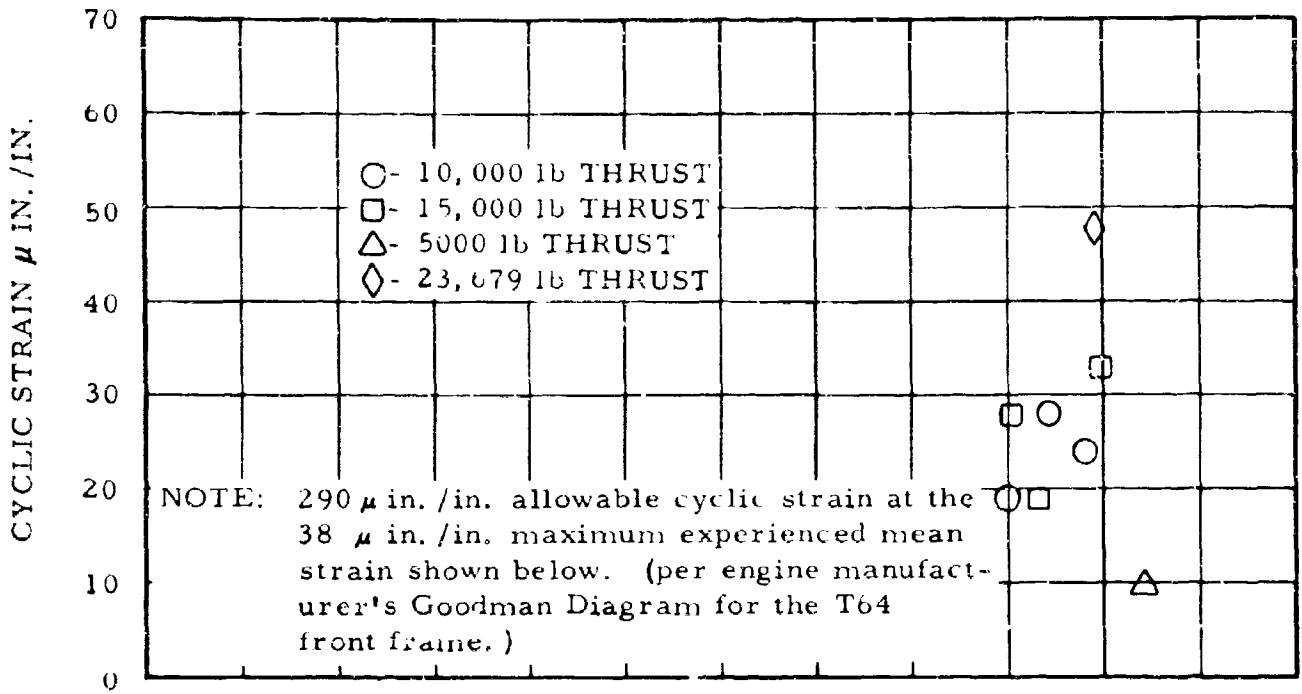


Figure 55. Engine No. 2 Lower L.H. Pad Strain

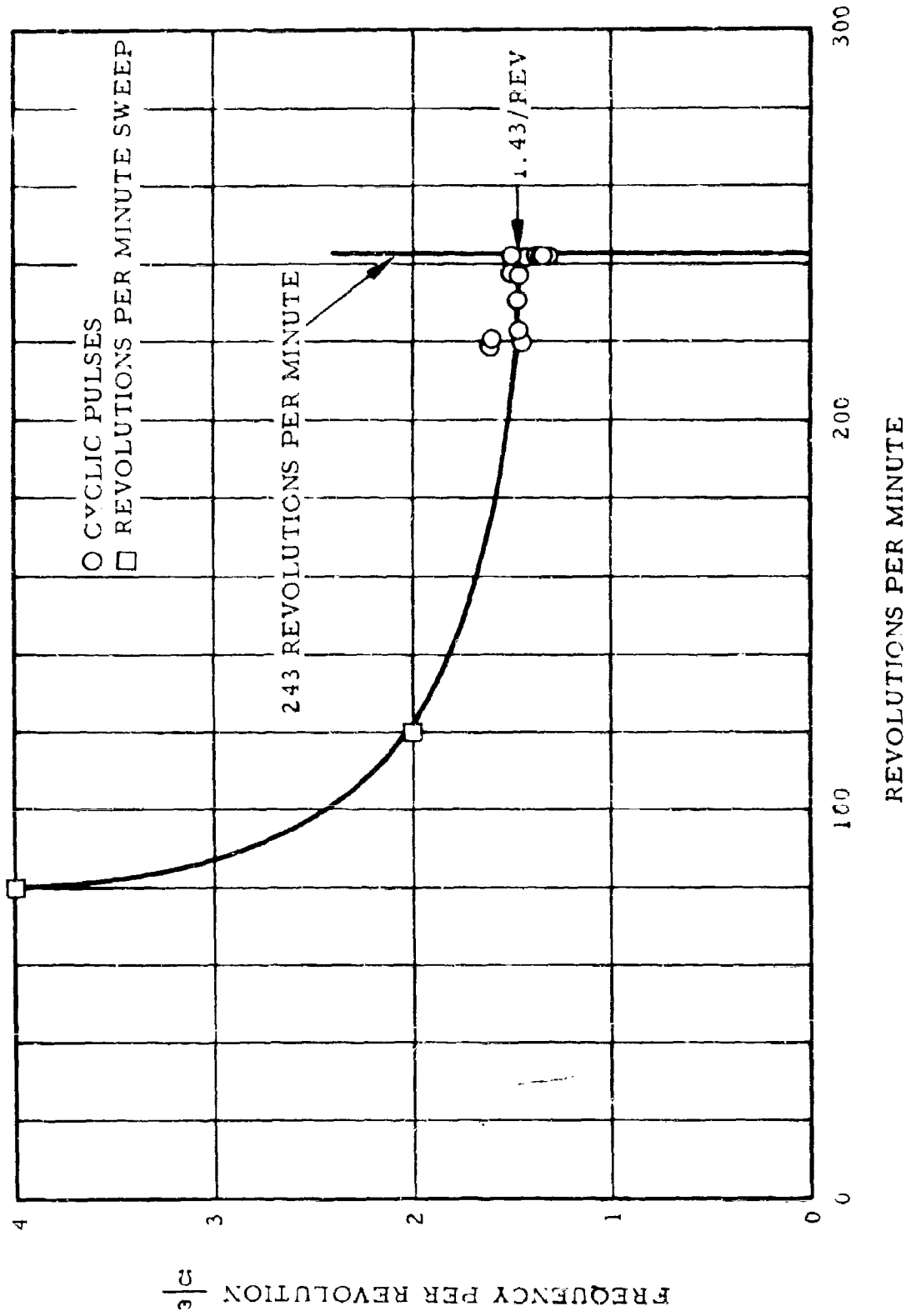


Figure 56. First Chordwise Cantilever Mode Natural Frequency per Revolution vs. RPM

### 5.5.3 Coupling Between Chordwise Blade Mode and Pylon Bending Mode

It was pointed out in the section on structural loads that large 2/rev chordwise bending moments were observed near full rotor speed (90 percent to 105 percent rpm). Such a chordwise response was not predicted in the frequency analysis of the rotor on a rigid pylon summarized in Figures 44 and 45 of Reference 7. Analysis of this 2/rev response indicated that it was due to coupling of the first chordwise bending of the blade with bending of the rotor pylon.

This analysis, which involved the coupled modes of a gimbaled rotor on a flexible pylon, considered motions in the plane of the rotor, including motions of the hub and chordwise bending of the blades. The coupled analysis required knowledge of the blade chordwise bending mode frequency (1.4/rev) and pylon bending frequency (measured as 8 cps, or 2/rev, with rotor attached, but not turning). The calculations are summarized in Figure 57, which shows frequency in the nonrotating system plotted against percent of rotor speed.

The calculations show that the coupled pylon-blade system (which can respond in the nonrotating system only to 3/rev, because the rotor has three blades) has four predicted resonance points in the range from 35 percent of rotor speed to 100 percent rotor speed. These four resonances occur due to the effect of rotor rotation on the pylon-blade system. The rotor rotation causes a two-branched curve to spring from each of the basic two resonance points of the nonrotating coupled blade-pylon system. The change in coordinates from rotating to nonrotating system (which will respond only to 3/rev) requires that excitation be caused by 2/rev and 4/rev excitation on the blade in the rotating system. Of the four resonance points predicted on Figure 57, three have been located on the oscillograph records (with the harmonic as indicated). The last one (4/rev on the blade at 61 percent rpm) was masked by a cyclic mode flapwise resonance predicted for this reduced rpm region (see Figure 45, Reference 7).

The results shown here indicate that the observed 2/rev blade stresses near 100 percent rpm are in fact due to coupling of the blade and pylon on the whirl stand. This same coupling was observed in whirl stand tests of a similar 3-bladed jet-driven rotor (the 75-foot McDonnell XHCH rotor) reported in Reference 8.

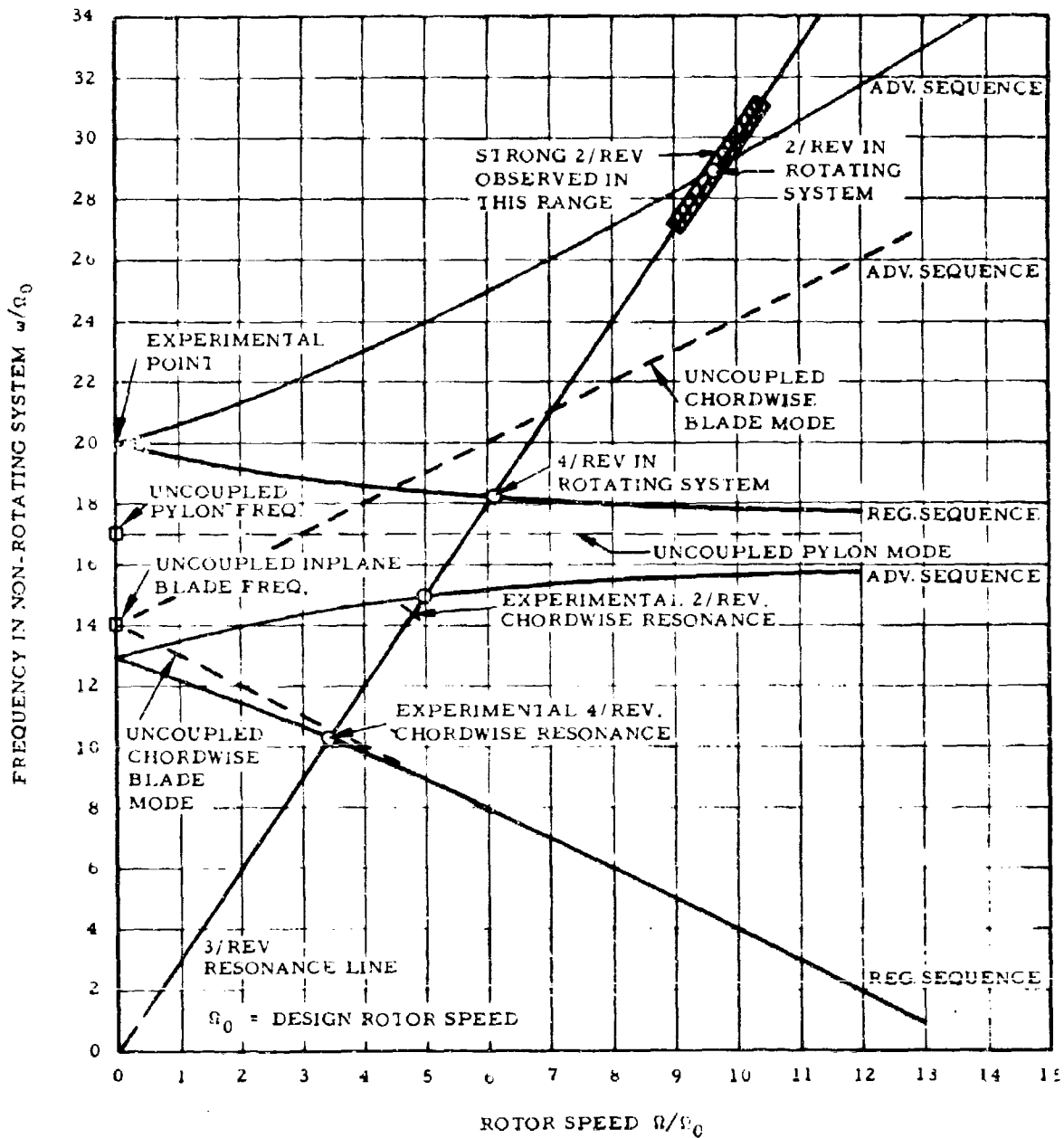


Figure 57. Coupled Pylon Blade Frequencies of Rotor on Whirl Stand vs. Rotor Speed

The 2/rev response noted during whirl testing is therefore characteristic of the system involving the rotor and the pylon mounted on the whirl stand. The situation that will be obtained with the rotor mounted on the actual aircraft will be different, due to different response characteristics of the rotor pylon when mounted on the XV-9A fuselage.

#### 5.6 ROTOR CONTROL DEFLECTIONS

Rapid cyclic control reversals were performed to evaluate control response, rotor stresses, and loads in control system components. Copies of oscillograph records taken during a typical lateral longitudinal reversal is shown on Figures 60 and 61. Cyclic control operation was smooth and stable with negligible control forces. Structural loads were low for these deflections.

Rapid collective power transients were performed to investigate effect on rotor stresses and to evaluate control response. A collective input from  $\theta = 2.25$  degrees to  $\theta = 9.85$  degrees and return to  $\theta = 2.25$  degrees is shown on Figures 62 and 63. Control response was smooth, and all structural loads were within the allowable limits. These collective power transient tests were performed using manually coordinated engine power control. The rotor droop at maximum thrust (15,800 pounds) was approximately 10 percent. The complete transient was performed in 10 seconds.

Copies of oscillograph setup sheets showing identification of traces and trace sensitivities for Figures 58 through 63 are included as Table 5.

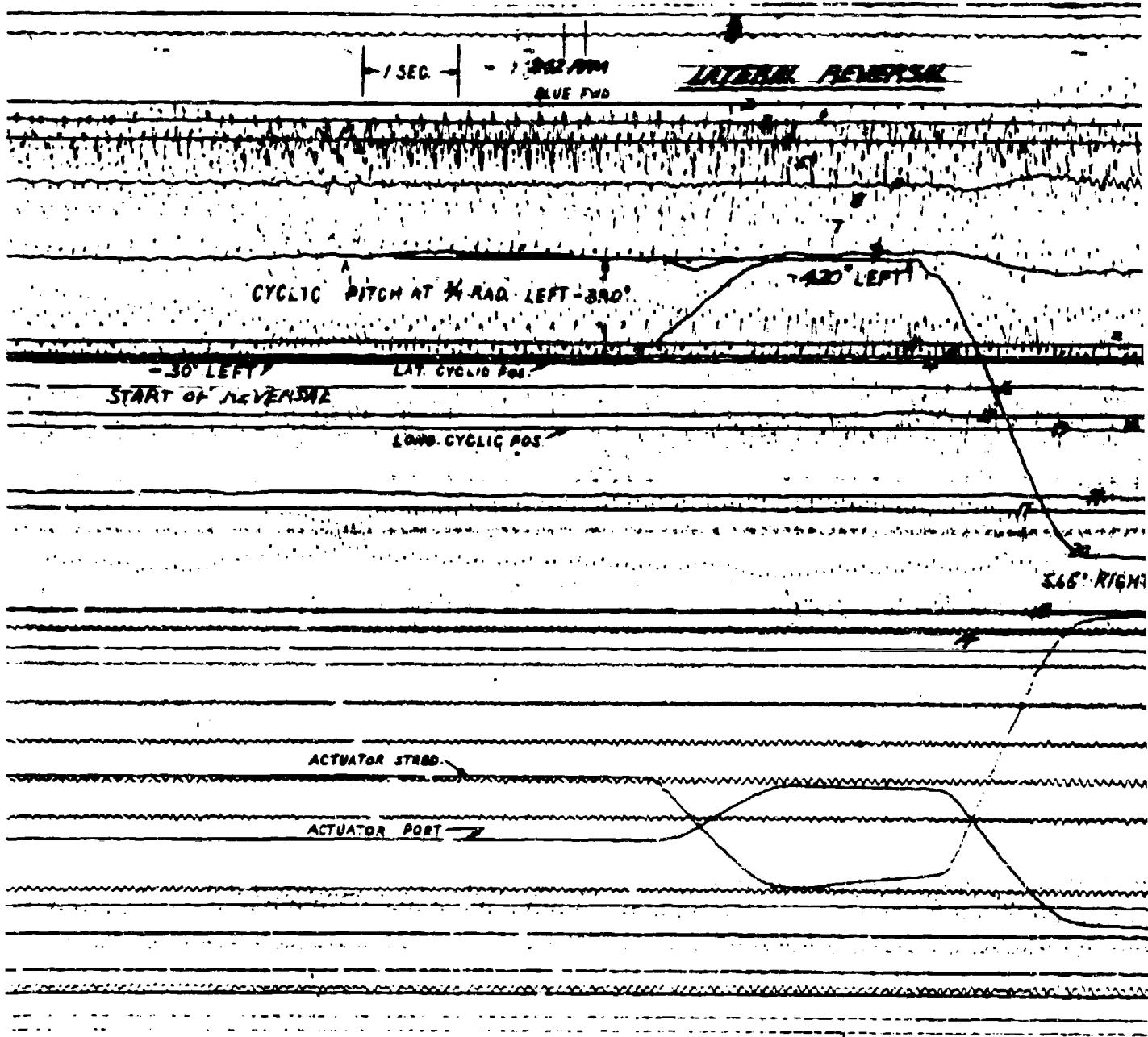


Figure 58. Lateral Cyclic Reversal,  $N_R = 99.6$  Percent

OSC 1

3-2

THROAT

15° RIGHT RAD. OF REVERSAL

550° RIGHT CYCLIC PITCH AT  $\frac{1}{4}$  RAD.

565° RIGHT

1 INCH

Reversal, Run 31, 14 May 1964  
percent

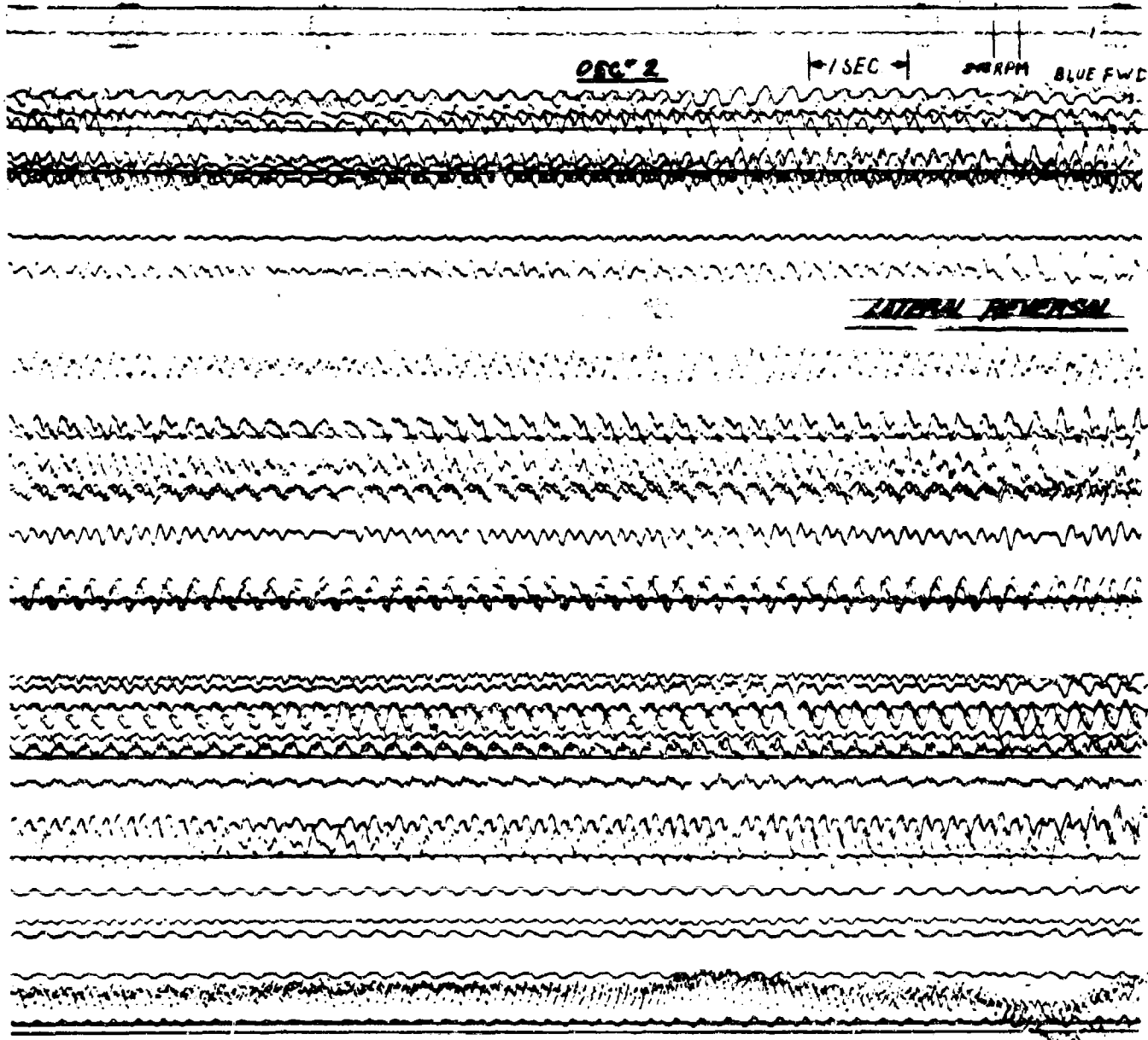
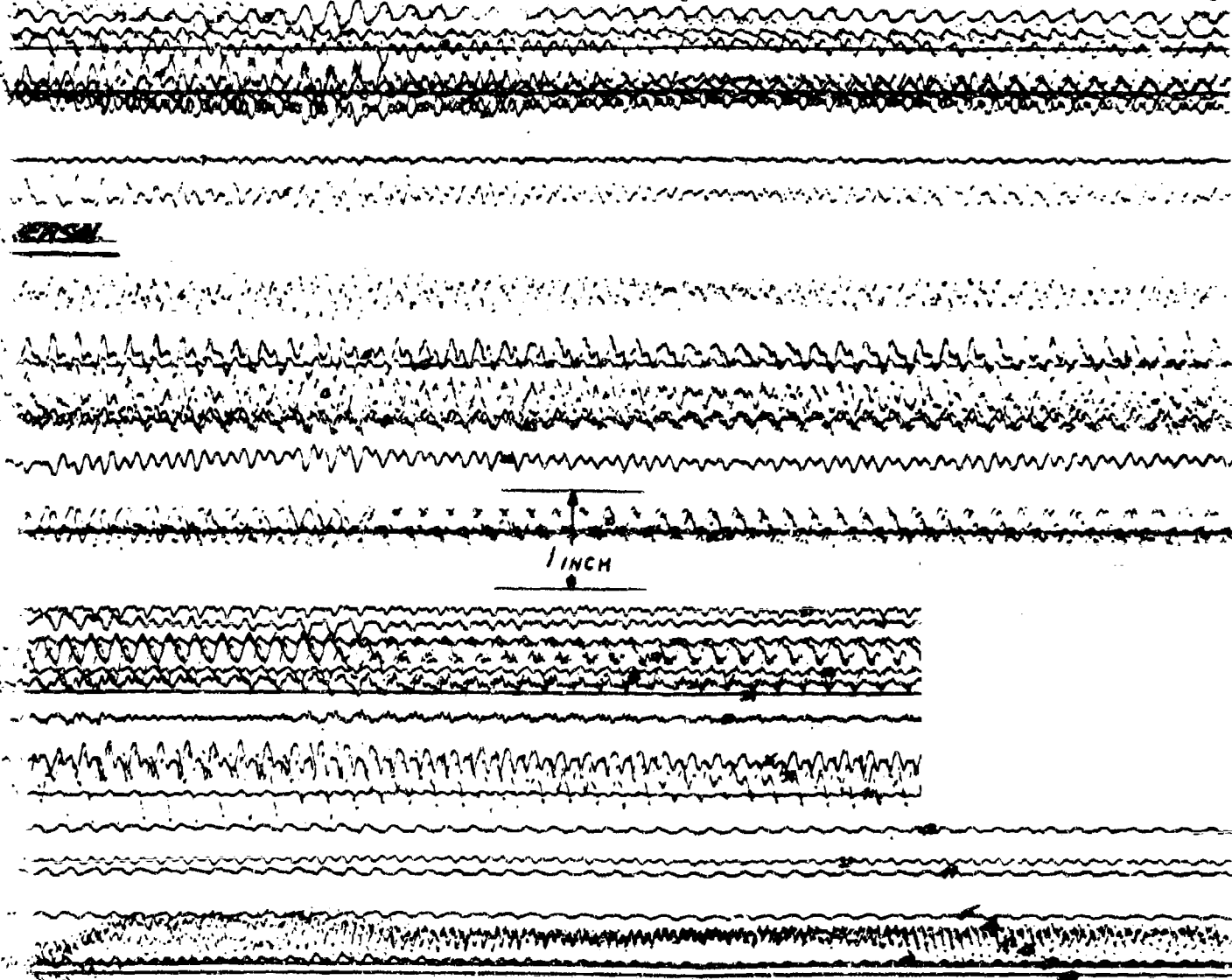


Figure 59. Lateral Cyclic Re  
 $N_R = 99.6$  Perc

BLUE FWD

MAY 21  
1964  
5-14-64



clie Reversal, Run 31, 14 May 1964  
6 Percent



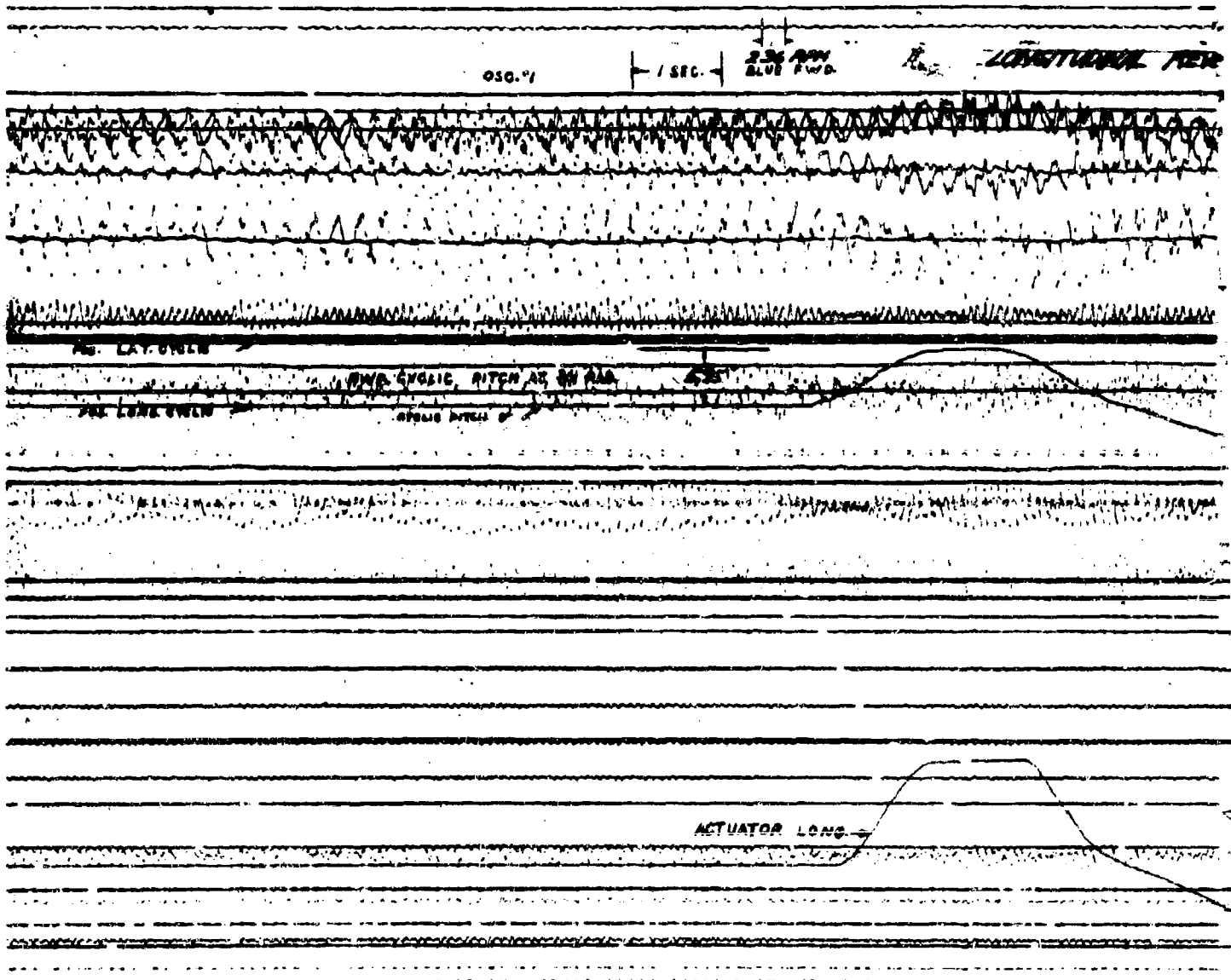
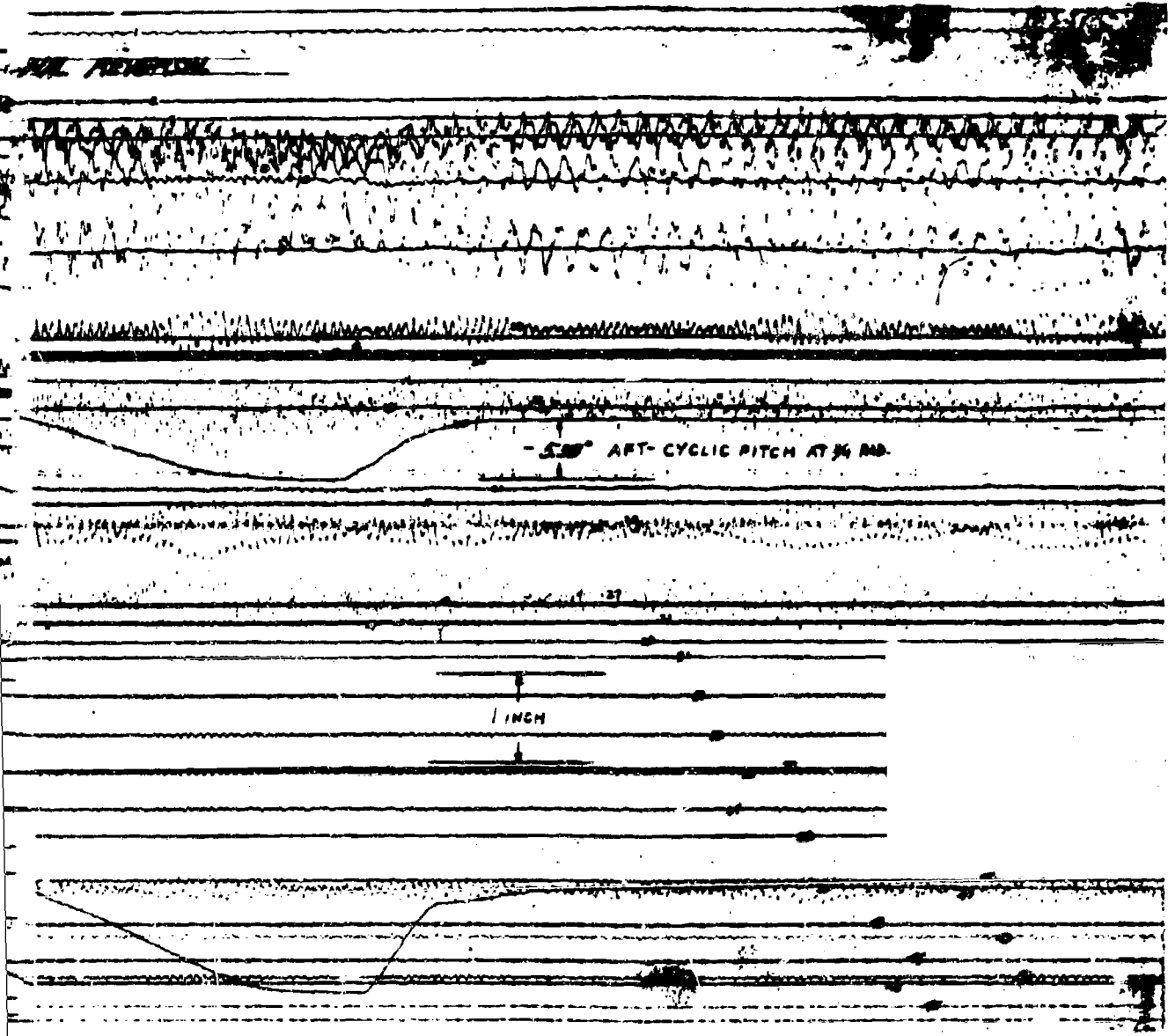


Figure 60. Longitudinal Cyclic Reverse  
 $N_R = 97.1$  Percent



- 500° APT- CYCLIC PITCH AT 36 MB

1 INCH

Reversal, Run 31, 14 May 1964

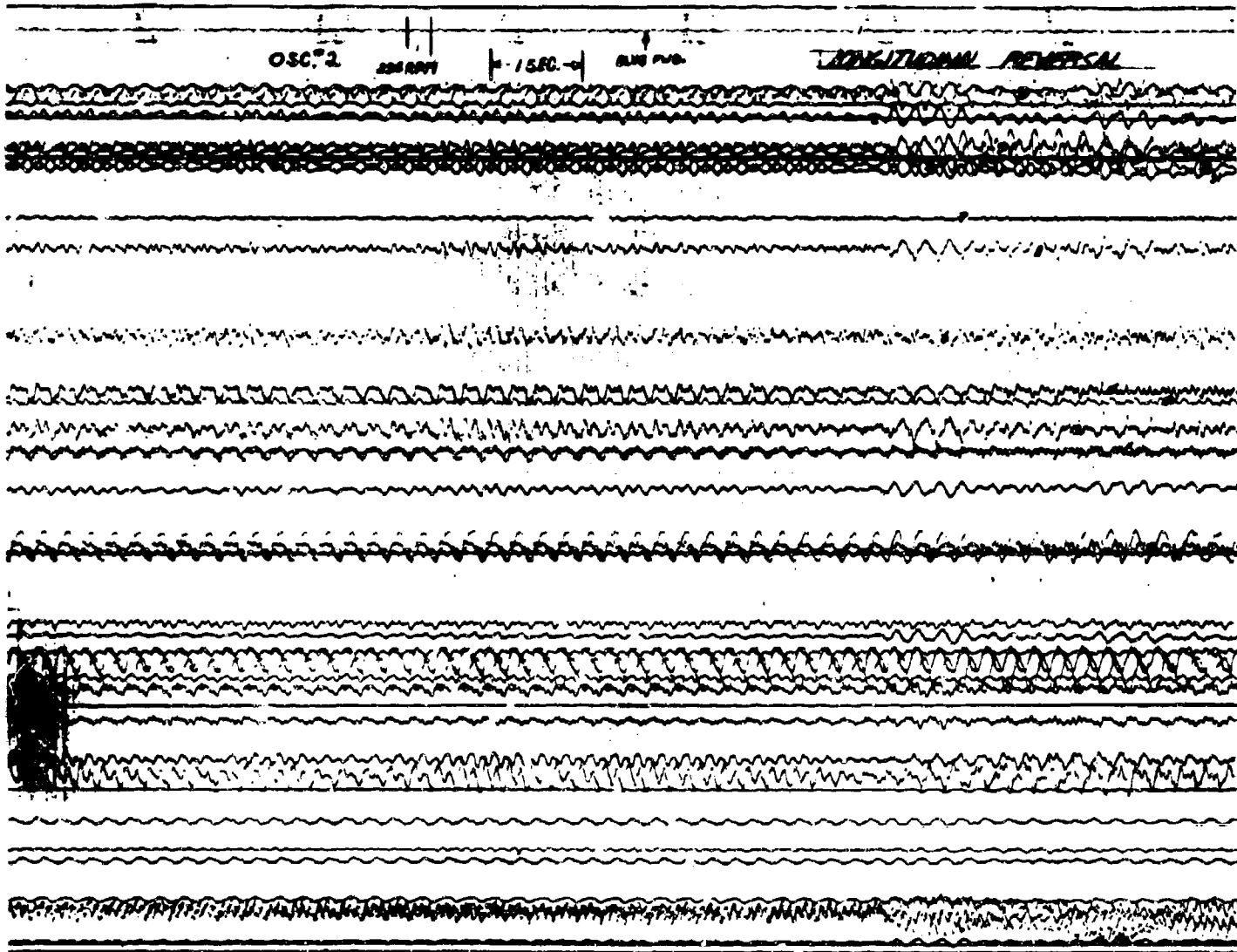
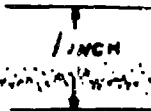


Figure 61. Longitudinal Cyclic Reversal,  
 $N_R = 97.1$  Percent

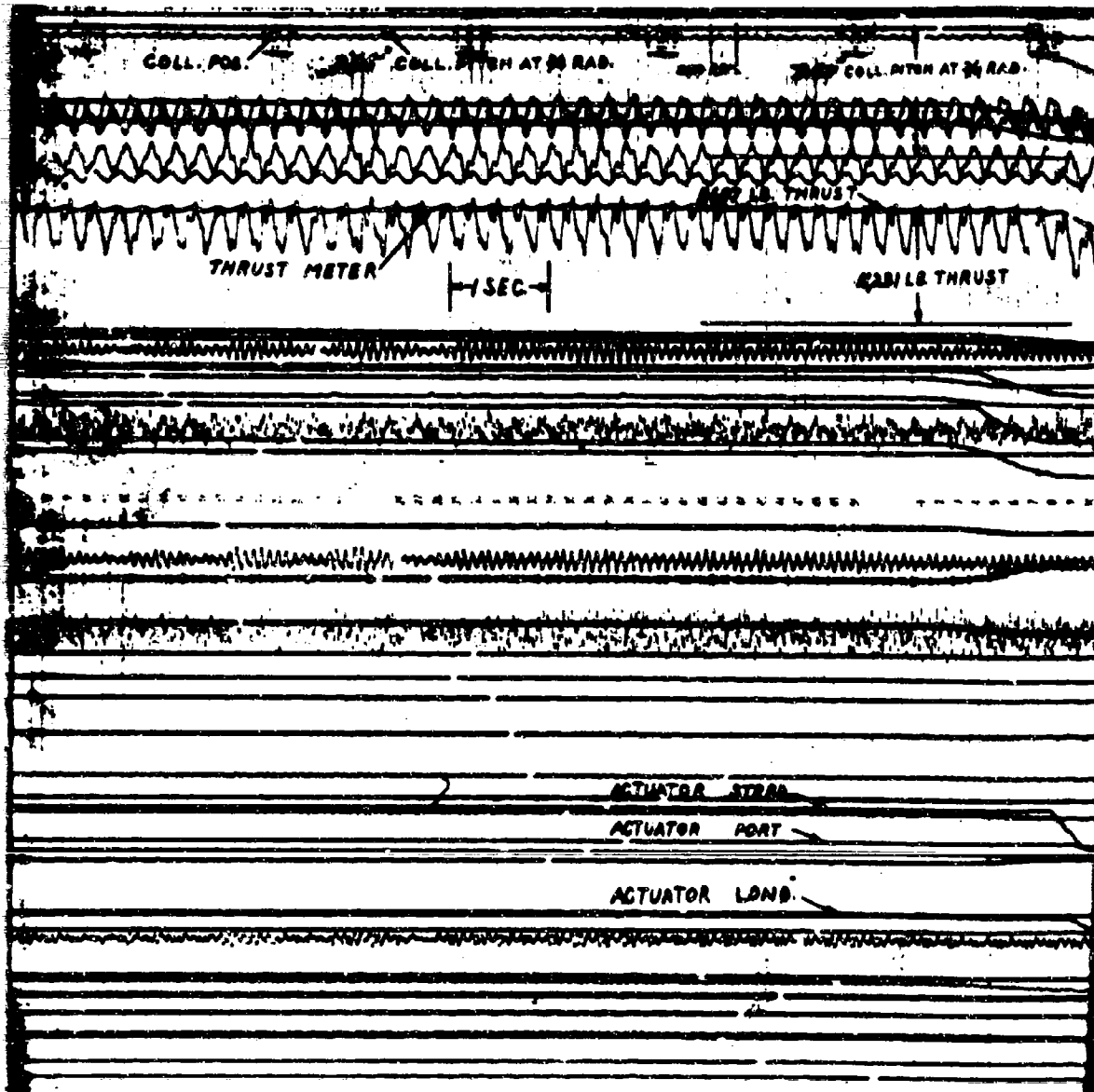
REVERSAL

31.3



Cyclic Reversal, Run 31, 14 May 1964

ent



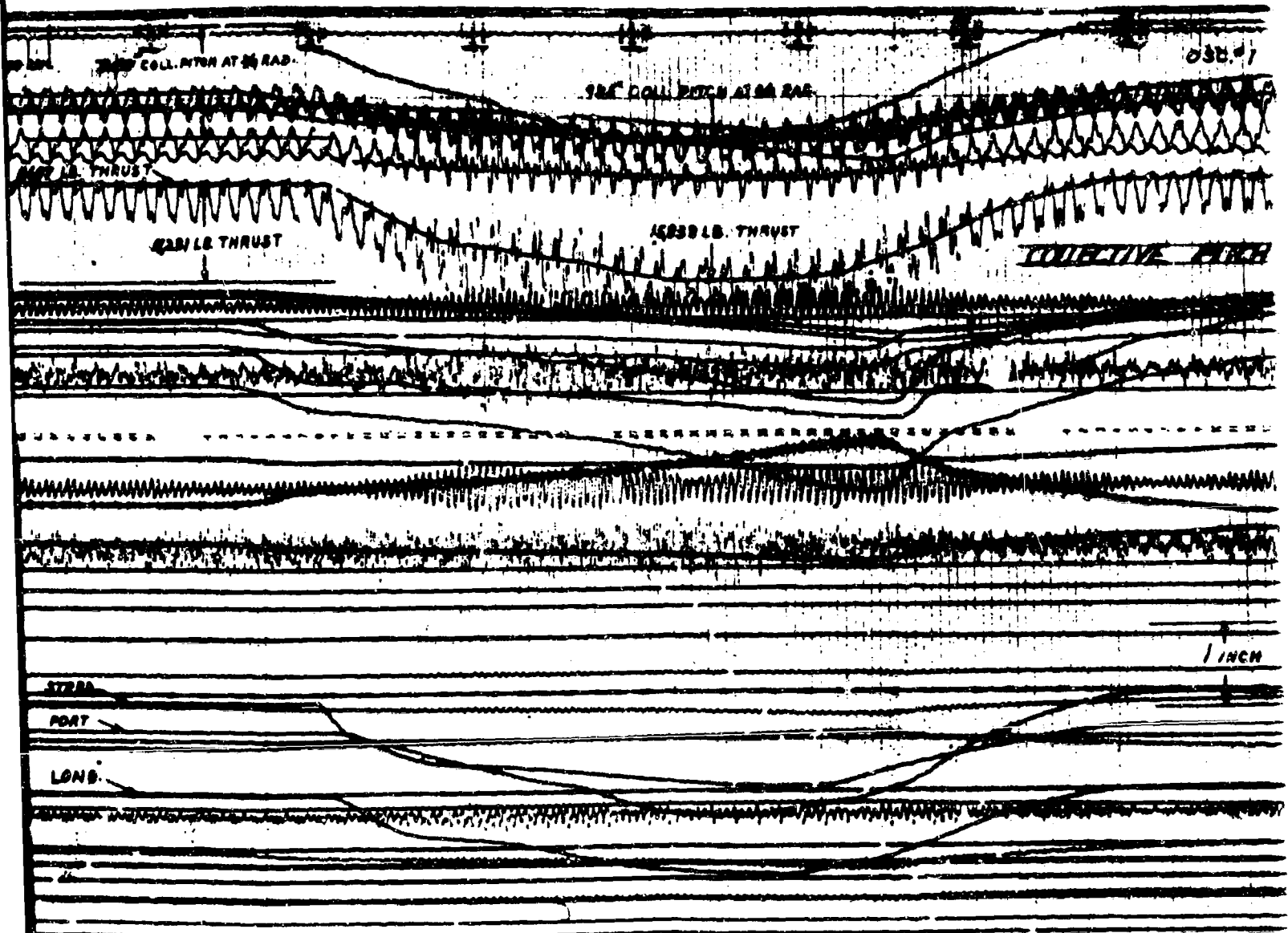


Figure 62. Collective Pitch Transient, Run 30, 11 May 1964  
 N<sub>R</sub> - 98.4 Percent

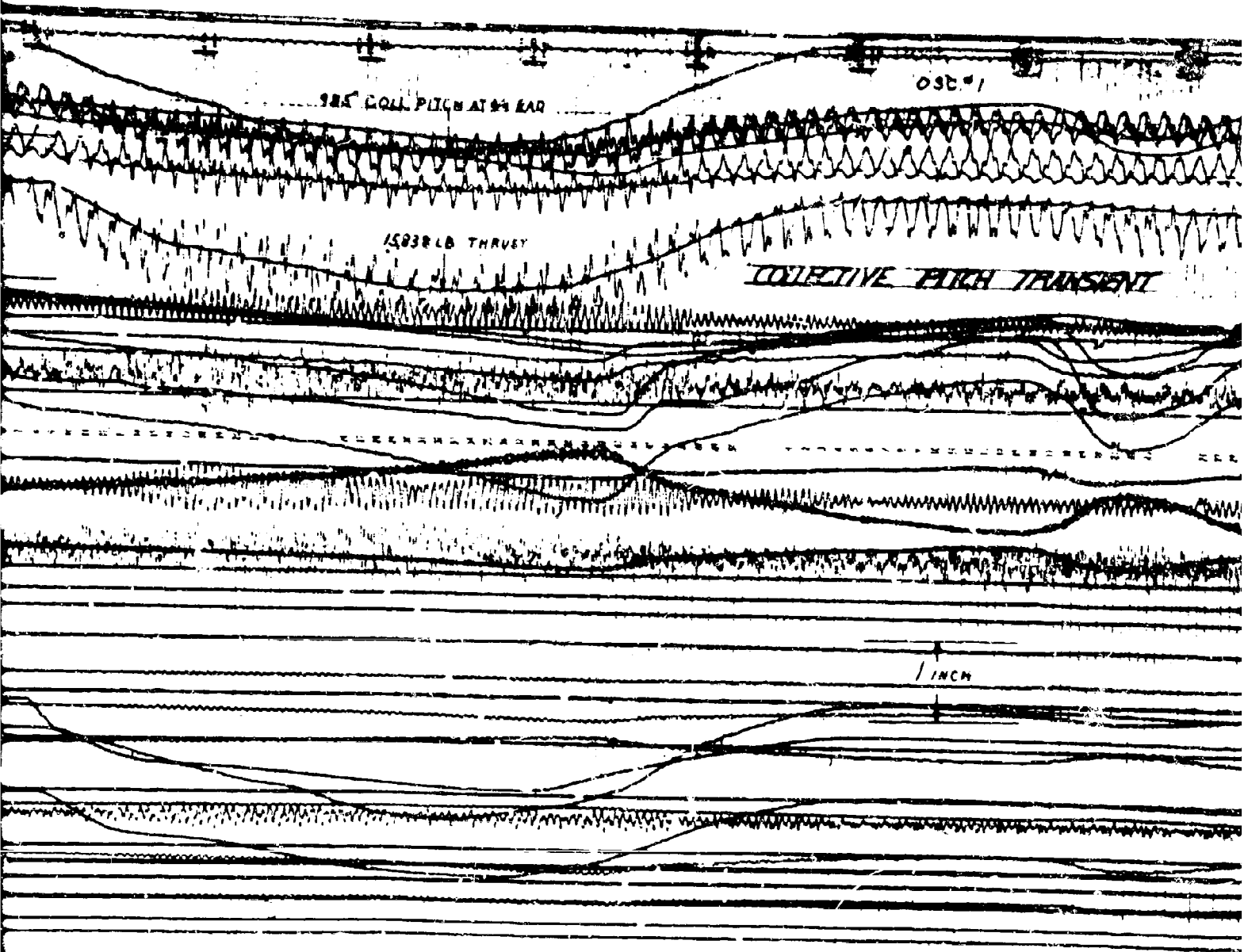
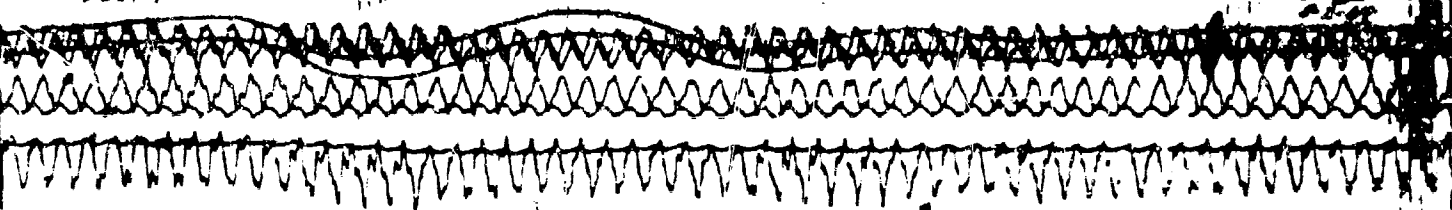


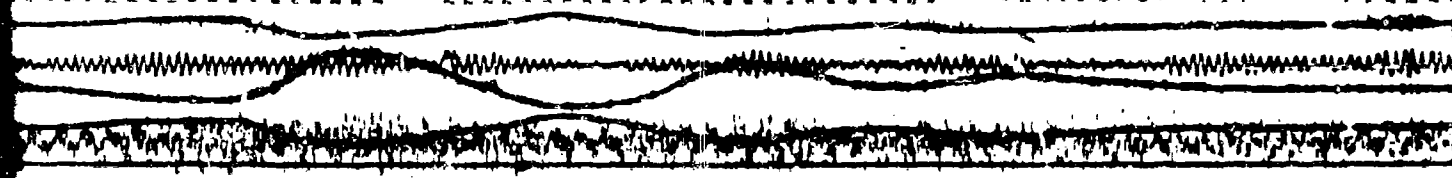
Figure 62. Collective Pitch Transient, Run 30, 11 May 1964  
NR = 98.4 Percent

C

OSC. 1



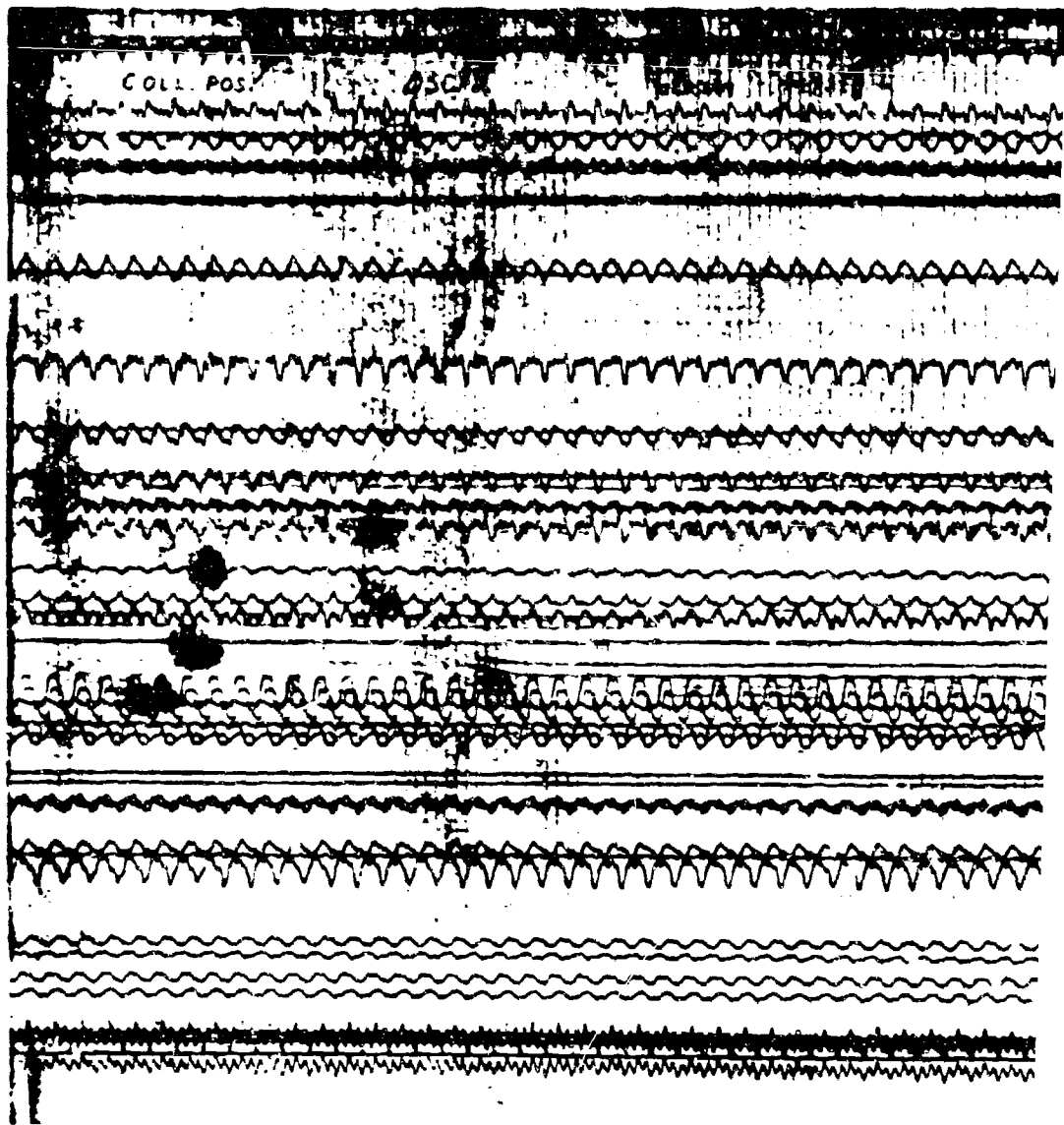
IVE HIGH TRANSIST



1 INCH

May 1964





A

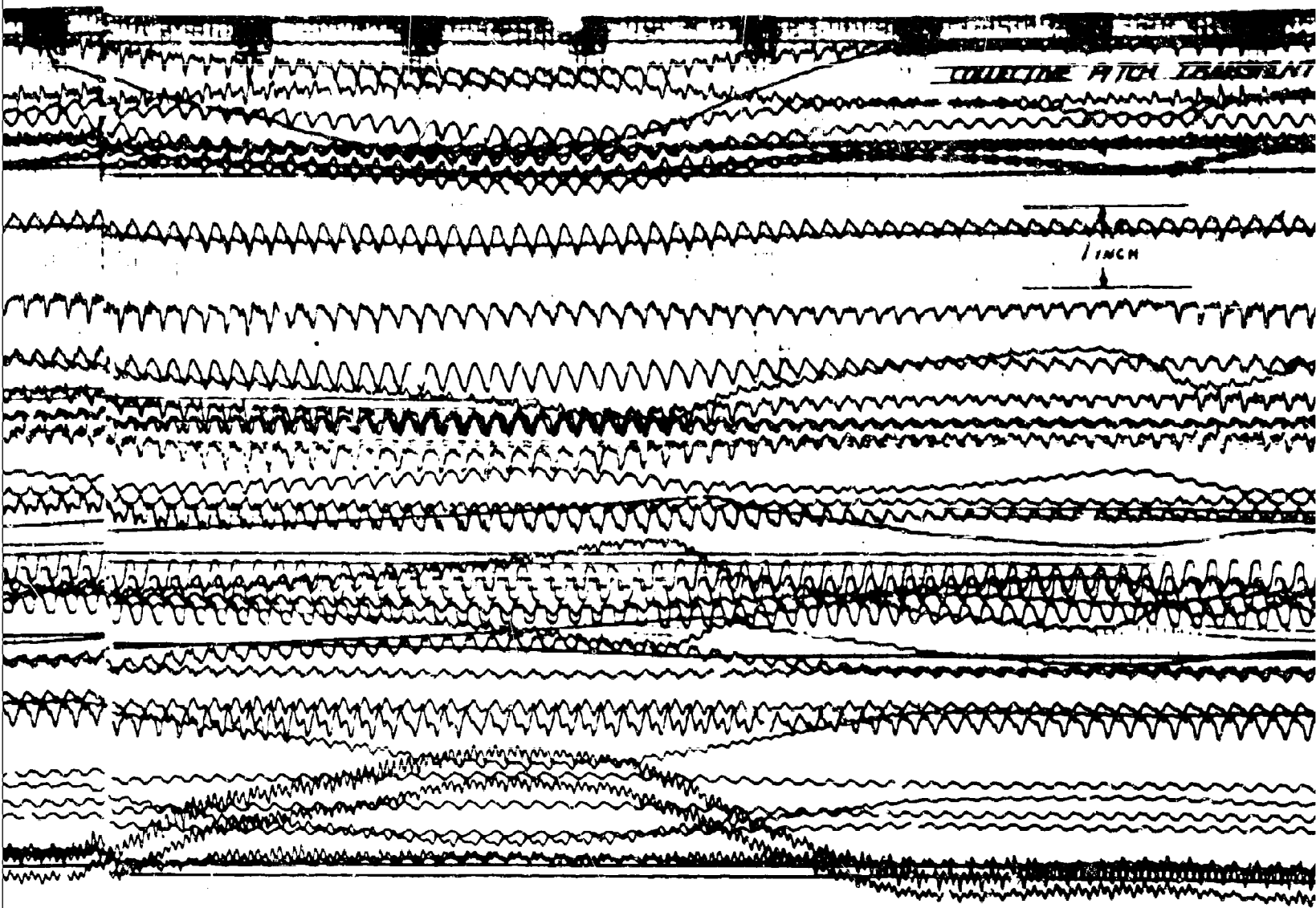
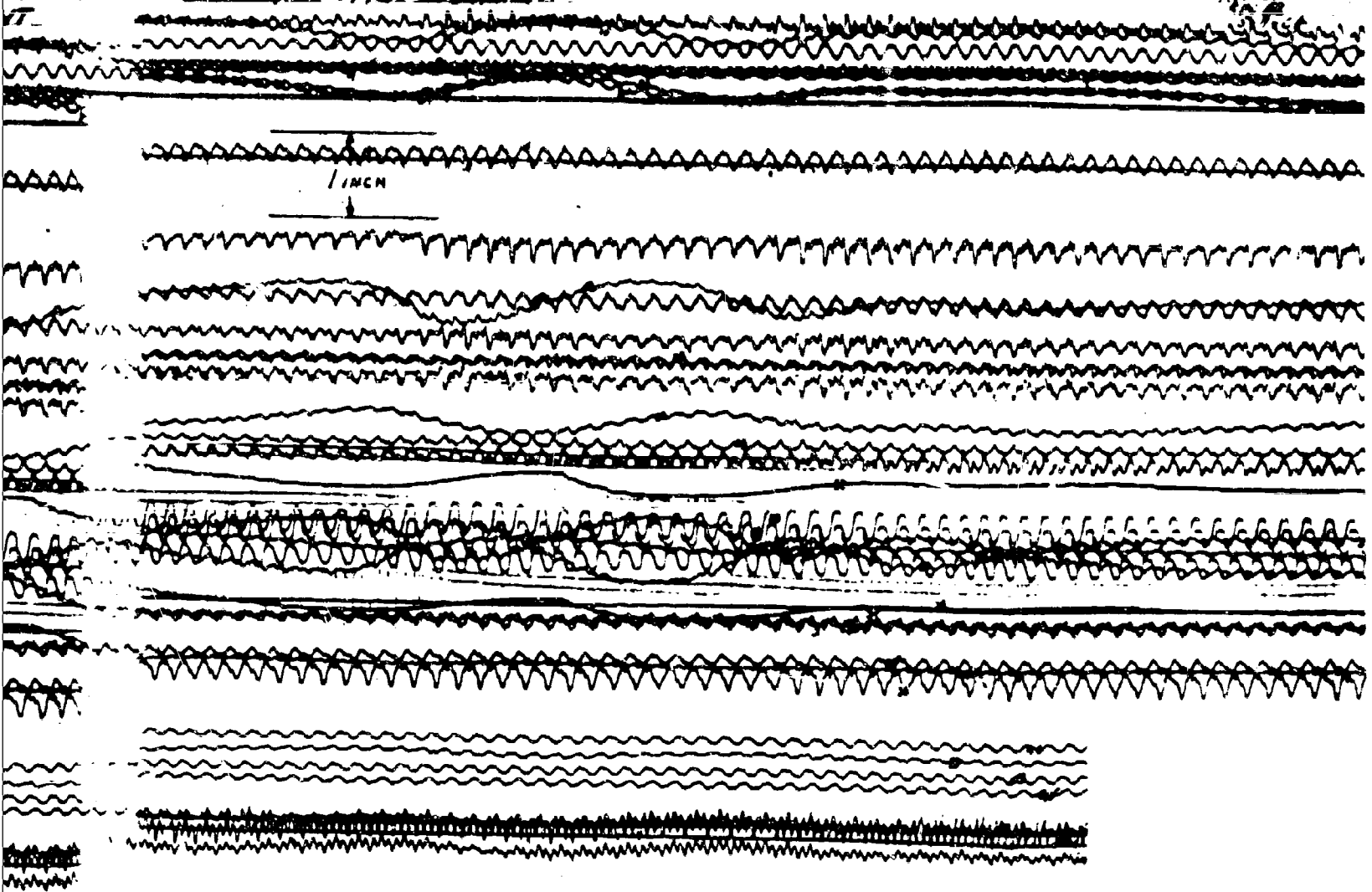


Figure 63. Collective Pitch Transient, Run 30, 11 May 1964  
 $N_R = 98.4$  Percent

COLLECTIVE PITCH TRANSIENT



May 1964

C

TABLE 5  
OSCILLOGRAPH SETUP SHEET

Ground Run 31		Record No's 45 & 46	Point 7-F	Oscillograph #1
Channel No	Transducer Location	Zero	Sensitivity Units/Inch	
1	Rotor rpm & Azimuth		Blue Blade Fwd	
2	Collective Pitch	11.21 dn	5.25 Degrees	
3	P-5 Engine #1	10.88	16.04 psi	
4	P-5 Engine #2	10.68	15.40 psi	
5	Thrust Load Cell #1	10.47	5114 lb	
6	Thrust Load Cell #2	10.28	5043 lb	
7	Thrust Load Cell #3	9.65	3256 lb	
8	Thrust Load Cell #4	9.96	5367 lb	
9	Thrust Meter	9.70	9497 lb	
10	Swashplate Drag Link	9.35	601 lb	
11	P-3 Engine #1	9.25	73.82 psi	
12	P-3 Engine #2	9.02	70.52 psi	
13	PLA Engine #1	8.63	See Curve	
14	PLA Engine #2	8.07	See Curve	
15	Variable Geometry Engine #1	8.52	1.0 in.	
16	Variable Geometry Engine #2	8.35	1.10 in.	
17	RPM Engine #1	8.11	1770 cycles	
18	RPM Engine #2	7.78	1316 cycles	
19	Longitudinal Cyclic	6.72 neut.	8.02 degrees	
20	Lateral Cyclic	7.33 neut	3.49 degrees	
21	Diverter Valve Pressure	7.36	7.33 psi	
22	Engine #1 Accel. Vert	7.77	1.97 G	
23	Engine #1 Accel. Lat	6.89	.53 G	
26	Engine #2 Accel. Vert	5.52	1.81 G	
27	Engine #2 Accel. Lat	4.75	.56 G	
28	P-5 Hub Pressure	4.93	11.56 psi	
29	Cross Flow Indicator	4.29	56.47 degrees	
30	AGP Parallel to Engine #2 $\perp$	4.54	531 $\mu$ in/in	
31	AGP 45° to Engine #2 $\perp$	4.02	600 $\mu$ in/in	
32	AGP 90° to Engine #2 $\perp$	3.73	545 $\mu$ in/in	
33	R/H Pad Lower	3.05	423 $\mu$ in/in	
34	R/H Pad Aft	2.23	448 $\mu$ in/in	
35	R/H Pad Upper	3.14	412 $\mu$ in/in	
36				
37	Control Actuator Starboard	3.92	3.25 degrees	
38	Control Actuator Port	2.27	6.27 degrees	
39	Control Actuator Long	1.35	4.54 degrees	
40				
41				
42	Diverter Valve #1 Rotor	1.65		
43	Diverter Valve #1 Overboard	.81		
44	Diverter Valve #2 Rotor	.26		
45	Diverter Valve #2 Overboard			
47	Diverter Valve #2 Lateral	1.46		
48	L/H Pad Upper	1.37	434 $\mu$ in/in	
49	L/H Pad Aft	1.09	448 $\mu$ in/in	
50	L/H Pad Lower	.48	363 $\mu$ in/in	

TABLE 5 (Continued)

## OSCILLOGRAPH SETUP SHEET

Ground Run 31    Record No. 45 & 46    Point No. 7-F    Oscillograph #2			
Channel No.	Transducer Location	Zero	Sensitivity Units/Inch
1	Rotor rpm & Azimuth		Blue Blade Fwd.
2	Collective Pitch	10.92 dn.	5.86 Degrees
3	Blue Blade Feathering Angle	10.93	14.6 Degrees
4	Blue Blade Flapping Angle	9.97	4.93 Degrees
5	Hub Tilt Angle	9.76	24.49 Degrees
6	Flapwise Bending Sta. 63.0 F/S	9.53	24,000 in-lb
7	Flapwise Bending Sta. 63.0 R/S	9.39	173,111 in-lb
8	Voltage Ref. A BB		
9	"    "    75.4 R/S	10.51	45,324 in-lb
10	"    "    100 F/S	7.94	14,082 in-lb
11	"    "    100 R/S	10.21	23,507 in-lb
12	"    "    140 F/S		
13	"    "    140 R/S	9.20	10,273 in-lb
14	"    "    220 F/S	10.57	9,517 in-lb
15	"    "    220 R/S	7.74	16,275 in-lb
16	"    "    270 F/S	6.44	24,606 in-lb
17	"    "    270 R/S	5.42	15,694 in-lb
18	Tip Press. Yellow Blade Fwd.	7.58	13.62 psi
19	Chordwise Bending Sta. 90.75 F/S	7.65	21,770 in-lb
20	Chordwise Bending Sta. 90.75 R/S	7.31	19,627 in-lb
21	Chordwise Bending Sta. 149 F/S	6.91	20,056 in-lb
22	Chordwise Bending Sta. 149 R/S	6.32	16,111 in-lb
23	Chordwise Shear Sta. 23	6.24	3841 lb
26	Vertical Shear Sta. 23	5.23	3441 lb
27	Duct Torsion Sta. 15 Blue	4.96	6653 in-lb
28	Duct Torsion Sta. 15 Red	4.19	6062 in-lb
29	Duct Torsion Sta. 15 Yellow	4.33	7574 in-lb
30	Tip Pressure Yellow Aft	4.85	13.38 psi
31	Skin Torsion Sta. 28	3.67	72,149 in-lb
32	Tip Pressure Blue Aft	4.54	13.52 psi
33	Skin Torsion Sta. 83	3.28	49,833 in-lb
34	Tip Pressure Blue Fwd.	4.00	13.28 psi
35	Main Shaft Bending Inplane	2.87	195,712 in-lb
36	Main Shaft Bending 90°	2.70	90,965 in-lb
37	Tip Pressure Red Fwd	3.50	10.21 psi
38	Tip Pressure Red Aft	3.05	13.66 psi
39	Gambal Lug Bending	2.03	
40	Gambal Lug Bending Aft	2.56	
41	Hub Plate Strain Fwd	2.42	1316 $\mu$ in/in
42	Hub Plate Strain Aft	1.81	2823 $\mu$ in/in
43	Pitch Link Blue	2.24	9035 lb
44	Pitch Link Red	1.77	10,256 lb
45	Pitch Link Yellow	1.25	9839 lb
46	Control Actuator Force Starboard	1.46	2092 lb
47	Control Actuator Force Port	1.44	2451 lb
48	Control Actuator Force Long.	.96	1971 lb
49	Voltage Ref. B BB		
50	Voltage Ref. C BB		

TABLE 5 (Continued)  
OSCILLOGRAPH SETUP SHEET

Ground Run 30      Record No. 82      Point 13-A      Oscillograph #1			
Channel No.	Transducer Location	Zero	Sensitivity Units/Inch
1	Rotor rpm & Azimuth		Blue Fwd.
2	Collective Pitch	11.23 dn	5.5 Degrees
3	P-5 Engine #1	10.80	16.04 psi
4	P-5 Engine #2	10.59	15.39 psi
5	Thrust Load Cell #1	10.50	5300 lb
6	Thrust Load Cell #2	10.31	5519 lb
7	Thrust Load Cell #3	9.63	3220 lb
8	Thrust Load Cell #4	9.97	5318 lb
9	Thrust Meter	9.70	9599 lb
10	Swashplate Drag Link	9.35	602 lb
11	P-3 Engine #1	9.25	72.8 psi
12	P-3 Engine #2	9.02	69.2 psi
13	PLA Engine #1	8.57	See Curve
14	PLA Engine #2	8.40	See Curve
15	Variable Geometry Engine #1	8.53	.98 inches
16	Variable Geometry Engine #2	8.37	.98 inches
17	rpm Engine #1	8.12	1754 Cycle
18	rpm Engine #2	8.40	1299 Cycle
19	Longitudinal Cyclic	6.71 neut.	8.01 Degree
20	Lateral Cyclic	7.20 neut.	See Curve
21	Diverter Valve Pressure	7.57	7.29 psi
22	Engine #1 Accel. Vertical	7.76	1.95 g
23	Engine #1 Accel. Lateral	6.93	.54 g
26	Engine #2 Accel. Vertical	5.52	1.79 g
27	Engine #2 Accel. Lateral	4.74	.56 g
28	P-5 Hub Pressure	4.94	11.60 psi
29	Cross Flow Indicator	4.25	55.51 Degrees
30	AGP Parallel to Engine #2 $\angle$	4.55	526 $\mu$ in/in
31	AGP 45° to Engine #2 $\angle$	4.04	
32	AGP 90° to Engine #2 $\angle$	3.73	545 $\mu$ in/in
33	R/H Pad Lower	3.02	423 $\mu$ in/in
34	R/H Pad Aft	2.22	449 $\mu$ in/in
35	R/H Pad Upper	3.12	413 $\mu$ in/in
36	Cascade Valve Position	2.40 open	1.23 close
37	Control Actuator Starboard	3.30	5.35 Degrees
38	Control Actuator Port	2.35	10.79 Degrees
39	Control Actuator Long.	2.75	7.57 Degrees
40			
41			
42	Diverter Valve #1 Rotor	1.06	
43	Diverter Valve #1 Overboard	.81	
44	Diverter Valve #2 Rotor	.66	
45	Diverter Valve #2 Overboard	.55	
46	Accel. Upper Bearing Long.	.87	.52 g
47	Accel. Upper Bearing Lateral	1.46	1.96 g
48	L/H Pad Upper	1.36	434 $\mu$ in/in
49	L/H Pad Aft	1.10	449 $\mu$ in/in
50	L/H Pad Lower	.53	356 $\mu$ in/in

TABLE 5 (Continued)  
OSCILLOGRAPH SETUP SHEET

Ground Run 30		Record No. 82	Point 13A	Oscillograph #2
Channel No.	Transducer Location		Zero	Sensitivity Units/Inch
1	Rotor rpm & Azimuth			Blue Fwd.
2	Collective Pitch		11.04 dn.	6.0 Degrees
3	Blue Blade Feathering		10.30	14.6 Degrees
4	Blue Blade Flapping		9.94	4.85 Degrees
5	Hub Tilt		9.87	24.49 Degrees
6	Flapwise Bending Sta. 63.0 F/S		10.98	
7	Flapwise Bending Sta. 63.0 R/S		10.75	22912 in-lb
8	Voltage Ref. A BB		9.50	
9	Flapwise Bending Sta. 75.4 R/S		10.52	46507 in-lb
10	Flapwise Bending Sta. 100 F/S		7.97	14082 in-lb
11	Flapwise Bending Sta. 100 R/S		10.25	23864 in-lb
12	Flapwise Bending Sta. 140 F/S		8.41	10383 in-lb
13	Flapwise Bending Sta. 140 R/S		9.11	10056 in-lb
14	Flapwise Bending Sta. 220 F/S		9.21	15956 in-lb
15	Flapwise Bending Sta. 220 R/S		7.69	16043 in-lb
16	Flapwise Bending Sta. 270 F/S		6.41	24606 in-lb
17	Flapwise Bending Sta. 270 R/S		5.42	15480 in-lb
18	Tip Press. Yellow Blade Fwd.		7.54	13.32 psi
19	Chordwise Bending Sta. 90.75 F/S		7.67	22201 in-lb
20	Chordwise Bending Sta. 90.75 R/S		7.23	19627 in-lb
21	Chordwise Bending Sta. 149 F/S		6.91	20056 in-lb
22	Chordwise Bending Sta. 149 R/S		6.36	15962 in-lb
23	Chordwise Shear Sta. 23		6.26	3877 lb
26	Vertical Shear Sta. 23		5.16	3673 lb
27	Duct Torsion Sta. 15 Blue		4.59	6653 in-lb
28	Duct Torsion Sta. 15 Red		4.23	6015 in-lb
29	Duct Torsion Sta. 15 Yellow		4.26	7574 in-lb
30	Tip Pressure Yellow Aft		4.83	13.09 psi
31	Skin Torsion Sta. 38		3.56	72149 in-lb
32	Tip Pressure Blue Aft		4.57	13.52 psi
33	Skin Torsion Sta. 83		3.30	50327 in-lb
34	Tip Pressure Blue Fwd.		3.92	13.80 psi
35	Main Shaft Bending Inplane		2.90	201,830 in-lb
36	Main Shaft Bending 90°		2.78	90965 in-lb
37	Tip Pressure Red Fwd.		3.52	10.27 psi
38	Tip Pressure Red Aft.		3.12	13.66 psi
39	Gimbal Lug Bending		2.11	
40	Gimbal Lug Bending Alt.		2.59	
41	Hub Plate Strain Fwd.		2.27	1315 $\mu$ in/in
42	Hub Plate Strain Aft		1.97	2822 $\mu$ in/in
43	Pitch Link Blue		1.70	9162 lb
44	Pitch Link Red		2.06	10,508 lb
45	Pitch Link Yellow		1.34	9692 lb
46	Control Actuator Force Starboard		1.94	2064 lb
47	Control Actuator Force Port		1.80	2358 lb
48	Control Actuator Force Long		.83	1971 lb
49	Voltage Ref B BB		.95	
50	Voltage Ref C BB		.81	

YAW CONTROL VALVE TESTING

In addition to functional check-out, the purpose of the yaw valve tests was twofold: (1) measurement of the available yaw thrust and (2) investigation of the effect that opening of the valve has on lift and/or power lever position. The measurement of yaw force was made in a sequence of steady-state points recorded at incremental opening of the valve. These tests were repeated in two modes of operation: at constant rotor lift and at constant power lever position (PLA). The results from the above tests are shown on Table 6 and Figure 64.

The operation of the valve at constant lift represents capability of yaw control in hovering. The maximum measured yaw thrust was 338 pounds, which exceeded the 300 pounds established as the design objective. When the valve was actuated at constant PLA, both rotor lift and yaw thrust notably decreased. In order to maintain constant lift, a coordinated movement between the directional control and the power lever was required.

The tests have shown that the adjustment of PLA associated with each valve opening was within practical limits. It is interesting to note that in the hot cycle helicopter the corrective PLA movement is always in the same direction, in a helicopter with a tail rotor, this movement is opposite for the opposite pedal deflection.

A neutral "no-force" position of the valve was found to extend over 18 degrees of the control valve movement. This was considered excessive for a smooth transition of the yaw thrust to the opposite direction. After the tests were completed, steps were taken to reduce this dead band to minimum.

ROTOR DOWNWASH VELOCITY

Rotor downwash velocities were measured during rotor performance tests using a downwash velocity boom and a movable probe with a standard pitot head approximately 9 feet below the plane of the rotor. These data are shown on Figure 65.

ROTOR-ENGINE SOUND LEVEL

Sound pressure level data were taken during the performance runs at high engine power and thrust levels. The YT-64 gas generators were run without sound suppression for inlet noise.

TABLE 6  
YAW CONTROL VALVE TEST DATA

Valve Opening at Constant Lift, Degrees	Rotor RPM %	Blade Pitch Degrees	Rotor Lift "b.	Yaw Thrust Lb.	P <sub>5</sub> Inches Hg. Absolute		Ng %		T <sub>5</sub> °C	
					Eng. #1	Eng. #2	Eng. #1	Eng. #2	Eng. #1	Eng. #2
0	100.0	7	15300	0	62.5	61.5	97.0	97.0	526	516
20	99.0	7	15300	112.2	61.5	60.7	97.9	98.1	514	498
33	99.2	7	15300	192.7	61.5	60.4	99.2	99.2	515	505
45.5	99.2	7	15300	274.0	62.5	60.6	100.9	100.7	522	504
58 (Full Open)	99.5	7	15300	338.3	62.5	60.3	101.0	102.5	520	512
Valve Opening at Constant P <sub>L,A</sub> , Degrees										
0	101.2	7	15500	0	63.0	62.0	97.1	97.1	529	510
20	98.8	7	15300	81.5	60.5	59.5	97.4	97.6	506	496
33	96.0	7	13800	156.3	58.5	57.0	97.7	98.0	488	478
45.5	93.1	7	12600	228.2	56.5	54.5	97.9	98.2	474	459
58 (Full Open)	91.0	7	11800	264.7	55.0	53.0	98.0	98.3	464	448

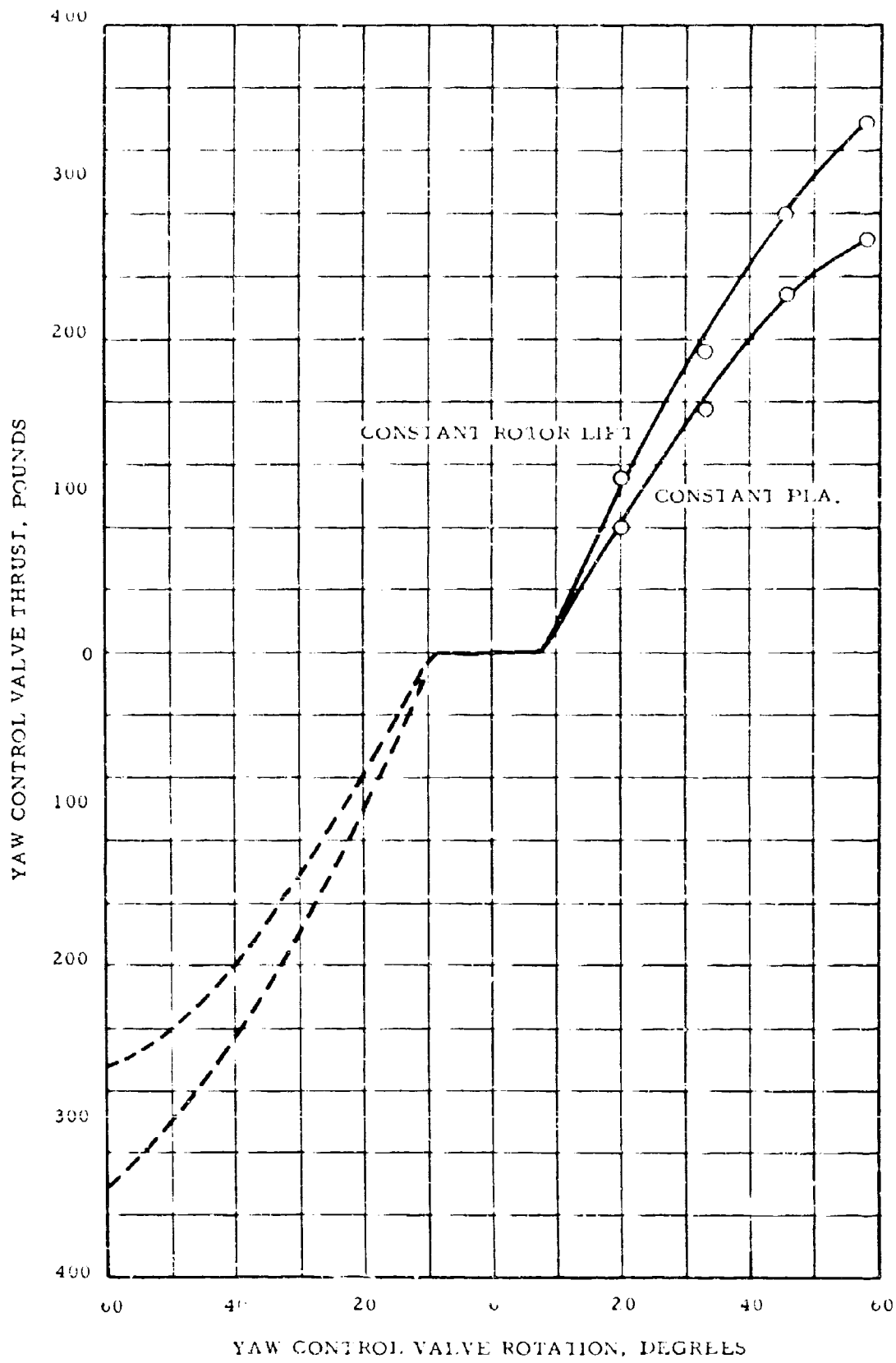
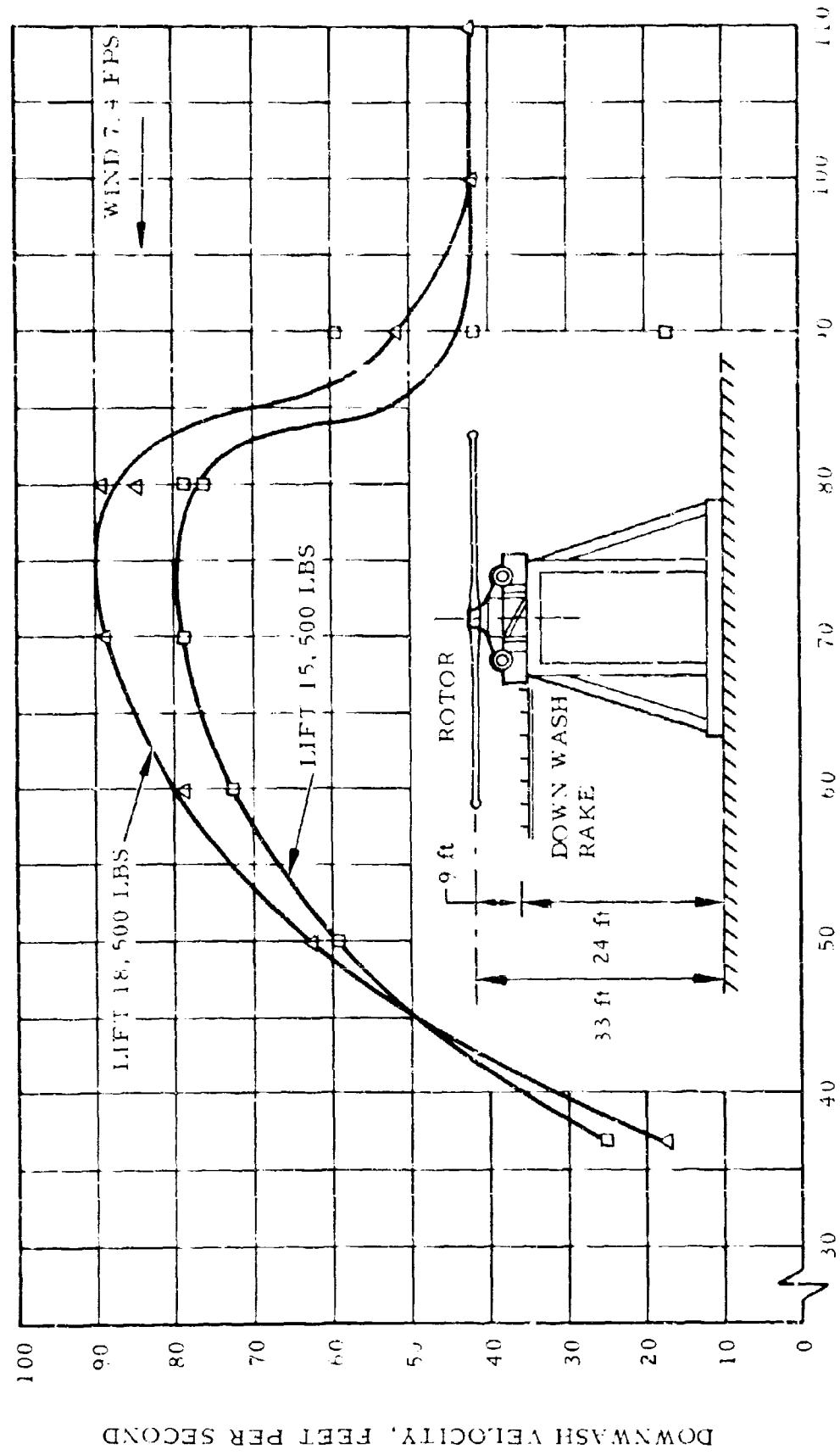


Figure 64. Yaw Valve Thrust Measurement



BLADE RADIAL STATION r/R, PERCENT

Figure 65. Rotor Downwash Velocity vs. Blade Radial Station

Sound spectral data were taken at 100-foot intervals from the base of the whirl tower from 100 to 400 feet. These data are presented on Figure 66 showing the over-all sound levels, and in Table 7, showing the sound levels for three frequency bands. An octave band noise analyzer was used to record these data.

The highest sound pressure levels were recorded directly in front of the power module and engine inlets. The over-all sound level measured at 112 decibels at a point 100 feet directly in front of the power module. Ambient sound level was 80 decibels. At a point 100 feet and 90 degrees to the right of the power module, the sound level was recorded at 108 decibels. The rotor thrust was approximately 16,000 pounds for these conditions.

Although the measured sound levels during these tests were as high as for the previous whirl tests where a J-57 engine with noise suppression was used, there were no cases of noise disturbance reported by nearby Loyola University during either the engine or the whirl test programs.

#### 5.10 ENGINE TEST RESULTS

Prior to twin-engine operation of the YT-64 gas generators with mixed exhaust flow, each engine was run individually with its diverter valve in the "overboard" position to obtain the engine operating line data for this fixed exit area and for military speed "topping" adjustment. The tailpipe exit area was 52.55 square inches for these tests.

The turbine speed,  $N_G$ , limit at topping was established as a function of the jet nozzle area and turbine discharge temperature,  $T_5$ , for a turbine inlet temperature limit which was defined by the manufacturer's calibration data supplied with the engines. Engine S/N 250010-4 had the lowest  $P_{T_5}$  at topping and was considered the reference engine. Engine 250026-1A had higher  $P_{T_5}$  at topping and was "topped" below its  $T_5$  limit for the effective exit area to match the  $P_{T_5}$  from Engine 010-4.

During this phase of testing it was noted that the apparent engine exit area was greater than 52.55 square inches by three to five square inches and that considerable gas flow was leaking past the diverter valve door into the upper common duct, even with the diverter valves locked in the overboard position. Rerigging and adjustment of

118

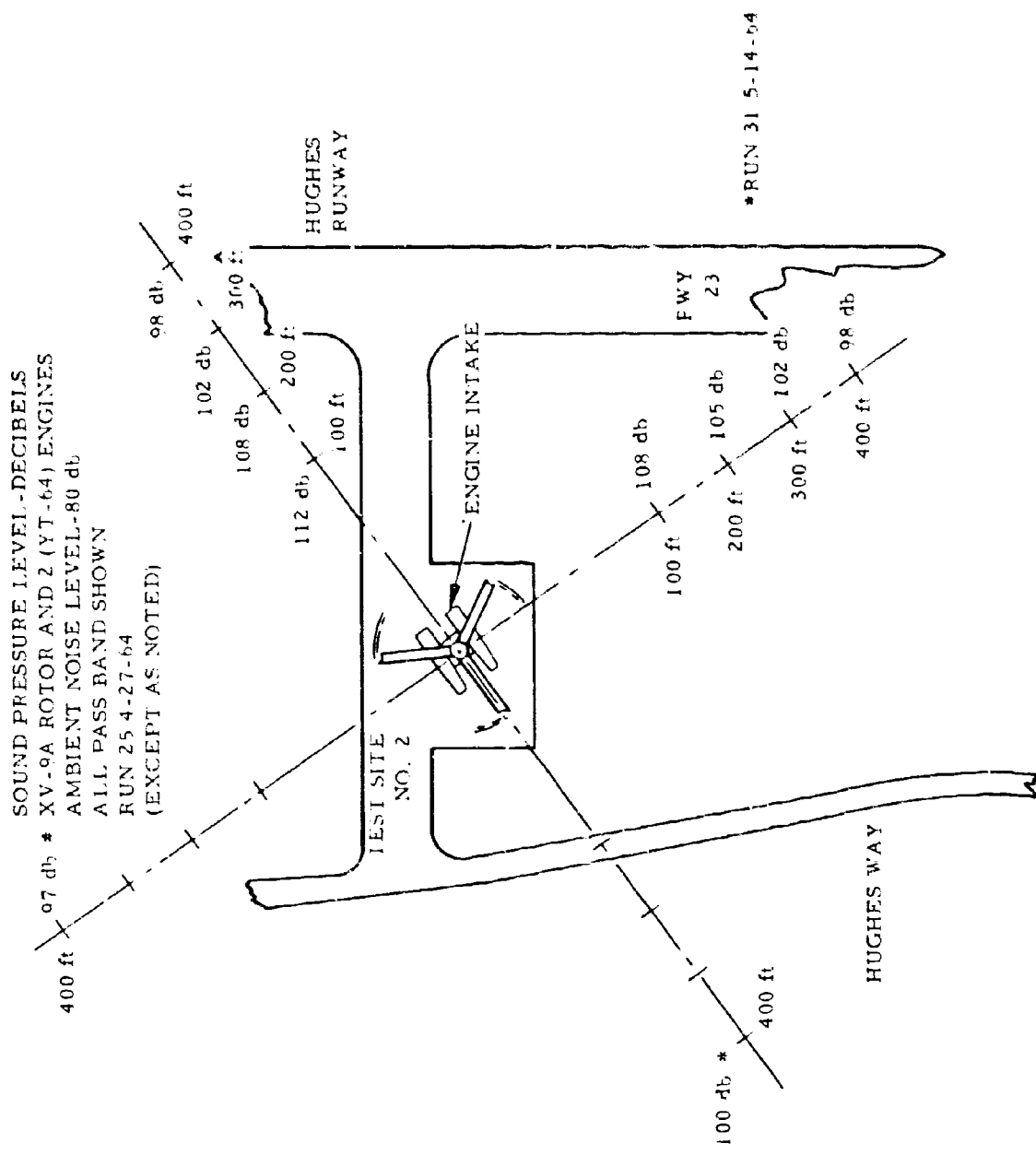


Figure 66. Sound Pressure Level

TABLE 7						
SOUND SPECTRAL DATA (DECIBELS)						
SOUND BAND FREQUENCY (CPS)						
Distance	Test Run No 25 Ambient 80 Db				Test Run No 31	
	600-1200 CPS	2400-4800 CPS	9600-19 2K CPS	All Pass	4800-9600 CPS	All Pass
Fwd of Power Module						
100	103	96	86	112	---	---
200	98	91	77	108	---	---
300	92	87	70	102	---	---
400	84	83	64	98	77	98
Aft of Power Module						
100	98	95	80	108	---	---
200	91	90	68	105	---	---
300	91	84	60	102	---	---
400	80	81	56	98	79	100
Right of Power Module						
400	---	---	---	---	77	96
Left of Power Module						
400	---	---	---	---	81	97

the diverter valve actuating mechanism reduced the leakage to some degree, but a completely tight seal was not obtainable.

The use of tailpipe "tabs" was employed to change the effective exit area and to permit "topping" the engine on the desired operating line. This procedure was used successfully on Engine 026-1A during topping to reduce the effective exit area, which was larger than desired because of diverter-valve leakage. The installation of tabs amounting to 5 square inches changed the effective exit area from 57 square inches to 52 square inches, and engine "topping" was set with the tabs installed.

The change-over from individual to twin-engine operation was accomplished by stabilizing both engines at idle with diverter valves in "overboard" position and then actuating the diverter valve switches simultaneously to "rotor" position. The exit area of the common exhaust nozzle was previously set for twice the nominal single-engine exit area.

Diverter-valve actuating time was approximately 0.5 second from "overboard" to "rotor" position. Engine operation was completely stable during the transition, and the only perceptible change in the engine instruments was an equalization of  $P_{T5}$  on both engines.

The power levers were then advanced simultaneously to produce a synchronized power lever angle until the desired twin-engine power setting was reached. Engine turbine speed,  $N_G$ , was used as the primary reference during the power setting process with fine balance adjustments made by matching compressor discharge  $P_{T3}$ ,  $N_G$ , and  $P_{T5}$ .

Air flow matching by setting equal  $P_{T3}$ 's was checked against the manometer board air flow measurement and found to be an accurate means of obtaining matched air flows.

Engine response during twin-engine accelerations and power lever changes was essentially the same as for single-engine operation, and no difficulty was encountered to control both gas generators by manual power lever manipulations using the standard reference instruments.

Good correlation between engine fuel flows was noted during engine matching, and this parameter could be particularly useful for power setting and engine matching during in-flight operation of the hot cycle system.

Twin-engine shutdown was accomplished by reducing both engines to idle power and simultaneously actuating the diverter valve switches to "overboard" position. Individual engine shutdown was then made by moving the individual power levers to "off" position.

Normal shutdown procedure was to start the MA-1 cart prior to engine shutdown in order to "motor" the engine in the event of a post-shutdown fire or residual fuel burning, however, all shutdowns were "clean" and post-shutdown motoring was never required.

#### 5.10.1 Test Results and Analysis

The engine and power module tests were conducted prior to the installation of the rotor in the propulsion system. Unlike the rotor, which had already demonstrated its capability in the 60-hour endurance test, the power module had never been tested as a complete unit. Many aspects of its operation thus remained unknown until the actual testing was completed. The same applied to the engines and diverter valves which, during the previous rotor feasibility testing, were in the development stage. The concept of the common exhaust system for a cluster of jet engines, though feasible theoretically, was yet to be checked in a practical application. The proof of practicality of twin-engine operation was of primary importance with regard to the whirl test program and to the hot cycle concept.

In effect, the power module test demonstrated excellent operating characteristics of the twin-engine system used in the XV-9A. The normal steady-state operation was exactly as predicted in the earlier studies made in connection with this program. The transient runs, as severe as any to be expected in emergency situations, demonstrated that the power plant operation is completely stable. This stability was proved by mismatching engines to a considerable degree in the steady-state and transient test runs.

Within the scope of performance evaluation, the following test objectives were accomplished:

1. Definition of engine operating line
2. Verification of engine manufacturer's test data
3. Selection of topping procedure and topping conditions for each engine
4. Twin-engine matched steady-state operation
5. Twin-engine matched transient operation
6. Mismatched engines in steady-state and transient operation
7. Simulation of engine or diverter valve failures
8. Comparison of various engine flow measuring methods
9. Measurement of pressure loss in the duct system

Most of the test objectives were accomplished during Runs 15, 16, and 17. The respective test data were used in the performance evaluation. Figures 67 through 76 illustrate the test results.

Figures 67 and 68 show a plot for each engine of corrected exhaust temperature  $\frac{T_M}{\theta^5}$  versus corrected engine speed  $\frac{N}{\sqrt{\theta}}$ . The operating lines established by the manufacturer at fixed nozzle areas, together with the turbine inlet temperature limit lines,  $\frac{T_4/\theta}{T_4 \text{ Limit}}$ , and exhaust pressure lines,  $\frac{P_5}{\theta^5}$ , form the background map on which test points and curves are indicated. These maps were used during the tests for a quick determination of operating lines, effective exit areas, and temperature limits. Figure 67 represents the operating record of Engine 010-4 from Runs 15, 16, and 17. Typical twin-engine matched and mismatched test runs are recorded. Each of these operations was run at the total geometric exit area of 109.6 square inches (curves A and B) and 98.6 square inches (curves C and D). The corresponding operating lines of Engine 026-1A (curves A, B, C, and D) are shown on Figure 68. Twin-engine topping was accomplished by topping Engine 010-4 at its temperature limit, while Engine 026-1A was adjusted to equal the lower exit pressure of its weaker counterpart. The power developed at topping speed is indicated on the plot in terms of shaft horsepower (SHP) as defined by the engine manufacturer. The tests showed no significant adverse effects caused by the common exit arrangement. When the engines remained essentially matched through the range of operation, they ran practically as they would run having

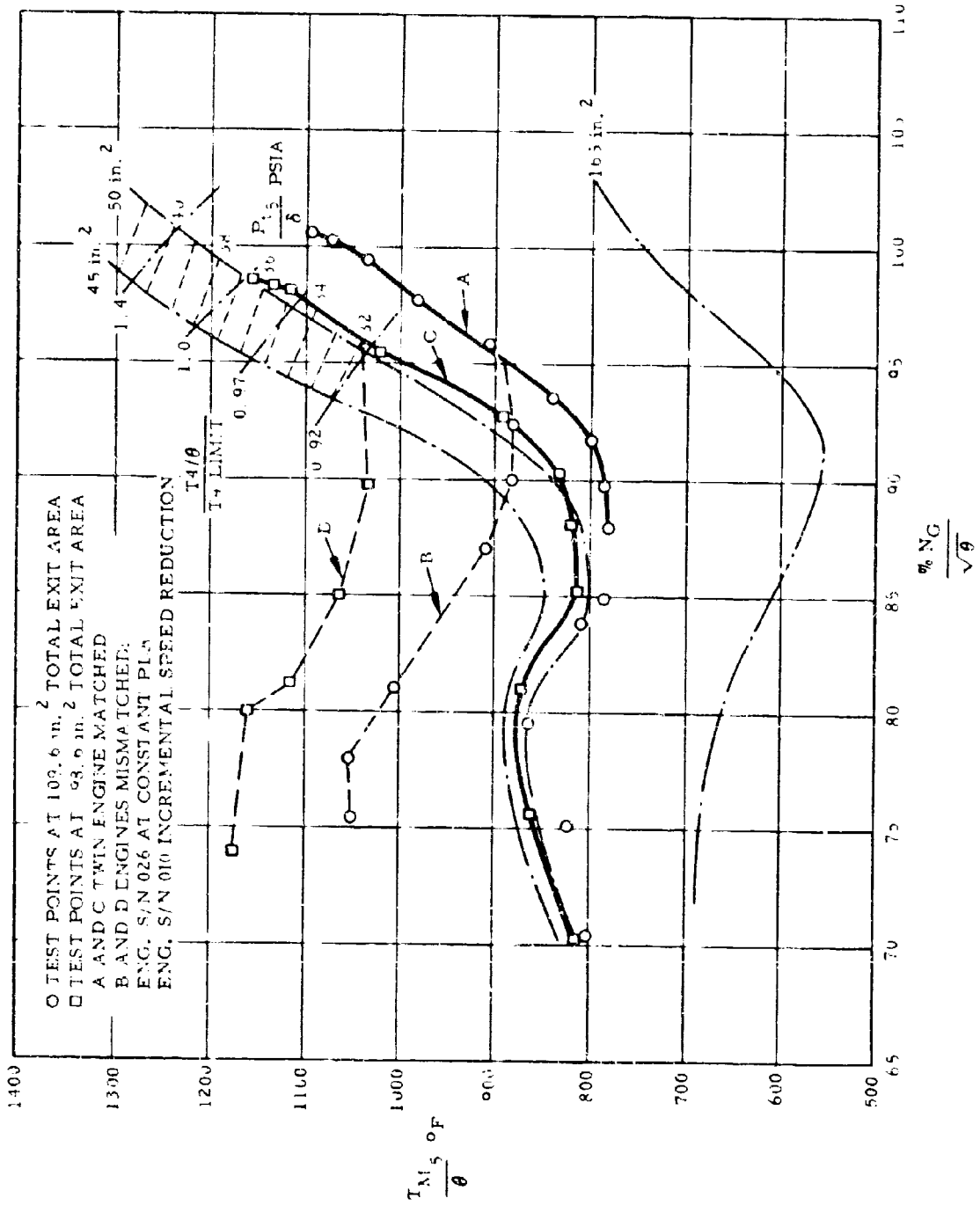


Figure 67. Engine 010 in Twin-Engine Operation

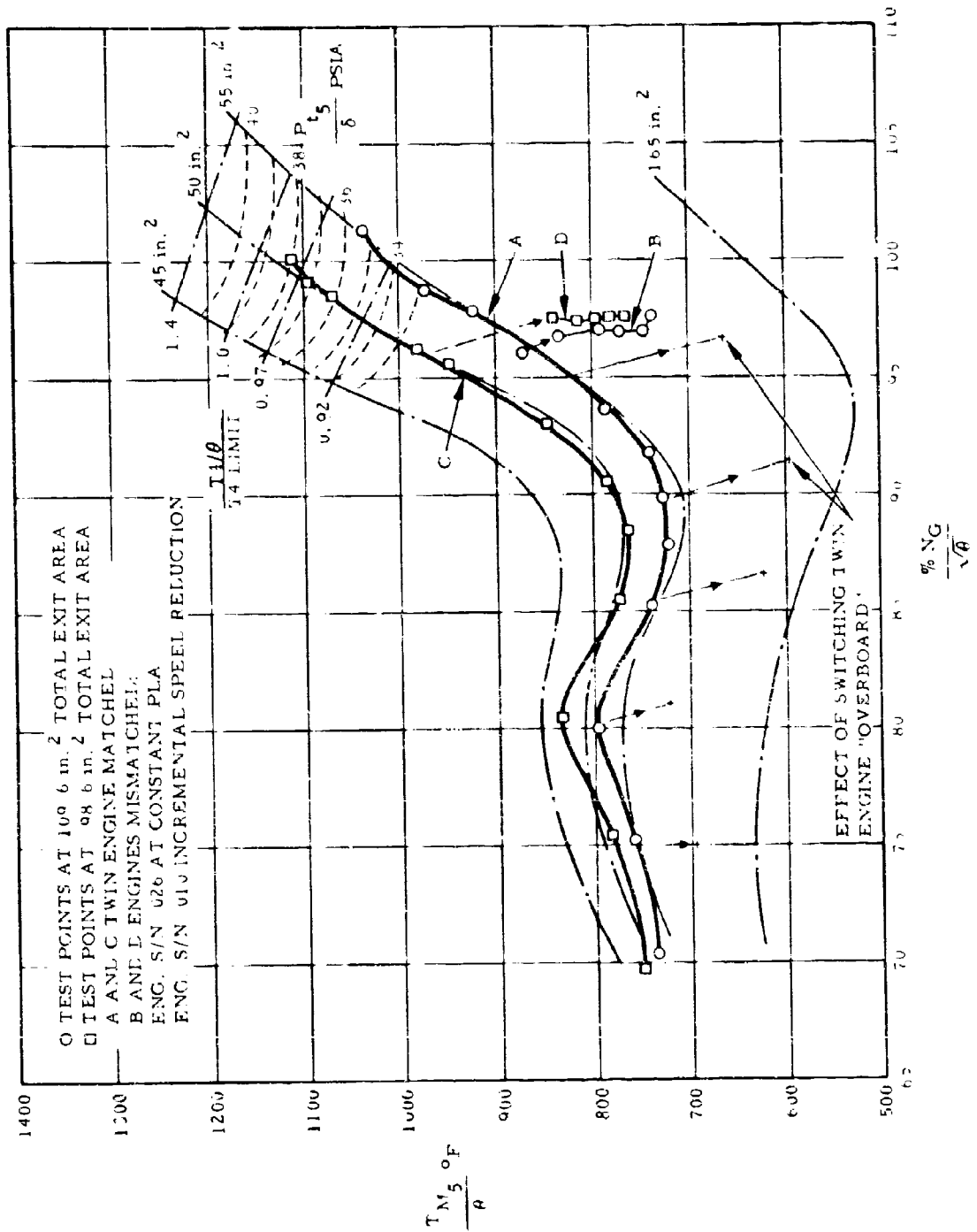


Figure 68. Engine 026 in Twin-Engine Operation

individual discharge nozzles. The steady-state engine operating characteristics at the differential power setting were checked by holding Engine 026-1A at a constant power lever angle of about 97 percent speed while reducing the speed of Engine 010. The degree of mismatch was increased incrementally until the speed ratio in one case was 97.5 : 74. There was no adverse effect of mismatching. Both tests constituted a sequence of stable steady-state points. The temperature of neither engine exceeded the limits.

To simulate one engine failure during twin-engine operation, the diverter valve on Engine 010-4 was switched "overboard." The effects of valve switching on the opposite engine are shown on Figure 68. At all speed levels the engine reacted in a normal and safe manner, with speed remaining within the droop line limits.

Figures 69 and 70 were used to compare the engine manufacturer's test data with the Hughes Tool Company test data. The corrected compressor flow curves  $\frac{W_2 \sqrt{\theta_2}}{\delta_2}$  versus compressor pressure ratio  $P_{T_3} / P_{T_2}$  on Figure 69, and the corrected compressor flow

versus corrected speed on Figure 70, provided the background on which test points were plotted. Figures 69 and 70 were prepared for Engine 026-1A; they show a good correlation between the engine manufacturer's and Hughes Tool Company test data. A similar plot made for Engine 010-4 was not so consistent with the engine manufacturer's test. However, as pointed in paragraph 5.10.2.4 a different approach toward correlation of engine manufacturer's test data and Hughes Tool Company test data for mass flow was developed, was found to provide good agreement and was utilized.

The next four figures are transcriptions from the oscillograph record. Figures 71, 72 and 73 show the effect of typical twin-engine transient operations on various engine parameters. They illustrate, respectively, rapid acceleration from idle to maximum power rapid acceleration to maximum power with differential starting speeds, and rapid power change from maximum to 80 percent  $N_G$  and return to maximum. Figure 74 shows a sequence of steady-state conditions at various differential power settings, followed by acceleration of the slow engine to its original power setting. This test is the same as one illustrated by curve D on Figures 67 and 68.

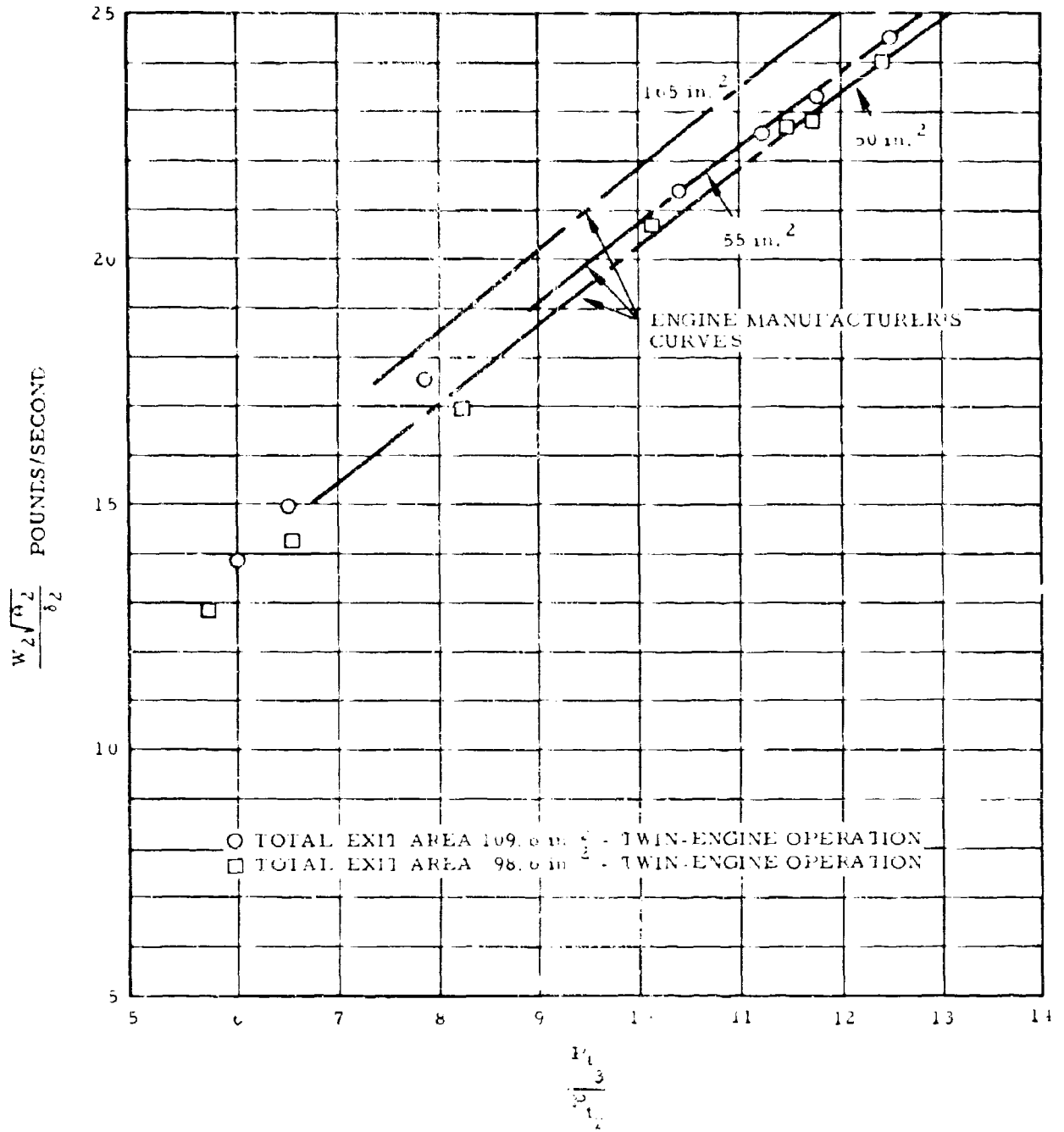


Figure 69. Engine 026 Compressor Corrected Flow vs. Compressor Pressure Ratio

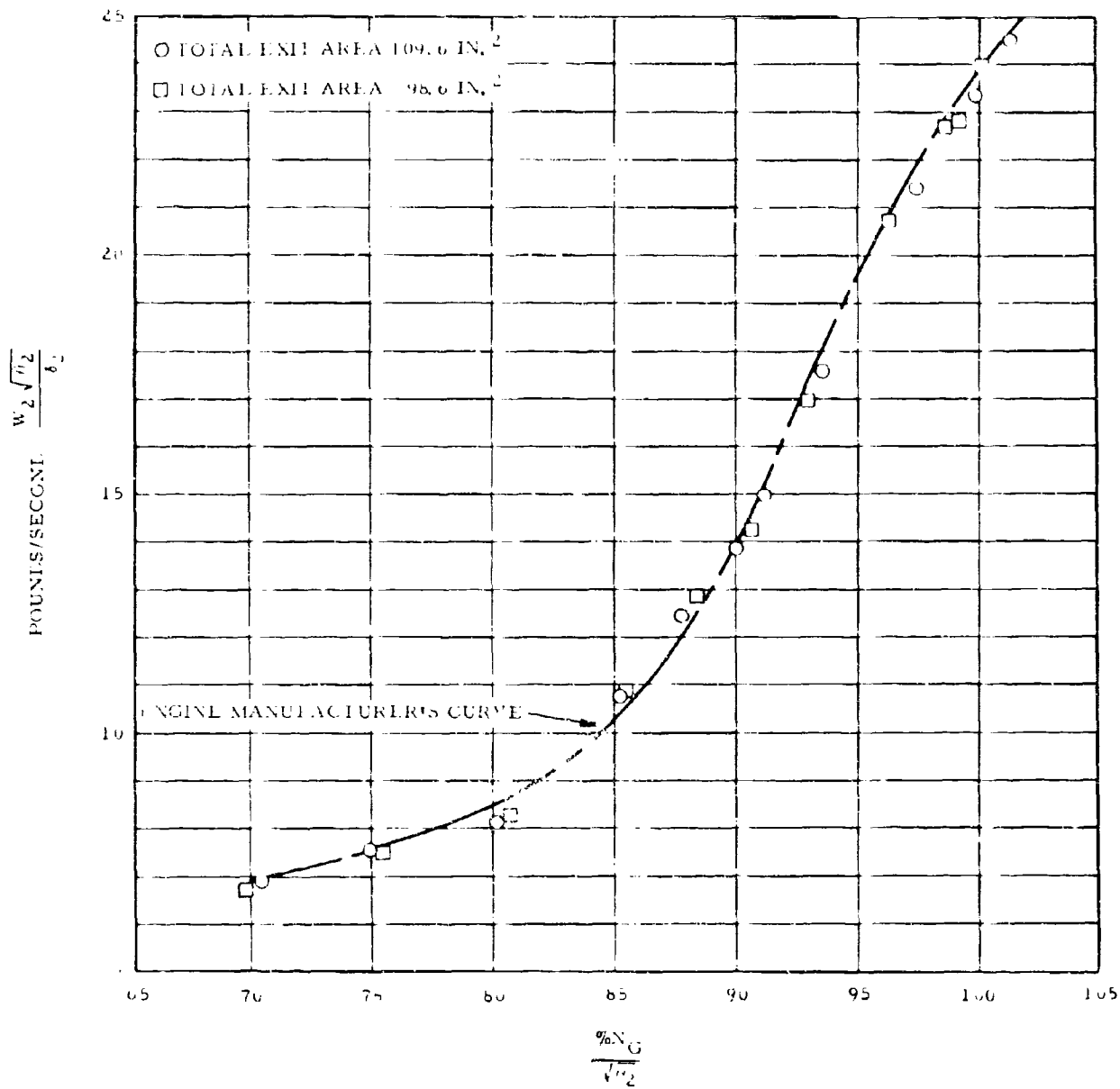
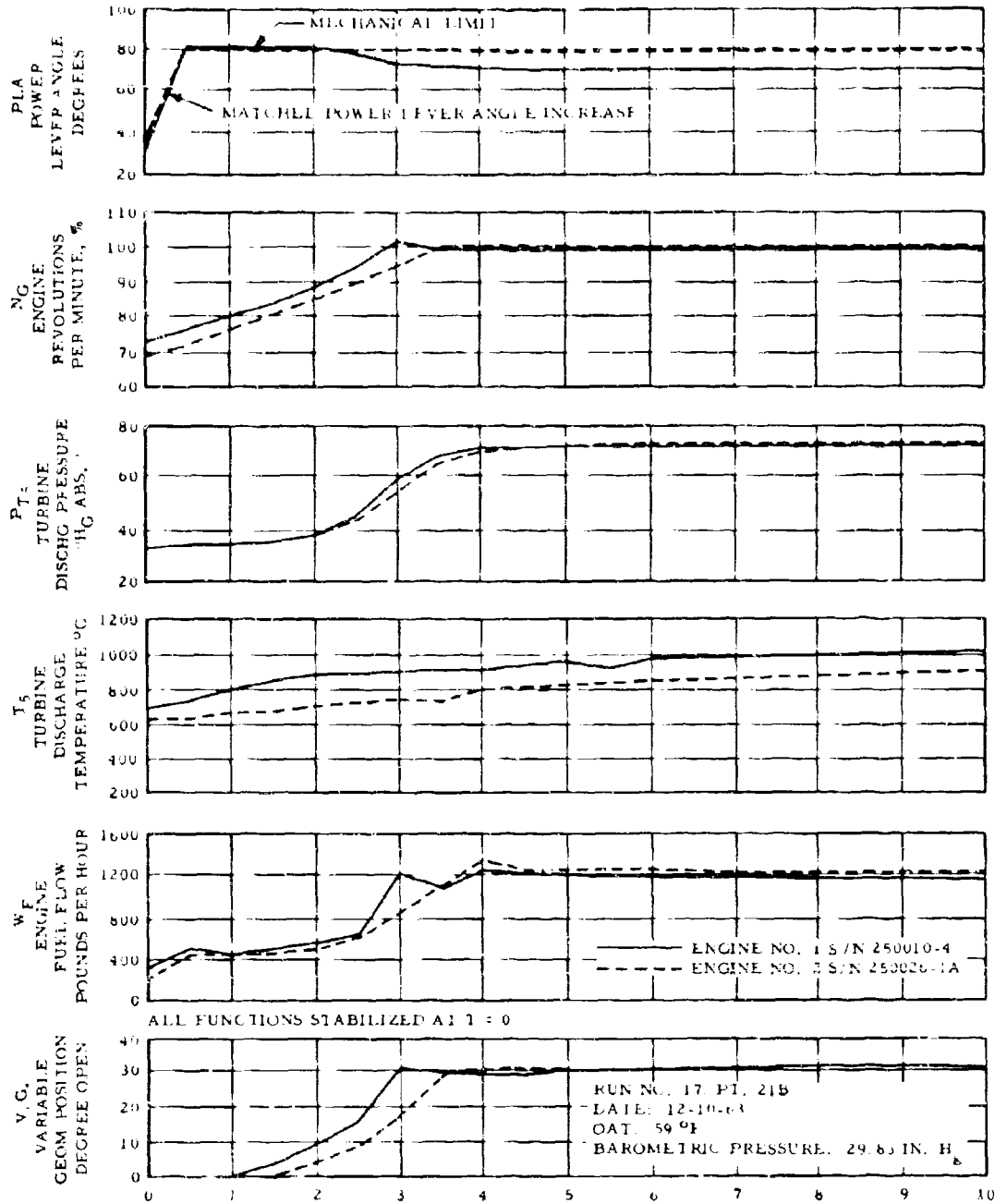
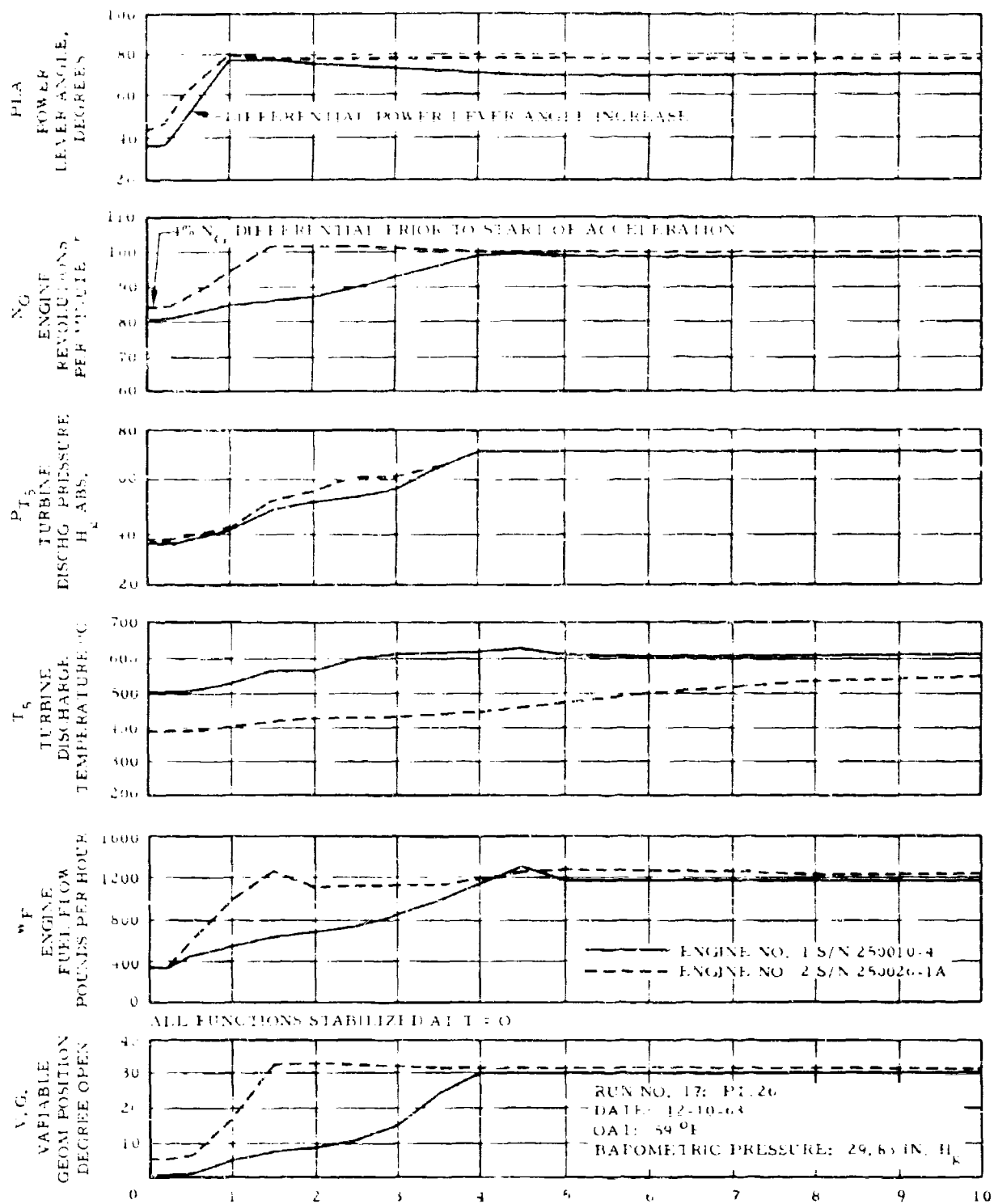


Figure 70. Engine 026 Compressor Corrected Flow vs. Corrected Engine Speed Twin-Engine Operation



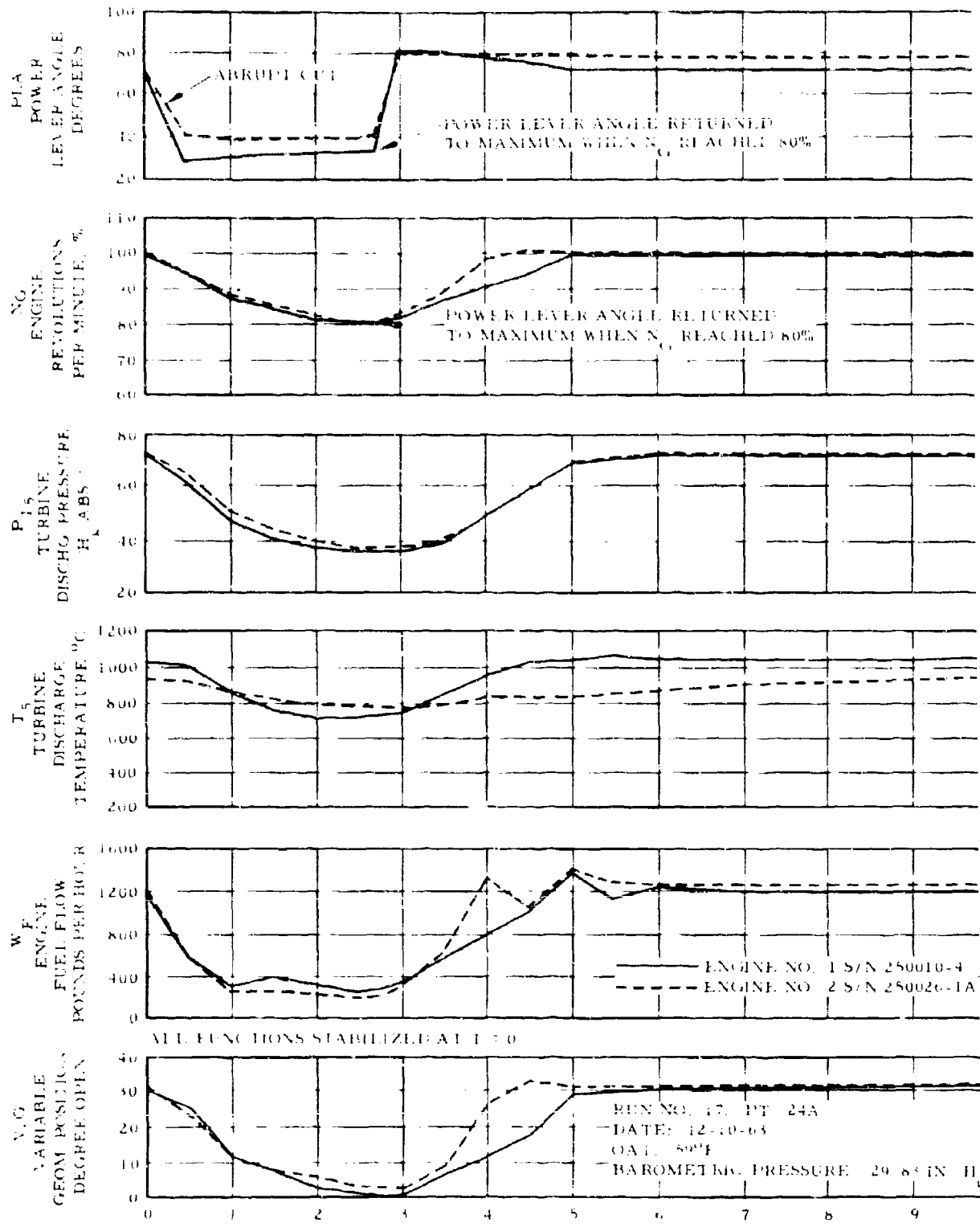
NOTE: GAS FLOW THROUGH DIVERTER VALVES & COMMON EXHAUST NOZZLE TWO Y1-64 GAS GENERATORS NOZZLE EXHAUST AREA = 98.6 IN<sup>2</sup>

Figure 71. Twin-Engine Operating Characteristics Rapid Acceleration from Idle to Maximum Power



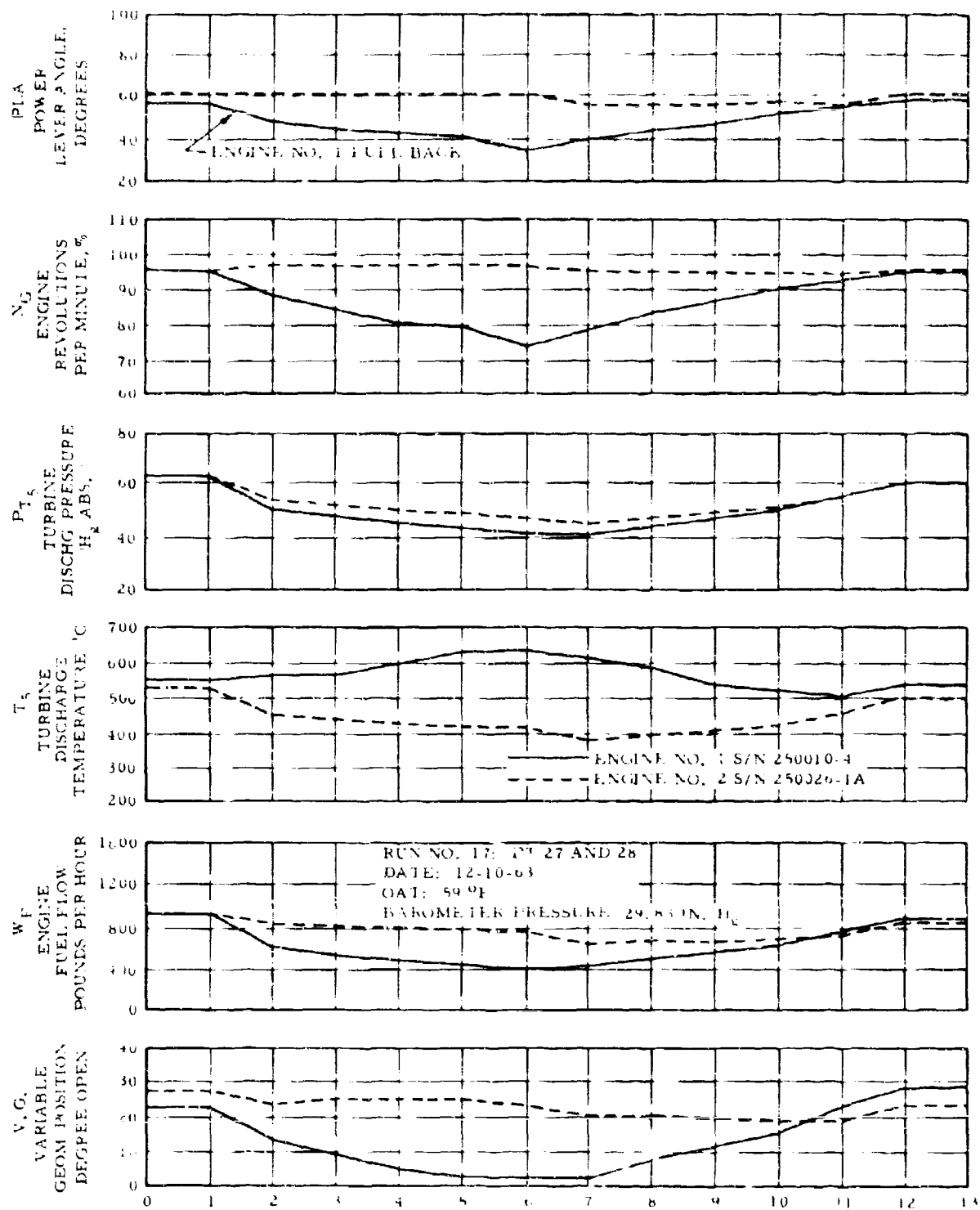
NOTE: GAS FLOW THROUGH DIVERTER VALVES & COMMON EXHAUST NOZZLE TWO Y1-64 GAS GENERATORS NOZZLE EXHAUST AREA = 98.6 IN<sup>2</sup>

Figure 72. Twin-Engine Operating Characteristics Rapid Acceleration to Maximum Power with Differential Starting Speeds



NOTE: GAS FLOW THROUGH DIVERTER VALVES & COMMON EXHAUST NOZZLE  
 TWO Y1-64 GAS GENERATORS  
 NOZZLE EXHAUST AREA 98.6 IN.<sup>2</sup>

Figure 73. Twin-Engine Operating Characteristics Rapid Power Change from Maximum to 80 percent N<sub>G</sub> and Return to Maximum 130



NOPL GAS FLOW THROUGH DIVERTER VALVES (POINT NO. (NO TIME SCALE))  
& COMMON EXHAUST NOZZLE,  
TWO YF-64 GAS GENERATORS  
NOZZLE A EXHAUST AREA = 98.6 IN<sup>2</sup>

Figure 74. Twin-Engine Operating Characteristics Steady-State  
Engine Data at Differential Power Setting

## 5.10.2 Flow Determination in Engine Testing

In the testing of the hot cycle system, the quality of performance evaluation depends much on the quality of air flow measurements. However, the problem of flow determination in the hot cycle duct system is complicated by various factors. In the first place, the internal ducting does not have a suitable section where any standard flow-measuring devices could be located. Secondly, the wide range of test conditions from stationary to flying is difficult to cover with any single conventional arrangement of instrumentation.

### 5.10.2.1 Bellmouth Measurements

The standard T64 bellmouth inlet was designed specifically for that engine to provide the measured values of inlet air flow. During the engine test program, the T64 bellmouth was considered as a primary standard for the purpose of calibration of pertinent system components. Until Run 17, which was the last in the series, the bellmouth was installed on Engine No. 1 (010-4). A water manometer was used to measure the pressure differential  $P_{T_2} - P_2$ . The calibration curve supplied by the engine manufacturer was used to convert manometer readings into corrected compressor flow. When some discrepancies were found between the results of the current tests and the manufacturer's test data, the complete bellmouth measuring system was thoroughly checked out. No leakage was detected in the system. The indications of the remote manometer were compared with the readings of sensitive gages mounted directly on the test rig. All readings were found to be the same. The bellmouth calibration curve was checked against the theoretical flow curve for compressible flow. The resulting flow coefficient for the bellmouth was found to be  $C_W = 0.985$ . Since this number was typical for bellmouths of this type, the calibration curve was concluded to be correct. In result, no reasons were found to question reliability of bellmouth measurement.

During the transient runs, the response of the manometer was checked with an electronic counter. The manometer attained steady state almost simultaneously with the counter and far ahead of the console  $P_{T3}$  pressure gages. This feat qualified the manometer indications as good for monitoring purposes.

#### 5.10.2.2 Hughes Tool Company Inlet Duct Measurements

The XV-9A inlet duct was designed with generous internal lip thickness to insure smooth inlet flow both statically and in flight. The instrumentation used with the inlet duct was identical to that installed with the standard bellmouth.

In all tests, with the exception of the last, the bellmouth was installed on Engine No. 1 (010-4) while Engine No. 2 (013-5 and 026-1A) was operated with XV-9A inlet. Prior to the last test, this arrangement was reversed to enable calibration of the inlet. The flow data recorded during that test had indicated that Hughes Tool Company inlet had essentially the same air flow calibration curve as the standard bellmouth.

#### 5.10.2.3 Engine Compressor Air Flow Measurements

The possibility of using the engine as a flowmeter has been discussed several times with the engine manufacturer.

Using compressor air flow curves, furnished by the engine manufacturer, is usually the most common method for determining the air flow in flight testing. The curves are generally plotted as  $\frac{W_2 \sqrt{\theta_2}}{\delta_2}$  vs.  $\frac{N}{\sqrt{\theta_2}}$  and  $\frac{W_2 \sqrt{\theta_2}}{\delta_2}$  vs.  $\frac{P_{T3}}{P_{T2}}$ . However, the T64 compressor has variable geometry which is related to a specific setting of the governor. Once the governor is removed for some reason or the variable geometry (V. G.) is reset, the calibration of the compressor is lost. The effect of hysteresis of V. C. mechanism may also result in an appreciable error, which adds to inaccuracy of the speed vs. flow curve.

The effect of the above limitations was noticeable in the test results. In Engine 010-4 and 013-5 the speed-flow relation was

different from that given by the manufacturer, and the flow versus compressor ratio was not consistent with other data. It is possible that the differences were caused by different V.G. settings and/or by some deterioration of the compressor. Contrarily, the new Engine 026-1A showed good correlation between all measurements (see Figures 69 and 70).

#### 5.10 2.4 Engine Turbine Inlet Air Flow Measurements

Not until the twin-engine testing was in progress was Station 4 (turbine inlet) considered for checking flow measurements. An evaluation study was made which proved that the turbine inlet used as a flow-measuring section is more accurate and better applicable in the test program than any other methods proposed previously. This is mainly due to the fact that Station 4 remains choked from maximum power down to the flight idle.

The turbine inlet also retains its geometry, unlike the compressor, and is unaffected by the changes in flow pattern associated with changes in flight conditions which cause inlet measurements to be meaningless.

Since the turbine inlet is not instrumented, its flow function cannot be expressed in terms of Station 4 parameters. However, it can be proved that when the turbine inlet is choked the following functional relation exists between the parameters measured at Stations 2, 3, and 5:

$$\frac{W_2 \sqrt{T_{t_3}}}{P_{t_3}} = \frac{f(T_{t_5} - T_{t_2})}{T_{t_3}}$$

In practice, the above relation represents a single curve which may be used to calibrate engine flow in any specific engine over the entire range of flight operation. Using this approach, Engines 010-4 and 026-1A have been calibrated. Test cell data and Hughes Tool Company engine test data were used in the calibration procedure. An example of a calibration curve is shown on Figure 75.

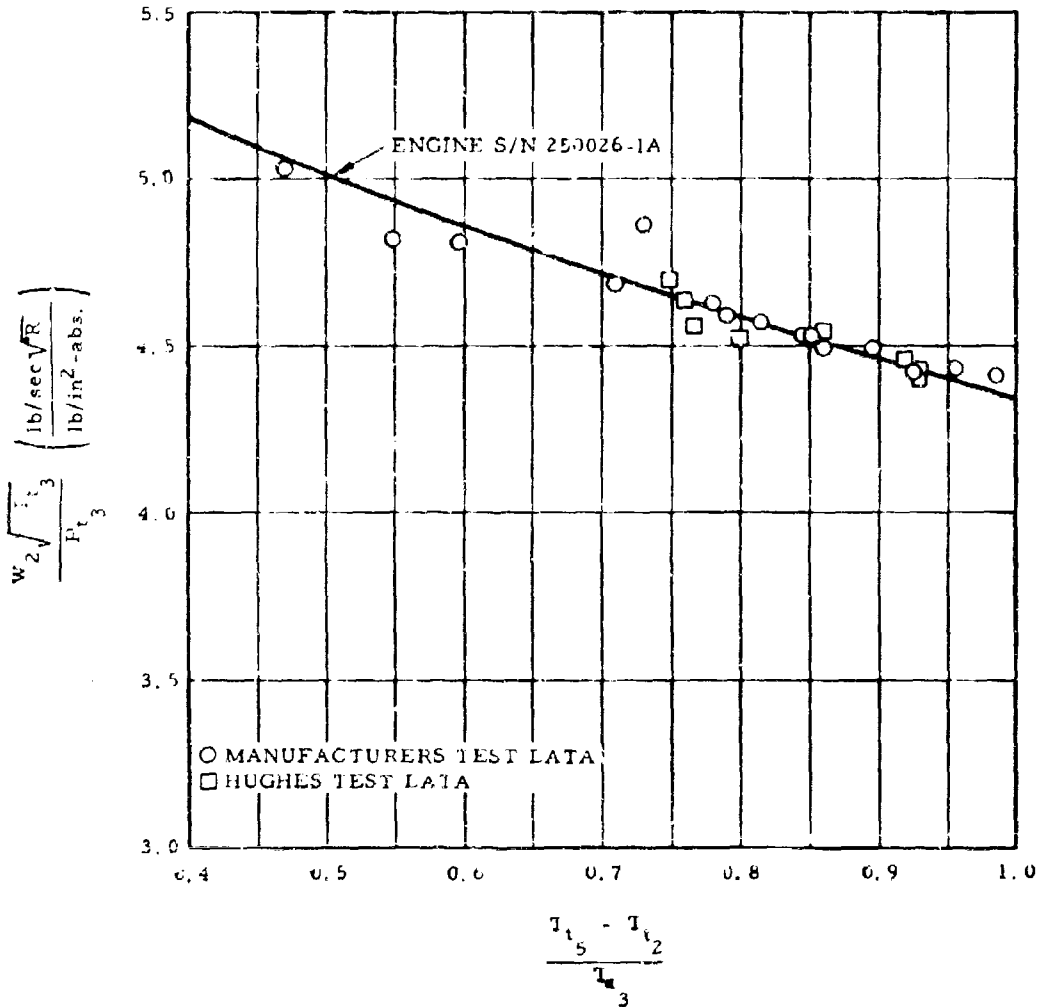


Figure 75. T-64 Gas Generator Air-Flow Characteristics

### 5.10.3 Pressure Loss in the Power Module

The absence of the rotor during the twin-engine test offered an opportunity to measure pressure losses in the nonrotating ducts of the power module. The straight annular duct of the common discharge nozzle was designed in anticipation of this particular test. Its location, which corresponded to the future location of the rotor hub, was suitable for this purpose. The duct was instrumented with 10 total pressure probes and 4 thermocouples equally divided between the opposite sides of the annulus. Gage pressure from the individual probes was recorded on the oscillograph. The temperatures were recorded on the strip chart recorder. As expected, the temperature in the module essentially remained unchanged. The results from total pressure measurements plotted versus engine discharge flow function are shown on Figure 76.

In the complete system, with the rotor operating between 90 and 100 percent rpm, the discharge flow function was found to vary between 53 and 54. At this value, the pressure loss between the engine exit and the rotor is about 4 percent.

### 5.10.4 Engine Test Instrumentation

The YT-64 gas generators were extensively instrumented to determine their operating characteristics and performance during twin-engine operation in the XV-9A propulsion system. The control van test operators' console which contained the basic engine instruments and controls was the primary reference for engine operation during all phases of testing, including starting, twin-engine steady state, and twin-engine transients. The instruments used for this purpose were of the standard sensitive type currently being used in multiengine jet aircraft. Most of these instruments were to be used subsequently in the XV-9A during flight testing.

A 50-channel oscillograph recording 30 data functions was used to record engine parameters during transients and conditions where rapid changes were expected. Strip chart and temperature recorders were used for engine gas flow and power module structural temperatures. A water manometer board with a 35mm camera for recording was used to record engine air flow data.

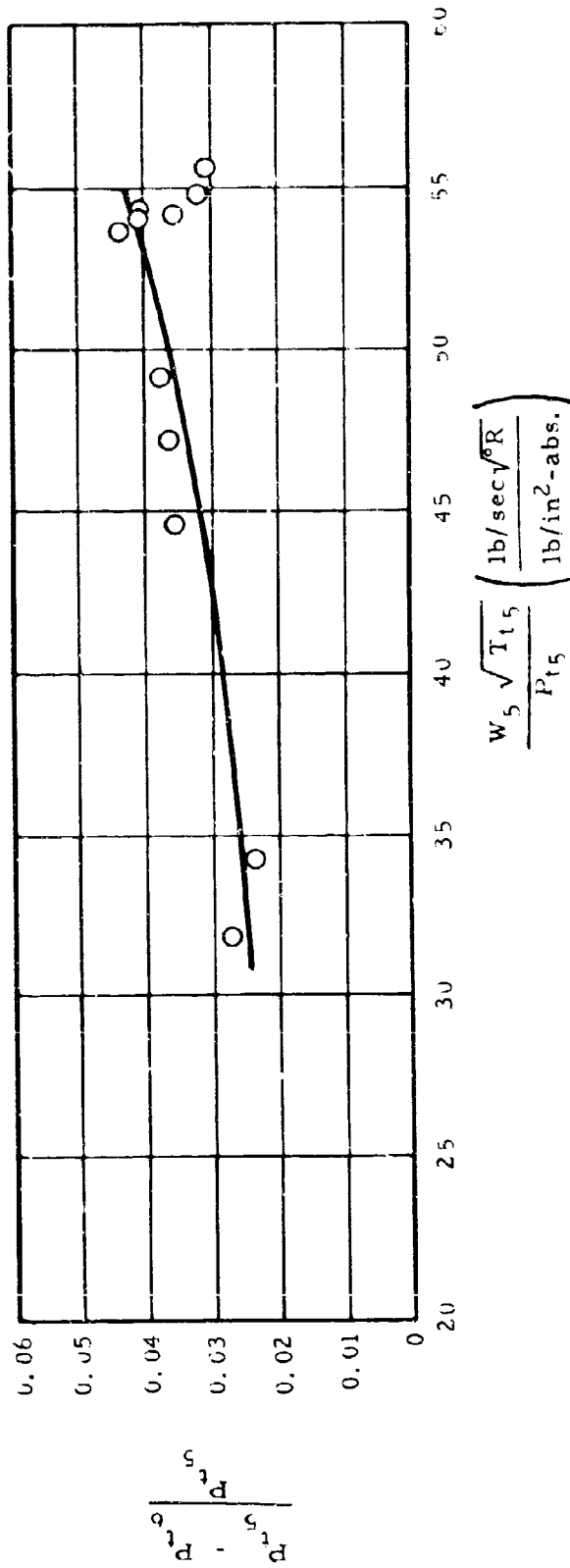


Figure 76. Pressure Loss Between Engine Exit (Station 5) and Hub (Station 6)

Engine air flow measurement was by means of a standard calibrated bellmouth, with instrumentation probes installed to measure total and static pressures and temperatures at six radial locations. Temperature probes consisted of three individual elements paralleled for single read-out at six radial locations and recorded on a multiple-point temperature recorder. The total and static pressure probes were connected to the water tube manometer located in the control van and recorded by the 35mm camera.

Although only one standard bellmouth was available during these tests, air flow calibrations were obtained for both engines by installing the bellmouth on each engine for calibration tests. The standard bellmouth was installed on Engine No. 1 (010-4) during Runs 1 through 16 and on Engine No. 2 (026-1A) during Run 17.

The Hughes Tool Company inlet with air flow instrumentation was installed on Engine 013-5 during Runs 1 through 6, on Engine 026-1A during Runs 8 through 16 and on Engine 010-4 during Run 17.

1. Control Console, Direct-Reading Aircraft Type Instruments  
(35mm Sequence Camera Used For Recording)

Engine Speed, $N_G$	Both Engines, % RPM
Turbine Discharge Temperature, $T_5$	" " °C
Turbine Discharge Pressure, $P_{T_5}$	" " "Hg ABS.
Fuel Flow, $W_F$	" " LBS/HR
Compressor Discharge Pressure, $P_{T_3}$	" " "Hg ABS.
Power Lever Angle, PLA	" " Units (calibrated)
Variable Geometry Position, VG	" " " "
Fuel Control Outlet Pressure	" " PSIG
Fuel Temperature	" " °F
Engine Oil Pressure	" " PSIG
Engine Oil Temperature	" " °F

Engine Vibration	Both Engines, Mils. displacement
Fuel Boost Pressure	PSIG

2. Oscillograph, 50-Channel with Magazine and Take-up Reel

Engine Speed, RPM	Both Engines	
Turbine Discharge Pressure, $P_{T5}$	" "	
Compressor Discharge Pressure, $P_{T3}$	" "	
Engine Power Lever Angle, PLA	" "	
Variable Geometry Position, VG	" "	
Fuel Flow, $W_F$	" "	(Limit Switches)
Diverter Valve Position	" "	(Limit Switches)
Acceleration Vertical	" "	Fwd. Engine Mount
Acceleration Horizontal	" "	Structure Sta. 279
Common Duct Total Pressure, $P_{T6}$	10 Probes	Total Pressure Rake
" " Static Pressure, $P_{S6}$		(4) Orifices Manifolded
Compressor Discharge Static Pressure, $P_{S3}$ Eng. #1		

3. Strip Chart Temperature Recorders (4) (Chromel-Alumel)

Turbine Discharge Temperature, $T_5$ ,	Both Engines
Compressor Discharge Temperature, $T_3$ ,	" "

4. Temperature Recorder #1 (Copper-Constantan)  
Engine Inlet Temperature,  $T_2$  (6), each engine
5. Temperature Recorder #2 (Iron-Constantan)  
Power Module Structural Temperatures
6. Strip Chart Temperature Recorder (Chromel-Alumel)  
Common Duct Gas Temperature,  $T_6$
7. Manometer Board & 35mm Sequence Camera  
Engine inlet total pressure,  $P_{T_2}$  (6) each engine  
Engine inlet static pressure,  $P_{S_2}$  (6) each engine

#### 5.11 SIMULATED EMERGENCIES

The following simulated emergencies were performed during whirl testing to determine the operating characteristics of the rotor, engines, and systems for these nonroutine operations.

##### 1. Rapid Rotor and Engine Shutdown

A rapid shutdown of the rotor and both engines was accomplished at the termination of Run 28 on 7 May 1964 when residual hydraulic fluid underneath the No. 1 diverter valve was ignited.

The shutdown was initiated from the following conditions:

<u>Rotor</u>	<u>Engine #1</u>	<u>Engine #2</u>
$\theta = 10^\circ$	$N_G = 99.9\%$	$N_G = 101.4\%$
$N_R = 97.5\%$	$T_5 = 604^\circ\text{C}$	$T_5 = 595^\circ\text{C}$
Lift = 20,800 lbs		

The shutdown was accomplished in the following sequence:

- a. Engine power reduced to  $N_G = 90\%$
- b. Both diverter valves actuated to "overboard" position.
- c. Reduced collective to  $0^\circ$  as rotor speed decreased below  $80\% N_R$

The shutdown was accomplished rapidly and smoothly and rotor structural loads were low.

The time intervals were as follows:

- t = 0                    Start engine power reduction.  
t = 13 seconds    Diverter valves positioned to "overboard".  
t = 45 seconds    Rotor speed reduced to  $27.5\% N_R$ .

## 2. Single Hydraulic System and Controls Operation

The rotor controls were operated through their normal range and rates with each hydraulic system at zero pressure during Run 31 on 14 May 1964. The procedure was to bypass each hydraulic system one at a time and to operate cyclic and collective controls with the remaining system providing hydraulic power at 3500 psi. Cyclic and collective control operation was smooth and stable while operating on each individual hydraulic system at 3500 psi. There were no control transients or any noticeable effects when either system was bypassed to zero pressure. Normal operation of both hydraulic systems was restored without any noticeable effect.

## 3. Simulated Engine Failure and Engine Isolation

An engine failure was simulated from an initial condition of  $N_R = 96.5\%$  during Run 31 on 14 May 1964. The procedure was to reduce power on engine No. 1 and simultaneously increase power on engine No. 2 until  $N_R$  dropped to  $81\%$ . The engine No. 1 diverter valve was actuated to "overboard" position, which isolated this engine from the system. This operation was accomplished without adverse effect to either engine. The power on engine No. 2 was increased to  $N_G = 100.4\%$ , and rotor operation continued at reduced lift with this engine operating at twice normal exit area. The

resultant rotor lift was considerably reduced since the two-position blade-tip closure valves were not installed.

4. Engine Shutdown by Means of the Fuel System Firewall Shutoff Valves.

Both engines were shut down from idle condition during Run 31 on 14 May 1964 by closing the firewall shutoff valves. The resultant engine shutdowns required approximately 60 seconds as a considerable amount of fuel is contained within the engine fuel control which is downstream of the shutoff valves. Both engine shutdowns were completely normal.

5.12 COMPONENT MAINTENANCE AND REPAIR

During the course of the test program, very limited maintenance, repair and/or replacement of power module or rotor components was required. The following assemblies required action during the program:

- a. Engine tailpipe assembly - Failed during engine tests due to insufficient penetration of a weld. Part was repaired and reinstalled.
- b. Engine failure - Engine S/N 250013-5 failed during engine tests due to compressor blade fatigue. Engine S/N 250026-1A was installed for the remainder of testing.
- c. Hydraulic system supply selector valve - Functioned improperly during initial check-out. Return spring was replaced with one of a higher force. Repair was satisfactory.
- d. Diverter valve - Units installed during engine tests had insignificant leakage and were replaced with previously reworked spare units prior to whirl test. Removed units were subsequently returned to manufacturer for seal rework.

- e. Diverter valve actuator - O-ring failed during whirl test and was replaced. Actuator performance was erratic during entire test program. New actuators were designed and fabricated and were installed subsequent to whirl test.

With the exception of the above items, the results from the mechanical and performance tests of the system showed that all components functioned satisfactorily.

## 6. RESULTS OF POST-TEST INSPECTION

Following completion of whirl testing, the power module and rotor were removed from the whirl tower and returned to the factory area for leakage tests, teardown inspection, and reassembly prior to mating the power module and rotor to the XV-9A fuselage. The results of leakage tests have been discussed previously in this report.

The complete rotor assembly was removed from the power module. The blades were removed from the hub, and all leading-edge segments, trailing-edge segments, fairings, and access panels were removed from the blades. The laminated spars were removed from each blade for inspection of the spars, attachment bolts, and blade segments. The Y-duct and tri-duct were removed from the hub, and the blade-articulate ducts were removed. The tip-cascade assembly was removed from each blade. The rotor hub and shaft were disassembled, including hub gimbals and the upper and lower bearings. The YT-64 gas generators, diverter valves, transition ducts and tailpipes were removed from the power module. The flight control system components were removed, including hydraulic servo actuators, control rods, and swash-plate assembly. The instrumentation slip-ring assembly and various transducers were removed for inspection and recalibration.

### 6.1 INSPECTION RESULTS

#### 6.1.1 Rotor Hub Assembly

Leakage of the Y-duct and tri-duct assembly was found to be negligible. Carbon seals were found to be in good condition. Replacement was not necessary. The C-102978 center seal was not compressing freely. This was remedied by locally grinding some material from the C-102978-2 composite. Approximately 3/16 inch interference existed between the hub structure and the tri-duct. This was eliminated by removing some of the hub material and raising the hub a small amount (1/8 inch). Hub tilt limits were changed from 10 degrees maximum to 9 degrees maximum.

A gap was found between the ends of the radial bearing oil seals. New seals, made from slightly longer material with their ends bonded together, were installed in an effort to minimize oil leakage.

Spacer blocks were remade using titanium to provide a more rigid path for the tri-duct thrust loads. The cooling-air curtain was torn from interference with an instrumentation bracket and was replaced. The outer carbon seal assembly clamp gasket was hard and brittle. A new gasket was installed. There was no noticeable wear found on the following:

1. Hub gimbal bearings
2. Shaft radial bearing
3. Shaft thrust bearing
4. Accessory drive belt

#### 6. 1. 2 Rotor Blades and Spars

Bolts attaching the spars were removed. No torque values were below drawing tolerance except one where a nut plate came loose. A new nut plate was installed and new attaching bolts were used even though there was no evidence of excessive fretting. This was done to make it possible to identify any fretting taking place during the next phase of testing. There was no evidence of cracks in laminations. Small marks were found on each spar in one area where the edge of a segment contacted the spar. Corrective action was taken to eliminate this by extending the Armalon antifretting material to cover this area entirely. No evidence of elongation of holes in the segments due to whirl test loads was found. Some holes were found out of tolerance and were reamed out and bushed as required. Small areas of spar delamination at the outer end of some of the laminates existed prior to whirl tests. These areas showed no evidence of having extended during tests. The root-end fitting and attachment were reworked to improve the fatigue strength of this area as substantiated by component testing.

#### 6. 1. 3 Articulate Ducts

There was no measurable leakage at the inboard spherical seal. The leakage rate of the outboard lip seal was measured at approximately 11 - 12 cfm. This is about the same rate as measured on a new seal. However, since approximately 1/3 inch was worn off the lips, new seals were installed.

## 7. TEST INSTRUMENTATION

Test instrumentation measurements recorded during whirl test are listed on Tables 8, 9, 10 and 11. The following portion of the test instrumentation was installed in the control van during whirl tests:

	<u>Description</u>	<u>Quantity</u>
1.	Oscillograph, 50-channel with Magazine and Take-Up Reel	(2)
2.	12-Point Temperature Recorders	(3)
3.	Manometer, Multiple Tube, H <sub>2</sub> O with 35mm Sequence Camera	(1)
4.	Strip Chart Temperature Recorders	(4)
5.	Engine & Rotor Instrument Panel with 35mm Sequence Camera	(1)
6.	Thrust Meter	(1)

### 7. 1 DESCRIPTION OF INSTRUMENTATION

#### 7. 1. 1 Strain Gage Installation

Foil strain gages with a high-temperature epoxy backing were used on the rotor and power module. In areas where temperatures above 200 degrees F were expected, a high-temperature cement was used. For application where the temperature was not expected to exceed 200 degrees F, a room-temperature curing epoxy was used. Each gage installation was subjected to a short cure at the expected operating temperature to prevent drift.

All strain-gage bridge installations had 4 active gages with the exception of the hub plate strain, which had 2 active gages, and the engine strain rosette, which had 1 active gage in each bridge.

All strain-gage bridges on the blade were waterproofed and protected by silastic-rubber compound. In addition, the compound was used to attach the strain-gage lead wiring to the spar. This was satisfactory except in areas where there was oil contamination. In these areas, the compound never hardened.

Information on the location of strain-gage bridges is given in Table 9 and Figure 77.

### 7. 1. 2 Blade Thermocouple Installation

Chromel-Alumel (K calibration) thermocouples were used exclusively on the rotor. These thermocouples were 30-gage wire with double-woven fiberglass insulation.

The thermocouples on the blade skins, flexures and duct walls were attached by spot-welding the thermocouple directly to the part. The spot-weld formed the junction at which the temperature was measured.

The temperature of parts subjected to fatigue loading, such as the spars, was measured by using a thermocouple with a junction fused by use of a mercury arc. These thermocouples were then cemented to the part. The thermocouple wire on the spars was attached directly to the spar with a silastic compound. The lead wire for the thermocouples installed on the blade was attached to the blade by three small sheet-metal clips spot-welded to the blade segment. The wire underneath these clamps was protected by wrapping it with fiberglass tape. Silastic compound was then applied to hold the wire in place. The arrangement worked very well.

The thermocouples installed in the blade-tip cascades were made from inconel sheathed Chromel-Alumel wire. Location of thermocouples is given in Table 10 and Figure 78.

### 7. 1. 3 Power Module Structural Thermocouples

Iron-Constantan (J calibration) thermocouples were used to monitor the temperatures in the critical areas of the power module. These thermocouples were attached directly to the parts by spot-welds. 30-gage wire with double fiberglass insulation was used. The location of the various thermocouples is given in Table 11.

### 7. 1. 4 Engine Performance Thermocouples

All engine performance temperatures were measured with probes furnished by the engine manufacturer. The engine inlet temperatures were monitored by Copper-Constantan thermocouples which were attached to the lead wire with compensated quick-disconnect plugs. The compressor outlet and turbine outlet temperatures were monitored using Chromel-Alumel probes attached to the lead wire

with compensated quick-disconnect plugs. These probes are shown in Figure 79.

#### 7. 1. 5 Rotor Thrust Measuring System

The rotor and power module were attached to 4 load cells at the 4 points where the power module attaches to the fuselage. The load cells then attached the power module to the tower in such a fashion that the force path of the rotor thrust was through the load cells. The side loads were reacted by adjustable links to prevent horizontal movement of the power module. The load cells were of the dual bridge type. One of the bridges of each load cell was connected to a summing circuit which provided the operating signal for a thrust indicator. This indicator was equipped with a retransmitting slide wire to provide a read-out of the sum in the oscillograph. The other bridge in each load cell was also connected to the oscillograph so that the load sensed by each individual load cell could be recorded. The installation of the load cells is shown in Figure 80. The indicator is shown in Figure 81.

#### 7. 1. 6 Pressure Measurements

##### 1. Engine Test

Engine inlet pressures ( $P_2$ ) were measured with a multi-tube water manometer. Compressor discharge pressures ( $P_3$ ) were measured with pressure transducers. Turbine discharge pressures ( $P_5$ ) were also measured with pressure transducers. Pressure transducers were used to measure the gas pressure ( $P_6$ ) in the variable area exit nozzle. Figure 82 shows the probe arrangement in the variable area exit nozzle.

##### 2. Whirl Test

All pressures described above with the exception of  $P_6$  were measured during the whirl test program. In addition, additional transducers were installed to measure the blade-tip cascade entrance pressure ( $P_7$ ) and the diverter-valve pressure. A differential pressure transducer was used to measure the pressure in the yaw control duct. Figure 83 shows installation of pressure transducers near the tip of the blade. The pressure transducer used to measure  $P_7$  was selected because of its low sensitivity at g forces in the plane of the diaphragm. The error at 500 g's was less than .3 percent of full range.

## 7. 1. 7 Additional Test Instrumentation

### 1. Rotor Shaft

The rotor shaft was strain gaged to measure shaft bending loads at the upper bearing. Two bending-type bridges were attached to the shaft 90 degrees apart to provide information about the bending moment at all times. The location of the individual strain-gage bridges is given in Table 9. In addition, thermocouples were attached to the shaft and spoke to record the temperatures experienced by the shaft.

### 2. Gimbal Lug

The gimbal lugs were strain gaged in such a fashion as to be sensitive to bending loads caused by a load along the axis of the bolts.

### 3. Swashplate Drag Link

The swashplate drag link was strain gaged to be used as a load cell to measure the swashplate drag loads. This was done by designing a reduced area section in the link so as to give a high and reliable signal level.

### 4. Blade Pitch Control Links

Each of the blade pitch control links was designed to serve as a load cell by incorporating a reduced area section to increase the strain level. The links were strain gaged with an axial-type bridge to measure the control forces.

### 5. Blade Pitch Control Cylinders

The blade pitch control cylinders were designed so that they could be used to measure the applied control forces. Each control cylinder had two strain-gage bridges of the axial type to provide an alternate in the event that one failed.

### 6. Blade Duct Torsion Bridges

The seal support ring was strain gaged to measure duct-torsion loads. The duct torque is reacted as a couple in the ring, and

so the ring was strain gaged to measure the bending moment in the ring.

#### 7. Yaw Control Valve Load Cells

Load cells were used as lateral supports for the yaw control valve when it was mounted on the whirl tower for test. Each load cell was wrapped with 1/4-inch copper tubing through which water passed to keep the load cell cool. This was done inasmuch as the load cells were subjected to the blast of the hot gases from the yaw control valve.

#### 8. Hub Tilt Indicator

The motion of the hub was measured by using a variable potentiometer which was actuated by an arm resting on a fitting attached to the hub. This fitting had a cylindrical surface covered with a sheet of Teflon. As the cylindrical surface cancelled out the component normal to the red-blade axis, the pickup sensed hub tilt about one axis only. The hub tilt indicator is shown in Figure 84.

#### 9. Blade Coning Angle Indicator

The coning and flapping angle of the blue blade was measured by using a pickup. The pickup consisted of a strain-gaged beam attached to an arm which rested on a teflon pad at the root end of the blade. The top of the blade at the root end is cylindrical about the feathering axis so that the blade flapping pickup is unaffected by a change in blade pitch. The blade coning angle indicator is shown in Figure 85.

#### 10. Strap Windup Indicator

The strap windup is a function of the relative movement between the blade and the hub. The strap windup indicator consisted of a strain-gaged beam attached to a link which pivoted at the hub and had one end fixed to the torque tube assembly. Figure 85 shows the installation.

#### 11. Rotor RPM and Azimuth Indicator

The rotor azimuth position was determined by using a magnetic pickup attached to the stationary structure with a steel pointer

attached to the rotor. As the blue blade passed the forward position, it caused a pulse which was then recorded.

### 12. Vibration Sensors

Vibrations were measured by accelerometers of the unbonded strain-gage type. Two were affixed to the upper bearing structure to measure longitudinal and lateral vibrations. Each engine also had two accelerometers attached. One was sensitive in the vertical direction and the other in the lateral direction. Figure 86 shows the engine accelerometer installation.

### 13. Control Movement Sensors

The movement of the pitch control cylinders was measured with a displacement transducer. The cable was attached to the pitch control cylinder, and the base was attached to the power module structure. The movements of the test conductors' control sticks were measured with similar transducers. One was connected to the collective stick. Two were connected to the cyclic pitch stick, one to measure longitudinal pitch and the other to measure lateral pitch.

### 14. Engine Variable Geometry

The position of the inlet guide vanes was measured using a potentiometer installed on the engines by the manufacturer. The output of potentiometers was connected in a Wheatstone bridge arrangement for convenience in calibrating and recording.

### 15. Engine Power Lever Angle

The position of the engine power lever was measured by attaching a displacement transducer to the engine fuel control cable. The internal wiring of the displacement transducer is a Wheatstone bridge circuit so that the output can be used with a balance box and calibrated easily.

## 7.2 CALIBRATION PROCEDURES

### 1. Rotor Blade

The initial calibration of the rotor blade was carried out as part of the component test program and is described in Reference 6. At the conclusion of the whirl test program, the calibration of the flap-wise bending bridges was checked by applying increments of 20 pounds dead weight up to a total of 100 pounds, and the output of each strain-gage installation was recorded.

### 2. Rotor Shaft

The rotor shaft bending bridges were calibrated by loading the rotor shaft as a simply supported beam with a concentrated load applied at the upper bearing by a static test machine. A strain indicator was used to record the output.

### 3. Rotor Thrust Measuring System

The thrust measuring system was calibrated by connecting the load cells in series and applying increments of load with a static test machine up to 10,000 pounds. The output of the summing circuit was read on the dial indicator, and the output of the individual bridges was recorded by an oscillograph. Later, when the load cells were installed on the whirl tower, this calibration was verified by applying a load to the system with a crane using a calibrated load ring to measure the applied load as shown in Figures 87 and 88. This same calibration was performed at the conclusion of the whirl test, and it was found that the calibration remained unchanged.

### 4. Gimbal Lug

The gimbal lug bending bridges were calibrated by applying a load in 500-pound increments to a total of 3500 pounds to the tip of the blue blade. This method also provided for a check on the spar axial-load bridges and the shaft-bending bridges. The output of the bridges was recorded with an oscillograph.

#### 5. Swash-Plate Drag Link

The swashplate drag link was loaded to 5000 pounds in 500-pound increments using a static test machine. The output of the strain-gage bridges was monitored with the use of a strain indicator.

#### 6. Pitch Link

The pitch links were loaded to a total of 5000 pounds in 500-pound increments in a static test machine. The output was recorded with a strain indicator.

#### 7. Control Cylinders

The control cylinders were calibrated in a test machine in 1000-pound increments up to a total of 6000 pounds. The output of each bridge was monitored by use of a strain indicator.

#### 8. Yaw Control Valve Load Cells

The yaw control valve load cells were calibrated in 25-pound increments up to a total load of 250 pounds each in a static test machine. The output of the strain gages was monitored with the use of a strain indicator.

#### 9. Duct Torsion Bridge

The duct torsion bridges were calibrated by placing the ducts in a fixture and applying a moment with the use of weights. The torsion was applied in 200-inch-pound increments up to a total of 1000 inch-pounds. The moment was applied in both directions. The output of the bridges was monitored using a strain indicator.

#### 10. Blue Blade Coning Angle Pickup

The blue blade coning angle pickup was calibrated by lifting the blade at the tip with a crane and measuring the angle of the pitch arm with a precision clinometer. The output of the bridge was recorded by an oscillograph.

### 11. Blue Blade Strap Windup Pickup

The strap windup pickup was calibrated by changing the pitch of the blade while the hub was blocked to prevent rotation. The angle of the blade was then measured with a precision clinometer. The blade pitch was increased in increments to full cyclic pitch, and then collective pitch was added to increments until full collective pitch was reached. The output of the pickup was recorded by an oscillograph.

### 12. Hub Tilt Pickup

The hub tilt pickup was calibrated by placing the precision clinometer on the hub parallel to the pitch axis of the red blade and another bubble level at right angles to it. The hub was then tilted by pulling down or pushing up on the red blade using the other blades to balance the hub so that the maximum tilt occurred at the red blade. The hub was tilted in increments until the tilt stop was reached. The output of the pickup was recorded by an oscillograph.

### 13. Pressure Transducers

The pressure transducers were calibrated using a standard deadweight tester. The pressure was increased in increments up to the full expected operating pressure of the transducer. The transducer output was measured with a strain indicator.

### 14. Accelerometer Calibrations

The accelerometers used as vibration pickups were calibrated by rotating the accelerometer 90 degrees each way from the center position. This gives a 1 g calibration in each direction of the sensitive axis. The accelerometer outputs were recorded by an oscillograph.

### 15. Engine Variable Geometry

The variable geometry pickups were calibrated by actuating the variable geometry control cylinder with air and measuring the extension of the actuator as well as reading the attached protractor provided by the manufacturer. The output of the pickup was recorded by an oscillograph.

## 16. Engine Power-Lever Angle

The engine power-lever angle sensor was calibrated by attaching a protractor to the power-lever shaft and then moving the throttles in increments until military power setting was reached. The output of the sensor was recorded by an oscillograph.

## 17. Thermocouple Calibrations

The thermocouple wire used had standard tolerances of  $\pm 4$  degrees F to 530 degrees F and 3/4 percent from 530 to 1000 degrees F. The various temperature recorders used were calibrated according to the manufacturer's instructions upon installation and at various times throughout the program. The calibrations included both zero setting and span.

### 7.3

## RECORDING INSTRUMENTATION

### 1. Strain-Gage Recording Instrumentation

The strain-gage bridges on the rotor were plugged into junction boxes on the rotor head that were connected to a 200-track slip ring. The slip ring installation is shown in Figure 89. From the slip ring, the wires ran to bridge balance boxes. These balance boxes had the capability of being used in a common power configuration. The use of common power greatly reduced the number of slip ring tracks required for a given number of bridges. For the strain gages and transducers whose outputs did not pass through the slip ring, additional balance boxes were used. These balance boxes employed an individual voltage adjustment on each channel for attenuation. Two 50-channel oscillographs were used to record the strain-gage and transducer outputs. Each oscillograph was equipped with a magazine which provided direct read-out. Take-up reels were attached to the magazines to spool the record as it was developed. The paper selected for use throughout the test was satisfactory. The oscillograph and balance boxes are shown in Figure 93.

### 2. Engine Temperatures

Engine  $T_3$  and  $T_5$  temperatures were recorded by 18-single-point strip chart recorders, two being used for each engine. Engine  $T_2$  temperatures were recorded by a 12-point recorder. Each  $T_2$  thermocouple was connected to a stepping switch so that six separate

temperatures on each engine were recorded. The  $T_3$  and  $T_5$  probes were each connected in parallel, and only one readout for each one was provided. These recorders are shown in Figures 90 and 91.

### 3. Power Module Structural Temperatures

The thermocouples attached to the power module structure in the critical areas were connected to a 48-point stepping switch. This switch in turn was operated by a 12-point recorder to provide a record of the temperatures encountered.

### 4. Rotor Thermocouples

All thermocouples on the rotor were connected to one of three 48-point stepping switches. The switch boxes were then connected to a hot reference junction. The hot reference junction was used to prevent end-junction dissimilar metals from forming a thermocouple which could introduce an error into the measurement. The wires from the hot reference junction to the 12-point recorder located in the control van were all copper; hence, no error would be introduced. The stepping switches are shown in Figure 92. The recorder can be seen in Figure 91.

### 5. Manometer

The multitube water manometer was recorded by using an automatic 35mm sequence camera. The pressures were then determined by reading the film on a microfilm reader. High contrast panchromatic film was used and provided excellent definition for enlarging. This installation is seen in Figure 94.

### 6. Engine and Rotor Instrument Panel

The engine and rotor instruments used by the test operators were also recorded photographically over the operators' heads. The film used along with a fine-grain developer gave excellent results. The camera used was a 35mm sequence camera. The installation can be seen in Figure 95.

TABLE 8  
 ROTOR & ENGINE PERFORMANCE, ROTOR GEOMETRY, & CONTROL  
 SYSTEM MEASUREMENTS

Function	No. of Transducers	Units of Calibration
Blade Tip Pressure ( $P_{T_7}$ )	6	PSIA
Turbine Discharge Pressure ( $P_{T_5}$ )	2	PSIG
Compressor Discharge " ( $P_{T_3}$ )	2	PSIG
Compressor Inlet Pressure ( $P_{T_2}$ ) (& $P_{S_2}$ )	12	Inches of Water
Variable Area Exit Nozzle ( $P_{T_6}$ )	11	PSIG (Engine Test Only)
Yaw Control Duct Pressure	1	PSID
Diverter Valve Pressure	1	PSIG
Rotor Thrust	4	Pounds Force
Yaw Control Valve Thrust	2	Pounds Force
Engine RPM	2	RPM
Engine Power Lever Angle	2	Degrees of Travel
Engine Compressor Variable Geometry	2	Inches of Movement
Engine Accelerations	4	G's
Cross Flow Vane Position	1	Degrees of Vane Movement
Diverter Valve Position	2	Rotor or Overboard
Control Actuator Position	3	Inches of Movement
Longitudinal Cyclic Stick Position	1	Degrees
Lateral Cyclic Stick Position	1	Degrees
Collective Position	1	Degrees
Rotor RPM	1	RPM

TABLE 8 (Continued)  
 ROTOR & ENGINE PERFORMANCE, ROTOR GEOMETRY, & CONTROL  
 SYSTEM MEASUREMENTS

Function	No. of Trans- ducers	Units of Calibration
Hub Tilt Angle	1	Degrees of Hub Tilt
Blade Flapping Angle	1	Degrees of Blade Coning
Blade Feathering Angle	1	Degrees of Blade Pitch
Upper Bearing Accelerometers	2	G's

TABLE 9  
STRAIN GAGE INSTALLATIONS WHIRL TEST

Bridge Name	Bridge Number	No. of Gages	Bridge Type	Bridge Location		Station
				Part Name	Part No.	
Flapwise Bending	1	4	Bending	Aft Spar	385-1108-5	63.0
"	2	4	"	"	"	75.4
"	4	4	"	"	"	100.0
"	5	4	"	"	"	140.0
"	7	4	"	"	"	220.0
"	8	4	"	"	"	270.0
Chordwise Bending	3	4	Axial	"	"	90.75
"	6	4	"	"	"	149.0
Flapwise Bending	9	4	Bending	Forward Spar	385-1108-3	63.0
"	10	4	"	"	"	75.4
"	12	4	"	"	"	100.0
"	13	4	"	"	"	140.0
"	15	4	"	"	"	220.0
"	16	4	"	"	"	270.0
Chordwise Bending	11	4	Axial	"	"	90.75
"	14	4	"	"	"	149.0
Horizontal Shear	17	4	Shear	Blade Struct.	285-0127	23.50
Vertical Shear	20	4	"	"	"	23.50

TABLE 9 (Continued)  
 STRAIN GAGE INSTALLATIONS WHIRL TEST

Bridge Name	Bridge Number	No. of Gages	Bridge Type	Bridge Location	
				Part Name	Station
Skin Torsion	18	4	Shear	Blade Structure	285-0166 38.00
"	19	4	"	"	285-0138 82.00
In-Plane Bending	32	4	Bending	Rotor Shaft	285-0517 W. L. -9.6
"	33	4	"	"	" W. L. -10.4
90° to In-Plane Bending	30	4	"	"	" W. L. -9.6
"	31	4	"	"	" W. L. -10.4
Gimbal Lug Bending	34	4	"	Hub Gimbal Beam	285-0526 W. L. +4.25
"	35	4	"	"	" W. L. +4.25
Hub Plate Strain Fwd Blue Blade	-	2	Axial	Lower Hub Plate	285-0564 11.5
Hub Plate Strain Aft Blue Blade	-	2	"	"	" 11.5
Blue Blade Duct Torsion	-	8	"	Duct Gimbal Ring	285-0178 19.0
		2-4 Gage In Parallel		Gages per-----	285-0995

TABLE 9 (Continued)  
STRAIN GAGE INSTALLATIONS WHIRL TEST

Bridge Name	Bridge Number	No. of Gages	Bridge Type	Bridge Location		Station
				Part Name	Part No.	
Red Blade Duct Torsion		8(2-4 Gage Bridges in Parallel)	Axial	Duct Gimbal Ring Gages Installed Per 285-0955	285-0178	19.00
Yellow Blade Duct Torsion		8(2-4 Gage Bridges in Parallel)	"	"	"	19.00
Strap Wind-up Blue Blade		4	Bending	Strap Wind-up Pickup	285-0948	Hub 19.0
Blue Blade Flapping Angle		4	"	Flapping Angle Pickup	285-0947	Hub 19.0
Pitch Load Blue Blade		4	Axial	Control Rod Assy	285-0305-9	Hub 19.0
Pitch Load Red Blade		4	"	"	"	Hub 19.0
Pitch Load Yellow Blade		4	"	"	"	"
Swash Plate Drag Link		4	"	Swash Plate Drag Link	385-9333	Shown 285-0300 W. L. -57.2
Lateral Actuator Load		4	"	Lateral Control Actuators (2)	385-6109	Shown 385-6110 W. L. -55.55

TABLE 9 (Continued)

## STRAIN GAGE INSTALLATIONS WHIRL TEST

Bridge	Bridge Number	No. of Gages	Bridge Type	Part Name	Bridge Location		Station
					Part No.	Part No.	
Longitudinal Actuator Load		4	Axial	Longitudinal Control Actuator	385-6109	Shown 385-6110 Fus. Sta. 286.0	
Engine Mtg. Pad Strains	R/H Pad Lower	"	"	#2 Engine	YT64 SNO26	Sta. 218.5	
Engine Mtg. Pad Strains	R/H Pad Aft	"	"	"	"	"	
Engine Mtg. Pad Strains	R/H Pad Upper	"	"	"	"	"	
Engine Mtg. Pad Strains	L/H Pad Upper	"	"	"	"	"	
Engine Mtg. Pad Strains	L/H Pad Aft	"	"	"	"	"	
Engine Mtg. Pad Strains	L/H Pad Lower	"	"	"	"	"	
Engine Mtg. Pad Strains	Accessory Gear Drive Pad Parallel To Eng. $\phi$	1	Axial	#2 Engine	YT64 SNO26	Sta. 218.5	
Engine Mtg. Pad Strains	Accessory Gear Drive Pad 45° to Engine $\phi$	1	"	"	"	"	

TABLE 9 (Continued)

STRAIN GAGE INSTALLATIONS WHIRL TEST

Bridge	Bridge Number	No. of Gages	Bridge Type	Bridge Location		Station
				Part Name	Part No.	
Engine Mtg. Pad Strains	Accessory Gear Drive Pad 900 to Engine $\text{C}$	1	Axial	#2 Engine	YT64 SNO26	Sta. 218.5

TABLE 10  
 ROTOR THERMOCOUPLE SUMMARY (CHROMEL-ALUMEL THERMOCOUPLES)  
 WHIRL TEST

General Location	Thermocouple Identification	Number of Thermocouples	Blade Sta. or Hub W. L.	Blade	Specific Location (Ref. Fig. 78)
Flexures	BC 2-1, 2, 3, 4	4	103.5	Blue	Flex #2, 285-1002
"	BC 4-1, 2, 3, 4	4	128.5	"	Flex #4, "
"	BC 6-1, 2, 4	3	153.5	"	Flex #6, "
"	BC 8-1, 2, 3, 4	4	178.5	"	Flex #8, "
"	BC 10-1, 2, 3, 4	4	203.5	"	Flex #10, "
"	BC 12-1, 4	2	228.5	"	Flex #12, "
"	BC 14-1, 3, 4	3	253.5	"	Flex #14, "
"	BC 16-3, 4	2	278.5	"	Flex #16, "
"	BC 18-1, 2, 3, 4	4	303.5	"	Flex #18, "
"	RC 2-1, 2, 3, 4	4	103.5	Red	Flex #2, "
"	RC 18-1, 4	2	303.5	"	Flex #18, "
"	YC 2-1, 2, 3, 4	4	103.5	Yellow	Flex #2, "
"	YC 18-1, 2, 3	3	303.5	"	Flex #18, "

TABLE 10 (Continued)  
 ROTOR THERMOCOUPLE SUMMARY (CHROMEL-ALUMEL THERMOCOUPLES)  
 WHIRL TEST

General Location	Thermocouple Identification	Number of Thermocouples	Blade Sta. or Hub W. L.	Blade	Specific Location (Ref. Fig. 78)
Blade Segments	BS 1-1, 2, 4, 5, 11, 12, 13, 14	8	96.0	Blue	Duct Walls, Segment #1 285-1002
"	BS 1-7, 8, 9, 10	4	96.0	"	Blade Skins, Segment #1 285-1002
"	BS 18-1, 2, 3, 4, 5, 6, 11	7	309.0	"	Duct Walls, Segment 18 285-1002
"	BS 18-8, 8, 9, 10	4	309.0	"	Blade Skins, Segment 18 285-1002
Blade Gas Temperatures	B-1, 2	2	330.0	"	Tip Cascade, 385-9629
"	R-1, 2	2	330.0	Red	"
"	Y-1 D, E	2	330.0	Yellow	"
Blade Cooling Air Temp.	BCDR	1	321.0	Blue	Aft Cooling Duct
"	BCDF	1	330.0	"	Forward Cooling Duct
"	B-57	1	57.0	"	Hub & Blade Cooling Air

TABLE 10 (Continued)  
 ROTOR THERMOCOUPLE SUMMARY (CHROMEL-ALUMEL THERMOCOUPLES)  
 WHIRL TEST

General Location	Thermocouple Identification	Number of Thermocouples	Blade Sta. or Hub W. L.	Blade	Specific Location (Ref. Fig. 78)
Blade Cooling Air Temp.	B-78	1	85.0	Blue	Hub & Blade Cooling Air
"	RCDR	1	321.0	Red	Aft Cooling Duct
"	RCDF	1	330.0	"	Forward Cooling Duct
"	R-57	1	57.0	"	Hub & Blade Cooling Air
"	R-78	1	85.0	"	Hub & Blade Cooling Air
"	YCDR	1	321.0	Yellow	Aft Cooling Duct
"	YCDF	1	330.0	"	Forward Cooling Duct
"	Y-57	1	57.0	"	Hub & Blade Cooling Air
"	Y-78	1	85.0	"	Hub & Blade Cooling Air
Blade Spars	B1A, B2A	2	63.0	Blue	Aft Spar, Upper & Lower Spar Caps
"	B1B, B2B	2	75.4	"	"
"	B3C	1	91.0	"	Neutral Axis of Aft Spar

TABLE 10 (Continued)  
 ROTOR THERMOCOUPLE SUMMARY (CHROMEL-ALUMEL THERMOCOUPLES)  
 WHIRL TEST

General Location	Thermocouple Identification	Number of Thermocouples	Blade Sta. or Hub W. L.	Blade	Specific Location (Ref. Fig. 7H)
Blade Spars	B4	1	100.0	"	Neutral Axis of Aft Spar
"	B5	1	140.0	Blue	"
"	B6	1	140.0	"	"
"	B7	1	220.0	"	"
"	B8	1	270.0	"	"
"	B11A, B11B	2	63.0	"	Forward Spar, Upper & Lower Caps
"	B12A, B12R	2	75.4	"	Forward Spar, Upper & Lower Caps
"	B13	1	91.0	"	Neutral Axis of Forward Spar
"	B14	1	100.0	"	"
"	B15	1	145.0	"	"
"	B17	1	220.0	"	"

TABLE 10 (Continued)  
 ROTOR THERMOCOUPLE SUMMARY (CHROMEL-ALUMEL THERMOCOUPLES)  
 WHIRL TEST

General Location	Thermocouple Identification	Number of Thermocouples	Blade Sta. or Hub W. L.	Blade	Specific Location (Ref. Fig. 78)
Blade Spars	BR	1	270.0	Blue	Neutral Axis of Forward Spar
Blade Structure	BR-1	1	45.0	"	Electroform Flexure
	BR-2	1	63.0	"	Inner Surface of Rib Sta. 63
	BR-3	1	73.0	"	"
	BRJ-1	1	19.0	"	Inner Surface of Tube
	BHD-1	1	15.0	"	Outboard Top of Disc Seal Ring
"	B-3	1	315.0	"	Tip Pressure Transducer Housing
Hub & Shaft	Hub #2	1	W. L. -13	-	On Rotor Shaft Below Rotating Seal
"	Hub #3	1	W. L. -8	-	On Rotor Shaft Below Spoke

10-11-68

TABLE 10 (Continued)  
 ROTOR THERMOCOUPLE SUMMARY (CHROMEL-ALUMEL THERMOCOUPLES)  
 WHIRL TEST

General Location	Thermocouple Identification	Number of Thermocouples	Blade Sta. or Hub W. L.	Blade	Specific Location (Ref. Fig. 7E)
Hub & Shaft	Hub #5	1	W. L. -6.5	-	Spoke, Inboard
"	Hub #6	1	W. L. -6.5	-	Spoke, Sta. 7.0
"	Hub #7	1	W. L. -6.5	Blue	Spoke, Sta. 14, at Tip
"	Hub #8	1	W. L. -2.5	Blue	Circum Fitting

TABLE 11

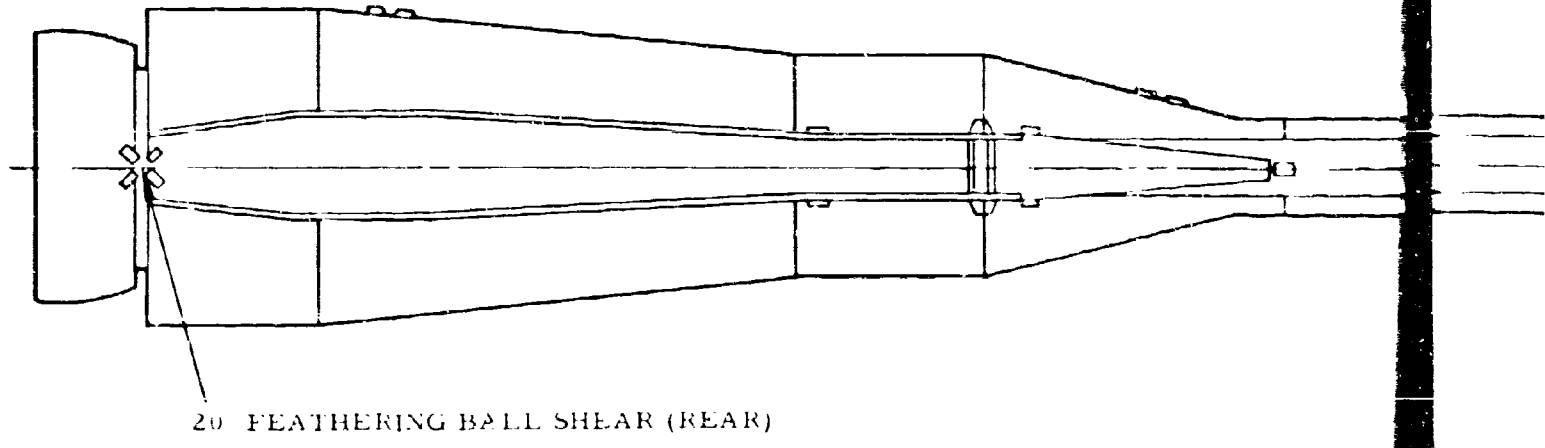
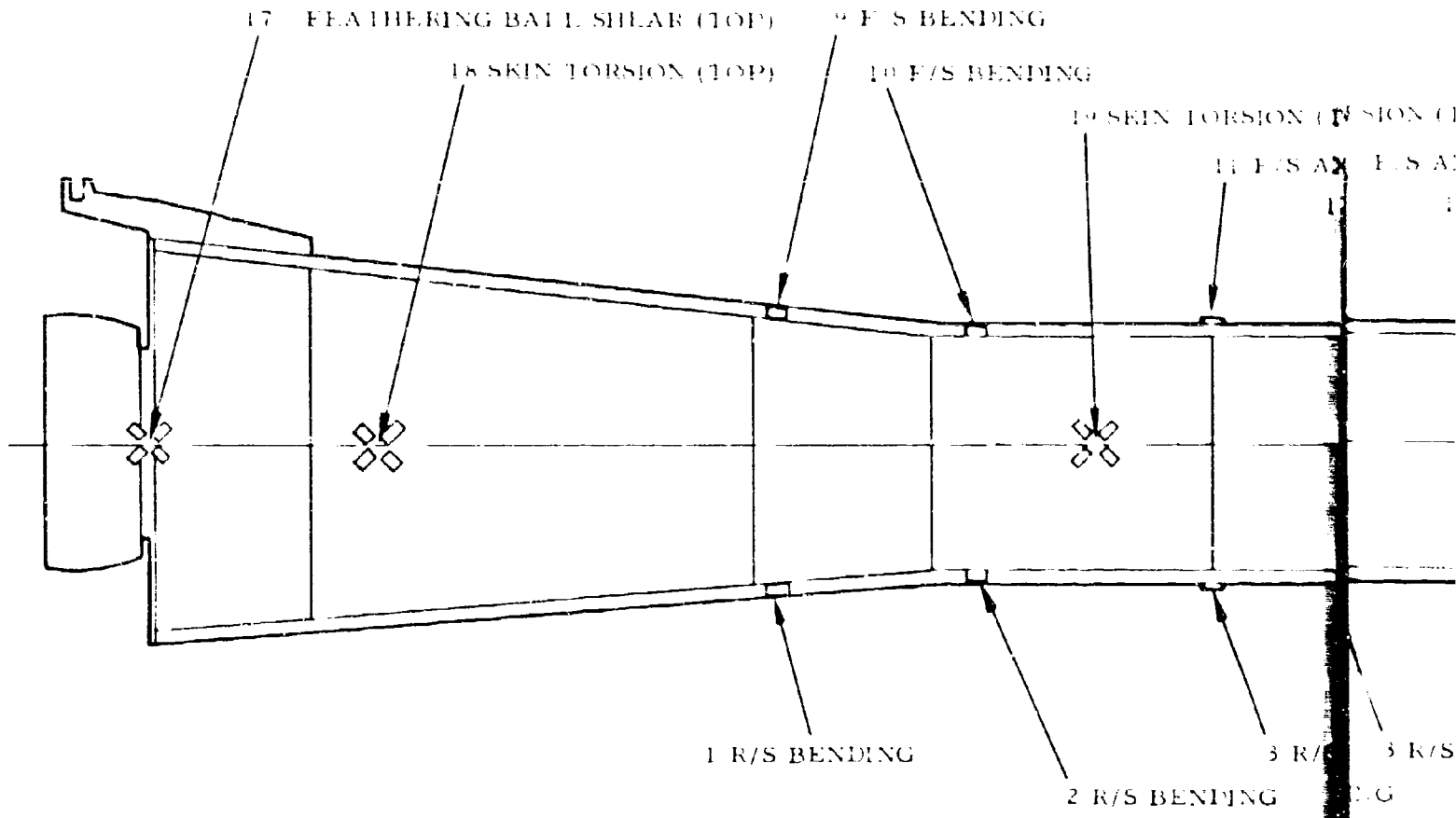
STRUCTURAL THERMOCOUPLE SUMMARY (IRON-CONSTANTAN THERMOCOUPLES)  
ENGINE & WHIRL TEST

LOCATION: (All Thermocouples are Located on the Left-Hand Engine &amp; Pylon Structure)

<u>Thermocouple Identification</u>	<u>Station</u>	<u>Location on Part</u>	<u>Part No.</u>
1	245.8	Top Aft Engine Mount	385-5007-17
2	255.0	Engine Truss Tube	385-5007-32
3	259.5	Engine Nacelle Panel Next to Engine	385-5007-41
4	270.0	" " " "	" "
5	275.18	Cross-Over Shroud	385-5007-37
6	272.8	Front Spar Ring @ 45° From Vertical	385-5014-3
7	279.8	Front Spar Aluminum Web Near Spar Ring	385-5007-15
8A	300.0	Nacelle Skin Over Diverter Valve Vertical	385-5014-33
8B	300.0	" " " 45° from Vertical	" "
8C	300.0	" " " 90° " "	" "
9	300.0	Rib Cap of Canted Rib Nearest Duct	385-5014-1
10	300.0	Aluminum Skin on Top of Pylon Nearest Duct	385-5014-3
11	300.0	Diverter Valve Mounting Link	385-4014-1

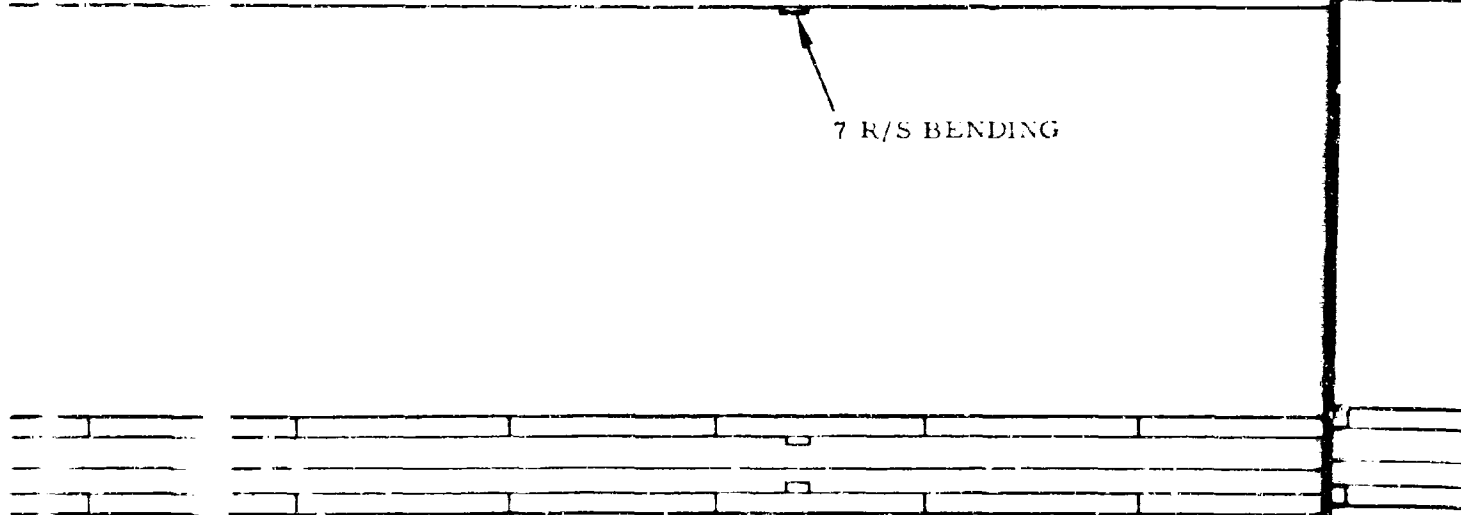
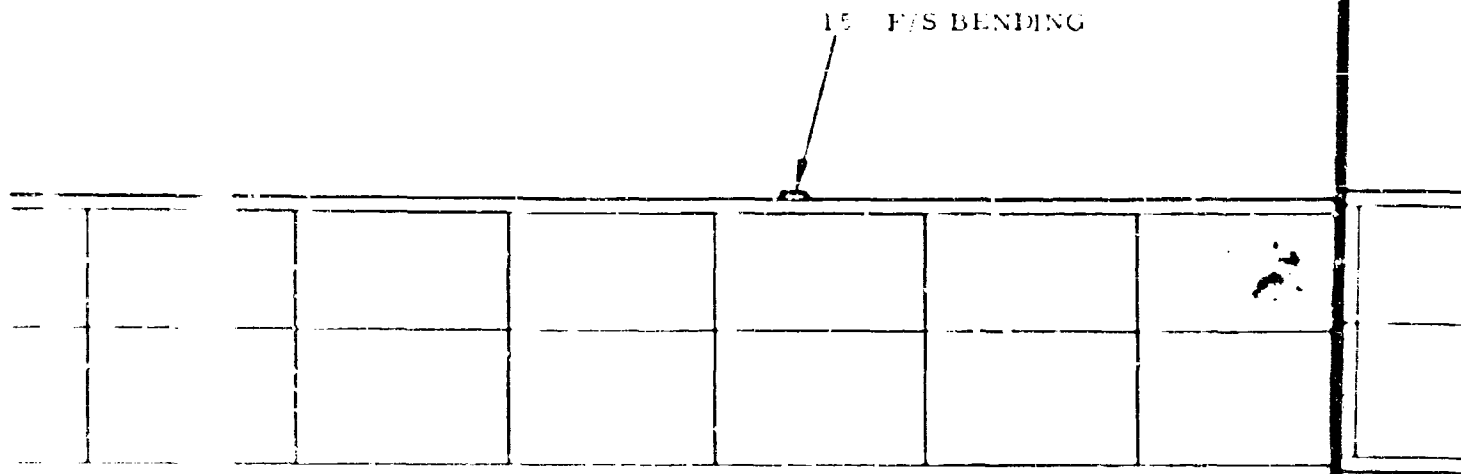
TABLE II (Continued)  
 STRUCTURAL THERMOCOUPLE SUMMARY (IRON-CONSTANTAN THERMOCOUPLES)  
 ENGINE & WHIRL TEST

<u>LOCATION (All Thermocouples are Located on the Left-Hand Engine &amp; Pylon Structure)</u>			
<u>Thermocouple Identification</u>	<u>Station</u>	<u>Location on Part</u>	<u>Part No.</u>
12	290.0	Aluminum Web Nearest Duct	385-5013-5
13	317.5	Tube Closest to Duct 4" Below Bearing	385-5025-0
14		Engine Fuel Control Body	
15		Engine Ignition Box	
16		Stator Vane Actuator	
17		Fuel into #1 Engine Heat Exchanger	
18		Fuel Out of #1 Engine Heat Exchanger	
19		Hydraulic Oil Out of Heat Exchanger System #1	
20		Fuel into #2 Engine Heat Exchanger	
21		Fuel Out of #2 Engine Heat Exchanger	
22		Hydraulic Oil Out of Heat Exchanger System #2	
23		Engine Generator	
24		Upper Bearing Mounting Ring	
25		Diverter Valve Leak Check	



23                      36    63                      75.4                      83.3                      90.75





Bridge Locations, Rotor Blades - Whirl Test 220

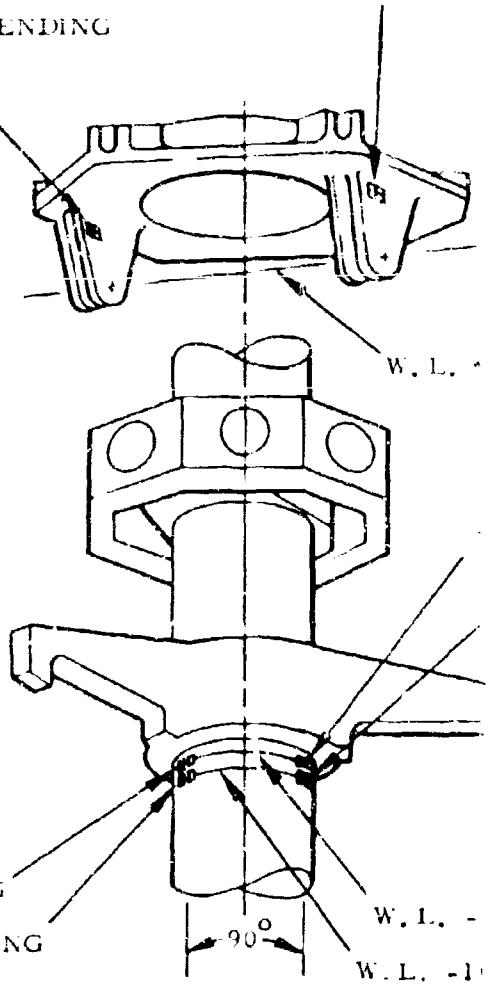
35 180° GIMBAL LUG BENDING

16 F/S BENDING

8 R/S BENDING

32 0° SHAFT BENDING

33 0° SHAFT BENDING



16

8 R

1919

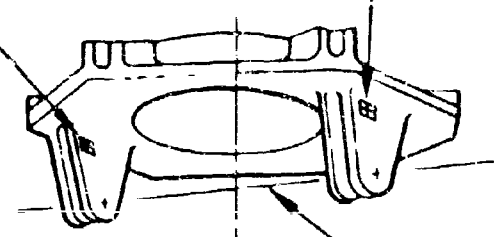
270

270

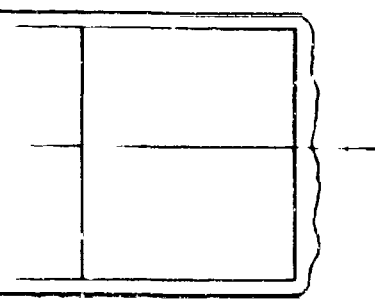
D

33 0° GIMBAL TUG BENDING

I/S BENDING

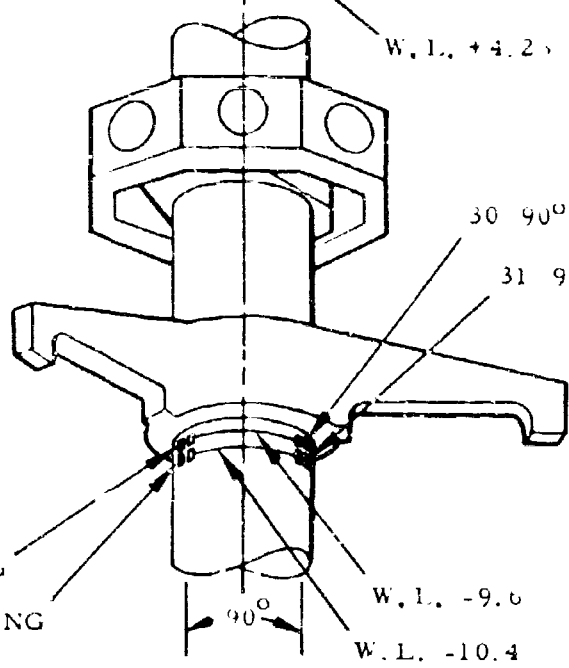


W.L. +4.2



30 90° SHAFT BENDING

31 90° SHAFT BENDING



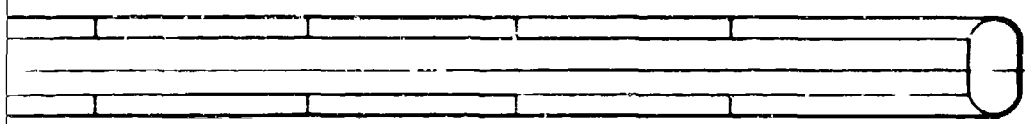
R/S BENDING

32 0° SHAFT BENDING

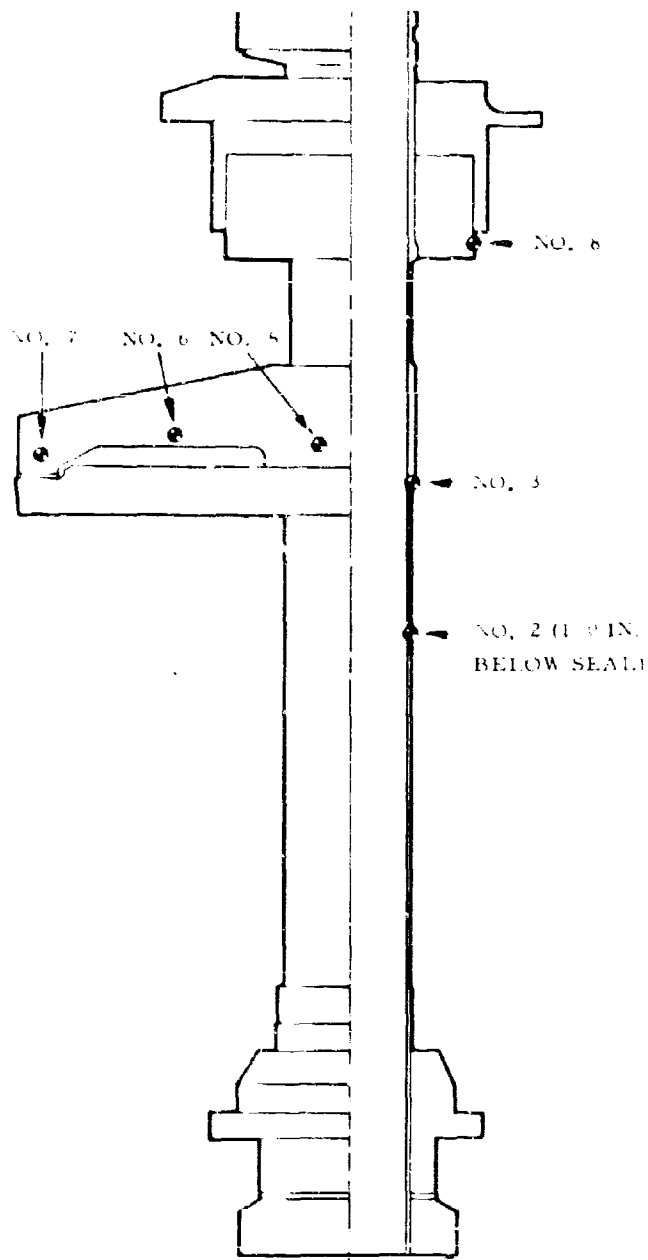
33 0° SHAFT BENDING

W.L. -9.6

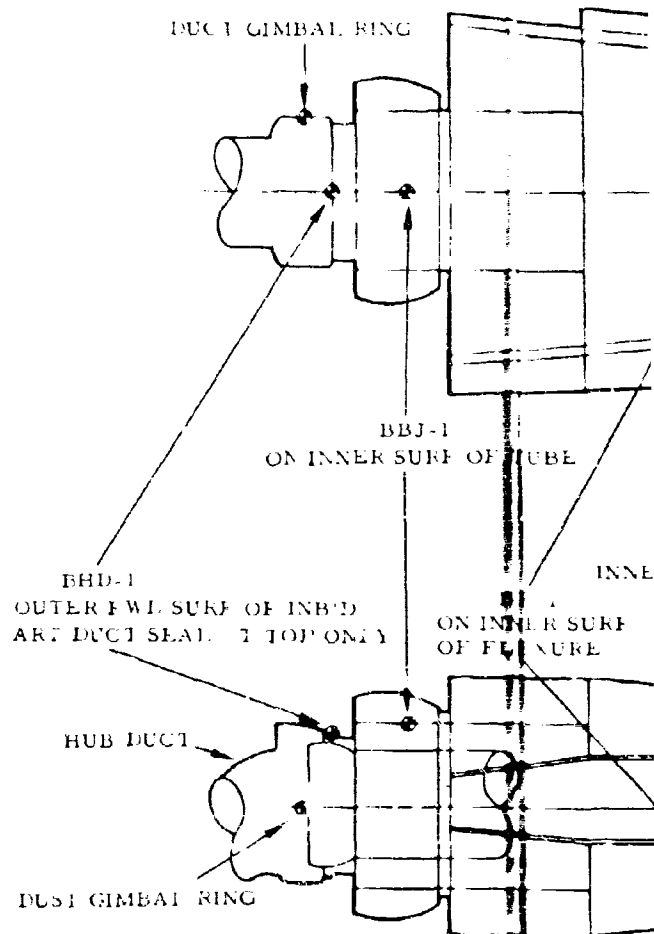
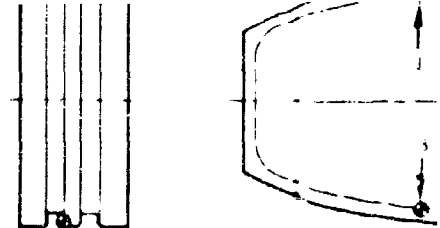
W.L. -10.4



E



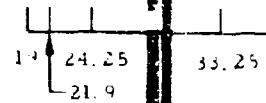
SHAFT AND HUB THERMOCOUPLES



NOTES:

1. ALL THERMOCOUPLES CHROMEL ALUMEL
2. REFERENCE DRAWINGS: 285-0937, -0949, -0950, -0951, -1002
3. INSTRUMENTATION INBD OF S1A 91 ON BLUE BLADE ONLY
4. THE COUNTERPART OF BCD-1 ON THE OTHER BLADES IS:  
RED RCDF, YELLOW YCDF
5. THE COUNTERPART OF BDC-2 ON THE OTHER BLADES IS:  
RED RCDR, YELLOW YCDR

**A**



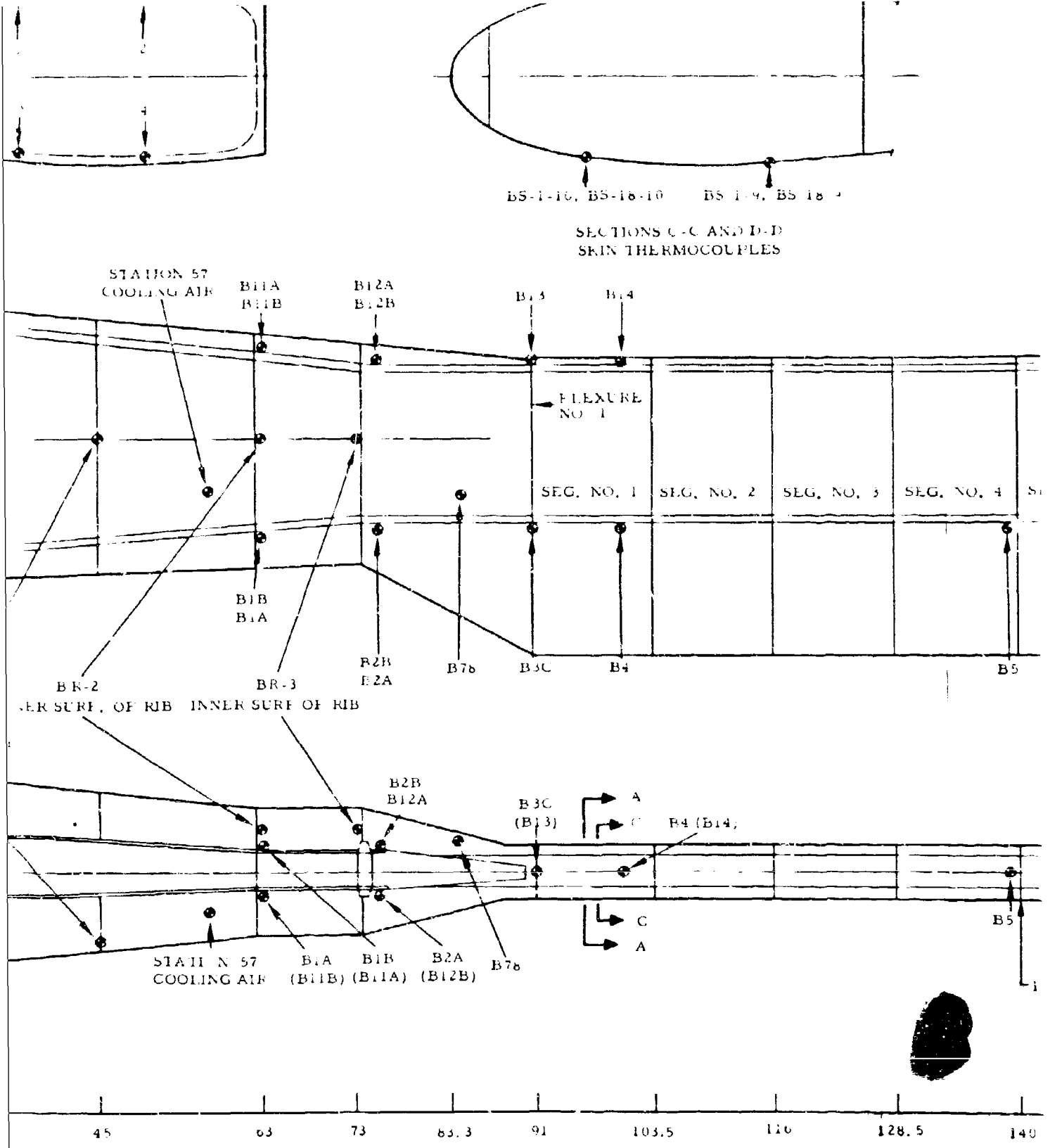
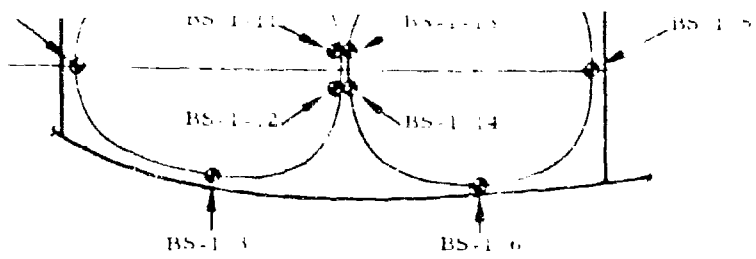


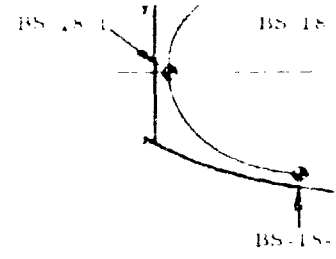
Figure 78. Thermocouple Locations, Rotor I

G. NO.

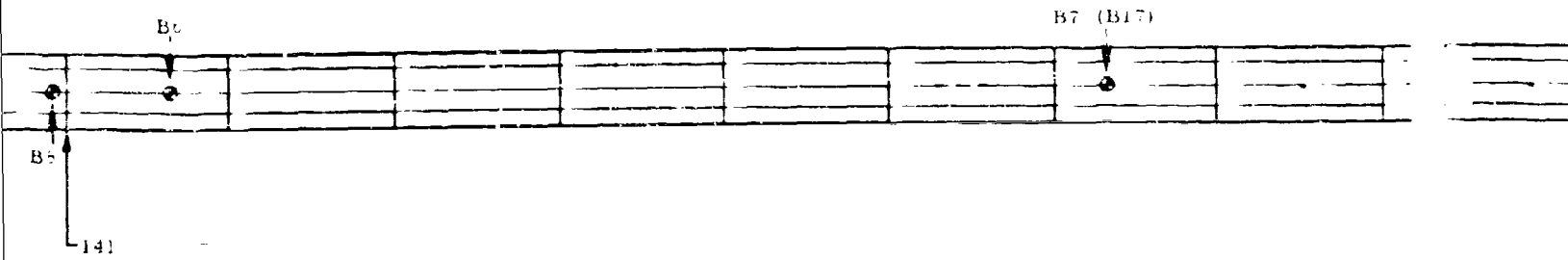
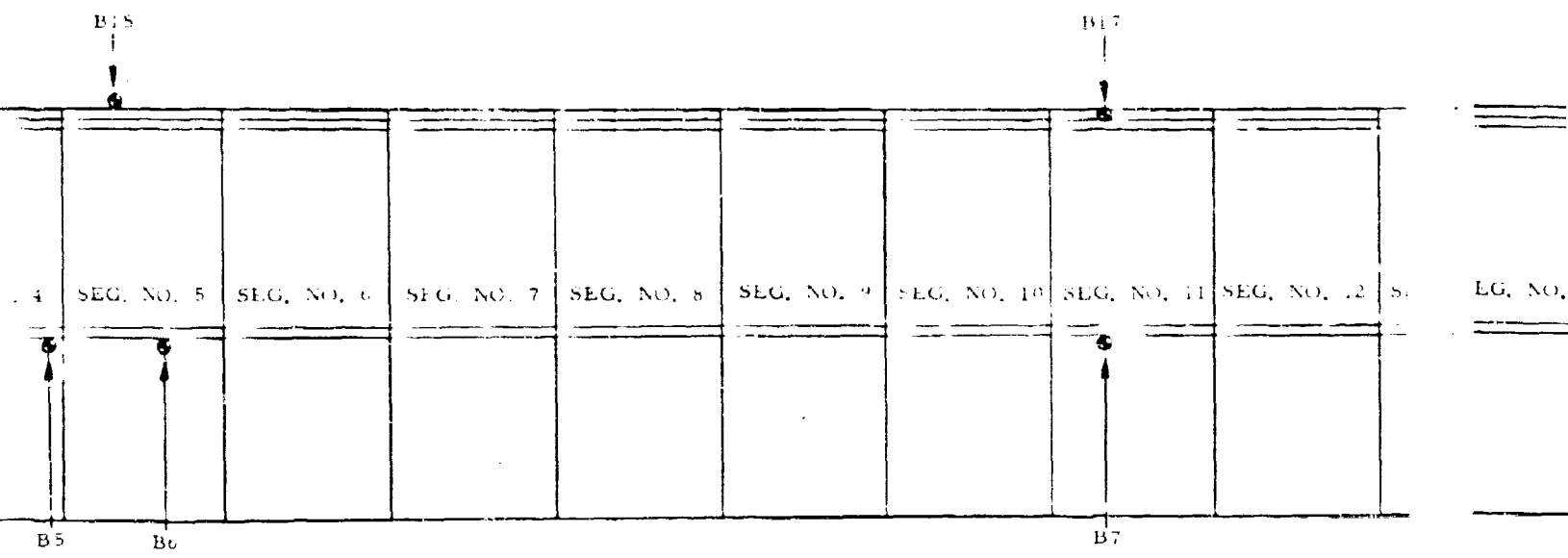
s, Rot



SECTION A-A  
BLADE SEGMENT NO. 4



BLA

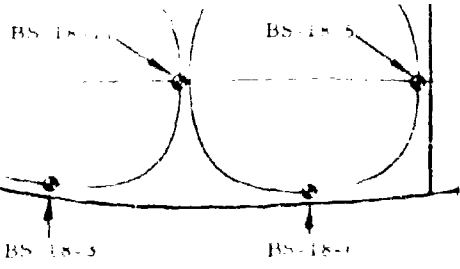


**C**

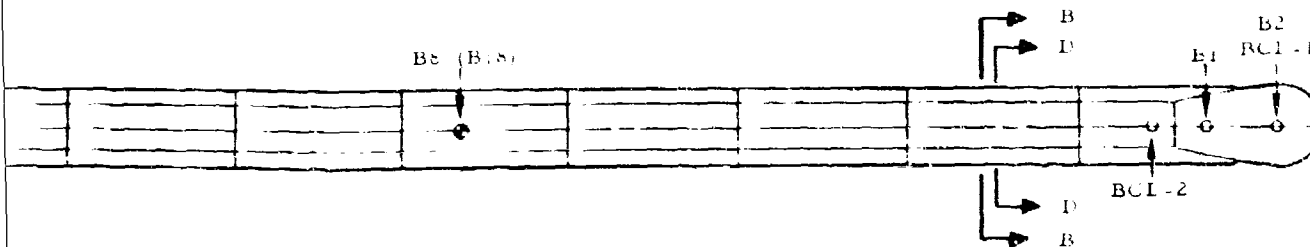
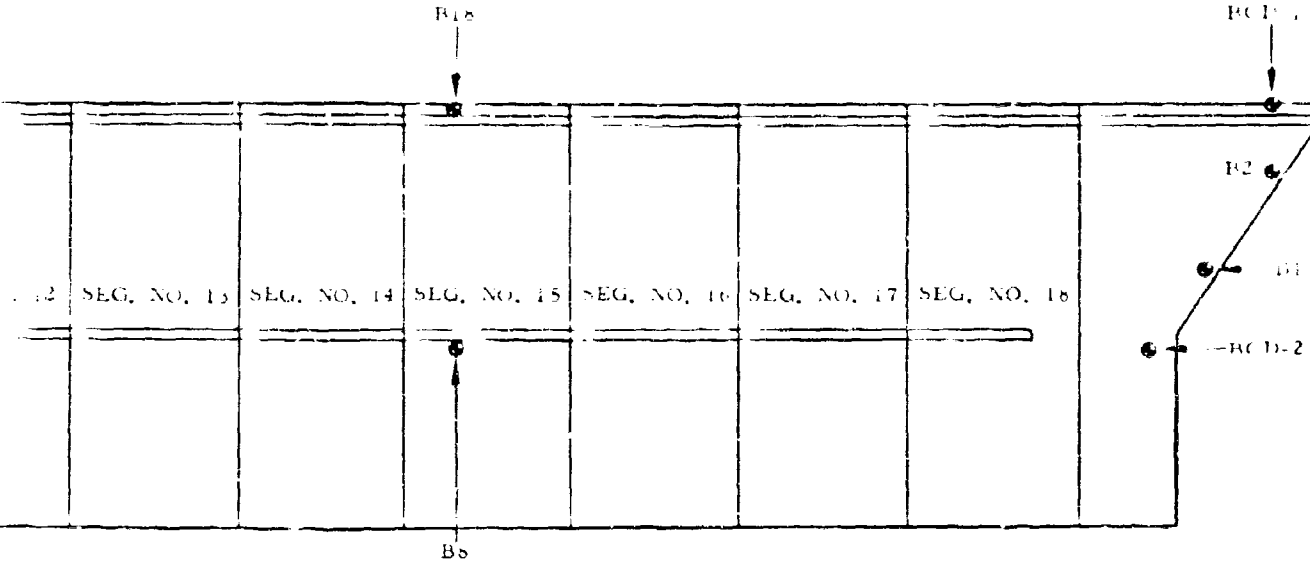
149      153.5      160      176.5      191      203.5      216      220      228.5      241  
STATION

Motor Blades and Hub Whirl Test

CODE: BC-2-3 - BLUE BLADE, FLEXURE 2  
 FROM ROOT TO NO. 3  
 RC-2-3 - RED BLADE, ETC.  
 YC-2-3 - YELLOW BLADE, ETC.  
 INSTR. FLEXURES:  
 BLUE BLADE - NOS. 2, 4, 6, 8, 10,  
 12, 14, 16 AND 18  
 RED BLADE - NOS. 2 AND 18  
 YELLOW BLADE - NOS. 2 AND 18



SECTION B-B  
 BLADE SEGMENT NO. 18



241      253.5      266   270      278.5      303.5      316

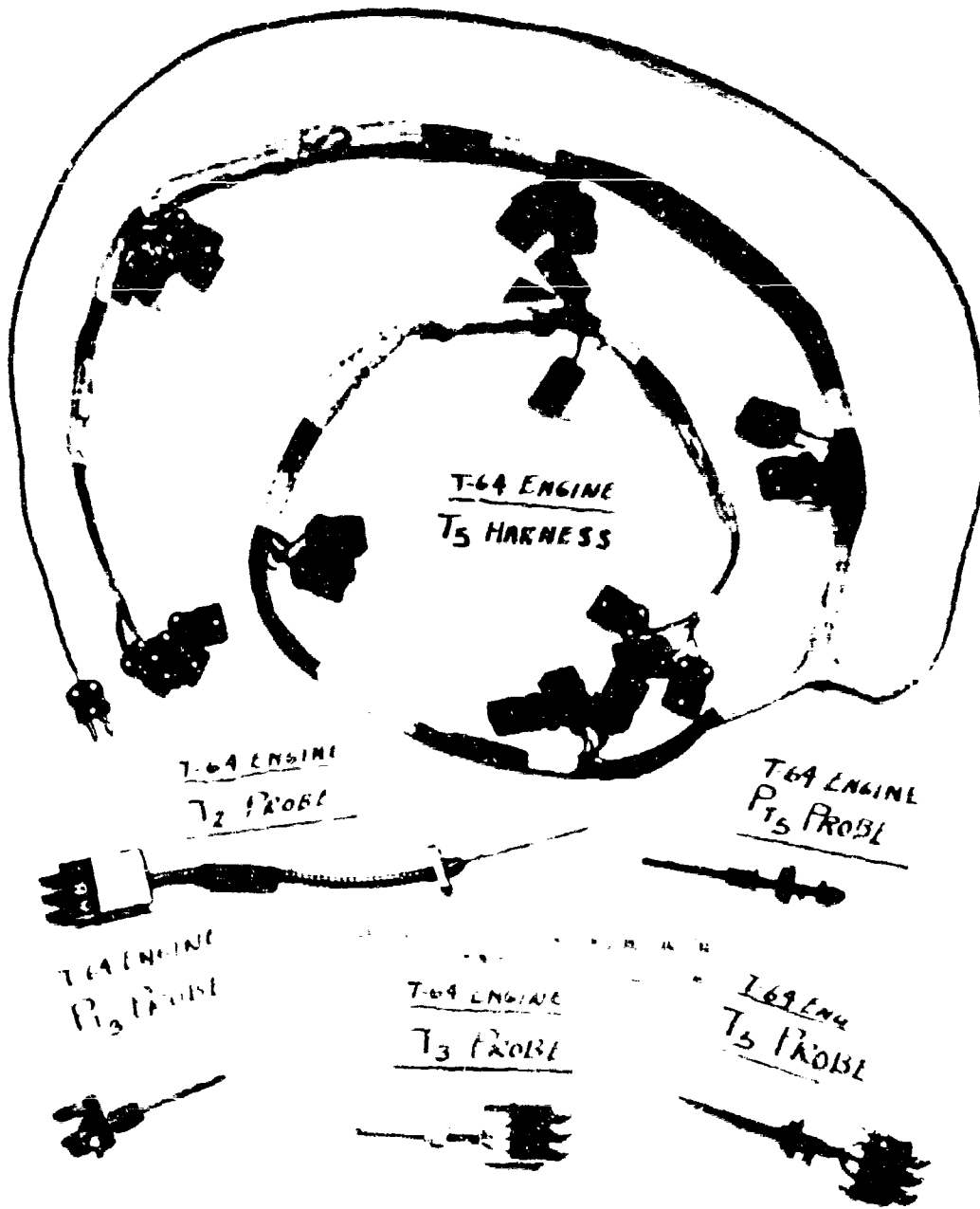


Figure 79. Engine Temperature and Pressure Probes

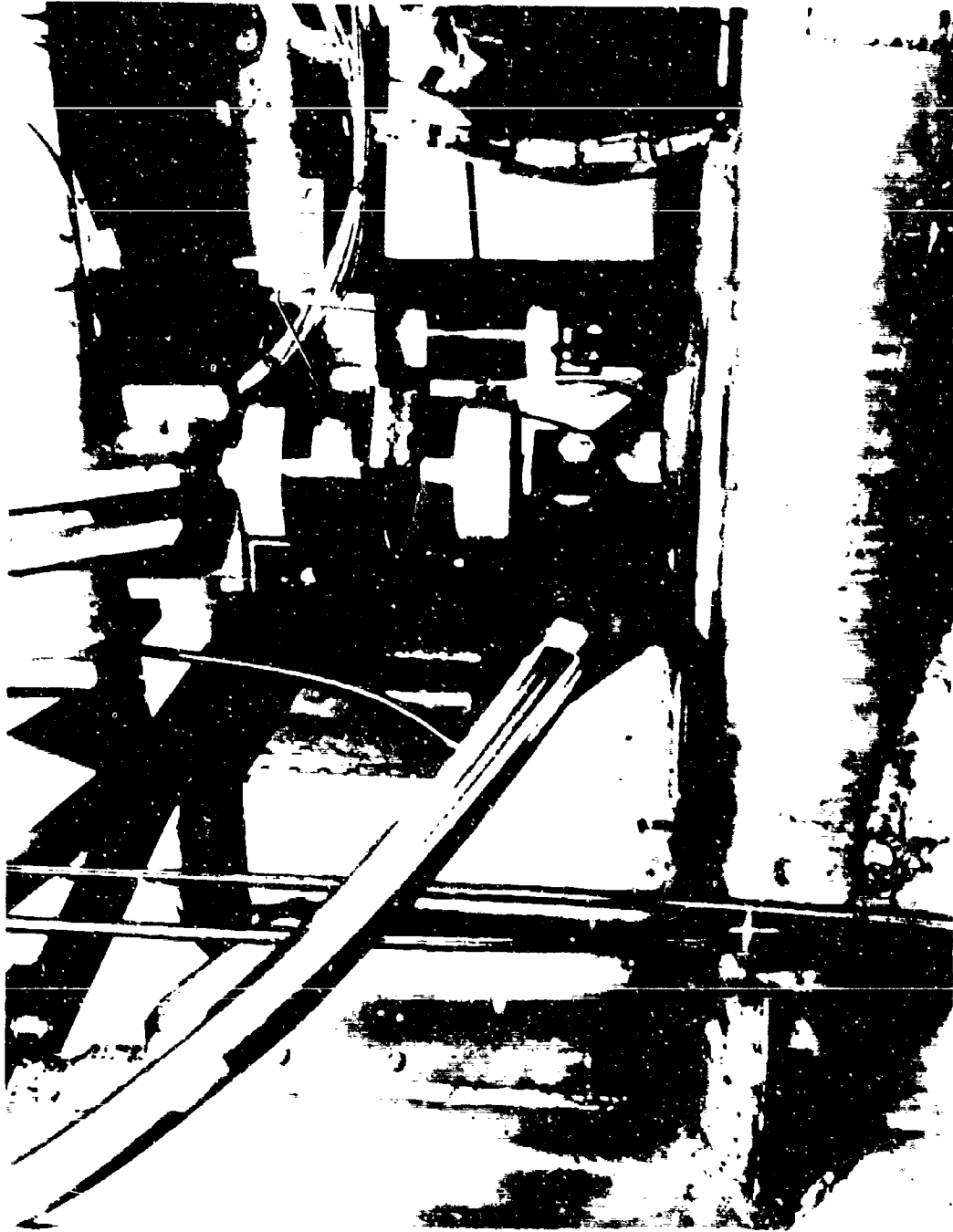


Figure 80. Thrust Load Cell Installation

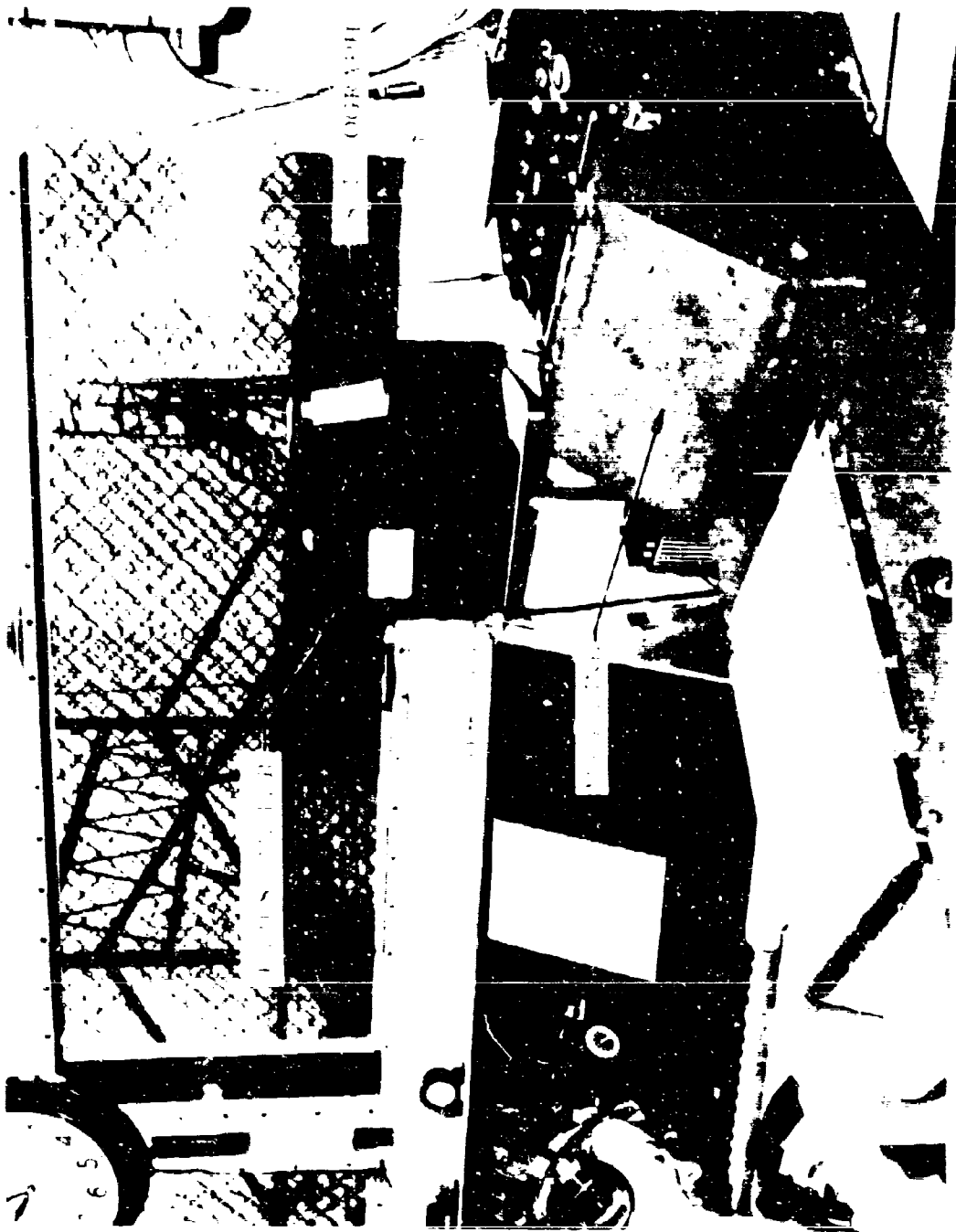


Figure 81. Thrust Meter and Oscillograph Installation

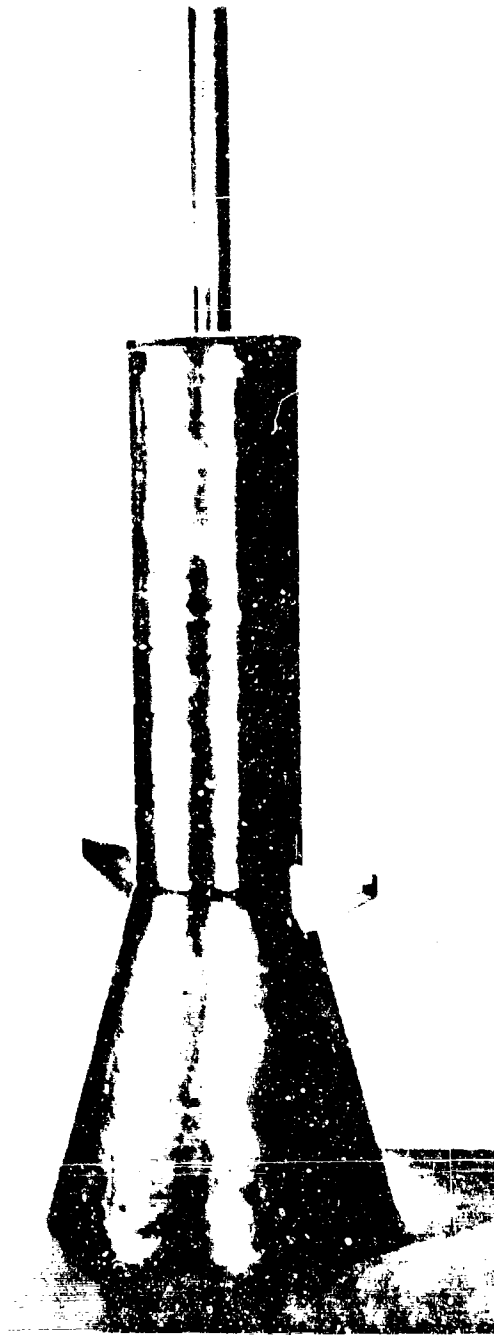


Figure 82. Variable Area Exit Nozzle Probe Arrangement



Figure 83. Tip Pressure Transducer Installation

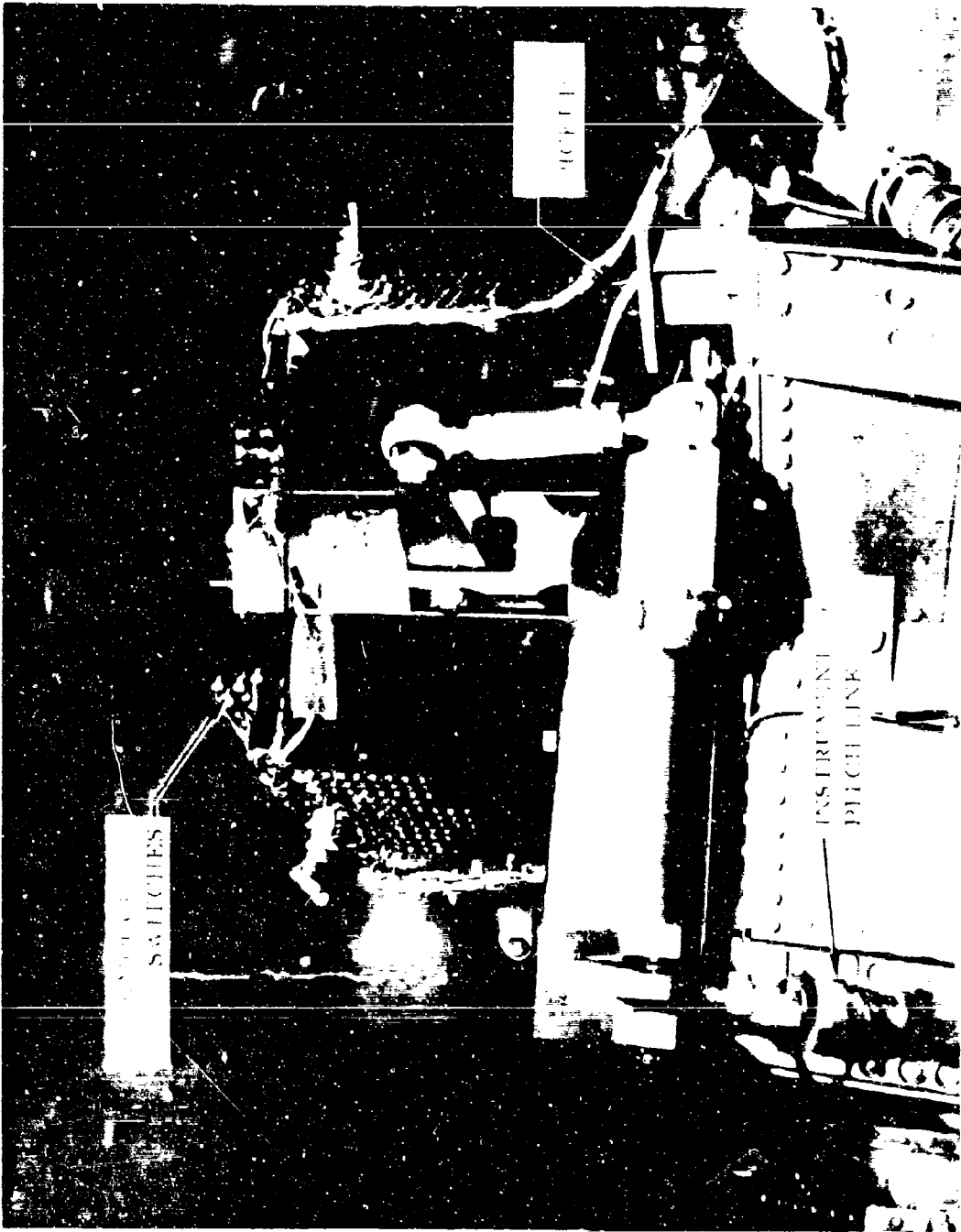


Figure 84. Hub Tilt Pickup Installation

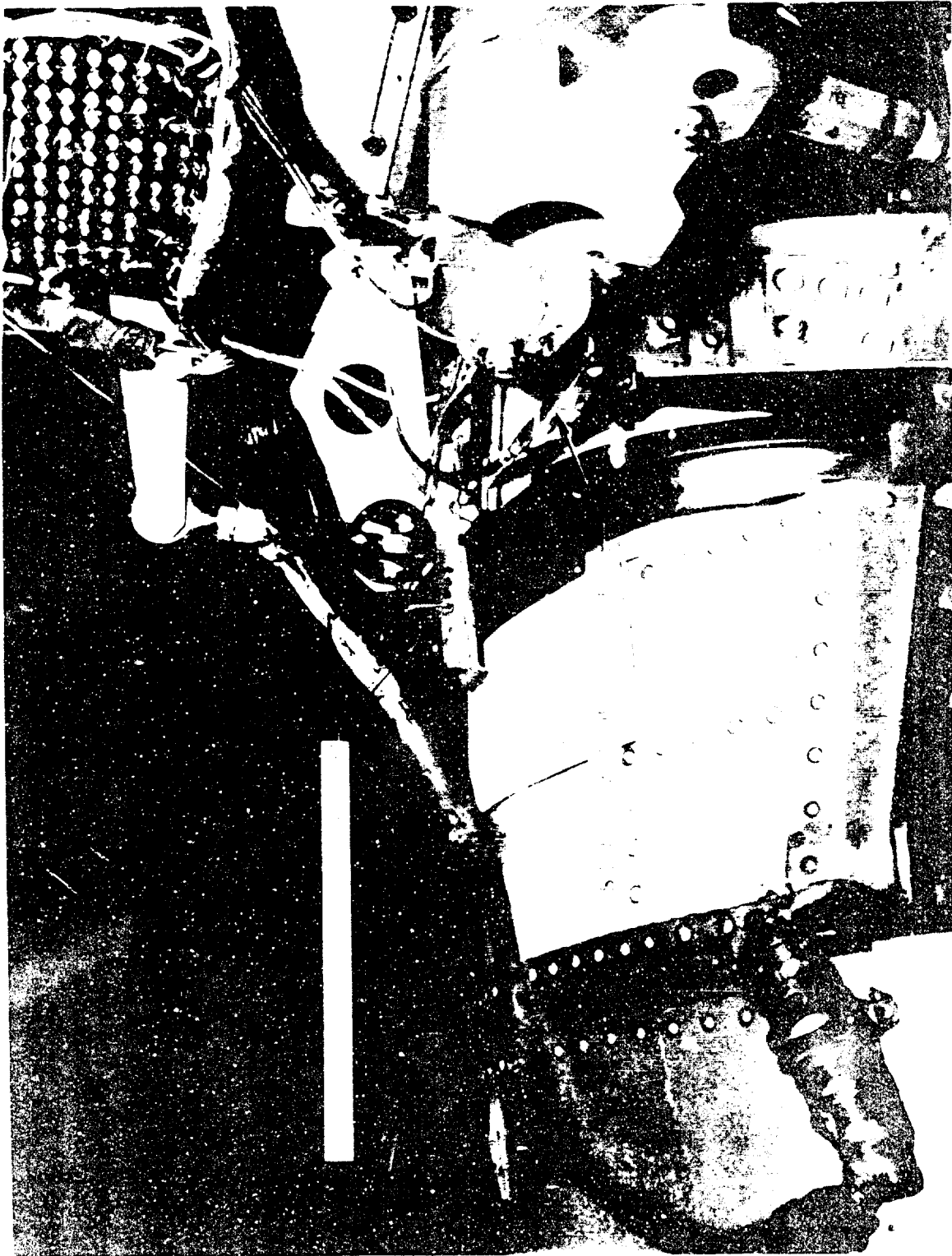


Figure 85. Blade Geometry Pickup Insulation Station

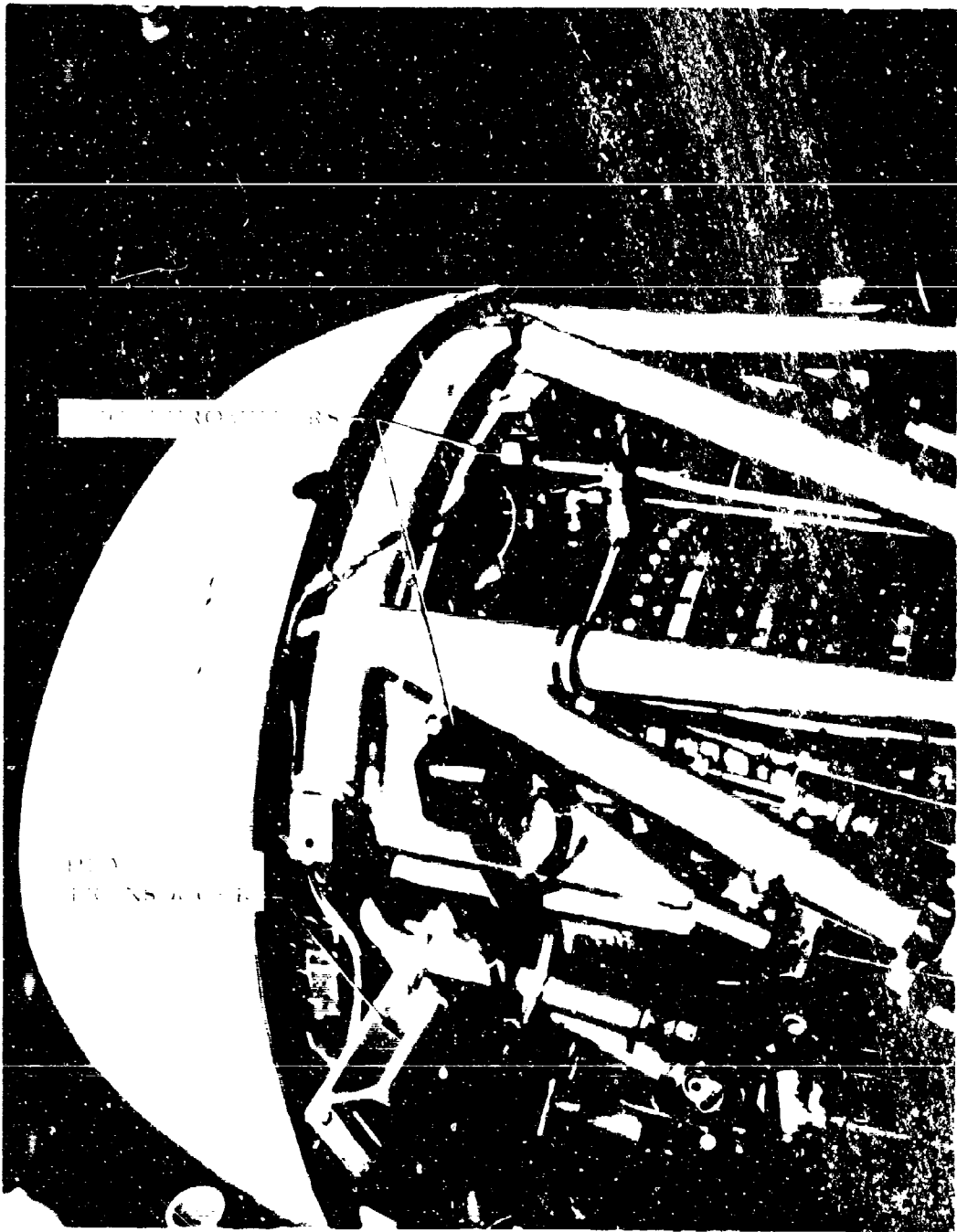


Figure 86. Engine Instrumentation Installation

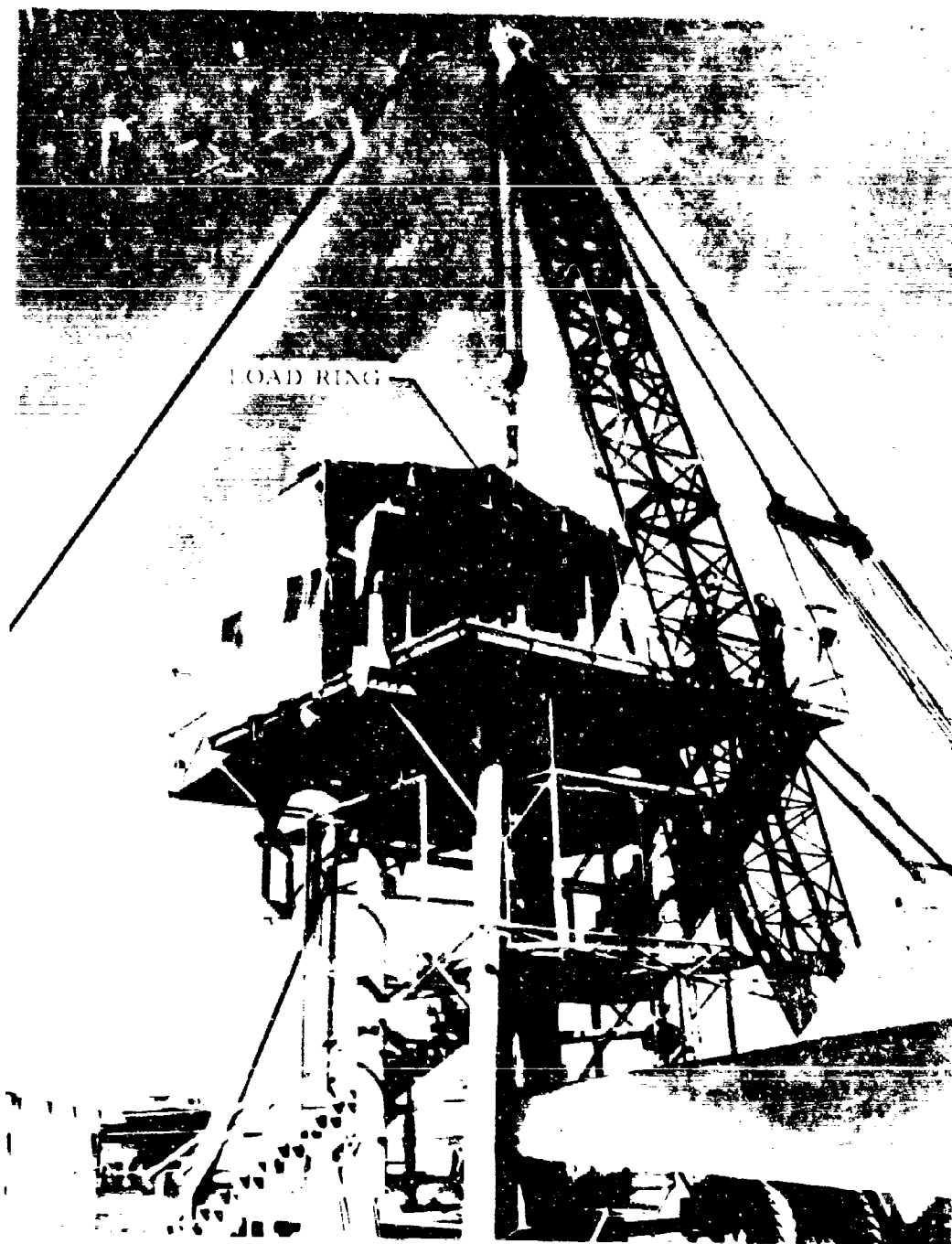
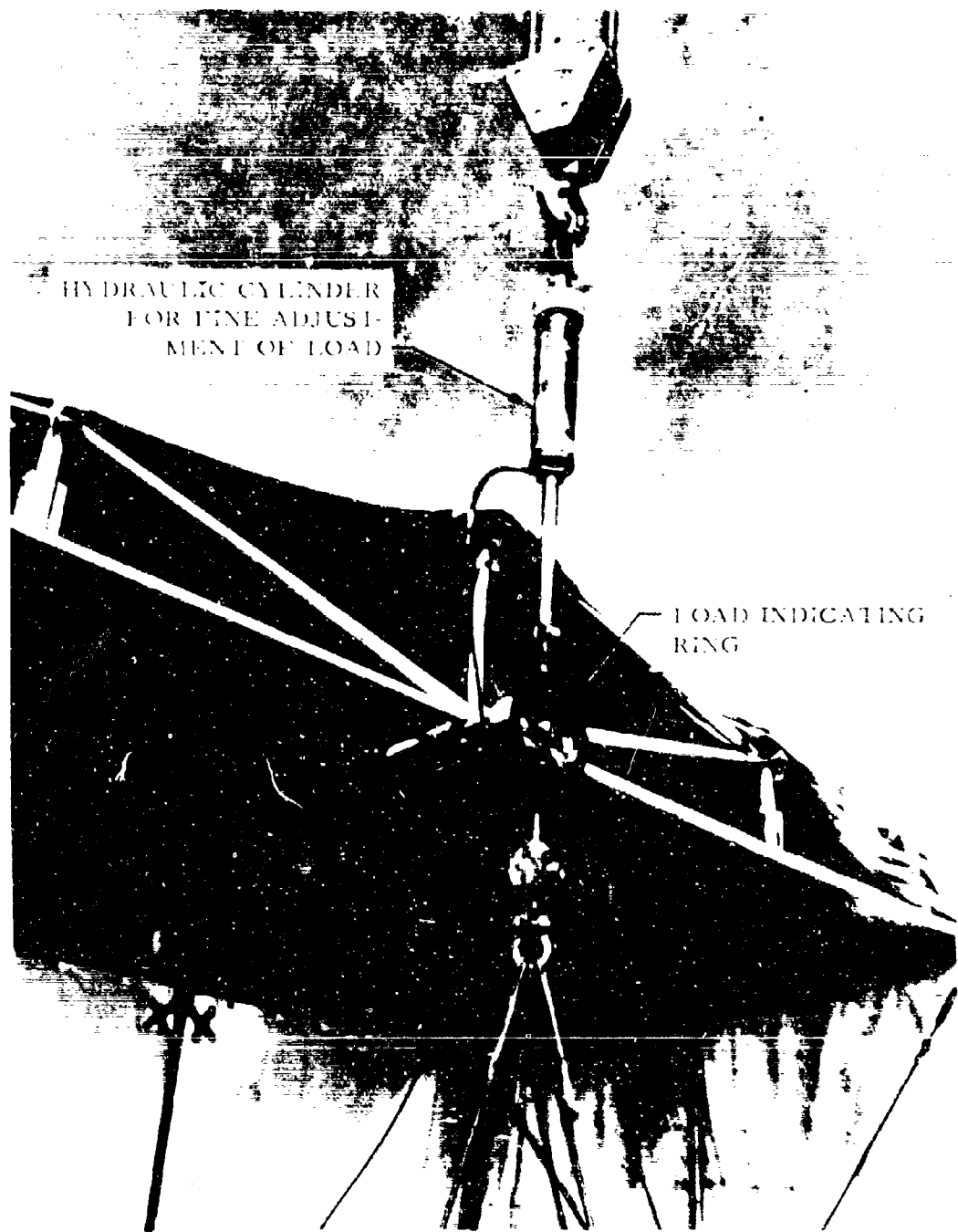


Figure 87. Thrust Measuring System Calibration



HYDRAULIC CYLINDER  
FOR FINE ADJUST-  
MENT OF LOAD

LOAD INDICATING  
RING

Figure 88. Close-up of Hookup Used To Calibrate Thrust Measuring System

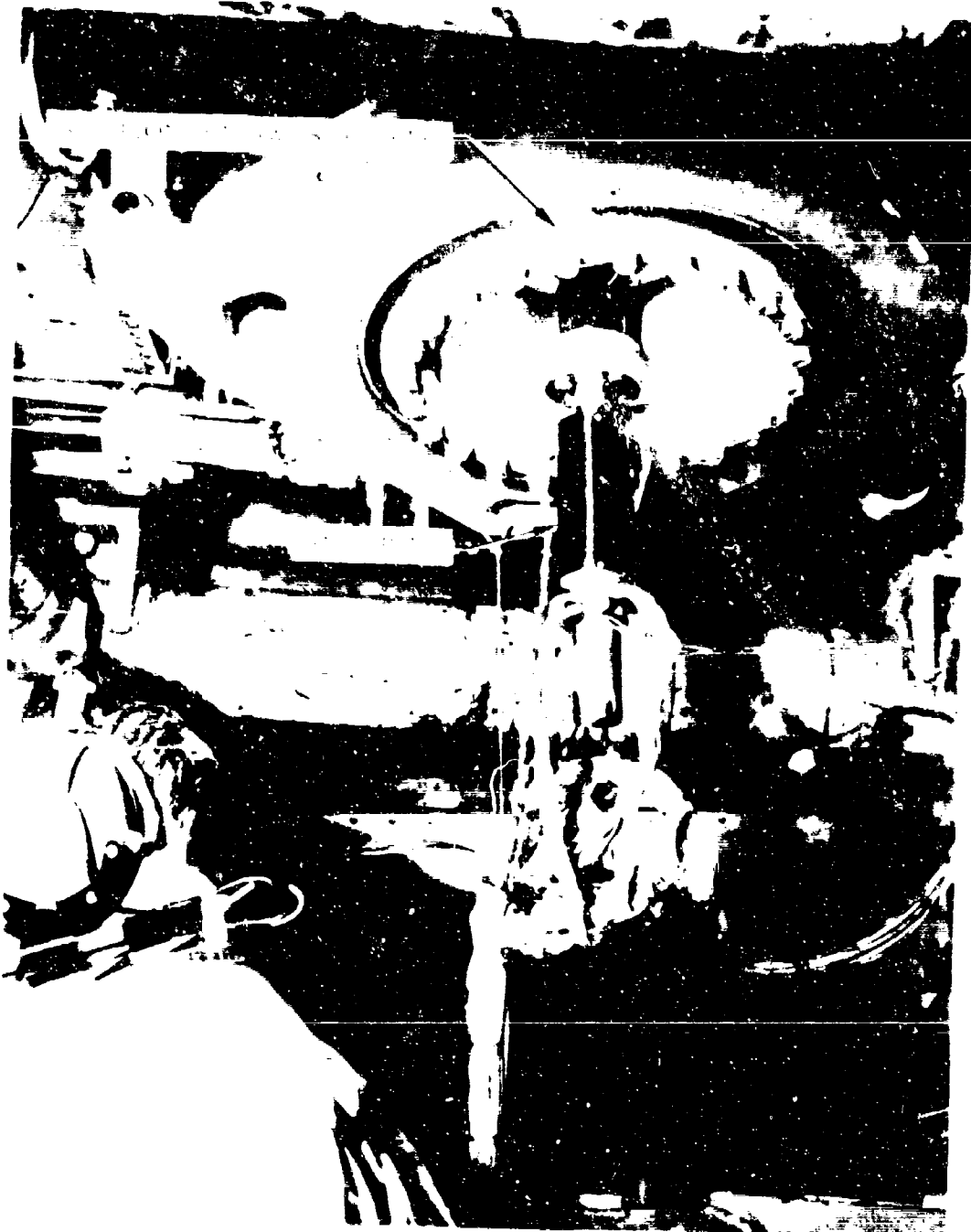


Figure 89. Slip Ring Installation



Figure 90. Engine T<sub>5</sub> Recorders

28  
25  
22  
20

1.0

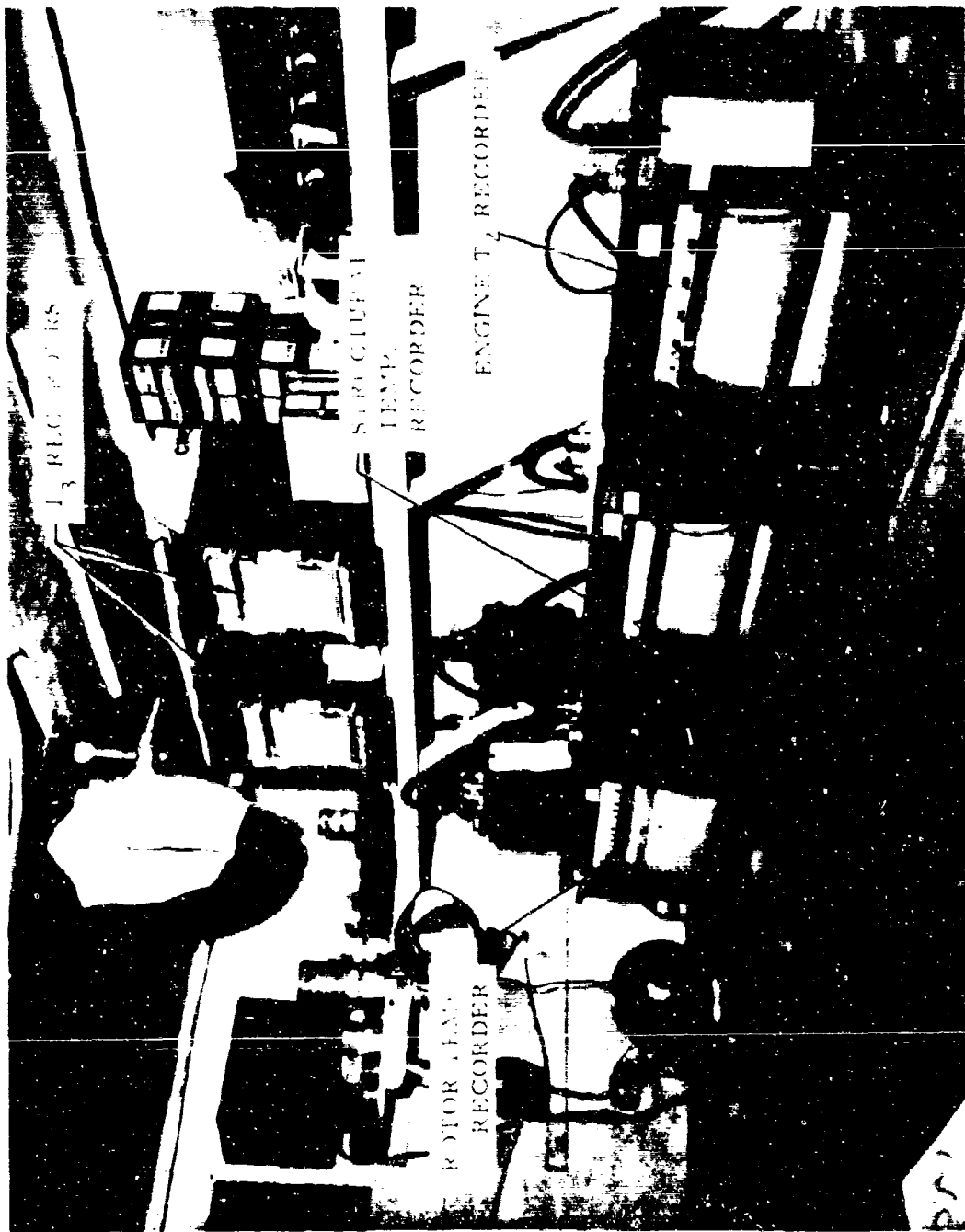


Figure 91. Temperature Recording Instrumentation

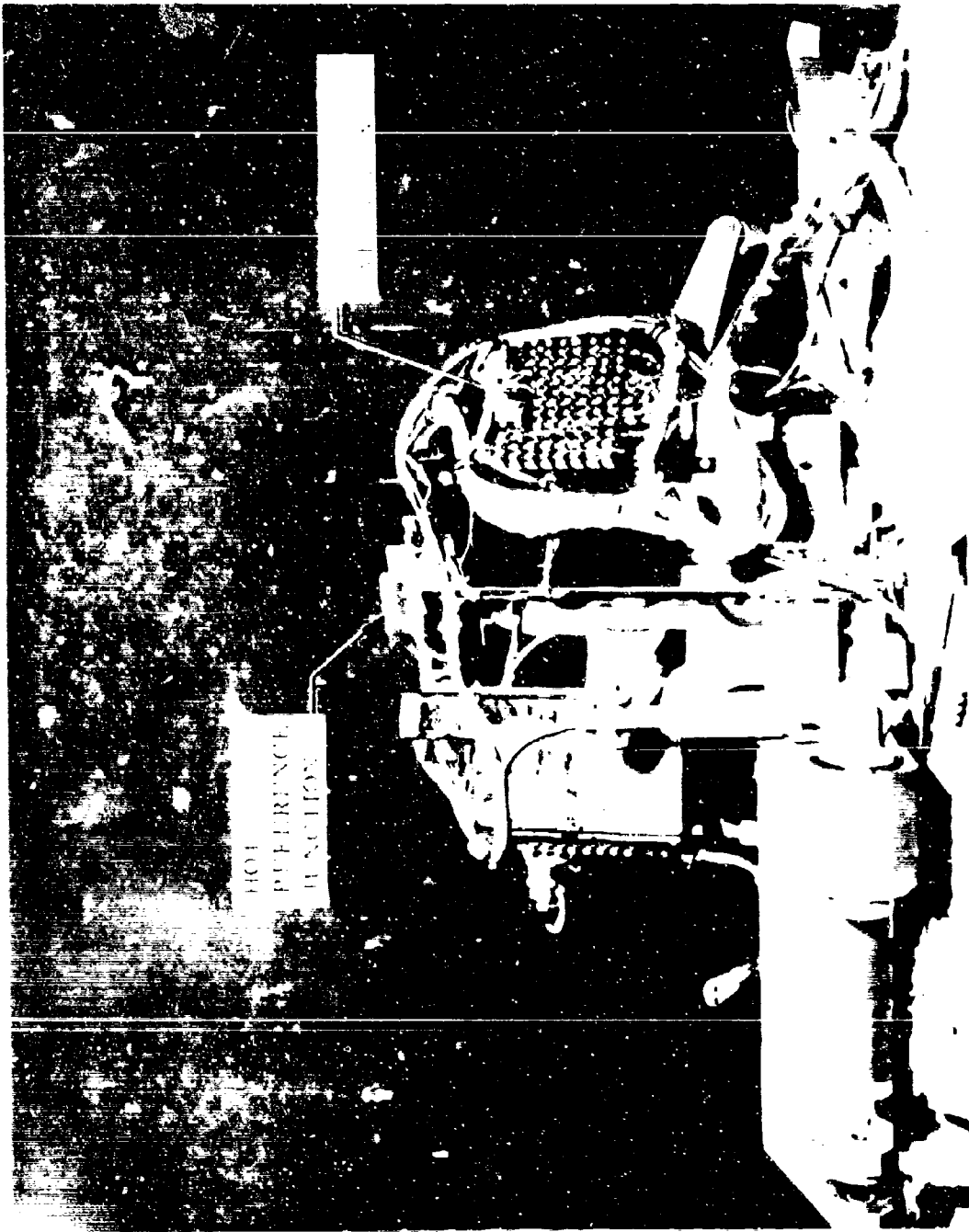


Figure 92. Rotor Thermocouple Switch Box Installation

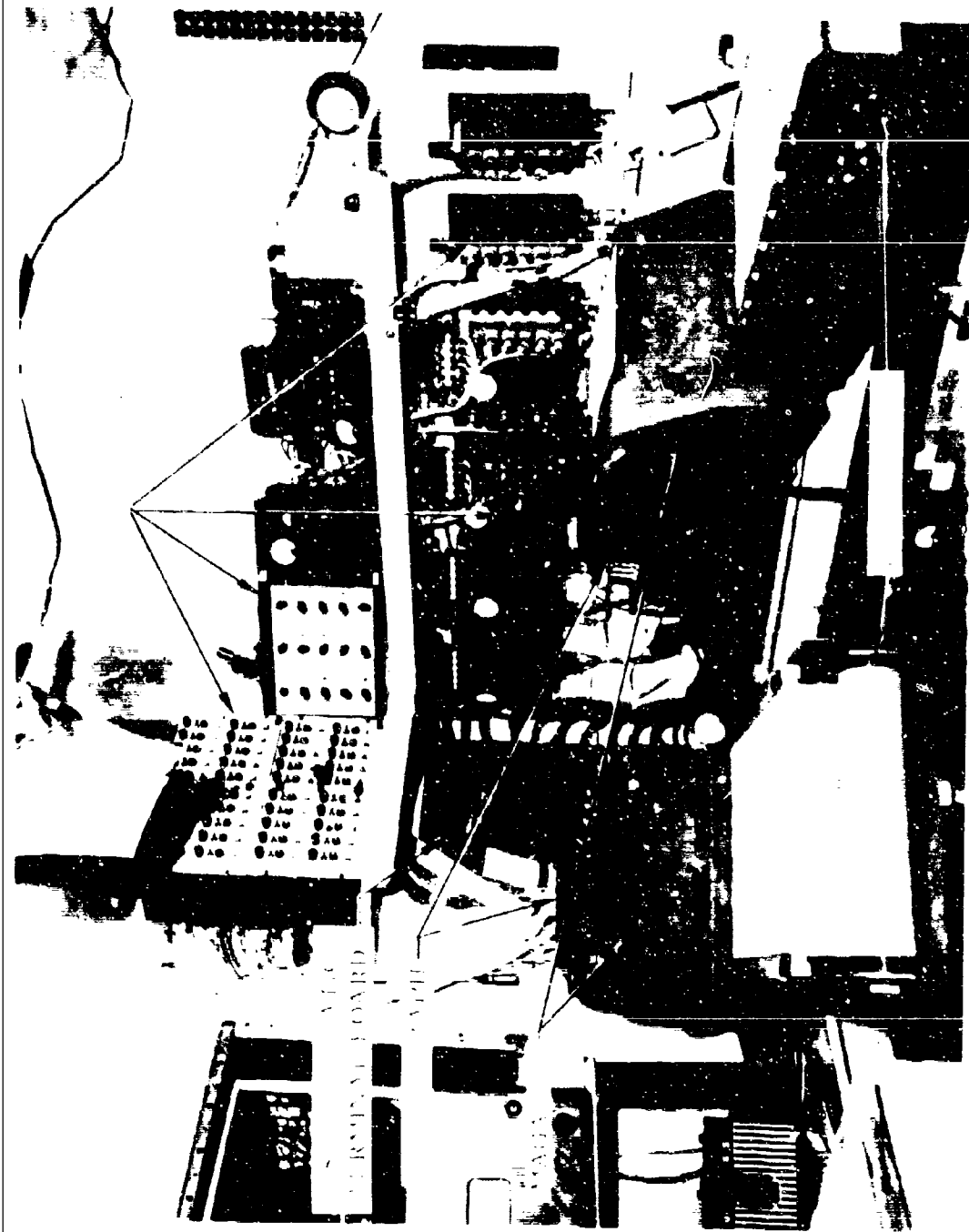


Figure 93. Oscillograph and Balance Box Installation

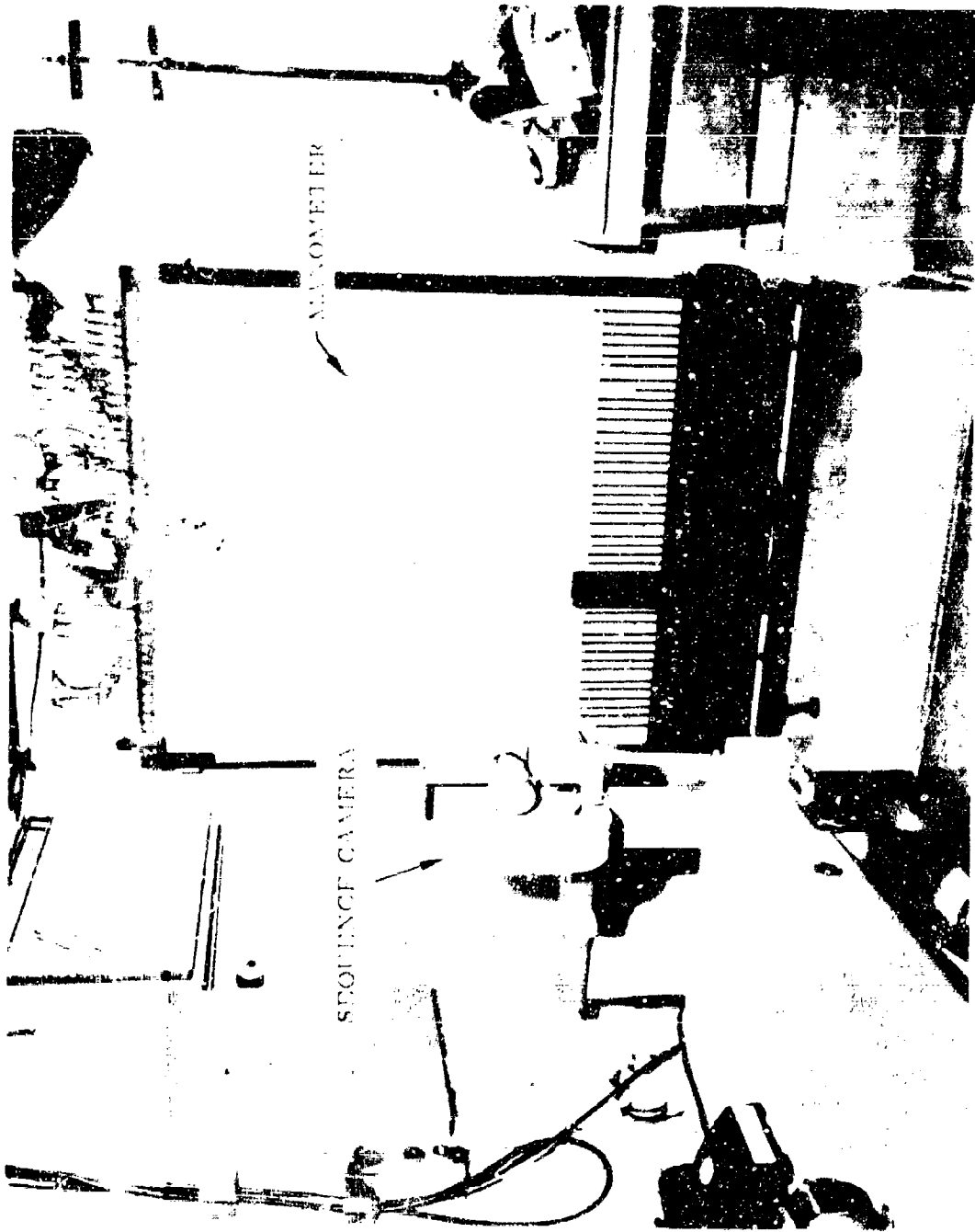


Figure 64. Manometer and Camera Installation

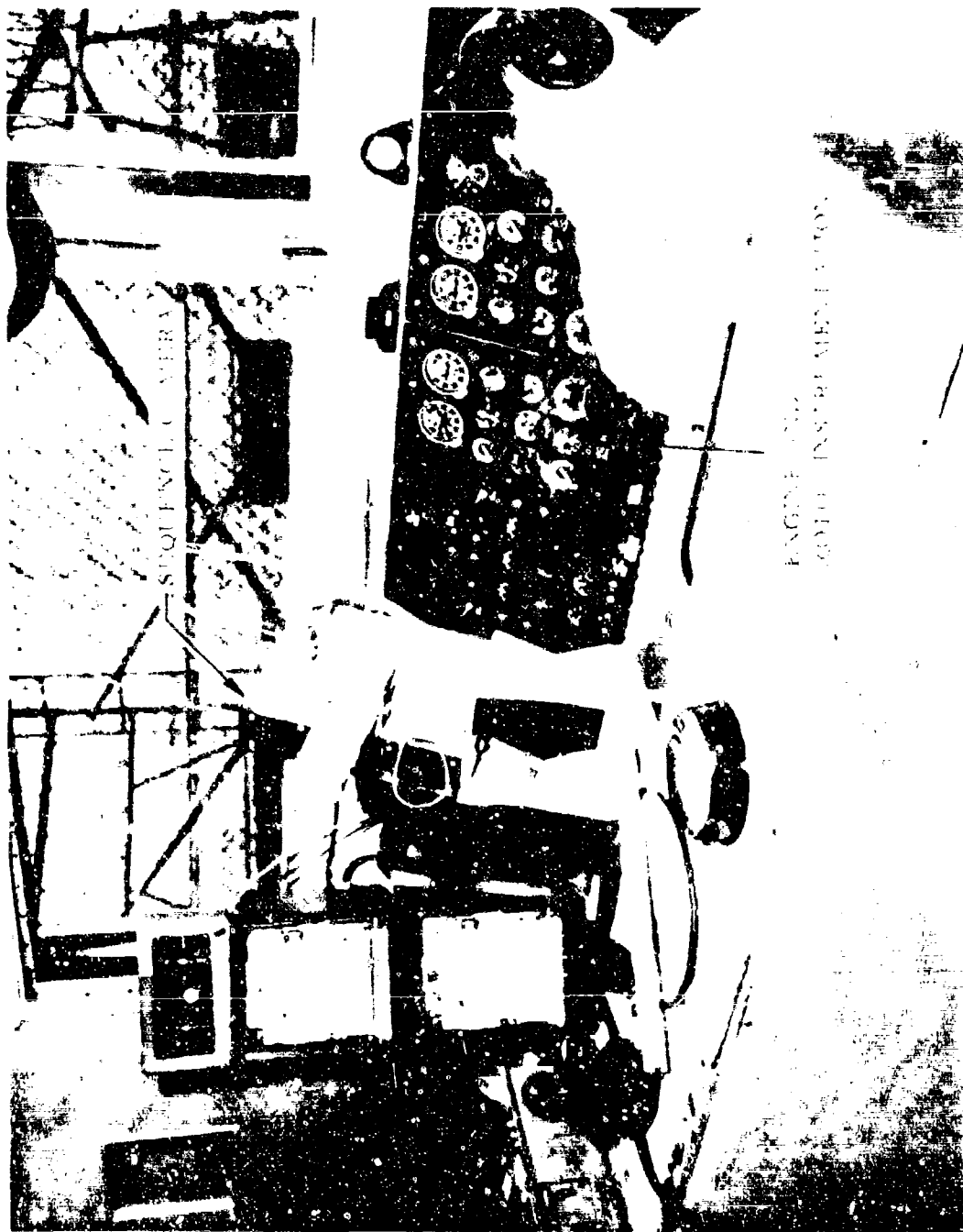


Figure 95. Engine and Rotor Instrumentation Photographic Installation

## REFERENCES

1. Program Plan, Engine and Whirl Tests, XV-9A Hot Cycle Research Aircraft, Aircraft Division Report 63-21 (385-T-02), Hughes Tool Company, Culver City, California, July 1963.
2. Hot Cycle Rotor System Whirl Tests, Aircraft Division Report 285-16 (62-16), Hughes Tool Company, Culver City, California, March 1962.
3. Gessow, A., and Myers, G., Aerodynamics of the Helicopter, The Macmillan Company, New York, New York, 1952.
4. Heyson, H. H., Ground Effect for Lifting Rotor in Forward Flight, NASA Technical Note TN D-234, May 1960.
5. Hot Cycle Rotor System Final Report, Thermal Analysis, Aircraft Division Report 285-10, Hughes Tool Company, Culver City, California, June 1960.
6. Summary of Component Tests, Aircraft Division Report 64-26 (385-T-16), Hughes Tool Company, Culver City, California, December 1964.
7. Summary Report, Aircraft Design, XV-9A Hot Cycle Research Aircraft, Aircraft Division Report 64-11, Hughes Tool Company, Culver City, California, December 1964.
8. Whirl Testing of the XHCH Rotor System, Report 6190, McDonnell Aircraft Corporation, St. Louis, Missouri, 31 October 1958.

DISTRIBUTION

US Army Materiel Command	2
US Army Mobility Command	4
US Army Aviation Materiel Command	5
Chief of R&D, DA	1
US Army Transportation Research Command	20
US Army R&D Group (Europe)	1
US Army Engineer R&D Laboratories	3
Army Research Office-Durham	1
US Army Test and Evaluation Command	1
US Army Combat Developments Command Aviation Agency	2
US Army Combat Developments Command Transportation Agency	1
US Army War College	1
US Army Command and General Staff College	1
US Army Transportation School	1
US Army Aviation School	1
US Army Aviation Test Board	1
US Army Transportation Engineering Agency	1
US Army General Equipment Test Activity	1
US Army Representative, AFSC, Andrews AFB	1
Air Force Systems Command, Wright-Patterson AFB	1
Air Force Flight Test Center, Edwards AFB	3
Air Proving Ground Center, Eglin AFB	1
Bureau of Naval Weapons	1
US Naval Air Station, Patuxent River	1
David Taylor Model Basin	1
Marine Corps Liaison Officer, US Army Transportation School	1
Testing and Development Division, US Coast Guard	1
Ames Research Center, NASA	1
NASA-LRC, Langley Station	1
NASA Representative, Scientific and Technical Information Facility	2
Research Analysis Corporation	1
National Aviation Facilities Experimental Center	1
Canadian Liaison Officer, US Army Transportation School	1
Defense Documentation Center	20
US Army Materials Research Agency	1
US Army Transportation Center and Fort Eustis	1

Unclassified

Security Classification

DOCUMENT CONTROL DATA - R&D

(Security classification of title, body of abstract and indexing annotation must be entered when the overall report is classified)

1. ORIGINATING ACTIVITY (Corporate author)		2a. REPORT SECURITY CLASSIFICATION	
Hughes Tool Company Aircraft Division Culver City, California		Unclassified	
3. REPORT TITLE		2b. GROUP	
ENGINE AND WHIRL TESTS, XV-9A HOT CYCLE RESEARCH AIRCRAFT		N/A	
4. DESCRIPTIVE NOTES (Type of report and inclusive dates)			
Summary Report			
5. AUTHOR(S) (Last name, first name, initial)			
Pieper, Carl W.			
6. REPORT DATE	7a. TOTAL NO OF PAGES	7b. NO OF REFS	
February 1965	195	8	
8a. CONTRACT OR GRANT NO	9a. ORIGINATOR'S REPORT NUMBER(S)		
DA 44-177-AMC-877(1) b. PROJECT NO	USATRECOM Technical Report 64-67		
Task 1D121401A14403	9f. OTHER REPORT NO(S) (Any other numbers that may be assigned this report)		
	DTC-AD 64-23 (385-T-15)		
10. AVAILABILITY LIMITATION NOTICES			
Qualified requesters may obtain copies of this report from DDC. This report has been furnished to the Department of Commerce for sale to the public.			
11. SUPPLEMENTARY NOTES		12. SPONSORING MILITARY ACTIVITY	
None		US Army Transportation Research Command Fort Eustis, Virginia	
13. ABSTRACT			
A summary of engine and whirl testing of rotor and power module portion of the XV-9A is presented. The results of engine testing include operation of two gas generators into a common exhaust duct with transient power conditions. Rotor whirl test results of the hot cycle rotor used on the XV-9A are reported and include functional check-out, performance evaluation and structural evaluation. Results of testing of a jet-reaction yaw control valve are included.			

DD FORM 1473  
1 JAN 64

Unclassified  
Security Classification

KEY WORDS	LINK A	LINK B	LINK C
	H E I W T	H E I W T	H E I W T

INSTRUCTIONS

1. **ORIGINATING ACTIVITY** Enter the name and address of the contractor, subcontractor, grantee, Department of Defense activity or other organization (*corporate author*) issuing the report.

2. **REPORT SECURITY CLASSIFICATION** Enter the overall security classification of the report. Indicate whether "Restricted Data" is included. Marking is to be in accordance with appropriate security regulations.

3. **GROUP** Automatic downgrading is specified in DoD Directive S200.10 and Armed Forces Industrial Manual. Enter the group number. Also, when applicable, show that optional markings have been used for Group 3 and Group 4 as authorized.

4. **REPORT TITLE** Enter the complete report title in all capital letters. Titles in all cases should be unclassified. If a meaningful title cannot be selected without classification, show title classification in all capitals in parentheses immediately following the title.

5. **DESCRIPTIVE NOTES** If appropriate, enter the type of report, e.g., interim, progress, summary, annual, or final. Give the inclusive dates when a specific reporting period is covered.

6. **AUTHOR(S)** Enter the name(s) of author(s) as shown on or in the report. Enter last name, first name, middle initial. If military, show rank and branch of service. The name of the principal author is an absolute minimum requirement.

7. **REPORT DATE** Enter the date of the report as day, month, year, or month, year. If more than one date appears on the report, use date of publication.

8a. **TOTAL NUMBER OF PAGES** The total page count should follow normal pagination procedures, i.e., enter the number of pages containing information.

8b. **NUMBER OF REFERENCES** Enter the total number of references cited in the report.

8c. **CONTRACT OR GRANT NUMBER** If appropriate, enter the applicable number of the contract or grant under which the report was written.

8d, 8e, & 8f. **PROJECT NUMBER** Enter the appropriate military department identification, such as project number, subproject number, system numbers, task number, etc.

9a. **ORIGINATOR'S REPORT NUMBER(S)** Enter the official report number by which the document will be identified and controlled by the originating activity. This number must be unique to this report.

9b. **OTHER REPORT NUMBER(S)** If the report has been assigned any other report numbers (*either by the originator or by the sponsor*), also enter this number(s).

10. **AVAILABILITY LIMITATION NOTICES** Enter any limitations on further dissemination of the report, other than those imposed by security classification, using standard statements such as:

- (1) "Qualified requesters may obtain copies of this report from DDC."
- (2) "Foreign announcement and dissemination of this report by DDC is not authorized."
- (3) "U. S. Government agencies may obtain copies of this report directly from DDC. Other qualified DDC users shall request through \_\_\_\_\_."
- (4) "U. S. military agencies may obtain copies of this report directly from DDC. Other qualified users shall request through \_\_\_\_\_."
- (5) "All distribution of this report is controlled. Qualified DDC users shall request through \_\_\_\_\_."

If the report has been furnished to the Office of Technical Services, Department of Commerce, for sale to the public, indicate this fact and enter the price, if known.

11. **SUPPLEMENTARY NOTES** Use for additional explanatory notes.

12. **SPONSORING MILITARY ACTIVITY** Enter the name of the departmental project office or laboratory sponsoring *(paying for)* the research and development. Include address.

13. **ABSTRACT** Enter an abstract giving a brief and factual summary of the document indicative of the report, even though it may also appear elsewhere in the body of the technical report. If additional space is required, a continuation sheet shall be attached.

It is highly desirable that the abstract of classified reports be unclassified. Each paragraph of the abstract shall end with an indication of the military security classification of the information in the paragraph, represented as (TS), (S), (C), or (U).

There is no limitation on the length of the abstract. However, the suggested lengths are from 150 to 225 words.

14. **KEY WORDS** Key words are technically meaningful terms or short phrases that characterize a report and may be used as index entries for cataloging the report. Key words must be selected so that no security classification is required. Identifiers, such as equipment model designation, trade name, military project code name, geographic location, may be used as key words but will be followed by an indication of technical context. The assignment of link numbers and weights is optional.